Final Report of the
Supplementary Comparison EURAMET.EM-S31
Comparison of capacitance and capacitance ratio

J. Schurr	PTB
N. Fletcher	BIPM
P. Gournay	LNE until March 2014, thereafter BIPM
O. Thévenot	LNE
F. Overney	METAS
L. Johnson and R. Xie	NMIA
E. Dierikx	VSL

Date: 31.05.2017

Jürgen Schurr
Physikalisch-Technische Bundesanstalt, PTB
Bundesallee 100, 38116 Braunschweig, Germany

Abstract

Within the framework of the Supplementary Comparison EURAMET.EM-S31, 'Comparison of capacitance and capacitance ratio', five participants (the BIPM, METAS, LNE, PTB, and VSL) inter-compared their capacitance realisations traced to the quantum Hall resistance measured at either ac or dc. The measurands were the capacitance values of three 10 pF standards and one 100 pF standard, and optionally their voltage and frequency dependences. Because the results were not fully satisfying, the circulation was repeated, augmented by a link to the NMIA calculable capacitor. Also two ac-dc resistors were circulated and their frequency dependences were measured in terms of the ac-dc resistance standards involved in the particular capacitance realisations, to allow inter-comparison of these resistance standards. At the end and in any case, a good agreement is achieved within the expanded uncertainties at coverage factor $k = 2$. Furthermore, the comparison led to new insight regarding the stability and travelling behaviour of the capacitance standards and, by virtue of the link to the NMIA calculable capacitor, to a determination of the von Klitzing constant in agreement with the 2014 CODATA value.

KEY WORDS FOR SEARCH
Inter-comparison, capacitance standard, ac-dc resistor, quantum Hall resistance, calculable capacitor, von Klitzing constant

Contents

1. Introduction

In this comparison, the values of capacitance standards traced to the quantum Hall resistance (QHR) have been tested. This shall guarantee consistent capacitance calibrations for the customers of the NMIs involved and is also important with respect to the forthcoming revised SI. For this comparison, the values of three travelling capacitors at a nominal value of 10 pF were derived from the quantum Hall resistance, measured at either ac or dc, by means of suitable chains of measuring bridges. The QHR is expressed in terms of the conventional value of the von Klitzing constant R_{K-90} = 25812.807 Ω. Because the measuring chains of the participants include several 10:1 steps, the comparison comprised one 100 pF capacitance standard to allow testing the 10:1 calibration of the participants.

This comparison was initiated by the EURAMET project REUNIAM (Foundations for a redefinition of the SI base unit ampere). In 2008 (before the comparison started), the EURAMET Technical Committee for Electricity and Magnetism decided to upgrade the comparison to a Supplementary Comparison in the MRA scheme under the identifier **EURAMET.EM-S31**, following the CCEM guidelines for planning, organizing, conducting and reporting key, supplementary and pilot comparisons.

A first circulation loop of the capacitance standards revealed significant discrepancies. Therefore, the participants circulated two Vishay ac-dc resistors with a nominal value of $R_{K-90}/2$ =12906.4035 Ω to allow comparison of the frequency dependence of the ac resistance standards which are involved in the measuring chain of each participant (i.e., either the ac QHR or calculable ac-dc resistors). Two ac-dc resistors (instead of one) were circulated for the sake of redundancy. This part of the comparison gave excellent agreement.

Therefore, after the participants had a chance to improve their measuring bridges and to submit corrections where needed, it was decided to repeat the circulation of the capacitance standards. To yield additional information, it was decided to transport the travelling capacitance standards also to NMIA to get a link to their calculable capacitor.

2. Organisation

2.1 Participants, coordinator, and support group

The following institutes participated in the comparison:

Table 2.1: Participants.

Institute	Acronym	Country	Comment
Physikalisch-Technische Bundesanstalt	PTB	Germany	pilot
Bureau International de Poids et Mesures	BIPM	International	support group
Laboratoire national de métrologie et d’essais	LNE	France	support group
Federal Institute of Metrology	METAS	Switzerland	
National Measurement Institute, Australia	NMIA	Australia	only at the 2nd capacitance loop
VSL Dutch Metrology Institute	VSL	Netherlands	only at the 1st capacitance loop

For contact details, see Annex 7.

2.2 Transportations

The transportation from each laboratory to the next one was at the responsibility and cost of the particular laboratory where the standards actually were. Within Europe, the travelling standards were transported by the car of a skilled driver of each participating institute. Courier services were not allowed, to avoid excessive mechanical shock due to inappropriate handling by the courier. The travelling capacitance standards should be thermostated during the transportations. For this purpose, a voltage converter from 12 V_{dc} to 230 V_{ac} connected to the cigarette-lighter socket of the particular car has been set up. At the first capacitance circulation loop, this system has partially failed due to unexpected incompatibility problems. Therefore, at the second capacitance circulation loop, an autarkic lead battery and the voltage converter from 12 V_{dc} to 230 V_{ac} has been used successfully. The capacitance standards, the lead battery and the voltage converter were packed into a suitable transport box with shock-absorbing foam. The box had no upper shell to avoid heat accumulation and overheating of the standards.

During the airfreight transportations to and back from NMIA, the capacitance standards were not thermostated and packed into a special airfreight box.

In the case of the travelling AC resistance standards, a thermostated transportation is less important. Nevertheless, the LNE ac resistance standard was powered by the car battery during each transport because it was prepared for this.

Immediately after the arrival at the laboratory of a participant, the travelling standards were placed in the particular laboratory and connected to the mains net. Immediately after the completion of the measurements, the standards were transported to the next participant.

3. Comparison of AC resistance standards

3.1 Travelling of AC resistance standards

Within the framework of this comparison, two Vishay ac resistance standards with a nominal value of $R_{K-90}/2$ were circulated. Vishay resistors were chosen because they have a small deviation from nominal, a low temperature coefficient, and they exhibit an *a priori* unknown, but linear, small and very stable, frequency dependence. Further, and in contrast to wire resistors with a calculable ac-dc difference, Vishay resistors are mechanically robust and their frequency dependence is insensitive to mechanical shock. For the sake of redundancy, two Vishay resistors, kindly provided by the BIPM and LNE, were circulated.

3.1.1 Description of travelling AC resistance standard of LNE

The LNE ac resistance standard has been built in such a way that its frequency dependence due to parasitic stray capacitances is as low as possible. It consists of an assembly of four Vishay resistors of equal nominal value and low temperature coefficients connected in series. The epoxy coating of these resistors in which dielectric losses may occur has been withdrawn and care has been taken to minimise, firstly, the capacitances between the individual resistors and the shield, and secondly, the capacitances between each resistor (by connecting the resistors in star configuration). The ac resistance standard has a relative deviation from the nominal value $R_{K-90}/2$ smaller than $50 \cdot 10^{-6}$. Its serial number is 1025665.

The assembled ac resistance standard is encased in a hermetical cylindrical brass shield (Figure 3.1.1) which in turn is placed in a temperature-controlled enclosure at about 25°C (Figure 3.1.2). The stability of the temperature regulator is better than 10 mK. The resistor has six terminal-pairs (UHF connectors), but only the four terminal-pairs labelled U_H, U_L, I_H, I_L were to be used for the comparison.

The temperature-controlled enclosure has two input-output connectors (Figure 3.1.3): one 6 pin Jaeger Rapid series connector for temperature regulation and one 5 pin Binder 680 series connector for enclosure temperature measurement. The Jaeger connector is connected to the power supply unit (Figure 3.1.4) and the Binder connector is connected to the thermometer Telna also provided for the comparison. The temperature regulation of the LNE resistor can be powered during transportation from a car battery.

A data logger model MSR 145 provided by PTB is mounted on the outer enclosure of the LNE standard resistor to record shock and vibration above a certain threshold. In addition, the data logger records the temperature in certain intervals (see also Annex 12.3).

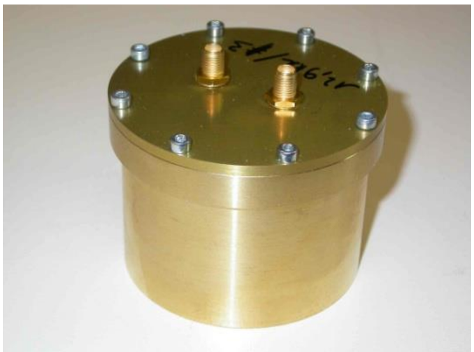

Figure 3.1.1: Hermetic brass enclosure containing the resistors assembly

Figure 3.1.2: Temperature-controlled enclosure containing the hermetic brass enclosure

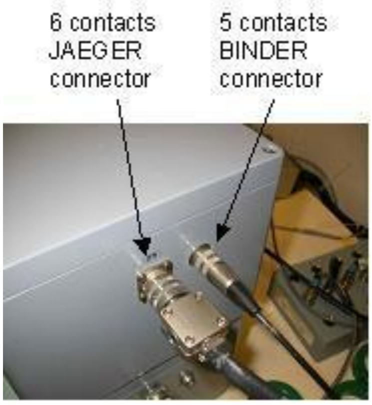

Figure 3.1.3: Electrical connections

Figure 3.1.4: Power supply

3.1.2 Description of travelling AC resistance standard of the BIPM

The BIPM Vishay ac resistance standard (labelled RES-ELEC-17 and shown in Figure 3.1.5) includes a temperature control, a thermistor for monitoring the internal temperature, and four BNC terminal-pairs for the main resistor connection (Figure 3.1.6). The nominal resistor value is $R_{K-90}/2$ within $\pm 10\cdot 10^{-6}$.

The internal temperature is regulated to approximately 25°C (by a controller providing heating only). It is designed to operate in a nominal lab temperature of 23°C. The value of the thermistor at the correct operating point is approximately 29.5 kΩ, with a sensitivity of 0.8 mK/Ω. To check that the controller works properly, the participants had to measure the thermistor value by means of a suitable multimeter.

Power for the temperature control is from an external 12 V dc supply, connected via the 4 pin DIN connector using the supplied cable.

Figure 3.1.5: Enclosure containing the Vishay resistor, with a 4-terminal-pair adaptor and the thermistor pins.

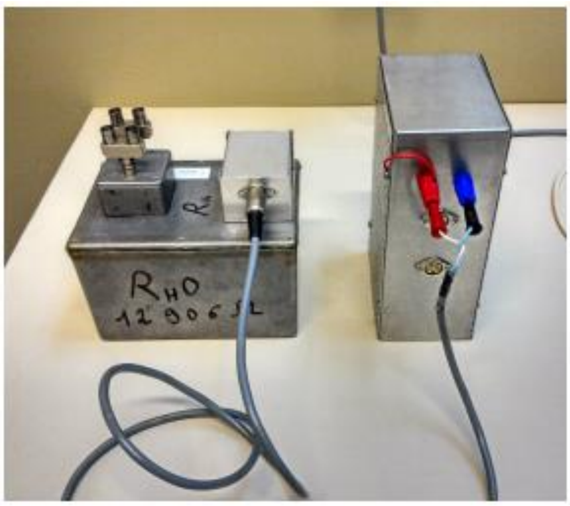

Figure 3.1.6: Vishay resistor and power supply of the temperature controller.

3.1.3 Quantities to be measured and nominal conditions

The main quantity to be measured is the frequency dependence of the two 12 906 Ω travelling resistors deduced from the measurements of their parallel equivalent resistance at several frequencies, either with respect to the actual, separately measured dc (or low-frequency) resistance value or with respect to the actual ac resistance value extrapolated to a frequency of zero hertz. The measurement conditions are as follows:

Test current: Maximum 1 mA

Test frequencies: Three frequencies between 400 Hz and 2500 Hz (mandatory). Optional measurements at other frequencies up to 5 kHz are welcome.

Environmental conditions: Ambient temperature: 20 to 23 °C
Relative humidity: (50 ± 10) %
Atmospheric pressure (only for the sake of completeness).

Resistor temperature: Immediately after the arrival, the standards have to be unpacked, placed in the particular laboratory, and the thermostats have to be powered again as soon as possible, at least 12 hours before the measurements. The temperature of the resistors has to be measured to verify a proper temperature regulation.

3.2 Time schedule and participants of AC resistance comparison

The AC resistance comparison was carried out in a loop, with additional re-measurements by the BIPM and LNE to establish the drift rate of their standards and to detect possible effects due to the transportation. A period of two weeks was assigned to each laboratory.

VSL did not participate in the AC resistance comparison and NMIA joined this comparison after this AC resistance comparison.

Period	Laboratory	Start date	End date
1	LNE	5 November 2012	16 November 2012
2	BIPM	26 November 2012	07 December 2012
3	PTB	12 December 2012	11 January 2013
4	LNE	18 January 2013	30 January 2013
5	METAS	4 February 2013	15 February 2013
6	BIPM	25 February 2013	8 March 2013
7	LNE	11 March 2013	22 March 2013

Due to a failure, only the LNE resistor, but not the BIPM resistor, was transported to METAS (which was accepted because one of the two resistors was only used for the sake of redundancy).

3.3 AC resistance measurement principles

3.3.1 Measuring principle of the BIPM

The resistors under test were measured on a coaxial bridge for the comparison of four-terminal-pair impedances using a calibrated 10:1 voltage ratio transformer. The variation of the in-phase component of the ac resistance standard was measured as a function of frequency over the range 400 Hz to 3200 Hz, using a coaxial (Haddad type) resistor of nominal value 1.2906 kΩ as the reference. An additional point was added at 2 Hz using a separate bridge for four-terminal resistance standards based on a room-temperature current comparator.

The coaxial reference resistor was not placed in an oil bath, to avoid unwanted dielectric effects of oil, and this limited the stability of the measurement system. For this reason, all measurements were performed as pairs of frequencies, always using the central reference frequency of 1610 Hz. Not the absolute values of the ac resistance standards, but only the changes at each frequency versus the reference frequency of 1610 Hz are reported. Finally, the results are converted with respect to the measured resistance value at a frequency of 2 Hz (which is practically equivalent to dc).

3.3.2 Measuring principle of LNE

The frequency dependence of the LNE and BIPM resistors have been measured against a 1290.6 Ω calculable resistor (Haddad type) using the 10:1 four-terminal-pair bridge described in Figure 3.3.2.

The main component of the bridge is a two-stage transformer, with 11 equal sections

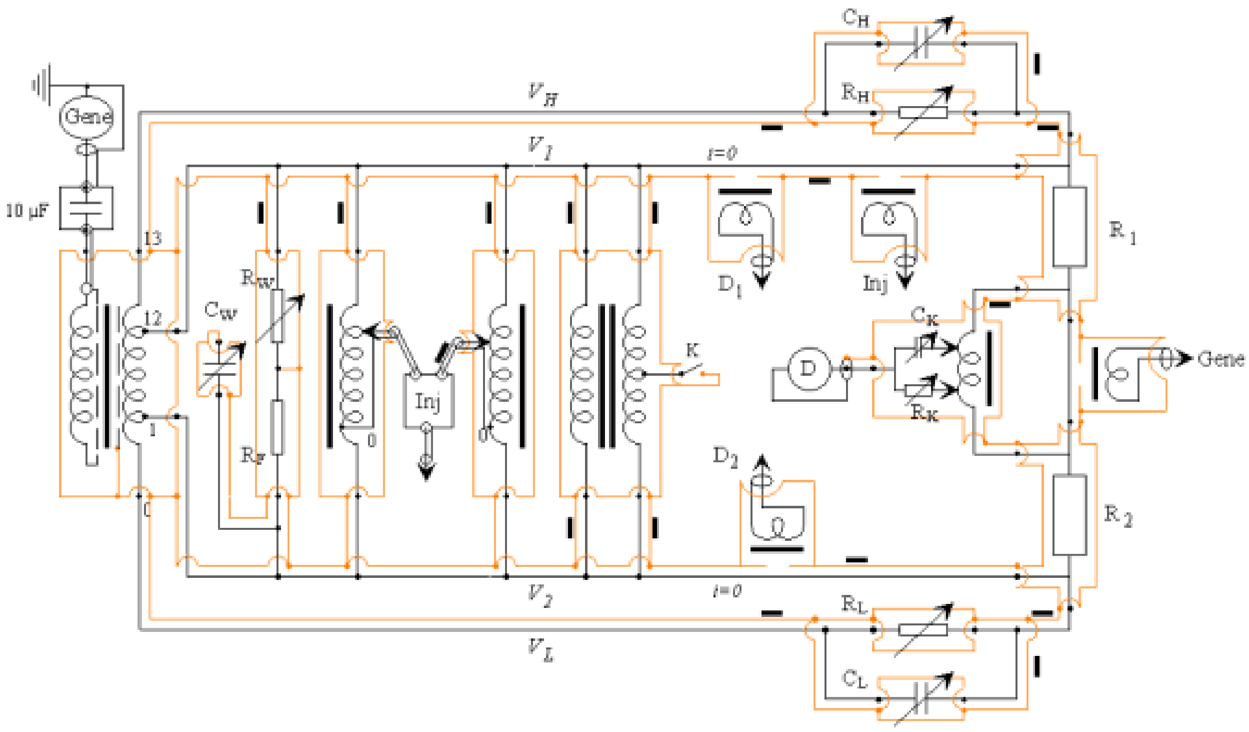

Figure 3.3.2: Four-terminal-pair resistance bridge.

wounded on high permeability cores. The transformer is kept unloaded by using a “Wagner” arm and compensating circuits. Their ratios are calibrated for each frequency value used in this comparison by using the “bootstrap” method.

Two adjustable current sources allow to obtain zero current at the potential ports of the resistors to be compared and a combining network at the detector node is adjusted so that a small auxiliary voltage injected in the connection cable between “R” and “10R” has no effect on the main detector D, thus producing a condition for which the voltage drop along this cable is zero.

Coaxiality of the bridge is ensured by insertion of high permeability cores (current equalizers) in each loop of the outer conductors of the coaxial connections. The efficiency of each current equalizer has been tested.

3.3.3 Measuring principle of METAS

Figure 3.3.3 shows the schematic of the new digitally assisted coaxial bridge configured for the comparison of the four-terminal-pair impedance standards Z_{top} and Z_{bot} [18]. This coaxial bridge has been used to measure the travelling Vishay resistors against a calculable quadrifilar 12.906 kΩ resistor. The precise voltage ratio is still given by a voltage ratio transformer. However, all the balances required to precisely compare the impedances are automatically performed - over a large bandwidth (100 Hz to 20 kHz) - by adjusting digital sources and detectors instead of IVDs and lock-in amplifiers. The main component is the double-screened

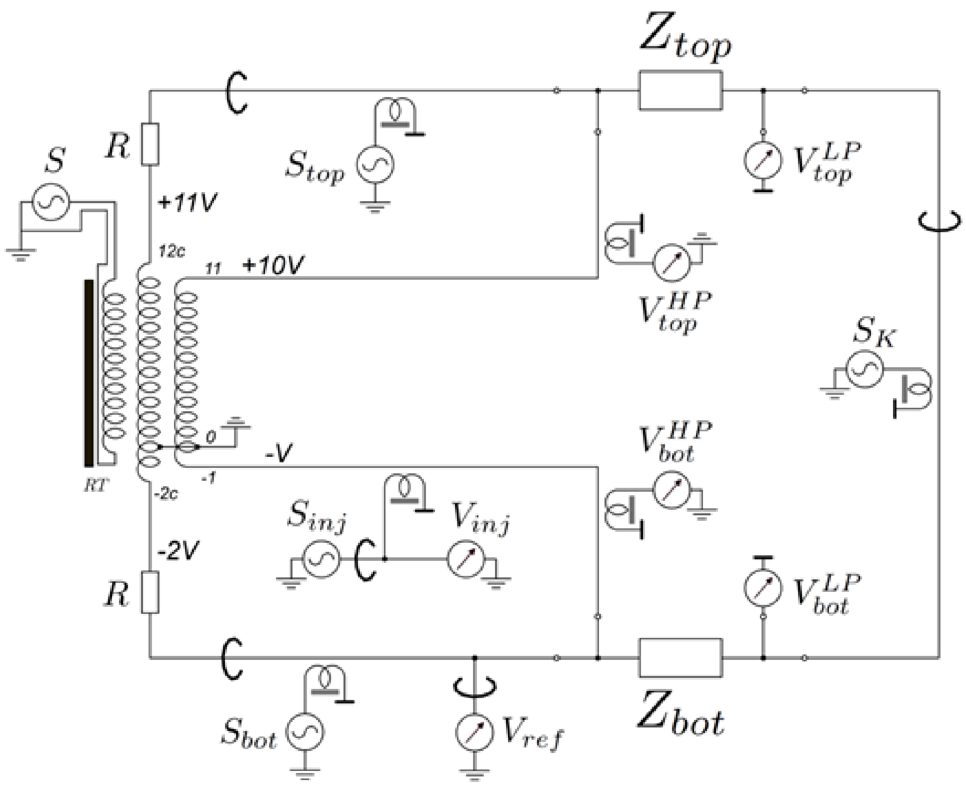

Figure 3.3.3: Simplified schematic of the digitally assisted coaxial bridge for the comparison of four terminal-pair standards in a 1:10 ratio. The outer conductors of the coaxial cables have been omitted for clarity. The bridge is formed by 1 ratio transformer RT; 5 signal generators S, S_{top}, S_{bot}, S_{inj} and S_K ; 6 digitizers Vref , V_{inj} , V^{HP}_{top}, V^{HP}_{bot}, V^{LP}_{top} and V^{LP}_{bot}; and 6 IDTs.

ratio transformer RT having one primary winding and two secondary windings. The first secondary winding, which has fourteen taps labelled from -2c to 12c, supplies the current to the impedance standards through the resistors R. The second secondary winding, which has twelve taps labelled from -1 to 11, gives the reference voltage ratio. In the configuration represented in Figure 3.3.3, the voltage ratio is 1:10. However, using different taps, the same bridge can also be used to compare impedances in a 1:1 ratio.

Operating the bridge requires the use of 5 signal generators, 6 digitizers and 6 double-screened injection-detection transformers (IDTs).

The signal generators and the digitizers are either the analogue outputs (AO) or the analogue inputs (AI) of high-performance, high-accuracy analogue I/O devices commercially available (NI PXI 4461). Each channel has its own 24-bit converter, amplifier/attenuator and anti-aliasing filter. The maximum generation/sampling rate is 204.8 kSa/s.

The 6 IDTs are home-made transformers with 100 turns at the primary winding and either 100 turns or 1 turn for the secondary winding. A double electrostatic shield is placed between the primary and secondary windings to avoid any leakage current between the different parts of the electrical circuit. Coaxial chokes [8] are also implemented, one in each mesh of the bridge, to guarantee the current equalization and the immunity of the bridge to external interferences [9]. Each AO channel generates a single tone signal at the same frequency f. The relative phase and amplitude of each generator can be independently adjusted.

Each AI channel simultaneously samples N values of the voltage at a sampling frequency f_s. The duration of the data set is therefore given by N/f_s and contains P periods of the measured signal. The amplitude, A, and the phase, ϕ, of the fundamental component of each measured signal is then obtained from the Discrete Fourier Transform (DFT) of the data sets. To avoid spectral leakages and to guarantee the accuracy of the DFT calculation, N and P have to be integers and $N \geq 2$. A preliminary characterization showed excellent results over the entire bandwidth.

3.3.4 Measuring principle of PTB

Each travelling Vishay resistor was measured by a coaxial 1:1 resistance bridge against a temperature-controlled 12.906 kΩ Vishay reference resistor. The frequency dependence of the reference resistor was determined by the same bridge against a double-shielded ac QHR device (as is applied in the quadrature bridge for the capacitance realisation). This means that each travelling resistor was measured in substitution against a double-shielded ac QHR device. (A direct measurement was not possible because at that time the cryo-magnetic system was not in operation.) The diagram of the coaxial 1:1 resistance bridge is shown in Figure 3.3.4.

The measuring current was set to 40 µA (rms) and the frequency was varied in the range from 507 Hz to 5007 Hz. The 1:1 deviation of the ratio transformer at each frequency was eliminated by a reversal measurement. The measurement of the frequency dependence of each travelling resistor was carried out two times, to verify the reproducibility. The equalisers in the coaxial bridge were tested and evaluated, and a cable correction has been applied to the results.

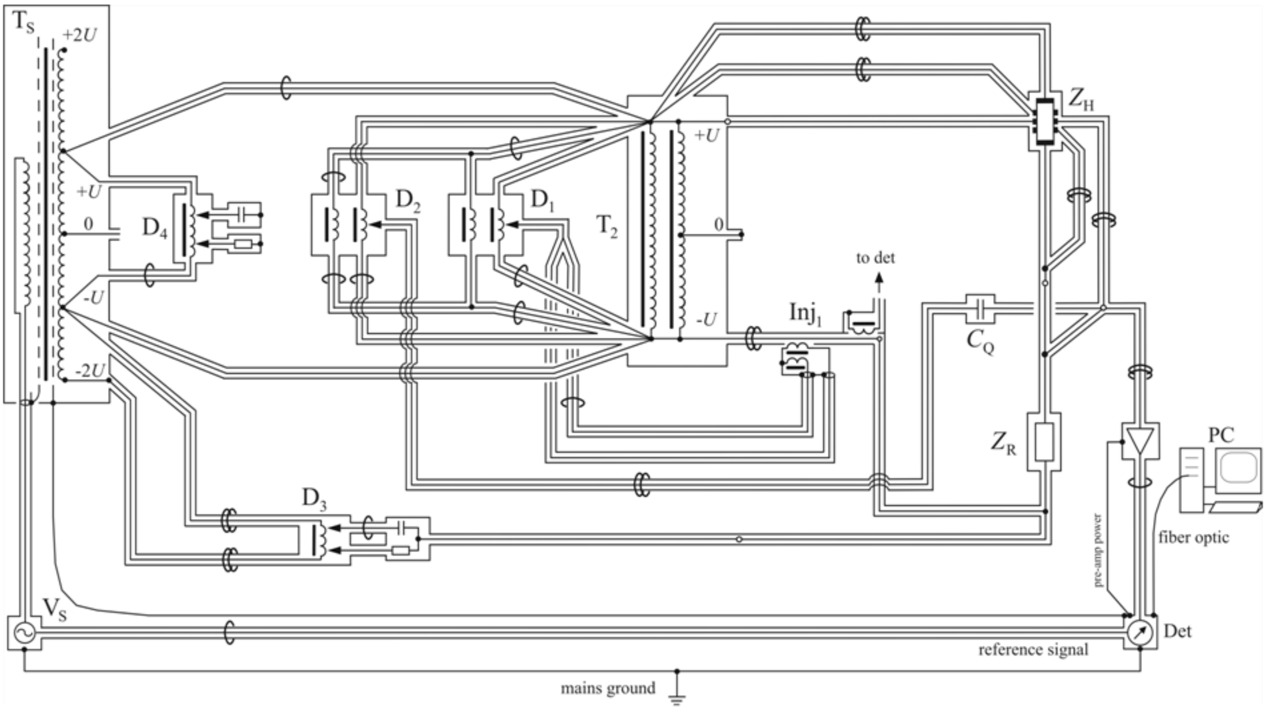

Figure 3.3.4: Diagram of the coaxial 1:1 resistance bridge. Z_H is the quantum Hall resistance in triple-series connection scheme and Z_R is the reference resistor. T_2 is the 1:1 ratio transformer. D_1 and D_2 are decade IVDs for the main balance, D_3 is a current source and D_4 is a Wagner arm.

3.3.5 Summary: reference resistors of participants

To summarise, the types of ac reference resistors which are used in the capacitance chain of each participant and against which the travelling Vishay ac resistance standards were measured are listed in Table 3.3.5.

Table 3.3.5: Reference resistors.

Participant	**Reference resistor**
BIPM	1290.6 Ω calculable resistor of Haddad type
LNE	1290.6 Ω calculable resistor of Haddad type
METAS	12906 Ω calculable resistor of quadrifilar type
PTB	ac quantum Hall resistance at i = 2

3.4 Results of AC resistance measurements

The measurand is the frequency-dependence of the ac resistance of the travelling Vishay resistors. The dc resistance values are not sufficiently stable during the comparison. To nevertheless allow a comparison of the ac resistances, it is necessary to refer the ac resistance either to the actual, separately measured dc (or low-frequency) resistance value (as was done by the BIPM and METAS) or to the ac resistance value extrapolated to zero hertz (as was done by LNE and PTB). In the latter case, a corresponding uncertainty has to be considered (which is the larger, the smaller the frequency range is).

Vishay resistors exhibit a frequency dependence which is practically linear and a characteristic property of Vishay resistors (at least in the audio frequency range). As shown in Figure 3.4.1, this linear frequency dependence occurs not only in the agreed frequency range of up to 5 kHz, but also continues at higher frequencies. The linear frequency dependence allows the description of the frequency dependence by a single parameter, the frequency coefficient, whose value can be determined by a least-squares fit. The uncertainty of the frequency coefficient is not only determined by the uncertainty of the particular ac measurements, but also by the particular frequency range and whether or not an extra dc (or low-frequency) measurement has been carried out.

We begin with the frequency dependence of the travelling LNE resistor as measured by LNE before, during and after the circulation period. The results are shown in Figure 3.4.2. More details and the associated uncertainty budgets are given in Annex 8.2. The frequency coefficient as measured at LNE as a function of time is given in Table 3.4.1 and is shown in Figure 3.4.3. As follows from χ^2 per degree of freedom, from the probability P of χ^2 being larger than the observed value and from the degree of equivalence, the distribution of the three values of the frequency coefficient is consistent and the individual measurements are without a discrepant result. (Note that a probability P < 5% is usually interpreted as a signifi-

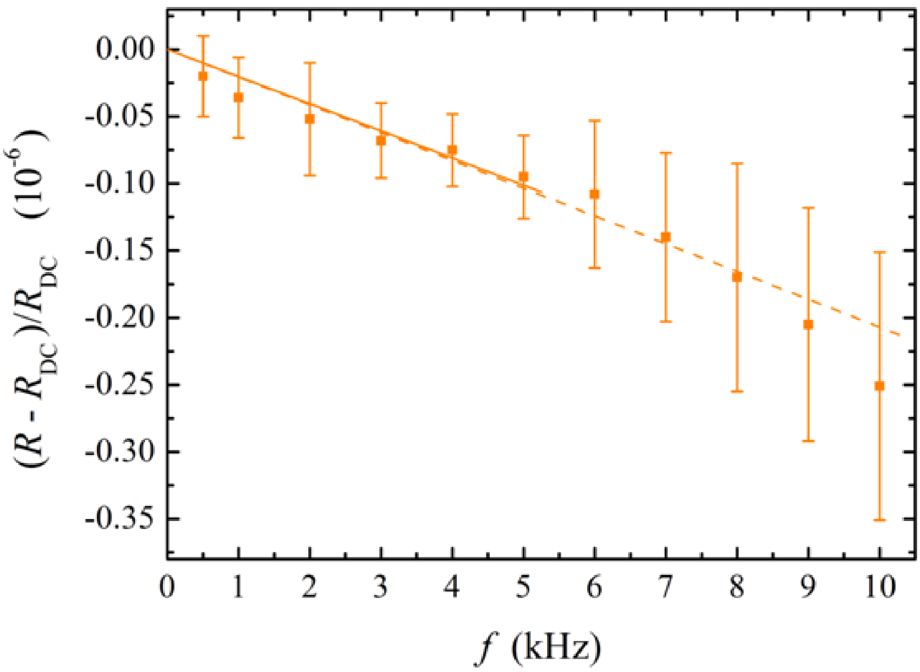

Figure 3.4.1: Frequency dependence of the travelling LNE resistor as measured by METAS. The uncertainty bars correspond to k = 2. The solid and the dashed line are linear least-squares fits and a guide to the eye.

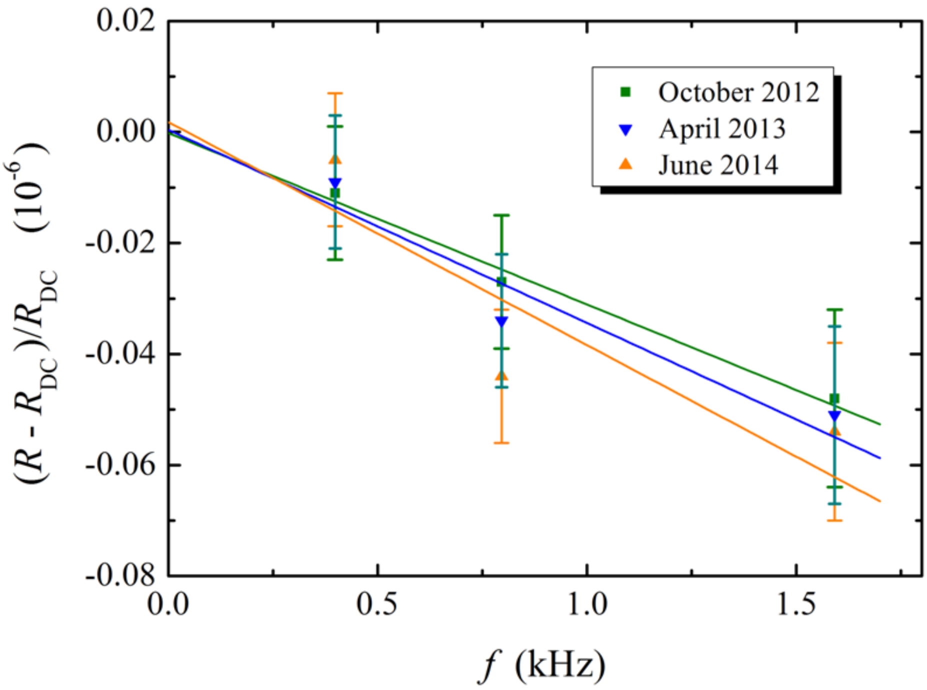

Figure 3.4.2: Frequency dependence of the travelling LNE resistor as measured by LNE before, during and after the circulation period. The uncertainty bars correspond to k = 2. The solid lines are linear least-squares fits and a guide to the eye.

cant failure, whereas $P > 95\%$ is usually interpreted as underestimated uncertainties.)

The LNE results show that the frequency dependence of the travelling LNE resistor exhibits neither a significant long-term drift nor a variation due to transportation. This is a very valuable finding and important to the interpretation of the following results.

Such an investigation was only carried out for the travelling LNE resistor, but not for the travelling BIPM resistor. However, since both resistors consist of similar Vishay-type elements and have a similar mechanical robustness, we assume a similarly convenient behaviour. This assumption is also justified by the good agreement of the individual results.

Table 3.4.1: Frequency coefficient of the travelling LNE resistor as determined by least-squares fits to the measurements of LNE. Quoted are also the weighted mean, the observed value of χ^2 per degree of freedom, and the cumulative probability P of χ^2 to be larger than the observed value.

Mean datum	Frequency coefficient (10^{-9}/kHz) and estimated k = 2 uncertainty
19.10.2012	-30.9 ± 17
12.04.2013	-34.8 ± 25
07.06.2014	-40.2 ± 16
mean value	**-35.3 ± 18**
$\chi^2/(N\text{-}1)$	**0.322**
$P(\chi^2 > \chi^2_{obs})$	**72%**

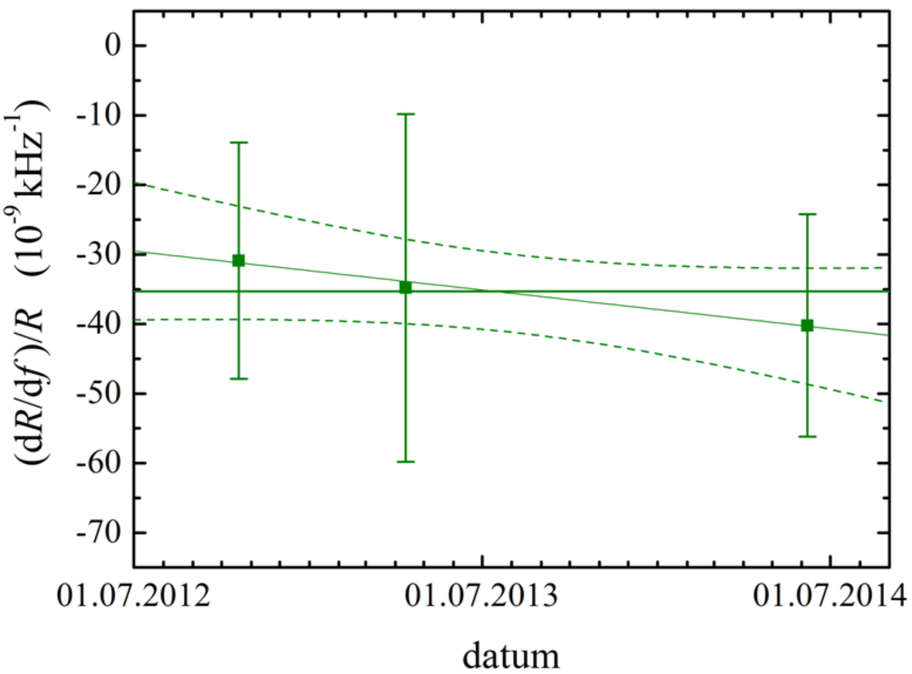

Figure 3.4.3: Frequency coefficient of the travelling LNE resistor as measured at LNE before, during and after the circulation period. The uncertainty bars correspond to *k* = 2. The thick solid line indicates the mean value. The thin solid line and the dashed lines indicate a linear least-squares fit and its 95% confidence band, respectively.

Figure 3.4.4 and Figure 3.4.5 show the results of the frequency dependence of the travelling resistors as measured by the participants. More details and the associated uncertainty budgets are given in Annex 8. As already mentioned above, the results show a linear frequency dependence which is parameterised by the frequency coefficients quoted in Table 3.4.2.

The linear frequency dependence of Vishay resistors, especially its negative sign, is attributed to the stray capacitance in parallel to the resistive film and through the lossy substrate which carries the resistive film. The LNE resistor is found to exhibit a very small frequency coefficient, which is attributed to the extra effort of LNE in minimising the stray capacitances (as described in Section 3.1). But also the frequency coefficient of the BIPM resistor is quite small (whereas single Vishay resistors of some other available types exhibit a much larger frequency dependence, for example, $-180\cdot10^{-9}$ kHz^{-1}).

As follows from the χ^2 test given in Table 3.4.2, the distribution of the results for the frequency coefficient is very reasonable. Analysis of the degree of equivalence shows that the results of all participants are fully consistent and without any discrepant result at the 95% level of significance. Also the associated uncertainties of all participants are considered to be reasonable. Therefore, the weighted mean of the frequency coefficients of each travelling resistor is taken as its CRV. The CRV has an expanded uncertainty of $4.9\cdot10^{-9}$/kHz and $3.3\cdot10^{-9}$/kHz, respectively, which is excellent.

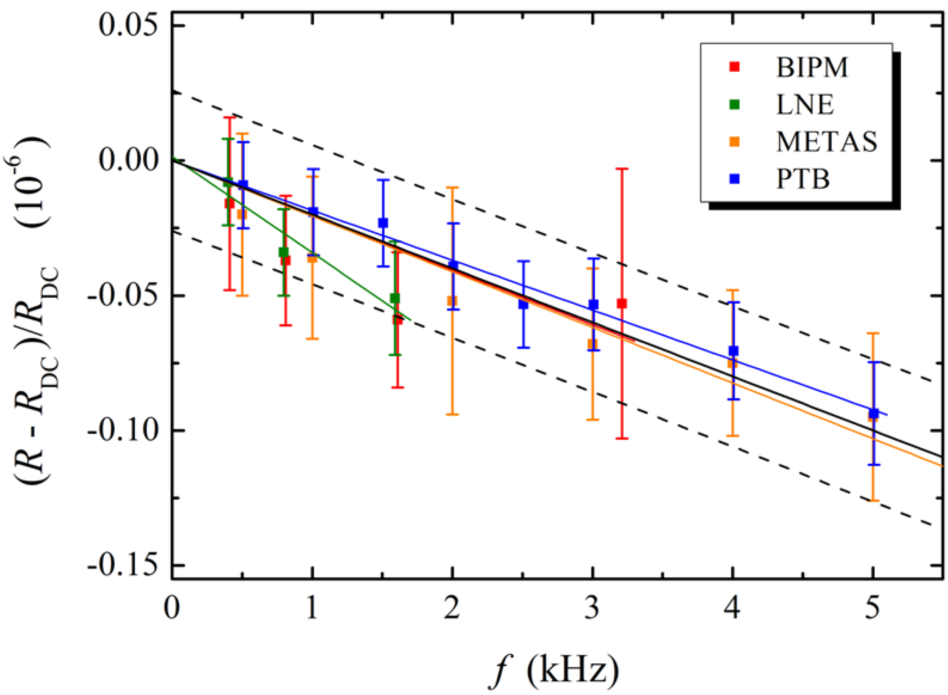

Figure 3.4.4: Frequency dependence of the travelling LNE resistor as measured by the participants. The uncertainty bars correspond to k = 2. The coloured lines are the particular least-squares fits to the data of each participant. The solid black line indicates a linear least-squares fit to all data and the dashed lines indicate the associated 95% prediction band.

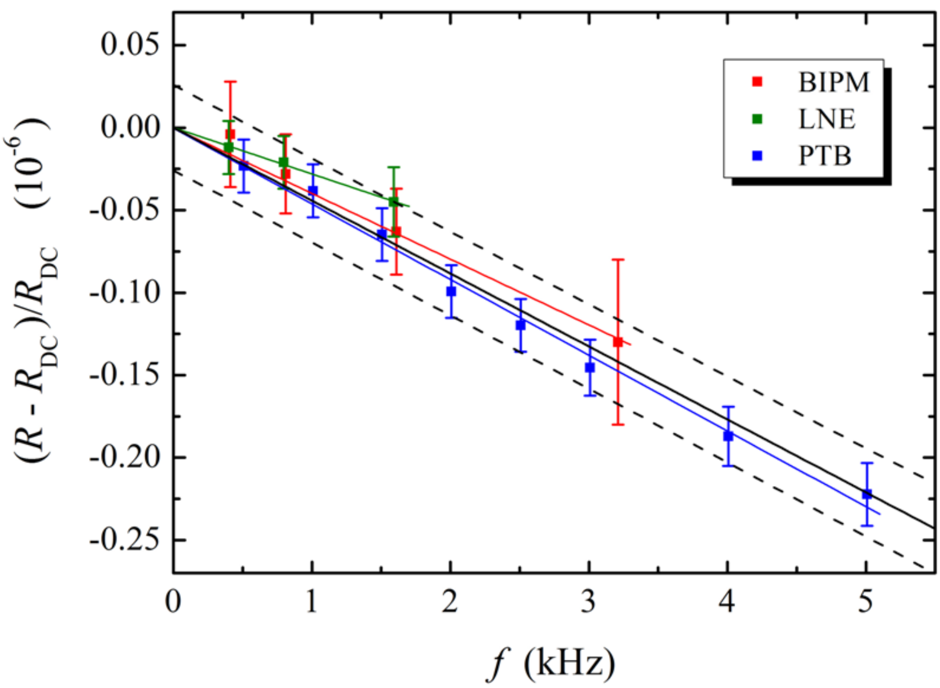

Figure 3.4.5: Frequency dependence of the travelling BIPM resistor as measured by the participants. The uncertainty bars correspond to k = 2. The coloured lines are the particular least-squares fits to the data of each participant. The solid black line indicates a linear least-squares fit to all data and the dashed lines indicate the associated 95% prediction band. (Due to a failure, the BIPM resistor was not transported to METAS. This has been accepted because one of the two resistors was circulated only for the sake of redundancy.)

Table 3.4.2: Frequency coefficients of the travelling BIPM and LNE resistors as determined by linear least-squares fits to the results of the participants (only at frequencies $f \leq 5$ kHz). Quoted are also the weighted mean, the observed value of χ^2 per degree of freedom, and the cumulative probability P of χ^2 to be larger than the observed value.

Participant	Frequency coefficient (10^{-9}/kHz) and estimated k = 2 uncertainty	
	BIPM resistor	LNE resistor
BIPM	-39.9 ± 11	-20.3 ± 12
LNE	-28.1 ± 18	-35.3 ± 18
METAS	(resistor was not available)	-20.6 ± 4.4
PTB	-45.9 ± 5.7	-18.5 ± 5.7
weighted mean	**-43.4 ± 4.9**	**-20.4 ± 3.3**
$\chi^2/(N\text{-}1)$ and P	**2.03, 13%**	**1.07, 36%**

3.5 Conclusion

The frequency dependence of two travelling Vishay ac resistance standards was measured by the participants either in terms of their calculable ac-dc resistor or at the pilot laboratory in terms of the ac QHR (see Section 3.3 and Table 3.3.5). The frequency dependences of the travelling ac-dc resistance standards do not show any significant drift or variation due to the transportations. The results of the participants are in a very good agreement and fully consistent. This means that the calculable ac-dc resistors involved in the measuring chain of each participant as well as the ac QHR involved in the measuring chain of the pilot laboratory are fully consistent and not a significant source of discrepancy of the particular capacitance realisations.

4. Comparison of capacitance standards

4.1 General aspects

4.1.1 Description of capacitance standards

The travelling standards are four commercial Andeen-Hagerling fused-silica capacitance standards, model AH11A, one at a nominal value of 100 pF (SN 1256) and three at 10 pF (SN 1257, 1258, and 1310). The standards were mounted into an Andeen-Hagerling frame, model AH1100. The 10 pF standard SN 1310 was kindly provided by the BIPM, the other ones and the frame were provided by PTB. A photograph of the travelling AH frame is shown in Figure 4.1. Three 10 pF capacitance standards were used to yield a high redundancy in the hypothetical case that one of the standards would fail or show a poor behaviour during the comparison, which fortunately did not happen.

The AH frame consists of the outer chassis and four inner enclosures. Each inner enclosure contains a separate thermostat with the shielded capacitive element. The capacitive elements are originally manufactured with an incomplete shield so that they suffer unwanted leakage capacitance and unnecessary pick-up noise. Therefore, home-made internal shields were added to all four standards already a long time before this comparison started, and it has been verified experimentally that no effects due to incomplete shielding remain. The front panel of the chassis is provided with four pairs of coaxial BNC sockets at which the apparent two terminal-pair capacitances to be measured are defined.

4.1.2 Quantities to be measured and nominal conditions

The test frequency was defined to be either f = 1233 Hz (reference frequency), 1592 Hz, 1000 Hz, or any other frequency in this range. The test voltages were defined to be 10 V_{rms} for the 100 pF standard and 100 V_{rms} for the 10 pF standards. The capacitance measurements were repeated several times during the whole period allocated to each participating laboratory. Participants were asked to measure the voltage and the frequency dependence of the travelling capacitance standards if possible.

The values of the capacitance standards can be determined by using, for example, either a two- or a four-terminal-pair measuring bridge, and the results were to be corrected for the effect of the connecting cables. In the case of a four-terminal-pair bridge, it was recommended to provide the two BNC sockets in the front panel of the particular AH standard with T-connectors to which the four measuring leads can be connected. Because the measurand is defined at the BNC sockets in the front panel of the chassis, the measured capacitance values

Figure 4.1: The travelling Andeen-Hagerling frame with four capacitance standards.

only have to be corrected for the defining cables from the measuring bridge to the T-connectors.

In the case of a two-terminal-pair bridge, the measured capacitance values have to be corrected for the defining cables from the bridge to the capacitive element and from the capacitive element back to the front panel of the chassis. Therefore, the internal cable parameters and the shield capacitances were provided to the participants. Depending on the cable lengths and the target uncertainty, it might be practically equivalent to correct the cables from the measuring bridge to the front panel of the chassis and to consider the residue as an uncertainty contribution.

The ambient temperature during the measurements was to be monitored by the participants. The nominal ambient temperature was defined to be (23.0 ± 0.5) °C.

The pilot laboratory has also investigated the effect of ambient humidity. For this purpose, an identical AH frame was placed into a temperature cabinet and the relative humidity was altered between less than 10% and about 90%, but no significant change of the capacitance was observed. This is reasonable since the AH standards are hermetically sealed and operated at a quite high internal temperature of about 55 °C. Therefore, the results of the participants do not need a humidity correction. Nevertheless, for the sake of completeness, also the relative humidity and the atmospheric pressure were to be monitored by the participants

Because the capacitive elements are operated at a quite high internal temperature, they suffer a considerable heat transfer to and from the direct surroundings and also exhibit temperature gradients on their surface. It is therefore important that the AH frame with the capacitance standards are not placed above or below heat-generating devices and stand free to allow sufficient air circulation.

4.1.3 Deviations from nominal conditions

At LNE, 100 pF were measured at both circulations at 45 V (instead of 10 V) and 10 pF only at the first circulation and at 398 Hz were measured at 63 V (instead of 100 V). Therefore, a correction with a corresponding uncertainty has been added by the pilot as described in Section 4.7.

LNE and NMIA ran their laboratory at a deviating temperature of 20°C (instead of 23°C). Therefore, the pilot corrected the LNE and NMIA results for the deviating temperature and added the corresponding uncertainty as described in Section 4.7 and Section 12.1.

The AH frame is powered by mains voltage. The nominal mains voltage within Europe is 230 V, but 240 V has been used at NMIA. Furthermore, the actual mains voltage was not monitored by each participant and may have deviated from nominal by a few volts. Therefore, the pilot laboratory has verified experimentally by means of a variable mains transformer that the capacitance of the travelling AH standards do not suffer a significant change within a relative uncertainty of $3\cdot10^{-9}$ per 10 V change of the mains voltage (see Section 12.2).

4.1.4 Time schedule and participants of the capacitance comparison

The capacitance comparison was carried out in a loop, with intermediate measurements at the pilot laboratory and at the BIPM to determine the long-term drift of the standards and to detect possible effects due to the transportation. A period of six weeks was assigned to each laboratory; it includes a period of 7 days for relaxation and acclimatisation of the travelling standards after each transport (which in the case of thermostated transportations was found to be sufficient).

Table 4.1.4.1: Time schedule of the first capacitance circulation loop:

Participant	Start and end dates		Mean datum of measurements	Datum of transportation to the next participant
PTB	08.07.2010	26.07.2010	17.07.2010	02.08.2010
VSL	05.08.2010	06.09.2010	24.08.2010	14.09.2010
METAS	01.10.2010	12.11.2010	21.10.2010	15.11.2010
PTB	24.11.2010	13.01.2011	08.12.2010	08.02.2011-09.02.2011
LNE	03.03.2011	31.03.2011	28.03.2011 (#1256: 15.03.2011)	01.04.2011
BIPM	12.04.2011	13.05.2011	05.05.2011	16.05.2011
PTB	26.05.2011	27.06.2011	11.06.2011	

At the second capacitance circulation loop, VSL did not participate. In addition, NMIA participated and contributed a link to their calculable capacitor. The BIPM carried out measurements before and after the NMIA measurements, to allow investigation of the behaviour of the unthermostated airfreight transportations to and back from Australia (which in fact differs from careful thermostated transportations by car, as described in Section 4.4).

Table 4.1.4.2: Time schedule of the second capacitance circulation loop:

Participant	Start and end datum of measurements		Mean datum of measurements	Datum of transportation to the next participant
PTB	19.09.2014	17.10.2014	02.10.2014	31.10.2014
LNE	*)			05.01.2015
BIPM	15.01.2015	12.02.2015	29.01.2015	13.-26.02.2015
NMIA	03.03.2015	24.03.2015	13.03.2015	08.-20.04.2015
BIPM	27.04.2015	01.06.2015	29.05.2015	03.06.2015
PTB	04.09.2015 **)	28.09.2015	16.09.2015	07.10.2015
METAS	12.11.2015	26.11.2015	19.11.2015	02.12.2016
LNE	18.01.2016	12.02.2106	31.01.2016	16.02.2016
PTB	09.03.2016	08.04.2016	22.03.2016	

*) No results delivered due to bridge problems.
**) Delay due to illness.

4.2 Principles of capacitance measurements

4.2.1 The measuring chain at PTB

PTB traces its capacitance unit to the ac quantum Hall resistance as schematically shown in Figure 4.2.1. In that, PTB is the first, and the only, national metrology institute. By means of a four-terminal-pair quadrature bridge, two 10 nF capacitance standards are linked to two ac QHRs. Then, by means of a four-terminal-pair ratio bridge, three 10:1 steps from the 10 nF capacitance standards to the 10 pF capacitance standards under calibration are carried out.

Using two ac QHR devices directly in the quadrature bridge has several advantages: (i) The measuring chain is shorter. (ii) A calculable ac-dc transfer resistor is not needed. (iii) The cryogenic QHRs generate much less thermal noise than conventional room-temperature resistors. As a consequence, the quadrature bridge is operated at a voltage level of 100 mV (which in the case of room-temperature resistance standards is practically impossible). Then, the whole measuring chain is carried out from 10 nF at 100 mV to 10 pF at 100 V so that every capacitance value is always operated at the same voltage level and, consequently, no correction for the voltage dependence of the capacitance standards is needed. (iv) Due to the properties of multiple-series connected QHR devices, several combining networks which are needed in a quadrature bridge with conventional resistors become obsolete so that the quadrature bridge can be simplified. This and the very low noise level drastically expedite the balancing process.

The quadrature bridge and the 10:1 ratio bridge are located directly beneath the cryomagnetic system with the two ac QHRs and also include a bank of capacitance standards: one pair of multi-layer ceramic capacitors at a nominal value of 10 nF and one pair at 5 nF, three General Radio 1 nF standards, one General Radio 100 pF, and up to three AH frames with 10 pF and 100 pF AH standards to be calibrated. All capacitance standards are thermostated. The frequency of the sine-generator of the quadrature bridge is coupled to PTB’s 10 MHz reference frequency.

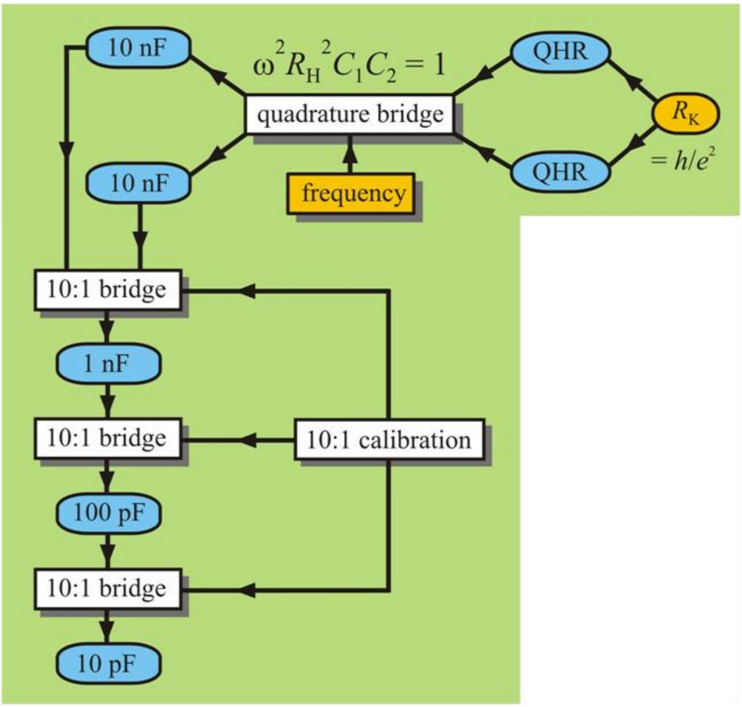

Figure 4.2.1: The impedance chain realised at PTB.

The quadrature bridge can be operated either with two 10 nF standards at a frequency of 1233 Hz or with two 5 nF standards at a frequency of 2466 Hz. The two 5 nF standards can be connected in parallel to yield a decade value 10 nF from which the measuring chain is continued to 100 pF and 10 pF. Thereby, all the capacitance standards can be measured at the two frequencies quoted above.

Finally, the 10:1 transformer of the ratio bridge is calibrated by a straddling bridge which is also located in the same laboratory. Because all the measuring bridges exhibit a very low noise level and require at maximum only one iteration for the main and auxiliary balances, the whole bank of capacitance standards can be linked to the ac QHR within one day. During this comparison, all capacitance calibrations were directly linked to the ac QHR.

More details on the method can be found in [4].

4.2.2 The measuring chain at the BIPM

The BIPM maintains a reference group of four fused-silica 10 pF capacitors (one of the NBS type and three of the General Radio 1408-A type). Since 1999, the mean value of the group has been measured twice a year using a measurement chain linking the 10 pF capacitances to the recommended value of the von Klitzing constant, R_{K-90}, as shown in Figure 4.2.2. The chain includes a capacitance bridge with ratio 10:1, a multi-frequency quadrature bridge, an ac-dc coaxial resistor with calculable frequency dependence of resistance, and a quantum Hall device operated at 1 Hz. The relative drift rate of the mean value of the reference group is about 3.5 parts in 10^8 per year. Details of the multi-frequency quadrature bridge can be found in [3].

The travelling standards were measured against members of the 10 pF reference group, directly on a 10:1 ratio bridge for the 100 pF standard, and via substitution (i.e. two 10:1 steps against a 100 pF buffer) in the case of 10 pF. The value of the reference group was determined (via the quadrature bridge chain and the QHR reference) within a few weeks of the comparison period in order to minimise the extrapolation uncertainty of the reference value.

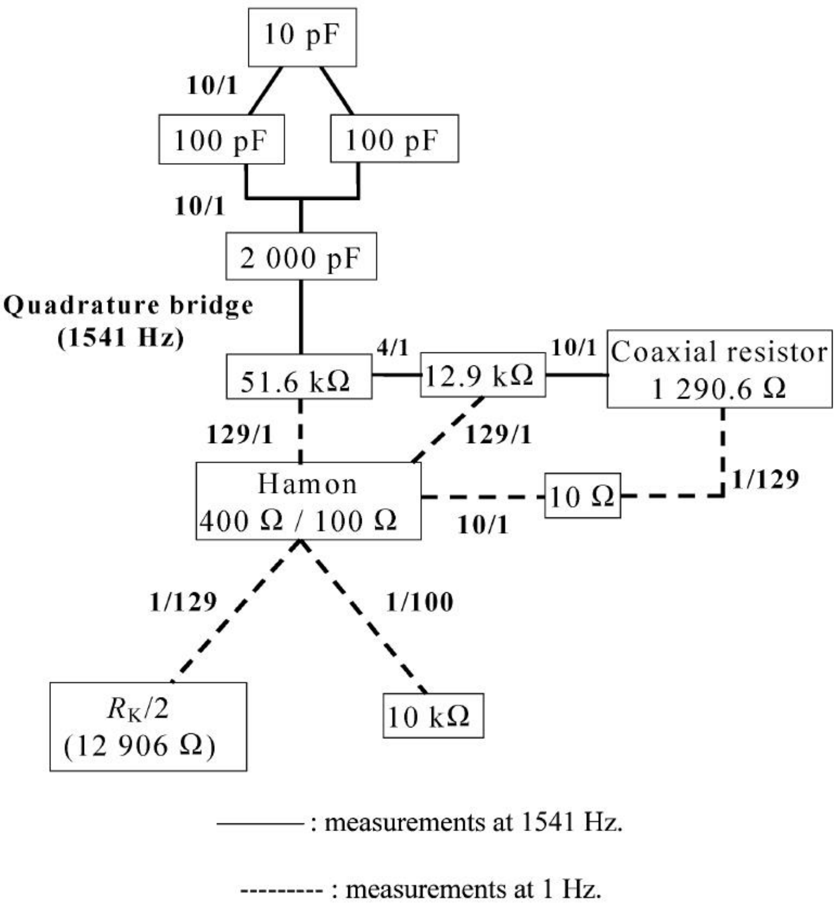

Figure 4.2.2: The impedance chain realised at the BIPM.

4.2.3 The measuring chain at LNE

At LNE, the value of a capacitor is traced to $R_{\text{K-90}}$ by means of the dc quantum Hall effect as shown in Figure 4.2.3. At first, three pairs of thermostated and sealed Vishay type resistances (at nominal values of 10 kΩ, 20 kΩ, and 40 kΩ) are compared to the dc quantum Hall resistance. After correction of their frequency dependences determined from a comparison with a coaxial calculable resistor, each pair of resistances is compared by means of a quadrature bridge to two 10 nF capacitors (home-made invar plates in vacuum) linking the farad to $R_{\text{K-90}}$ and the second. The quadrature bridge is a four-terminal-pair bridge derived from the classical models described in [5,6]. These measurements are carried out at three frequencies corresponding to ω=2500 rad/s, ω=5000 rad/s and ω=10000 rad/s.

Next, a four-terminal-pair 10:1 ratio bridge is used successively to link the two 10 nF standards to a 1 nF transfer standard and a 100 pF capacitance standard. The 1 nF transfer standard is a nitrogen sealed General Radio capacitor placed in an oil bath. Then, a two-terminal-pair 10:1 ratio bridge is used to link the 100 pF capacitor to a 10 pF capacitor. This bridge is also used to compare a 10 pF capacitor to a 1 pF capacitor. The 10:1 ratio can be easily rearranged to obtain a 8:3 ratio. Thus, it is also used to compare the 1 pF capacitor against the capacitance variation generated by the LNE Thompson-Lampard calculable capacitor.

The main components of these two capacitance bridges are two-staged transformers, with 11 equal sections wound on high-permeability cores. The transformers are kept unloaded by using a Wagner arm and compensating circuits. Their ratios are calibrated for each frequency value by the bootstrap method.

All equipment necessary to perform the successive measurements is located in two adja-

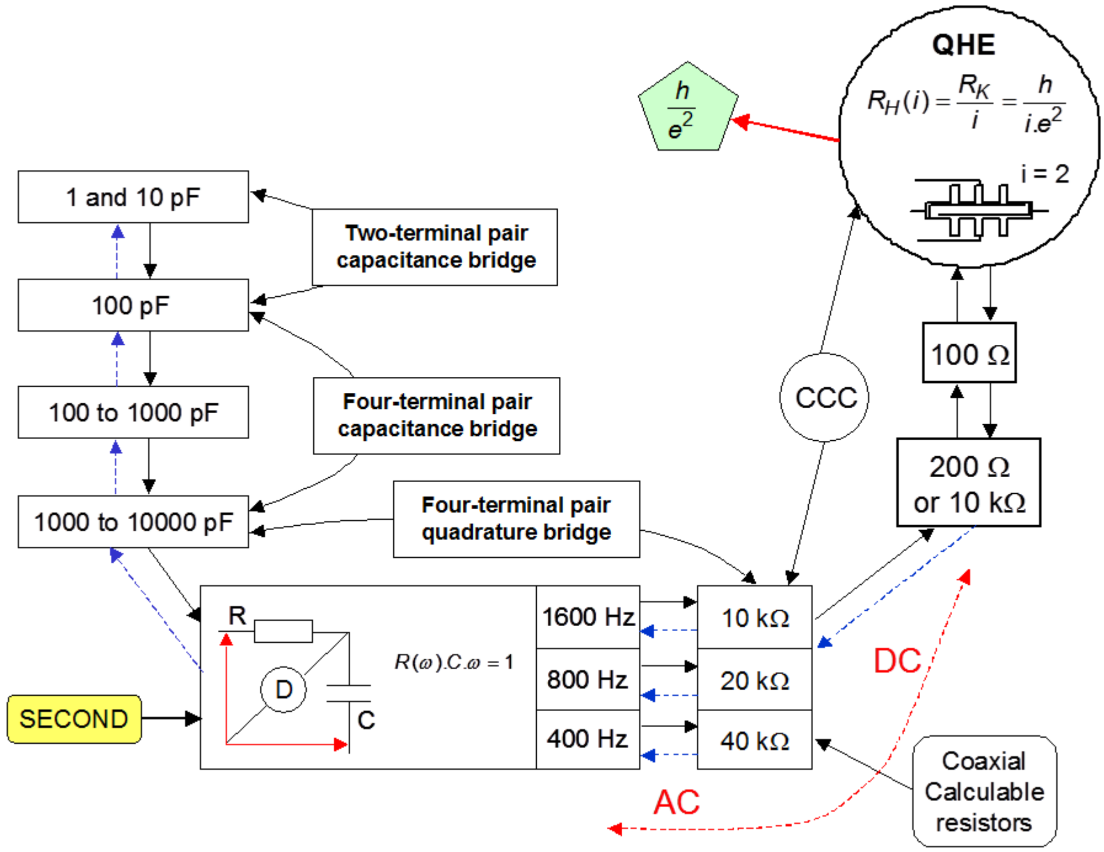

Figure 4.2.3: The impedance chain realised at LNE.

cent rooms. The first one is devoted to the AC measurements and the second one to the DC quantum Hall effect measurements. A 6 meter long cable (two shielded twisted pairs) getting through the corridor separating the two rooms is used to compare the quadrature bridge resistances to the quantum Hall resistance. This configuration allows all the measurements to be carried out without moving any transfer standard.

4.2.4 The measuring chain at METAS

The measuring chain realised at METAS is shown in Figure 4.2.4. The starting point is a 100 Ω secondary resistance standard that is regularly compared to the quantum Hall resistance at dc in terms of R_{K-90}. The dc values of two calculable quadrifilar resistance standards are then calibrated by a direct comparison to the 100 Ω secondary resistance standard using a direct cryogenic current comparator (CCC). The values of the quadrifilar resistance standards at 1233 Hz are then calculated using their known frequency dependence. The frequency dependence between dc and 1233 Hz of the calculable resistances has been assessed by an intercomparison [7] and by a direct comparison to the ac quantum Hall effect [8].

A quadrature bridge is then used to compare two 10 nF capacitance standards to the two quadrifilar resistance standards. It is a manual four-terminal-pair ratio bridge.

Then, the 10 nF capacitance standards are compared to a 1 nF capacitance standard using a four-terminal-pair 10:1 ratio bridge. The 1 nF capacitance standard is compared to a 100 pF capacitance standard using the same four-terminal-pair bridge. Finally, the 100 pF capacitance standard is compared to the 10 pF capacitance standard using a three-terminal-pair ratio bridge. These two ratio bridges are computer controlled and the balance procedure is automated making the repetition of the measurements easier.

The 10:1 transformer is calibrated by direct comparison to a reference IVD which has been calibrated using the so-called "boot-strap" method [17].

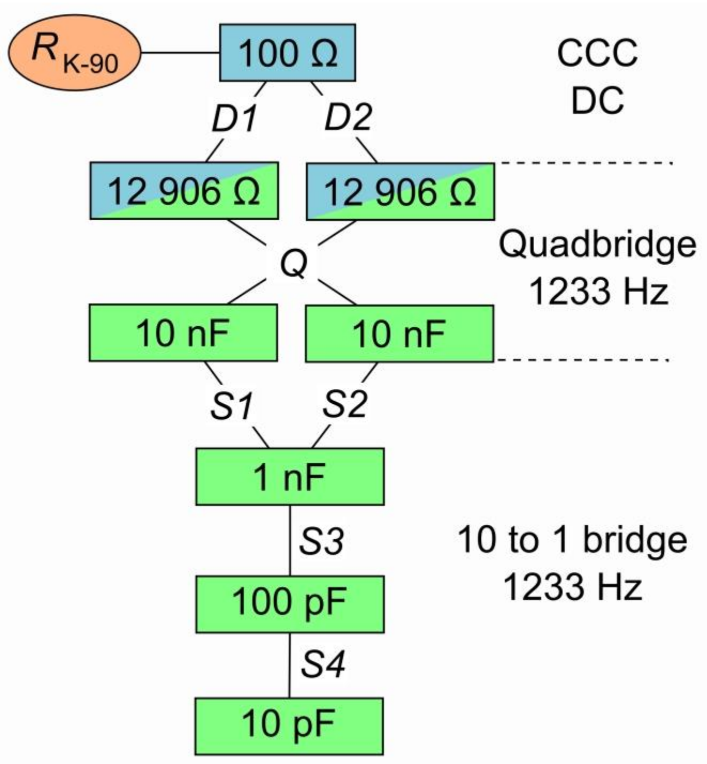

Figure 4.2.4: The impedance chain realised at METAS.

4.2.5 The measuring chain at NMIA

The NMIA derives its capacitance unit from a Thompson-Lampard calculable capacitor [9-12] traceable to the SI via NMIA's length standard (see Figure 4.2.5.1). The two-terminal pair transformer substitution bridge used to compare the calculable capacitor with fixed reference capacitors in a 1:1 ratio is shown in Figure 4.2.5.2. The calculable capacitor is in the top arm of the bridge and stable, fixed capacitors of equivalent value (1/6 pF) in the lower arm of the bridge. Capacitance and conductance balances are provided via additional windings on the main bridge transformer.

Initially, the cross-capacitance between bars 1 and 3 of the calculable capacitor, with the guard bar in the upper position, is compared with a ballast capacitance (refer to Figure 4.2.5.2 (a)). The guard bar is then lowered, and the 1/6 pF reference capacitor to be measured is connected in parallel with the calculable capacitor. The bridge is rebalanced to compare this parallel connection with the ballast capacitance (refer to Figure 4.2.5.2 (b)). These measurements are then repeated with bars 2 and 4 of the calculable capacitor.

The same transformer substitution bridge is also used to compare the 1/6 pF reference capacitor with two further 1/6 pF reference capacitors, see Figure 4.2.5.2 (c). The three 1/6 pF capacitors are then connected in parallel to constitute a reference of known value, nominally 0.5 pF (see Figure 4.2.5.1).

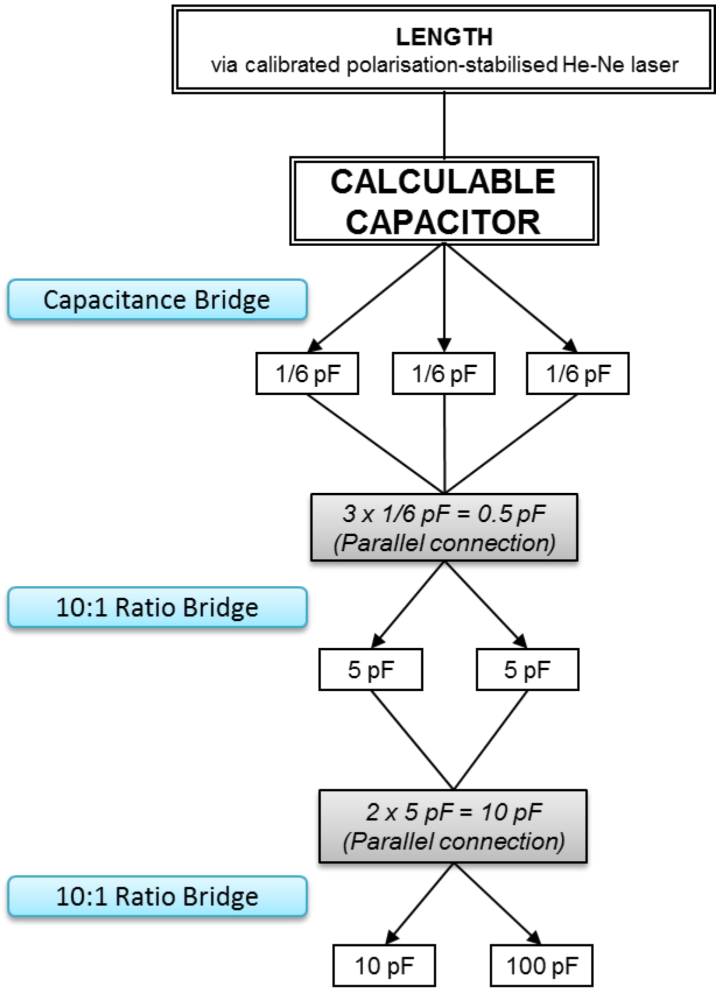

Figure 4.2.5.1: The impedance chain realised at NMIA.

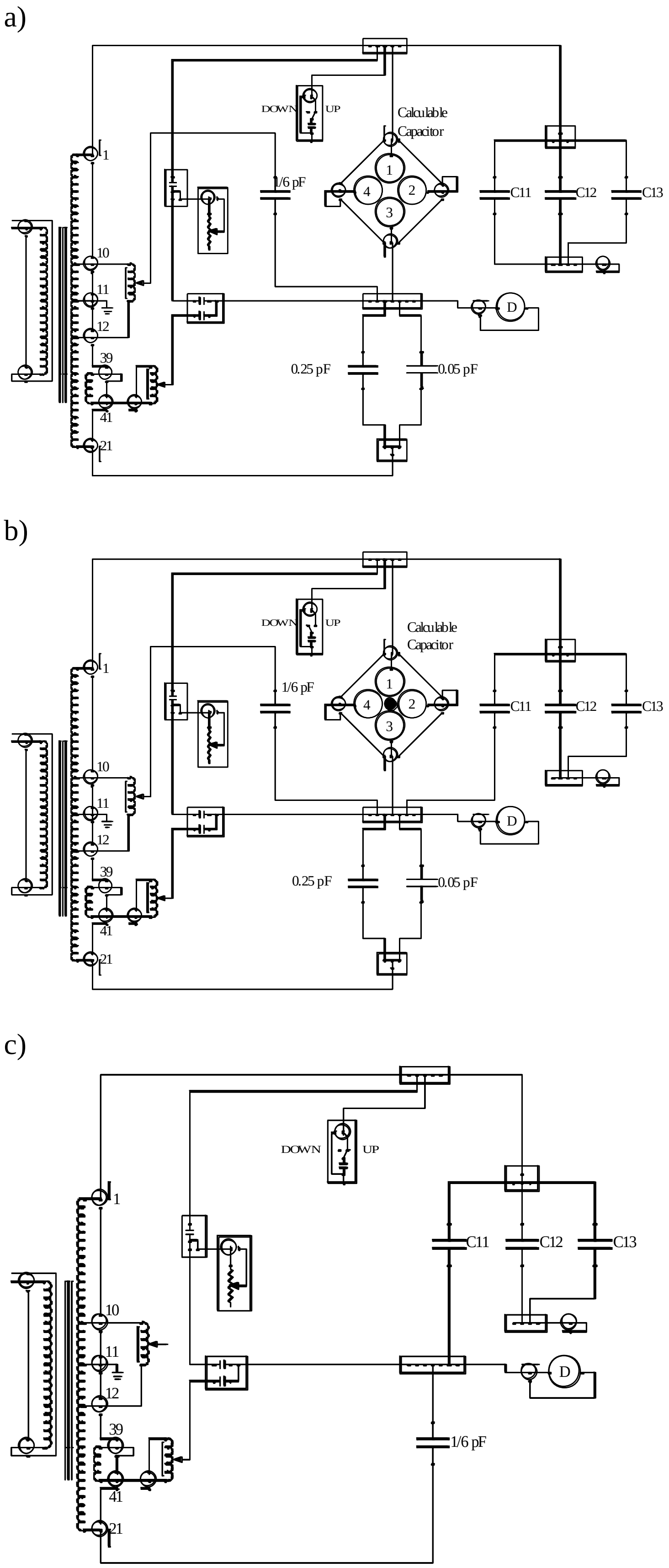

Figure 4.2.5.2: Capacitance bridge to compare calculable capacitor to 1/6 pF reference capacitor, C11: calculable capacitor guard bar in (a) upper position and (b) lower position. (c) Capacitance bridge reconfigured to measure two further 1/6 pF reference capacitors, C12 and C13, with respect to C11.

This 0.5 pF reference capacitor is used to measure two 5 pF reference capacitors using a two-terminal pair 10:1 transformer ratio bridge and the direct comparison method. The 10:1 ratio bridge is based on a three-winding voltage transformer (see Annex 9.5). The two 5 pF reference capacitors are then connected in parallel to constitute a reference of known value, nominally 10 pF (see Figure 4.2.5.1).

The comparison artefacts were measured relative to the 10 pF reference using the same 10:1 transformer ratio bridge and either the substitution method (for the 10 pF comparison artefacts) or the direct comparison method (for the 100 pF comparison artefact).

Measurements of each comparison artefact were made using the following procedure:

1. Each of the four comparison artefacts were measured in turn relative to the parallel combination of the two 5 pF reference capacitors.
2. Measurements were made from the calculable capacitor to determine the value of the two 5 pF reference capacitors.
3. Measurements of the comparison artefacts (step 1 above) were repeated.
4. Based on the measurements in steps 1 to 3 above, a value for the capacitance of each comparison artefact was calculated.

Each measurement was performed within one day. A total of six measurements of the capacitance of each comparison artefact were made at each measurement frequency.

4.2.6 The measuring chain at VSL

The capacitance unit at VSL is derived from resistance standards which in turn are traced to the dc quantum Hall resistance, as shown in Figure 4.2.6. The QHR is run a few times per year. In between these runs, the unit of resistance is maintained by a set of three ESI SR104 10 kΩ resistors and one ESI SR102 100 Ω resistor. This is accomplished by a cryogenic current comparator (CCC) bridge [13] via the 100 Ω transfer standard or directly by means of a potentiometric comparison bridge [14].

The potentiometric bridge is also used to compare three ac-dc resistors with nominal values of 12.906 kΩ (manufactured by Normal Lloyd (NL) Engineering) against the 10 kΩ reference resistors. In two of our standards, the wire is folded 4 times; the so-called quadrifilar resistor. And in one standard, the wire is folded 8 times; the so-called octofilar resistor. To limit the effect of environmental temperature on the dc resistance value, the ac-dc resistors are contained in thermostatic controlled enclosures. The behaviour of these types of resistors has been studied and described in the literature [15,16].

The impedance of the ac-dc resistors is compared with the impedance of two 10 nF capacitors in a four-terminal-pair quadrature bridge operating at a frequency of 1233 Hz. The 10 nF capacitors are ceramic dielectric capacitors, manufactured by NPL (UK), type C03. The frequency of the sinusoidal signals in the impedance bridges is traceable to the VSL time and frequency standard which generates the UTC (VSL) timescale.

Finally, a four-terminal-pair 10:1 ratio bridge is used to successively step down from 10 nF to lower values of capacitance like the 100 pF and 10 pF of the travelling standards. The 10:1 transformer is calibrated by the method of permuting capacitors.

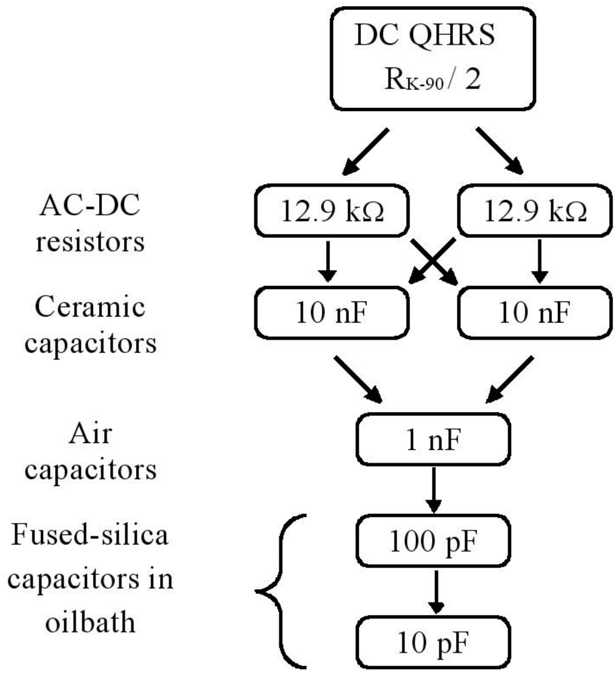

Figure 4.2.6: The impedance chain realised at VSL.

4.3 Definitions

The value of the travelling 100 pF capacitance standard (serial number #1256) and the values of three travelling 10 pF standards with serial number X (X being either #1257, #1258, or #1310) measured by a participant N are written here according to

$$C(100\ \mathrm{pF}, \mathrm{N}) = 100\ \mathrm{pF} \cdot \left(1 + d^{\mathrm{N}}{}_{100\ \mathrm{pF}}\right)$$

$$C(10\ \mathrm{pF}, \mathrm{X}, \mathrm{N}) = 10\ \mathrm{pF} \cdot \left(1 + d^{\mathrm{N}}{}_{10\ \mathrm{pF,X}}\right)$$

with $d^{\mathrm{N}}{}_{100\ \mathrm{pF}}$ and $d^{\mathrm{N}}{}_{10\ \mathrm{pF,X}}$ the relative deviations from nominal, quoted either in parts in 10^6 or in parts in 10^9.

The comparison reference value (CRV) of each travelling standards is written here as

$$d^{\mathrm{CRV}}{}_{100\ \mathrm{pF}}(t) = d^{\mathrm{PTB}}{}_{100\ \mathrm{pF}}(t) + \Delta_{100\ \mathrm{pF}}$$

$$d^{\mathrm{CRV}}{}_{10\ \mathrm{pF,X}}(t) = d^{\mathrm{PTB}}{}_{10\ \mathrm{pF,X}}(t) + \Delta_{10\ \mathrm{pF,X}}$$

with $d^{\mathrm{PTB}}{}_{100\ \mathrm{pF}}(t)$ and $d^{\mathrm{PTB}}{}_{10\ \mathrm{pF,X}}(t)$ the time-dependent relative deviations from nominal as measured by PTB. $\Delta_{100\ \mathrm{pF}}$ and $\Delta_{10\ \mathrm{pF,X}}$ are time-independent parameters to be determined from a weighted least-squares fit optimisation process to determine the best estimate of this deviation, as described in Section 4.7.

4.4 Effect of transportation

To investigate the effect of transportation of the thermostated AH standards on the capacitance values, the pilot measured the AH travelling standards at one occasion beginning already half a day after the end of a thermostated transportation. As shown in Fig. 4.4.1, only one of the AH standards shows a clear effect due to the transportation whereas the three other standards show only a tiny effect (if significant at all).

To allow differentiation between thermal and mechanical effects, the behaviour of the travelling standards was measured after switching off the thermostat for about 8 hours (corresponding to a typical travel time, but without a transport). Switching off the thermostat causes a relative change of the capacitance values by about $-450\cdot10^{-6}$ (because the fused-silica elements cool down from about 55°C to 23°C), but after switching the thermostat on again, the capacitance values come back to the initial values with a remarkably small hysteresis (Fig. 4.4.2): Whereas one AH standards shows a small transient effect of $5\cdot10^{-8}$ at maximum, the other ones exhibit only a tiny effect of less than $1\cdot10^{-8}$ (if significant at all).

In any case, the effect of a temporarily switched off thermostat and the effect of a thermostated transportation are quite small and the standards fully relax within about one week.

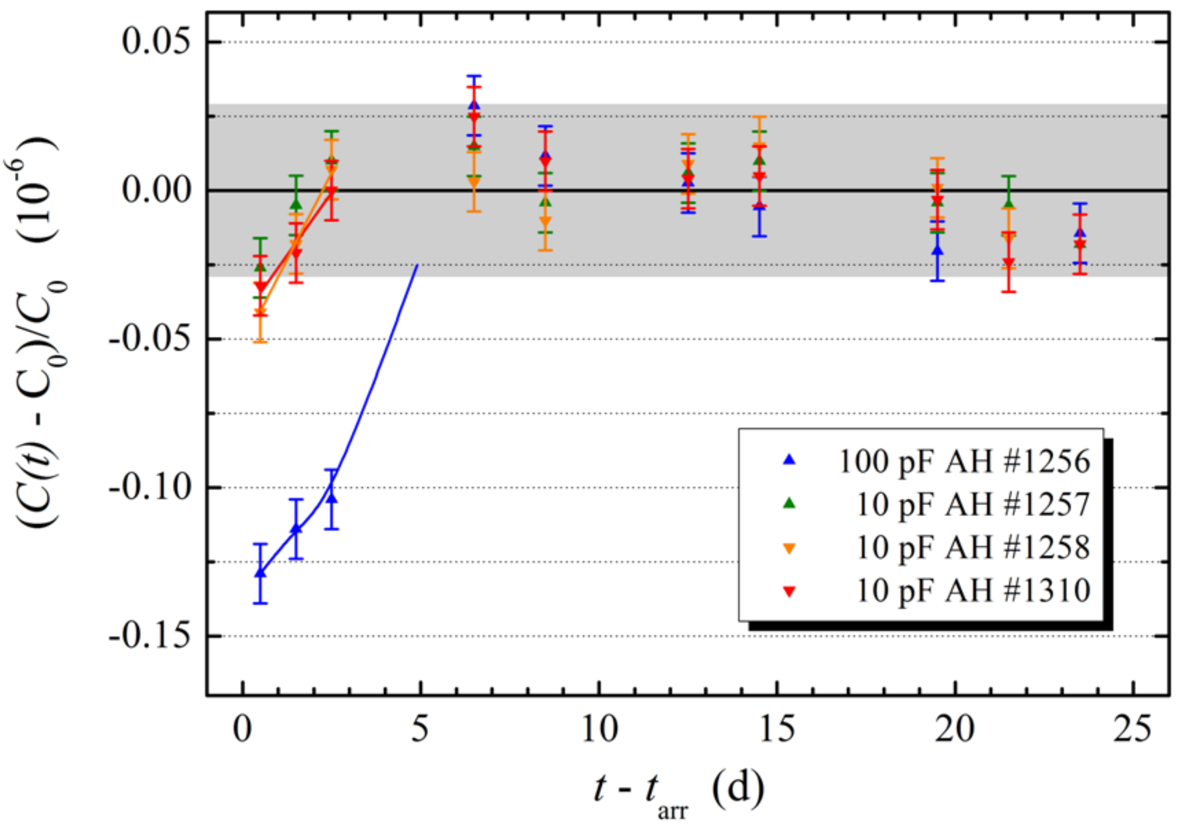

Figure 4.4.1: The capacitance values of the travelling standards measured at PTB after a transportation from the BIPM to PTB, with respect to an arbitrary reference value C_0. t_{arr} is the time of arrival at PTB. The grey band indicates the standard deviation of the measurements by the pilot laboratory at this early time of the first circulation loop.

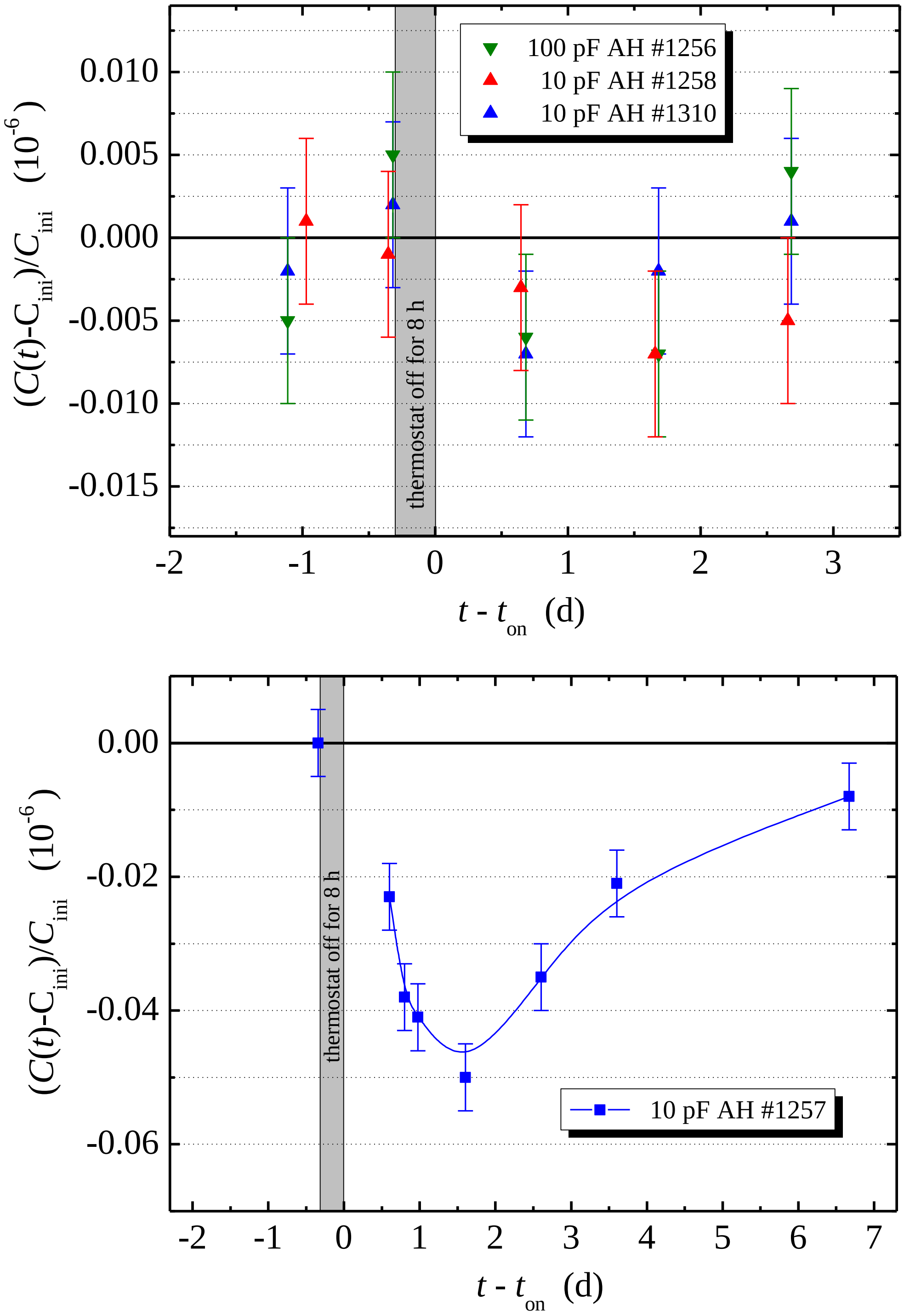

Figure 4.4.2: Drift behaviour of the AH standards measured at PTB. The thermostats were temporarily switched-off for 8 hours and switched on again at the time t_{on}. C_{ini} is the (mean) capacitance value before the switch-off. For better visibility, the data in the lower diagram are connected by splines.

At the second capacitance circulation, the travelling standards were also sent to NMIA, and for this purpose, unthermostated airfreight transportations were practically unavoidable. The BIPM measured the travelling standards before and after the NMIA period. In contrast to the previous findings, unthermostated transportations gave rise to long-lasting relaxation effects and to persistent changes of the capacitance values. The behaviour of the travelling standards showing the largest and the smallest effect are shown in Fig. 4.4.3. The intermediate behaviour of the other two travelling standards can be found in Annex 11.2. The magnitudes of the jumps are given in Table 4.4.

Obviously, the effect of an unthermostated transportation is not equal to the superposition of the effects of a temporarily switched-off thermostat and a thermostated transportation, presumably because the capacitance standards do not constitute a sufficiently linear system. (For example, when a capacitance standard is not transported and the temperature controller is switched off, the resulting mechanical stress vanishes after the controller is turned on again. But if the mechanical stress caused by a switched-off controller partially relaxes due to mechanical vibration and shock during an airfreight transportation, the later switching-on of the controller causes mechanical stress which has to relax subsequently.)

Remarkably, the magnitude of the jumps and relaxation effects is found to be clearly correlated with the ambient temperature coefficient of the particular standard (Table 4.4; see also Annex 12.1). This seems to indicate that the jumps and relaxation effects do not directly originate from the fused-silica element itself, but from the temperature controller. This finding is also discussed in Section 4.9.1.1.

To conclude: At some of the transportations of the first capacitance circulation loop, the power supply has failed, but the mechanical shocks during a careful car trip are much smaller than during airfreight. Further, the timeout of the power supply of about 8 hours was much shorter than the 22 days and 13 days in the case of the transportations to and back from NMIA, respectively (including customs clearance). There is no indication that the first capacitance circulation might be significantly affected by jumps or long-lasting relaxation effects, even though the procedure was not optimum. At the second capacitance circulation, the improved power supply worked without failure, but it was not used at the transportations to and back from NMIA.

Table 4.4: The difference of the travelling capacitance standards measured by the BIPM before and after the NMIA period and the ambient temperature coefficient of the travelling standards. The quoted uncertainties are only the statistical uncertainties.

Standard	difference of the two BIPM series (10^{-9})	ambient temperature coefficient [10^{-9}/°C]
100 pF AH #1256	50 ± 14	-12.3 ± 2.0
10 pF AH #1257	145 ± 14	-18.1 ± 2.0
10 pF AH #1258	91 ± 14	-11.4 ± 2.0
10 pF AH #1310	-4 ± 14	-7.1 ± 2.0

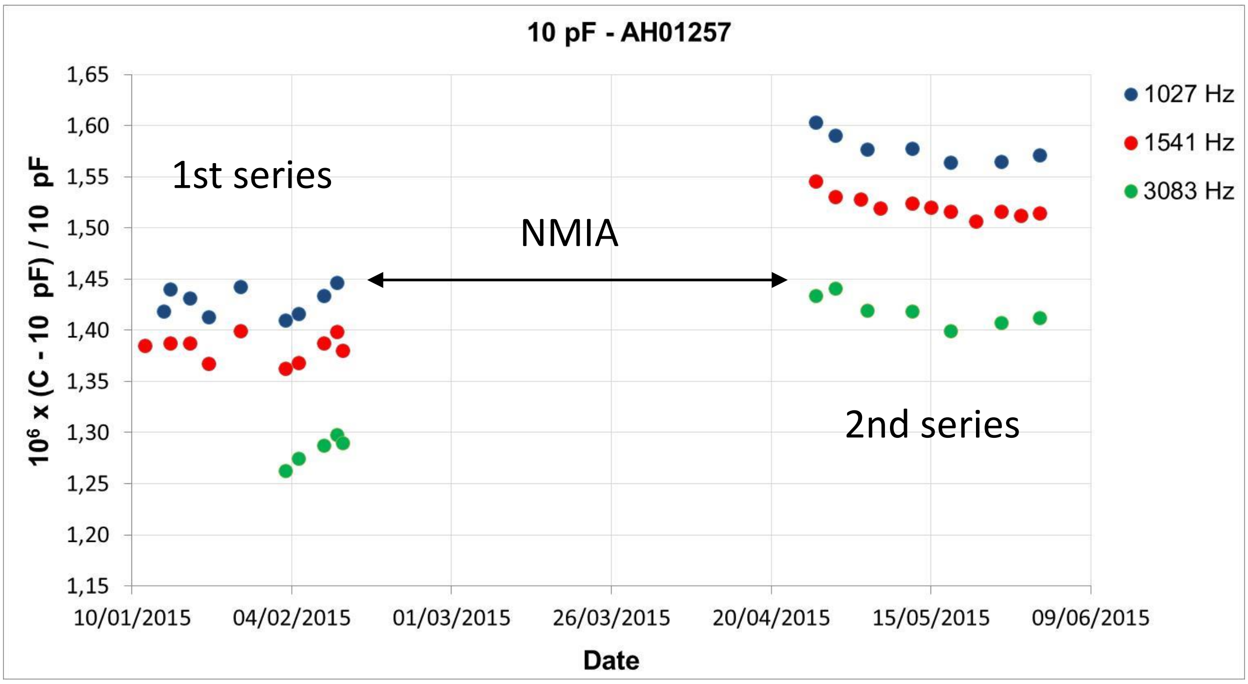

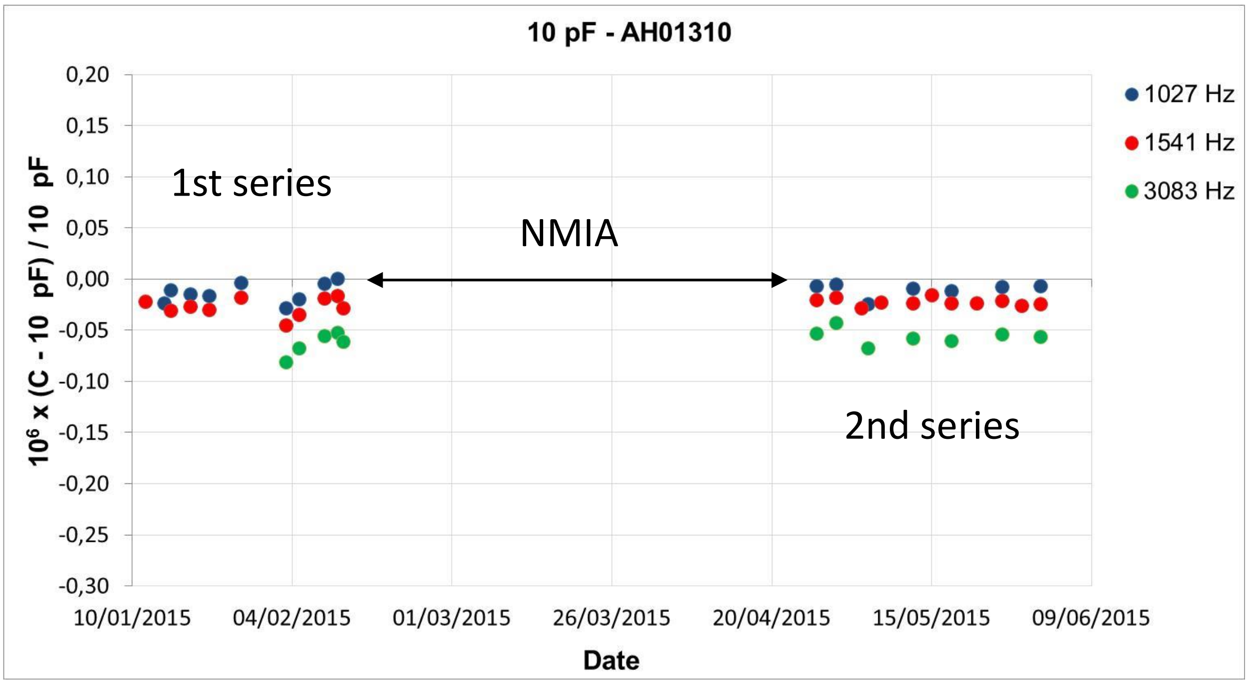

Figure 4.4.3: Drift behaviour of two AH standards measured by the BIPM before and after the NMIA period, at different frequencies as indicated.

4.5 Corrections submitted by the participants

As already mentioned, the original results of the first capacitance circulation revealed significant discrepancies. While the participants carried out an ac resistance comparison to test the frequency dependence of the ac resistance standards involved in their capacitance chains (as described in Section 3), they had time to check their measuring bridges for systematic errors. In fact, PTB, LNE and the BIPM discovered systematic errors and submitted corrections *after* the distribution of the initial results among the participants. They are listed in the top part of Table 4.5. The corrections submitted were determined experimentally either by a re-calibration of the affected component or a measurement of the change between the imperfect initial state and an improved state. We would like to point out that these corrections, even though revealed by the comparison, were determined *independent* of the discrepancy between the participants and were submitted *before* the second capacitance circulation started.

At the second capacitance circulation, only LNE has submitted a correction *after* the distribution of the initial results, as given in the bottom part of Table 4.5.

Table 4.5: Corrections of the capacitance values as supplied by the participants for the first capacitance circulation (light grey) and for the second capacitance circulation (light blue).

<table>
<tr><th>Participant</th><th>Origin of error</th><th>Frequency (Hz)</th><th>Correction relative to nominal (k = 1) (10^{-6})</th></tr>
<tr><td rowspan="2">PTB</td><td>Underestimated lead effect of the acQHR in the quadrature bridge and underestimated lead effect of the 10:1 calibration
(Later, a correction was determined as the difference of results obtained in the initial configuration and a strongly improved configuration.)</td><td>1233
1233</td><td>-0.117 at 100 pF
-0.143 at 10 pF</td></tr>
<tr><td>Faulty cable configuration which could not be identified in retrospect</td><td>2466</td><td>withdrawn</td></tr>
<tr><td>BIPM</td><td>Underestimated long-term drift of the frequency dependence of the reference capacitor
(Later, a correction was determined by a re-calibration of the frequency dependence of the reference capacitor.)</td><td>1000</td><td>-0.06 at both 100 pF and 10 pF</td></tr>
<tr><td>LNE</td><td>Underestimated change of transformer ratio
(Fixed by a later re-calibration of the transformer ratio.)</td><td>397.9
795.8
1591.6</td><td>-0.023
+0.020
+0.066</td></tr>
<tr><td>LNE</td><td>Overlooked magnetisation of the injection system affecting the injection phase angle
(Fixed by a later re-calibration.)</td><td>397.9
795.8
1591.6</td><td>-0.09 ± 0.04
-0.05 ± 0.02
+0.12 ± 0.02</td></tr>
</table>

4.6 Drift behaviour at the pilot laboratory

Figure 4.6.1 and Figure 4.6.2 show the individual capacitance values of the four travelling standards as measured at the pilot laboratory at the reference frequency of 1233 Hz, together with the mean value for each measuring period. The long-term behaviour is non-linear in time and the available data are just random spot samples of a more complex, incompletely known time dependence. This time dependence can be modelled in different ways. One possibility is a subdivision into intervals in which the time dependence can be reasonably described by either a linear or a polynomial least-squares fit. The disadvantage is that this procedure is somewhat arbitrary and that the slope changes abruptly at the interval boundaries, which is unphysical. However, the interval boundaries are by chance not within the relevant circulation periods. Another possibility is to interconnect the mean values with a spline function. This function is smooth and, even though not all apparent structures might be real, within the two circulation periods it agrees quite well with the composite least-squares fits. Therefore, the spline function has been chosen to define the time dependence of the CRV. Since any model can yield only an approximation, an additional uncertainty contribution has been taken into account. Furthermore, as will be shown later, the method to eliminating the effect of an unthermostated transportation of the capacitance standards is quite robust and yields practically the same results even for other, much less appropriate model functions.

During the first measurement periods at the pilot laboratory, an unexpected scattering of the results became apparent (see Figure 4.6.1 and Figure 4.6.2 or Figure 4.4.1). This scattering has been identified as an underestimated instability of the phase-shifter of PTB's 10:1 ratio bridge. Since this was improved, the standard deviation of 10 pF or 100 pF measurements is reduced to values as low as $6{\cdot}10^{-9}$ (in accordance with the measurement uncertainty given in Annex 10.1). However, the first measurement periods at the pilot laboratory were already affected and a corresponding uncertainty contribution is taken into account.

In the following, some findings are listed which obviously indicate instabilities of the capacitance standards: (i) During a few weeks, the four capacitance standards show a sometimes similar and a sometimes different time pattern with a standard deviation of up to $15{\cdot}10^{-9}$ which is larger than the measurement uncertainty of $6{\cdot}10^{-9}$. An example is shown in the insert of Figure 4.6.1. (ii) The standard deviation of a 10 pF standard can be significantly smaller than for the 100 pF standard measured in the chain prior to this. (iii) Also the 100 pF:10 pF ratios show a variation which is up to 10 times larger than the measurement uncertainty of $2.4{\cdot}10^{-9}$ (as given in Annex 10.1). All these observations cannot be attributed to hypothetical fluctuations originating from the measuring bridges. Obviously, the AH capacitance standards really feature a slow variation on a time scale of a few days, presumably due to instabilities of the internal temperature. Therefore, each measurement period lasted about four weeks to obtain a reasonably accurate mean value. In addition, four travelling standards were circulated so that these fluctuations practically average out in the final degrees of equivalence.

As can be seen in Figure 4.6.1 and Figure 4.6.2, the capacitance standards also show instabilities on a longer time scale. (i) The drift rate changed in the interval between the two circulation periods where the standards were neither moved nor have suffered a power blackout or any mechanical shock. (ii) The short-term drift rates of each four-week measuring interval do not conform to the corresponding slope of the spline function (see the example in the insert of the top part of Figure 4.6.1). The maximum deviation from a linear long-term drift is found to be the larger, the larger the ambient temperature coefficient of the particular standard is (see Annex 12.1). This seems to indicate that both the short- and long-term variations of the AH capacitance standards are due to a variation of the internal temperature. In Annex 13, the properties of the capacitance standards obtained at this comparison are compared to the specifications of the manufacturer. Even though the behaviour of the capacitance standards when carefully handled and transported is excellent, it partially exceeds the specifications.

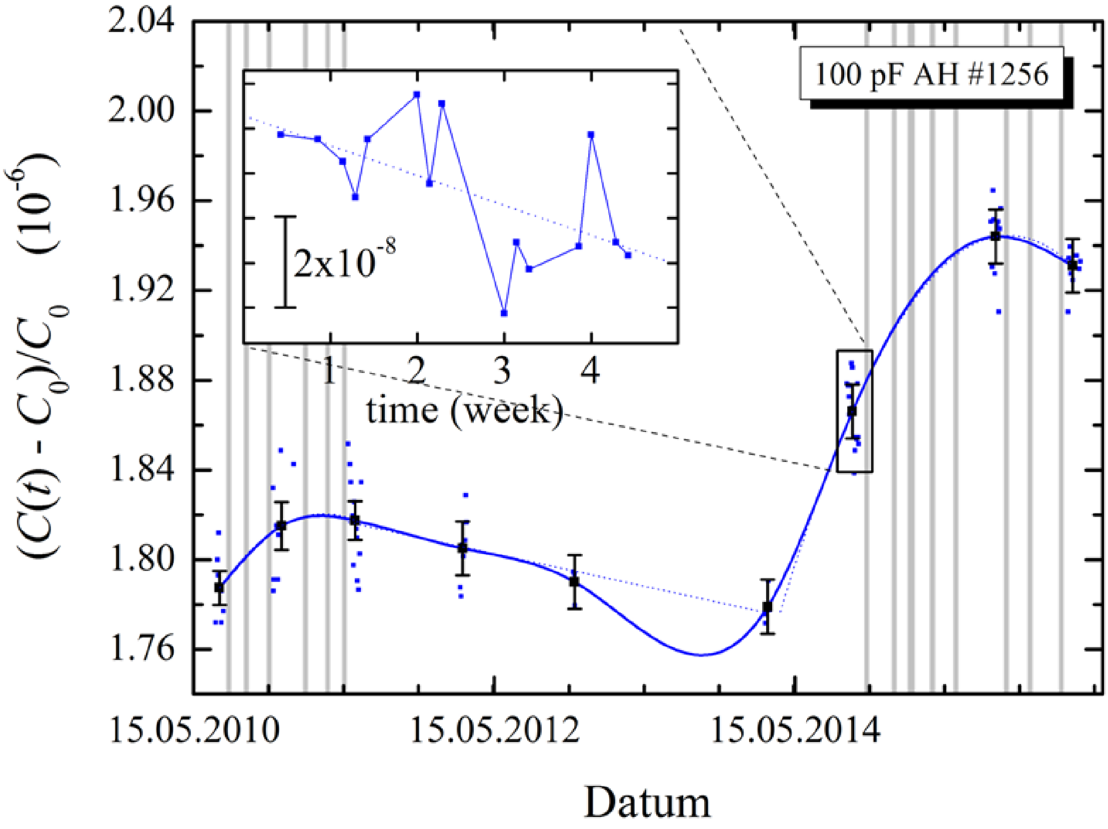

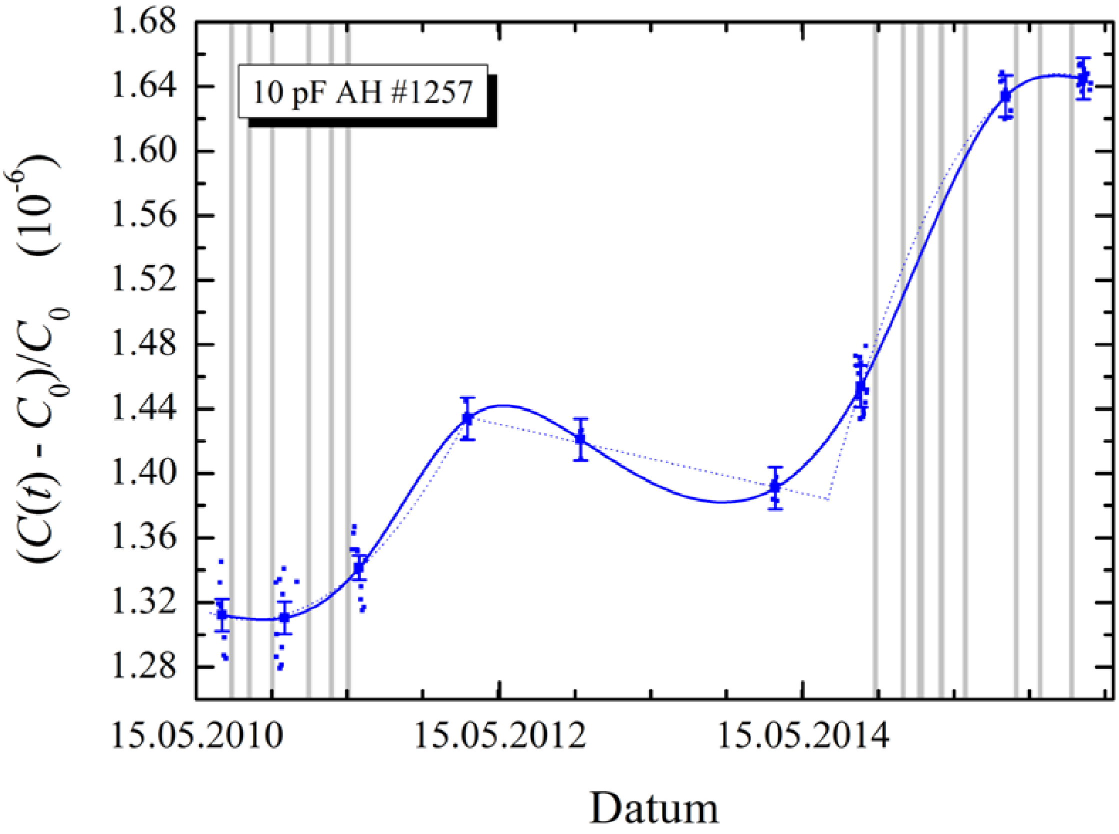

Figure 4.6.1: The capacitance of the travelling standards 100 pF AH #1256 (top) and 10 pF AH #1257 (bottom) measured by the pilot laboratory at the reference frequency of 1233 Hz as a function of time. C_0 is the particular nominal value. The uncertainty bars correspond to coverage factor k = 1. The transportations and allocated relaxation intervals are indicated in light grey. The insert in the top diagram shows the individual results of one measurement period at a higher resolution.

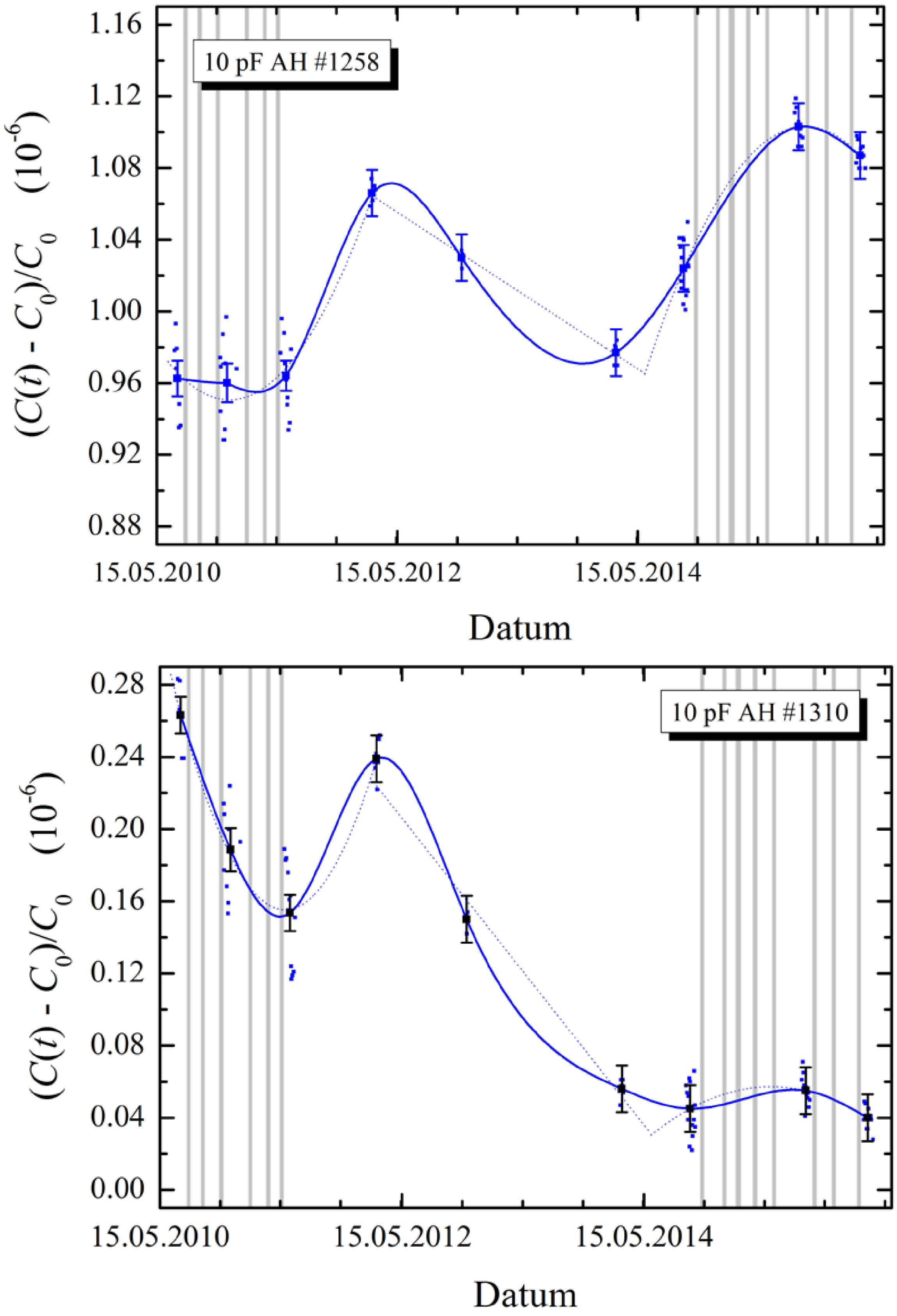

Figure 4.6.2: The capacitance of the travelling standards 10 pF AH #1258 (top) and 10 pF AH #1310 (bottom) measured by the pilot laboratory at the reference frequency of 1233 Hz as a function of time. C_0 is the particular nominal value. The uncertainty bars correspond to coverage factor k = 1. The transportations and allocated relaxation intervals are indicated in light grey.

4.7 Method of computing the reference value

The comparison reference value (CRV) is evaluated following the principles laid down in [1] and [2]. The proposed principles of the analysis are:

- The results of the two capacitance circulation loops are analysed separately.
- The results of the travelling 100 pF capacitance standard (serial number #1256) and the results of the three travelling 10 pF capacitance standards with serial number X (X being either #1257, #1258, or #1310) measured by a participant N are expressed as the relative deviations from nominal, $d^{\mathrm{N}}{}_{100\ \mathrm{pF}}$ and $d^{\mathrm{N}}{}_{10\ \mathrm{pF,X}}$, defined here according to

$$C(100\ \mathrm{pF}, \mathrm{N}) = 100\ \mathrm{pF} \cdot \left(1 + d^{\mathrm{N}}_{100\ \mathrm{pF}}\right)$$
$$C(10\ \mathrm{pF}, \mathrm{X}, \mathrm{N}) = 10\ \mathrm{pF} \cdot \left(1 + d^{\mathrm{N}}_{10\ \mathrm{pF,X}}\right)$$

- All participants measured the capacitance values either at least at the frequency of 1233 Hz or at other frequencies in the range between 400 Hz and 3 kHz so that an interpolation to 1233 Hz is possible. Therefore, the frequency of 1233 Hz is chosen as the reference frequency. The frequency dependence of each capacitance standard relative to its value at the reference frequency is considered as a separately compared quantity.
- The time-dependent capacitance values measured by the pilot laboratory at the reference frequency of 1233 Hz define the time dependence of the CRV. The capacitance values of the pilot laboratory are traced to the ac quantum Hall resistance, as described in [4].
- For the calculation of the CRV of each travelling capacitance standard, the following procedure is used. The CRV of each travelling capacitance standard, $d^{\mathrm{CRV}}(t)$, is defined as the time-dependent deviation from the particular nominal value as measured by the pilot laboratory at the reference frequency of 1233 Hz, $d^{\mathrm{PTB}}(t)$, plus an *a priori* unknown deviation $\Delta_{100\ \mathrm{pF}}$ and $\Delta_{10\ \mathrm{pF,X}}$, respectively:

$$d^{\mathrm{CRV}}_{100\ \mathrm{pF}}(t) = d^{\mathrm{PTB}}_{100\ \mathrm{pF}}(t) + \Delta_{100\ \mathrm{pF}}$$

$$d^{\mathrm{CRV}}_{10\ \mathrm{pF,X}}(t) = d^{\mathrm{PTB}}_{10\ \mathrm{pF,X}}(t) + \Delta_{10\ \mathrm{pF,X}}$$

  The parameters $\Delta_{100\ \mathrm{pF}}$ and $\Delta_{10\ \mathrm{pF,X}}$ are assumed to be time-independent and are calculated as the best estimate by a χ^2 minimisation process based on all sufficiently equivalent results of the participants either measured at, or interpolated to, the reference frequency of 1233 Hz, weighted with the uncertainty of the particular participant. For the 100 pF standard, the result of $\Delta_{100\ \mathrm{pF}}$ is given by

$$\Delta_{100\ \mathrm{pF}} = \frac{\sum_{\mathrm{N}=1}^{\mathrm{M}} \left(\frac{d^{\mathrm{N}}_{100\ \mathrm{pF}}(t_{\mathrm{N}}) - d^{\mathrm{PTB}}_{100\ \mathrm{pF}}(t_{\mathrm{N}})}{u_{\mathrm{N}}{}^2} \right)}{\sum_{\mathrm{N}=1}^{\mathrm{M}} (1/u_{\mathrm{N}}{}^2)}$$

  with M the number of all contributing participants (including PTB as the pilot), t_{N} the mean time of measurement of participant N, $d^{\mathrm{PTB}}{}_{100\ \mathrm{pF}}(t_{\mathrm{N}})$ the PTB result interpolated to that time, and u_{N} the uncertainty of participant N. Note that the sum in the denominator also includes the PTB uncertainty whereas in the numerator the deviation of the PTB result from itself cancels. For the 10 pF standards, the values of $\Delta_{10\ \mathrm{pF,X}}$ are calculated correspondingly.

- The degree of equivalence of the capacitance measurements, DoE, is calculated as follows: The capacitance value of each participant N either measured at, or interpolated to, the reference frequency of 1233 Hz is expressed as the deviation from the CRV at the mean time of the participant's measurement, t_N, together with the expanded uncertainty of this deviation at the 95% level of confidence:

$$\mathrm{DoE^N}_{100\ \mathrm{pF}} = d^{\mathrm{N}}_{100\ \mathrm{pF}}(t_{\mathrm{N}}) - d^{\mathrm{CRV}}_{100\ \mathrm{pF}}(t_{\mathrm{N}}) \ \pm u^{\mathrm{N,CRV}}_{100\ \mathrm{pF}}(95\%)$$
$$\mathrm{DoE^N}_{10\ \mathrm{pF,X}} = d^{\mathrm{N}}_{10\ \mathrm{pF,X}}(t_{\mathrm{N}}) - d^{\mathrm{CRV}}_{10\ \mathrm{pF,X}}(t_{\mathrm{N}}) \ \pm u^{\mathrm{N,CRV}}_{10\ \mathrm{pF,X}}(95\%)$$

  The degree of equivalence includes not only the measurement uncertainties of the participant N and the pilot laboratory, but also an uncertainty contribution due to the incomplete knowledge of the true time-dependence of the travelling standards and their imperfect transport behaviour.

  The degree of equivalence of the results of a pair of participants can be expressed as the difference of their deviations from the CRV at the respective time, together with the uncertainty of this difference at the 95% level of confidence.

- In the case of the optionally measured frequency coefficients of the travelling capacitance standards, which as far as known do not change with time and are also not affected by transportation, the weighted mean value of all sufficiently equivalent individual results is taken as the CRV of the frequency coefficient. The degree of equivalence of a participant's value of the frequency coefficient is the deviation from the CRV of the frequency coefficient, together with the uncertainty of this deviation at the 95% level of confidence.

- LNE and NMIA ran their laboratory at a temperature of 20°C which deviates from the nominal 23°C. Because they both have neither placed the AH frame into a temperature cabinet at the specified temperature nor have they measured a temperature correction, the pilot measured the effect of the ambient temperature on the travelling capacitance standards. For this purpose, the capacitance standards were placed in a temperature cabinet and the capacitance values were monitored while the temperature was varied (see Section 12.1). Then, the pilot corrected the LNE and NMIA results for the deviating temperature and added an appropriate uncertainty.

- The NMIA results are measured in the SI whereas the results of all other participants refer to the conventional (non-SI) value $R_{\mathrm{K}\text{-}90}$. To allow a comparison and for the sake of simplicity, the NMIA results are converted to farad-90. The actual SI value of R_K as recommended by the CODATA commission in 2014 is

  $R_\mathrm{K} \equiv h/e^2 = 25812.8074555\ (59)\ \Omega$ whereas
  $R_{\mathrm{K}\text{-}90} \equiv 25812.807\ \Omega$.

  Because the SI value of R_K is larger than the conventional value $R_{\mathrm{K}\text{-}90}$, it follows from the quadrature bridge equation $\omega RC = 1$ that the SI capacitance value is smaller than its farad-90 value. To convert the SI capacitance values of NMIA to farad-90, the pilot thus has added a relative correction of $(+17.6 \pm 0.2)\cdot 10^{-9}$. To determine an R_K value, it is necessary to convert all capacitance results to the SI.

- If a participant could not comply with the requested voltage level, he was allowed to carry out his measurements at a different voltage level. The corresponding effect on the results is very small (if significant at all) and could be determined by the particular participant himself, otherwise the pilot laboratory had to assign a correction according to the weighted mean voltage coefficient determined in this comparison and to add a reasonable uncertainty contribution. This case applies only to LNE (see Section 4.1.3).

4.8 Results of the first capacitance circulation

4.8.1 Capacitance values at the reference frequency

In this section, the capacitance values at the reference frequency of 1233 Hz are discussed, including the corrections discussed in Section 4.5 and Section 4.7. A graphical representation is given in Figure 4.8.1 and Figure 4.8.2. For the sake of completeness, also the initial results (without the corrections submitted by the participants, as given in Section 4.5) are shown (but not included in the following analysis). The results of the pilot laboratory were already discussed in Section 4.6 (Figure 4.6.1 and Figure 4.6.2); the assigned uncertainty covers not only the calculated measurement uncertainty, but also includes the uncertainty of the submitted corrections and an uncertainty contribution due to the permanent instability of the travelling standards. The results of all participants agree within the expanded uncertainties, apart from METAS whose results are a bit off. The CRV is calculated by a weighted least-squares fit optimisation process (as described in Section 4.7) and includes the results (and uncertainties) of all participants (including METAS).

Numerical differences between the results of the participants and the pilot laboratory are given in Table 4.8.1. Numerical differences between the results of the participants and the CRV are given in Table 4.8.2. As follows from this table, all results are fully equivalent, apart from METAS whose uncertainty seems to be somewhat underestimated. However, it is also true that the results of PTB, LNE, and the BIPM became equivalent because they applied corrections to their results and correspondingly increased their uncertainties. On the other hand, the equivalence also indicates that the corrections applied are reliable. It is also worth mentioning that the standard deviation of the three 10 pF differences of each participant is well within the quoted uncertainty.

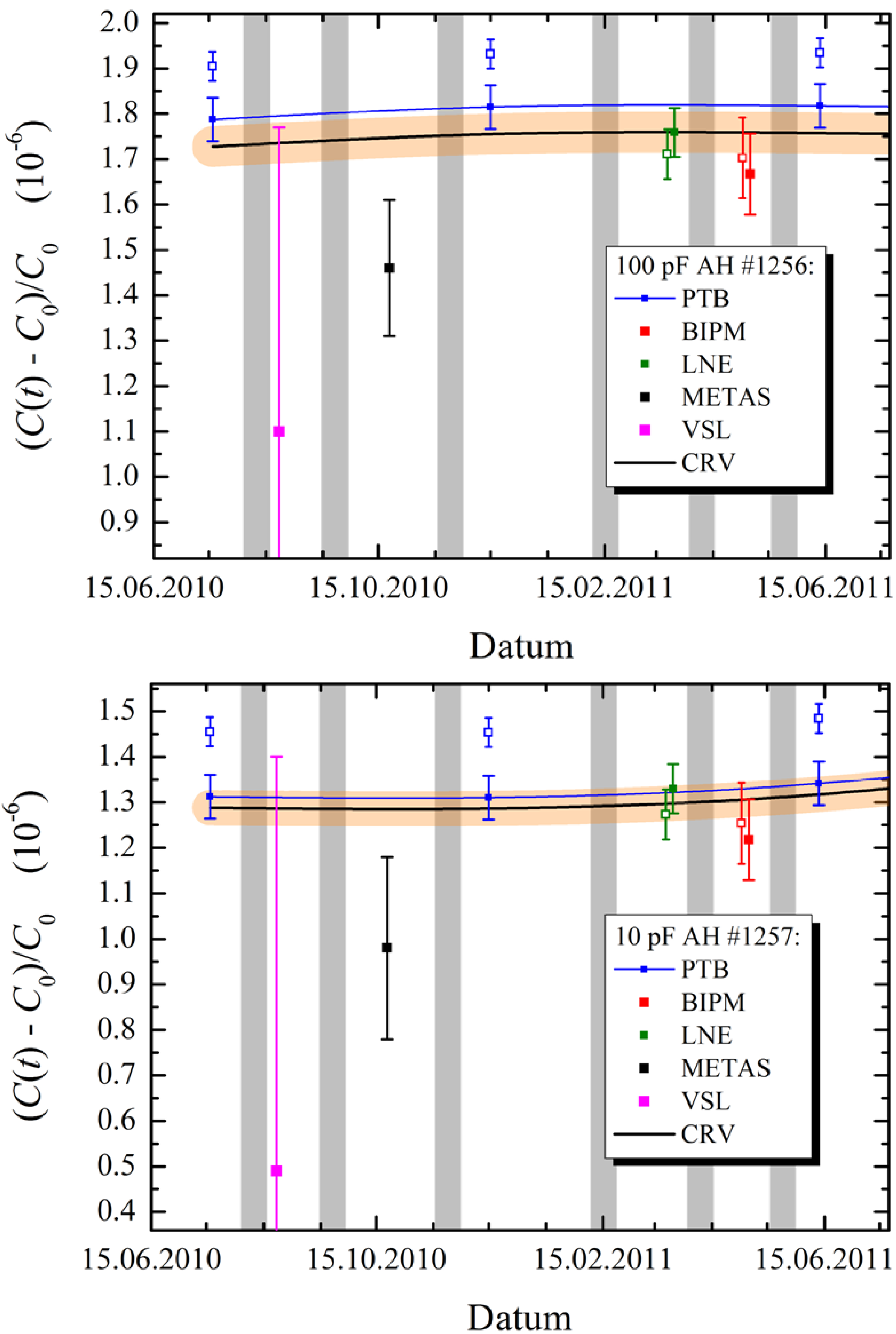

Figure 4.8.1: The capacitance of the travelling standards 100 pF AH #1256 (top) and 10 pF AH #1257 (bottom) as measured by the participants. C_0 is the particular nominal value. The uncertainty bars correspond to coverage factor k = 2. The transportations and the allocated two-week relaxation intervals are indicated in light grey. The black solid line is the CRV with the 95% confidence band in light orange. The open symbols indicate the initial results and are partially shifted in time for better visibility.

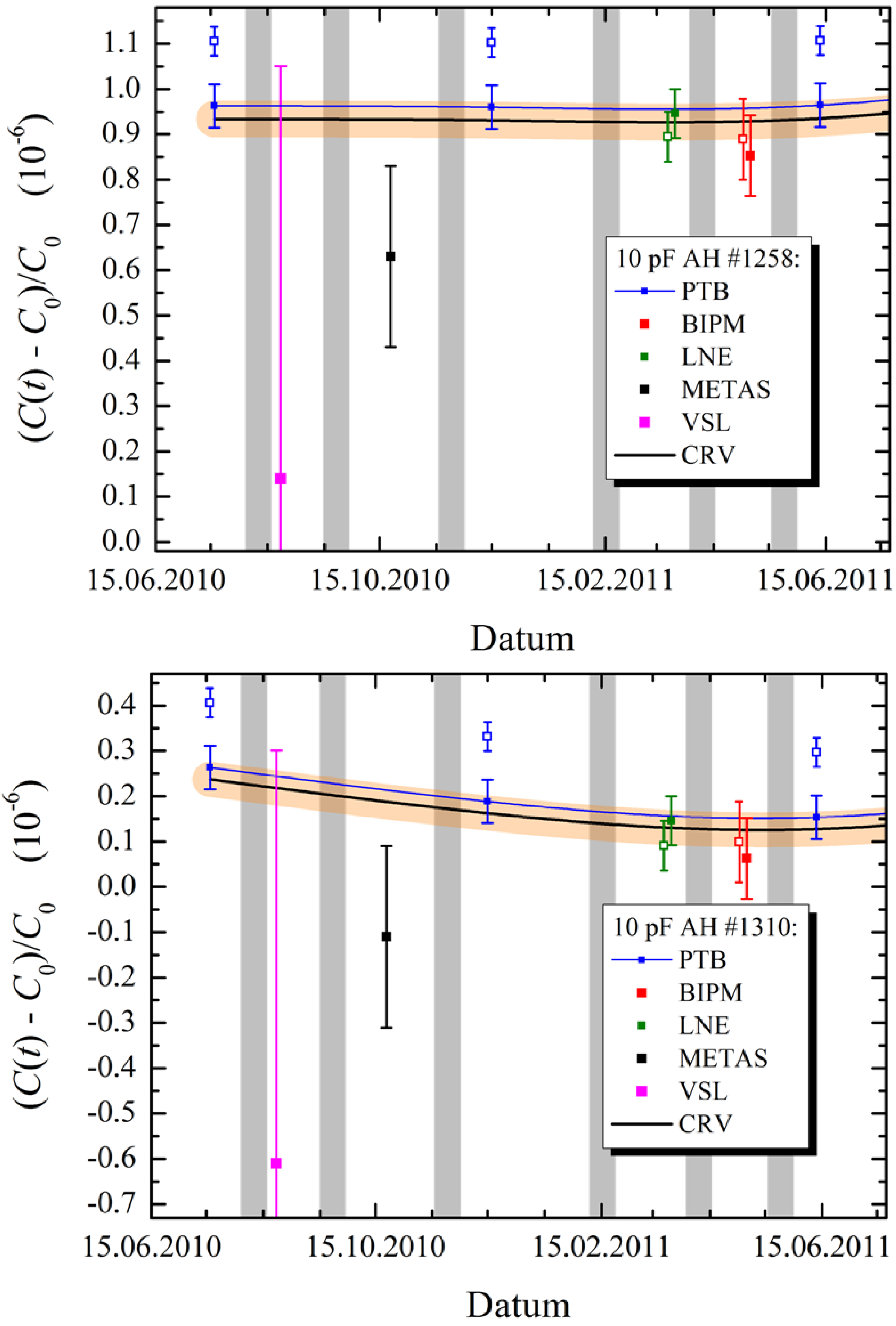

Figure 4.8.2: The capacitance of the travelling standards 10 pF AH #1258 (top) and 10 pF AH #1310 (bottom) as measured by the participants. C_0 is the particular nominal value. The uncertainty bars correspond to coverage factor k = 2. The transportations and the allocated two-week relaxation intervals are indicated in light grey. The black solid line is the CRV with the 95% confidence band in light orange. The open symbols indicate the initial results and are partially shifted in time for better visibility.

Table 4.8.1: The difference between the results of the 10 pF standards as measured by a participant N and PTB (interpolated to the mean time of the measurement of the particular participant), either measured at, or interpolated to, the reference frequency 1233 Hz. Also the mean 10 pF differences and the standard deviation of the three individual differences are quoted. All uncertainties refer to coverage factor *k* = 2. The 100 pF values are also quoted for later calculation of the 10:1 ratios.

Quantity	$dx^{N} - dx^{PTB}$ [10^{-9}]			
	BIPM - PTB	**LNE - PTB**	**METAS - PTB**	**VSL - PTB**
100 pF AH #1256	-152	-60	-347	-695
X = AH #1257	-113	8	-329	-821
X = AH #1258	-104	-10	-332	-823
X = AH #1310	-89	-10	-324	-855
mean 10 pF $d^{N} - d^{PTB}$	-102 ± 35	-4 ± 9	-328 ± 3	-833 ± 16
uncertainty of d^{N}	89	54	200	910
uncertainty of d^{PTB}	48			
total uncertainty	101	72	206	911
final result	-102 ± 101	-4 ± 72	-328 ± 206	-833 ± 911

Table 4.8.2: The difference between the results of the 10 pF standards of a participant N, either measured at, or interpolated to, the reference frequency 1233 Hz, and the CRV. Also the mean 10 pF differences and the standard deviation of the three individual differences are quoted. All uncertainties refer to coverage factor *k* = 2. The 100 pF values are also quoted for later calculation of the 10:1 ratios.

Quantity	$dx^{N} - dx^{CRV}$ [10^{-9}]				
	PTB - CRV	**BIPM - CRV**	**LNE - CRV**	**METAS - CRV**	**VSL - CRV**
100 pF AH #1256	53	-99	-7	-294	-642
X = AH #1257	22	-91	30	-307	-799
X = AH #1258	28	-76	18	-304	-795
X = AH #1310	26	-63	16	-298	-829
mean 10 pF $d^{N} - d^{CRV}$	25 ± 3	-77 ± 11	21 ± 6	-303 ± 4	-808 ± 15
uncertainty of d^{N}	48	89	54	200	910
uncertainty of d^{CRV}	33				
total uncertainty	59	95	63	203	911
degree of equivalence	25 ± 59	-77 ± 95	21 ± 63	-303 ± 203	-808 ± 911

4.8.2 10:1 capacitance ratio at the reference frequency

The 100 pF:10 pF ratio measured by a participant N is defined here according to

$$\frac{C(100\ \mathrm{pF,N})}{C(10\ \mathrm{pF,X,N})} = 10\left(1 + d^{\mathrm{N}}{}_{100\ \mathrm{pF}} - d^{\mathrm{N}}{}_{10\ \mathrm{pF,X}}\right) = 10(1 + d^{\mathrm{N}}_{\mathrm{X}})$$

with $d^{\mathrm{N}}{}_{100\ \mathrm{pF}}$ the relative deviation of the 100 pF standard #1256 from nominal, $d^{\mathrm{N}}{}_{10\ \mathrm{pF,X}}$ the relative deviation of the 10 pF standard X from nominal (with X either #1257, #1258, or #1310), and $d^{\mathrm{N}}{}_{\mathrm{X}}$ the relative deviation from the nominal ratio 10. The results of those participants who did not measure at the reference frequency of 1233 Hz were interpolated to the reference frequency using the frequency dependence measured by the particular participant.

The 100 pF:10 pF ratios are not constant in time, but exhibit a non-linear drift behaviour shown in Figure 4.8.3 and Figure 4.8.4. For the sake of completeness, also the initial PTB results (without the corrections given in Section 4.5) are shown (but not included in the following analysis), whereas the corrections submitted by the other participants do not (or not significantly) affect their 100 pF:10 pF ratios.

The CRV of each 100 pF:10 pF ratio is written as

$$d^{\mathrm{CRV}}_{\mathrm{X}}(t) = d^{\mathrm{PTB}}_{\mathrm{X}}(t) + \Delta_{\mathrm{X}}$$

with Δ_{X} a time-independent parameter determined by a weighted least-squares fit optimisation process including the results (and uncertainties) of all participants. Numerical differences between the results of the participants and the pilot laboratory are given in Table 4.8.3. The 10:1 ratios of all participants are in excellent agreement within the expanded uncertainties. Further, the standard deviation of the three individual ratio measurements of each participant is well within the quoted uncertainty. Therefore, the CRV is calculated by a weighted least-squares fit optimisation process (as described in Section 4.7) and includes the results (and uncertainties) of all participants. Numerical differences between the results of each participant and the CRV are given in Table 4.8.4. As follows from these tables, all 10:1 ratios are fully equivalent with the CRV and with each other.

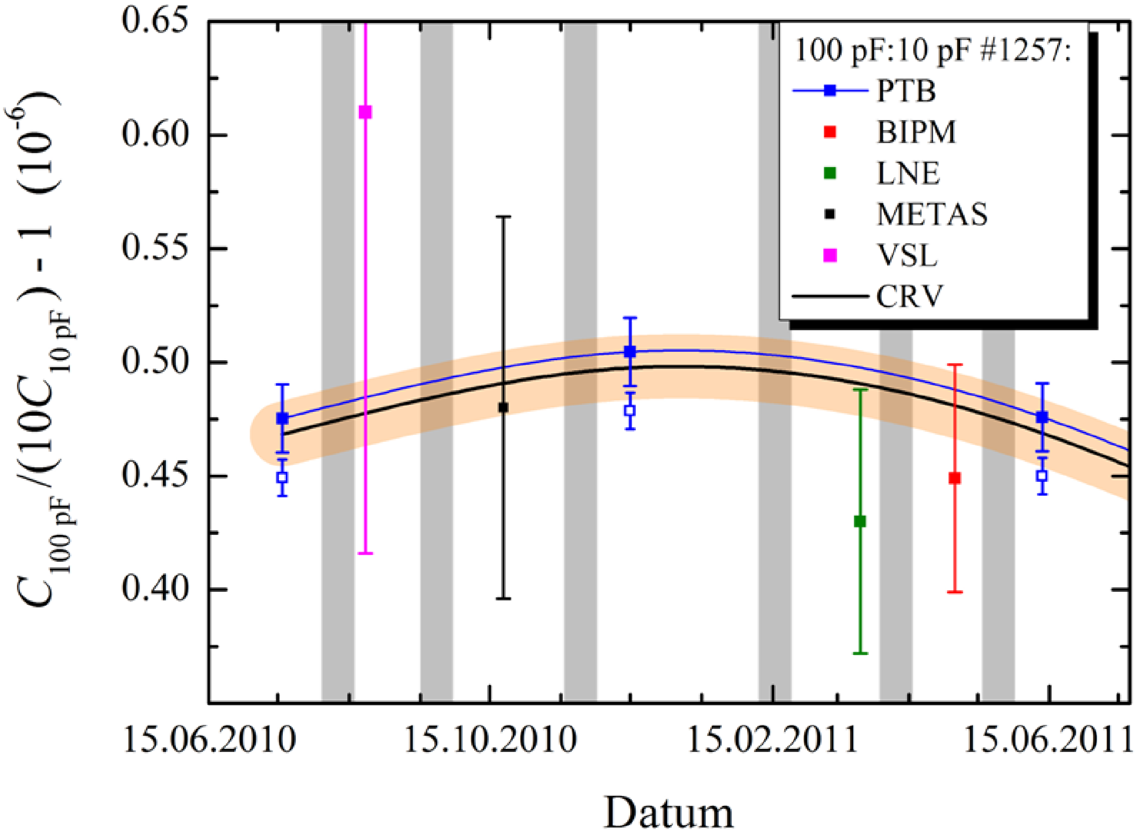

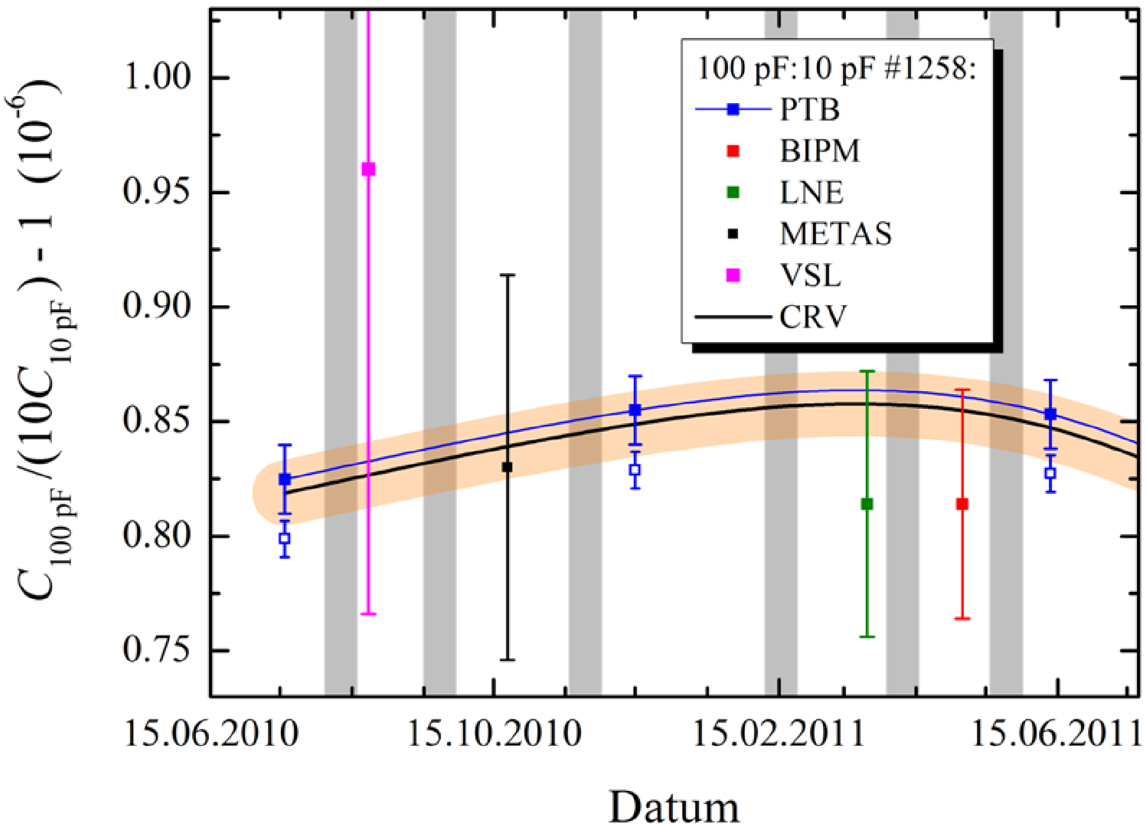

Figure 4.8.3: The ratio of 100 pF AH #1256 to 10 pF AH #1257 (top) and to 10 pF AH #1258 (bottom) as measured by the participants. The uncertainty bars correspond to coverage factor *k* = 2. The transportations and the allocated two-week relaxation intervals are indicated in light grey. The solid black line is the CRV with the 95% confidence band in light orange. The open symbols indicate the initial PTB results.

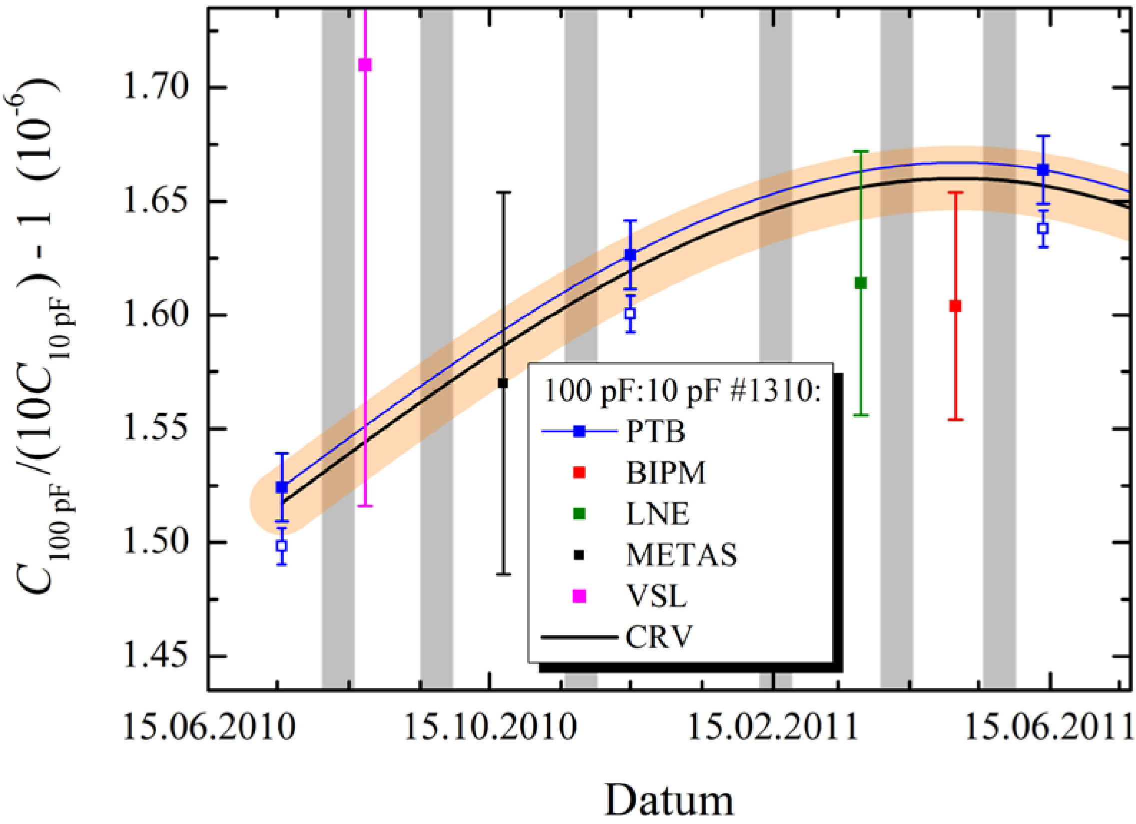

Figure 4.8.4: The ratio of 100 pF AH #1256 to 10 pF AH #1310 as measured by the participants. The uncertainty bars correspond to coverage factor *k* = 2. The transportations and the allocated two-week relaxation intervals are indicated in light grey. The solid black line is the CRV with the 95% confidence band in light orange. The open symbols indicate the initial PTB results.

Table 4.8.3: The differences between the 100 pF:10 pF ratios d_X^N measured by a participant N and PTB (interpolated to the mean time of the measurement of the particular participant), measured at or interpolated to the reference frequency of 1233 Hz. Also the mean differences and the standard deviation of the individual differences are quoted. All quoted uncertainties refer to coverage factor k = 2.

Quantity	$d_X^N - d_X^{PTB}$ [10^{-9}]			
	BIPM - PTB	**LNE - PTB**	**METAS - PTB**	**VSL - PTB**
X = AH #1257	-39	-68	-18	126
X = AH #1258	-48	-50	-15	128
X = AH #1310	-63	-50	-23	160
mean value $d^N - d^{PTB}$	-50 ± 10	-56 ± 9	19 ± 3	138 ± 16
uncertainty of d^N	50	58	84	194
uncertainty of d^{PTB}	15			
total uncertainty	52	60	85	195
final result	-50 ± 52	-56 ± 60	19 ± 85	138 ± 195

Table 4.8.4: The differences between the 100 pF:10 pF ratios d_X^N measured by a participant N at or interpolated to the reference frequency of 1233 Hz and the CRV. Also the mean differences and the standard deviation of the individual differences are quoted. All quoted uncertainties refer to coverage factor k = 2.

Quantity	$d_X^N - d_X^{CRV}$ [10^{-9}]				
	PTB - CRV	**BIPM - CRV**	**LNE - CRV**	**METAS - CRV**	**VSL - CRV**
X = AH #1257	7	-32	-61	-11	133
X = AH #1258	6	-42	-44	-9	134
X = AH #1310	7	-56	-43	-16	167
mean value $d^N - d^{CRV}$	7 ± 1	-43 ± 10	-49 ± 8	-12 ± 3	145 ± 16
uncertainty of d^N	15	50	58	84	194
uncertainty of d^{CRV}	14				
total uncertainty	21	51	59	85	194
degree of equivalence	7 ± 21	-43 ± 52	-49 ± 60	-12 ± 85	145 ± 194

4.8.3 Frequency dependence of the capacitance standards

The frequency dependence of the travelling standards was an optionally task for those participants which are capable of operating their measuring bridges at multiple frequencies. In particular, it requires a quadrature bridge which can be operated at different frequencies and at each frequency the whole measuring chain to 10 pF has to be measured separately. Results were provided by the BIPM, LNE, and PTB. As explained in Section 4.5, PTB has withdrawn the results at 2466 Hz and thus is not able to contribute to the frequency dependence. The available data of the BIPM and LNE with respect to the reference frequency of 1233 Hz are shown in Figure 4.8.5 and Figure 4.8.6. The initial results are also shown, but not included in the following analysis.

Since a physical model accurately describing the frequency dependence of an AH capacitance standards is not available, the frequency dependence in a limited range can be empirically described by a linear or polynomial function or by a power law (also known as Jonscher law). The BIPM data allow only a linear fit whereas the LNE data are fitted by a polynomial of 2nd order. The frequency dependence around the reference frequency can be described by a single parameter, the frequency coefficient. The results of the BIPM and LNE are given in Table 4.8.5 and reasonably agree with each other within the quoted uncertainties. The first three AH standards listed in Table 4.8.5 have practically the same frequency coefficient whereas the AH standard #1310 has a somewhat smaller frequency coefficient.

The frequency dependence of the travelling standard #1310 has also been measured at the BIPM in 2004 [3] and the frequency coefficient around 1233 Hz was $(-20 \pm 16)\cdot 10^{-9}$/kHz (as can be read from Figure 4 in Ref. 3). The actually measured frequency dependence is in good agreement with the former BIPM measurement.

Table 4.8.5: Frequency coefficient of the travelling standards and the associated expanded uncertainty (*k* = 2).

Nominal value and SN	Frequency coefficient (10^{-9}/kHz)		
	BIPM	LNE	weighted mean
100 pF #1256	-150 ± 108	-106 ± 72	-120 ± 60
10 pF #1257	-182 ± 108	-54 ± 78	-98 ± 63
10 pF #1258	-191 ± 108	-63 ± 74	-104 ± 61
10 pF #1310	-115 ± 108	-14 ± 74	-46 ± 61

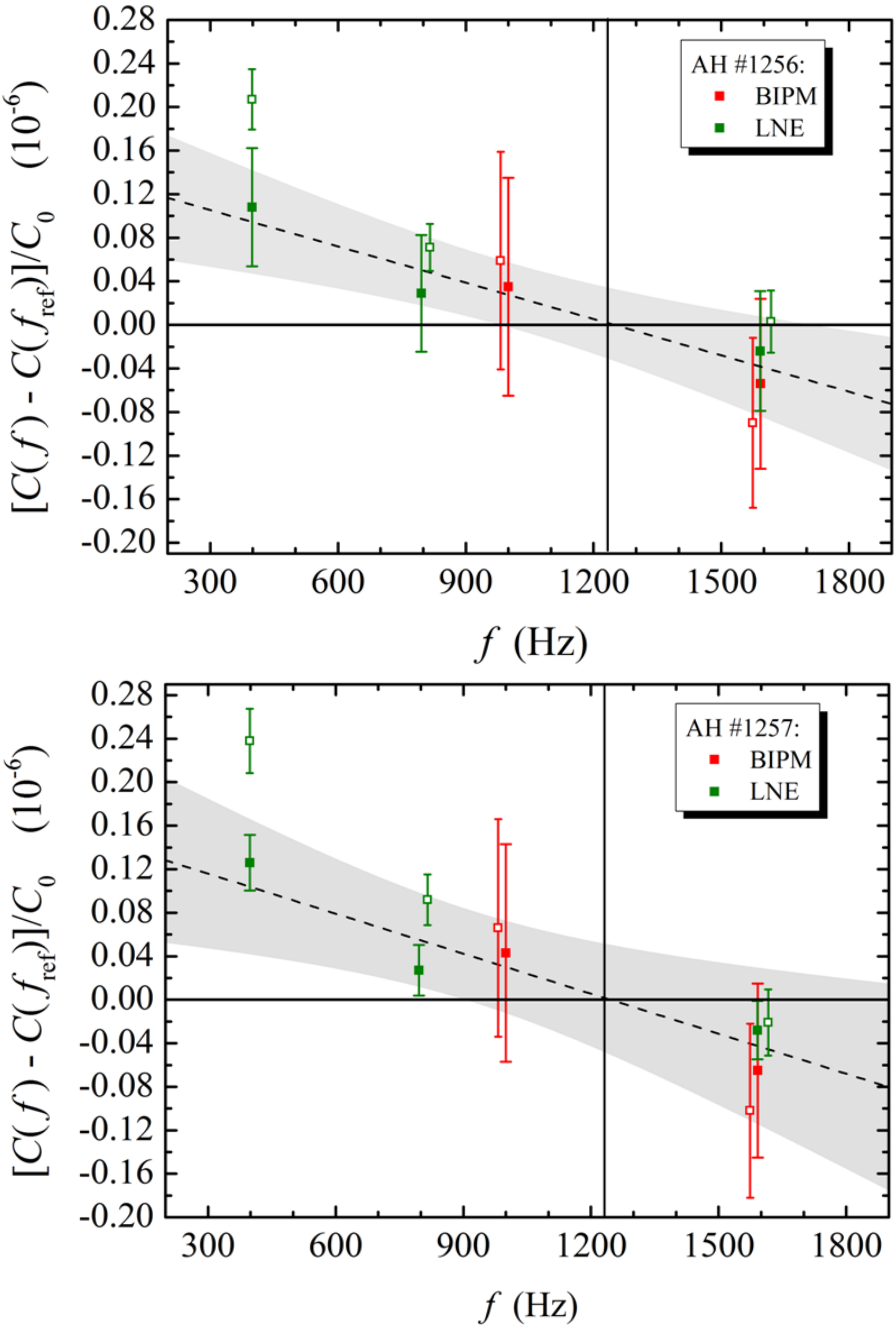

Figure 4.8.5: The frequency dependence of the capacitance standards 100 pF AH #1256 (top) and 10 pF AH #1257 (bottom) with respect to the particular value interpolated to the reference frequency 1233 Hz, as measured by the BIPM and LNE. C_0 is the particular nominal value. All uncertainty bars refer to coverage factor $k = 2$. The dashed line is a linear least-squares fit with the 95% confidence band in light grey. The open symbols indicate the initial results and are slightly shifted in frequency for better visibility.

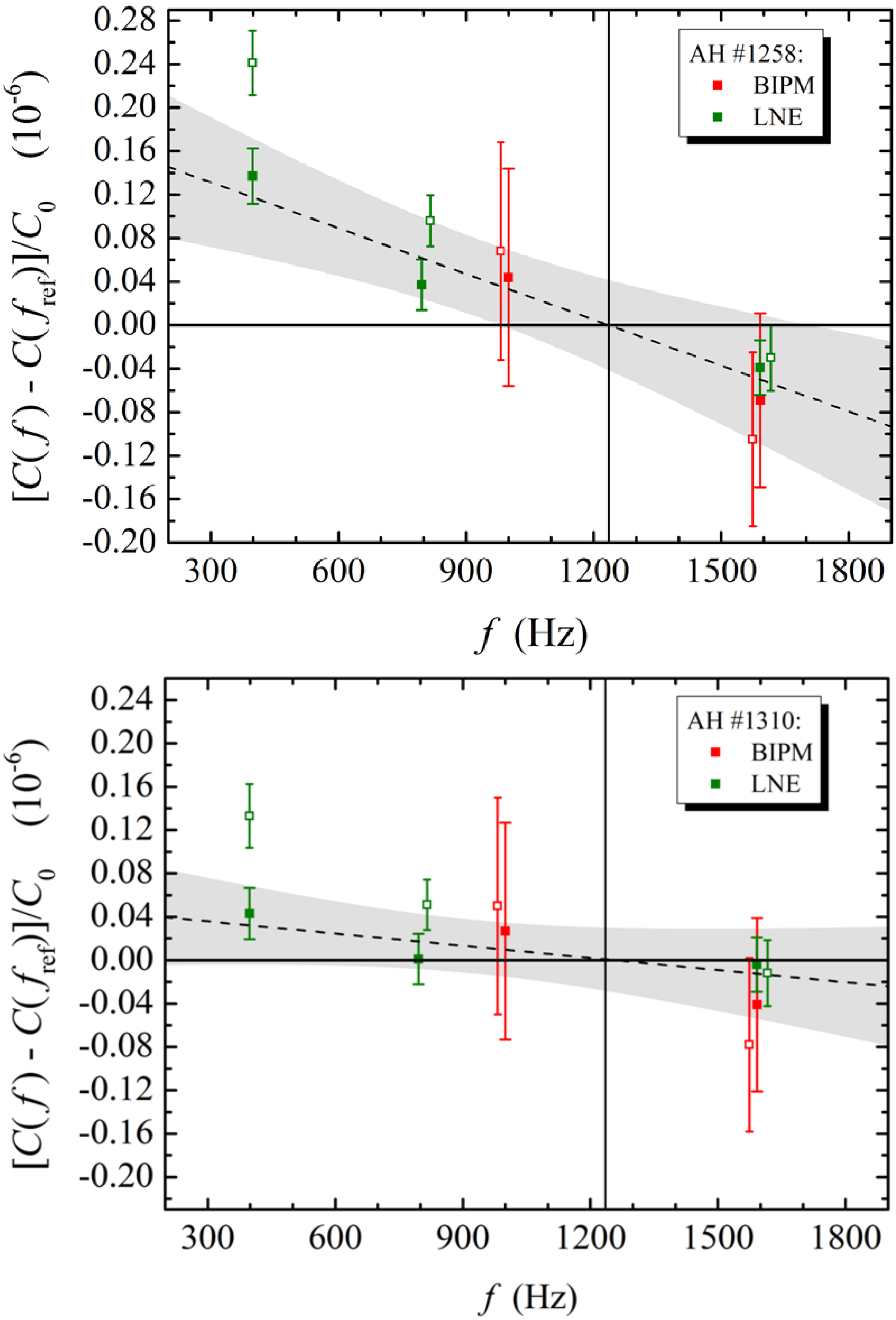

Figure 4.8.6: The frequency dependence of the capacitance standards 10 pF AH #1258 (top) and 10 pF AH #1310 (bottom) with respect to the particular value interpolated to the reference frequency 1233 Hz, as measured by the participants. C_0 is the particular nominal value. All uncertainty bars refer to coverage factor k = 2. The dashed line is a linear least-squares fit with the 95% confidence band in light grey. The open symbols indicate the initial results and are slightly shifted in frequency for better visibility.

4.8.4 Voltage dependence of the capacitance standards

Measurement of the voltage dependence of the travelling standards was an optionally task. For the purpose of such a measurement, it is assumed that the ac resistance used as the starting point of the measuring chain (either the ac QHR or an ac-dc transfer resistor and the dc QHR) does not depend on voltage. Then, the whole measuring chain to 10 pF has to be separately measured at different voltage levels. Usually, the voltage dependence is very small (if significant at all) and linear so that it can be characterised by a single parameter, the voltage coefficient. Results were provided by PTB and the BIPM (see Table 4.8.6). The 100 pF standard does not show significant voltage dependence. For the 10 pF standards, only the uncertainty of the PTB result is low enough to state that the voltage coefficients of two of the individual 10 pF standards is significantly different from zero. The BIPM results have a larger (maybe overestimated) uncertainty, but nicely match the PTB results.

Table 4.8.6: Voltage coefficient of the travelling standards and the associated uncertainty (k = 2).

Nominal value and SN	Nominal voltage	Relative change of capacitance with applied voltage, measured at voltages in the specified ranges	
		PTB, f = 1233 Hz	**BIPM, f = 1592 Hz**
100 pF #1256	10 V	$(0.6 \pm 1.4)\cdot10^{-9}$/V at (6 to 12) V	$(-0.3 \pm 6.0)\cdot10^{-9}$/V at (5 to 10) V
10 pF #1257	100 V	$(2.9 \pm 1.4)\cdot10^{-10}$/V at (60 to 120) V	$(1.9 \pm 6.0)\cdot10^{-10}$/V at (50 to 100) V
10 pF #1258	100 V	$(4.0 \pm 1.4)\cdot10^{-10}$/V at (60 to 120) V	$(4.7 \pm 6.0)\cdot10^{-10}$/V at (50 to 100) V
10 pF #1310	100 V	$(0.3 \pm 1.4)\cdot10^{-10}$/V at (60 to 120) V	$(1.0 \pm 6.0)\cdot10^{-10}$/V at (50 to 100) V

4.8.5 Summary of the first capacitance circulation

The initial results of the first circulation had revealed discrepancies, but the participants had time to check their measuring bridges and some participants have submitted corrections after the distribution of the initial results. Then, the results turned out to be reasonably good and fully equivalent. The expanded relative uncertainties are as low as $34\cdot10^{-9}$ for the 10 pF standards and $15\cdot10^{-9}$ for the 100 pF:10 pF ratios. In addition, the frequency and voltage coefficients have been determined. Because of the initial discrepancies and because not all aspects and uncertainties of this circulation were satisfying, it has been decided to repeat the circulation of the capacitance standards.

4.9 Results of the second capacitance circulation

4.9.1 Capacitance results at the reference frequency

The measurements of the second capacitance circulation were carried out in nominally the same manner as at the first capacitance circulation. The measuring bridges of the participants (where needed) got improved *before* the second capacitance circulation started. In contrast to the first capacitance circulation, every transport of the travelling standards within Europe was carried out with the thermostats being powered by an autarkic lead battery. This was not possible at the airfreight transportation to NMIA and eventually caused unexpected difficulties.

A general, and very important, precondition of any comparison is that the participants do not know the results beforehand. In our case of a repetition, this aspect is still granted: Compared to the first capacitance circulation, the capacitance standards have slightly changed their values; the changes are in the range of $-0.15\cdot10^{-6}$ to $0.3\cdot10^{-6}$ for the individual standards (see also Section 4.6) and exhibit different sign. Further, the final values of the correction for a deviating ambient temperature were measured by the pilot at the very end of the second circulation period and also a correction of the imperfect airfreight transportations to and back from NMIA was worked out after the second capacitance circulation was completed. Therefore, all participants (including the pilot) saw the final picture of the second capacitance circulation for the very first time after the final measurements at the pilot laboratory. This means that *all* participants were practically unbiased from the first capacitance circulation.

Before the results will be presented, the mentioned effect of the airfreight transportations has to be discussed.

4.9.1.1 Unthermostated airfreight transportation

As shown by the two BIPM series before and after the unthermostated transportations to and back from NMIA (see Section 11.2 or Figure 4.4.3), the unthermostated transportations caused a jump and long-lasting relaxation effects. The amplitudes of the jumps are listed in Table 4.9.1. It is conspicuous that the larger the jump of a particular standard, the larger is also the instability, the drift rate, the non-linearity of the drift, and the ambient temperature coefficient (see Table 4.9.1). **Therefore, the difference of the two BIPM series can be taken as a measure of the instability of the capacitance standards.** Further, the observation that the changes of the capacitance standards are correlated with their ambient temperature coefficient seems to indicate that mechanical shock or thermal hysteresis does not directly affect the fused-silica elements themselves, but the AH temperature controllers, and this leads to small changes of the internal temperature which indirectly affects the capacitance values.

For *all* pairs of measurement periods with an *unthermostated* transportation in between, the differences of the particular results are found to show a significant correlation with the BIPM difference, as shown in the top part of Figure 4.9.1 and in Figure 4.9.2. This also applies to the difference between the first BIPM series and the PTB spline as well as to the difference between the NMIA measurement and the PTB spline, probably because the PTB spline function interconnects data taken before and after the unthermostated transportations.

For *all* pairs of measurement periods with no unthermostated transportation in between, the differences of the particular results do not show a significant correlation with the BIPM difference. Reversely, the absence of a significant correlation during a certain time interval shows that no significant instabilities of the travelling standards have occurred. An example is shown in the bottom part of Figure 4.9.1 (which also shows that mainly the first of the two unthermostated transportations to NMIA affected the standards). Finally, applying the same analysis to the results of the first capacitance circulation shows that probably no significant jumps have occurred even though the travelling standards were not thermostated during some of the transportations. (The reason for this might be that the timeout of the thermostats was much shorter, and the mechanical vibrations were much weaker, than at an airfreight transportation, as already discussed in Section 4.4.)

The main point here is that the measured correlations allow correcting for the instability of the travelling standards (i.e., extrapolation to zero instability), without the need to know the true and complete time dependence of the travelling standards, without arbitrary assumptions, and without a significant increase of the total uncertainty. Reversely, the absence of correlated instabilities during a certain time interval shows that no significant variation of the travelling standards has occurred and that the simple spline function is a reasonable approximation. Note also that a hypothetical systematic measurement error of a participant, which is to be tested in this comparison, is *not* eliminated or affected by this correction. It is also worth mentioning that other alternative measures of the instability of the standards could be used; they yield practically the same result, but appear to be slightly less suitable or require more assumptions.

Table 4.9.1: Summary of quantities measuring the instability of the standards: The change of the travelling capacitance standards measured by the BIPM before and after the transportation to NMIA, the drift rate between the two BIPM series measured by PTB, the maximal non-linear drift, and the ambient temperature coefficient. The quoted uncertainties are only the statistical uncertainties.

Standard	difference of the two BIPM series (10^{-9})	drift between the two BIPM series (10^{-9})	maximal non-linear drift (10^{-9})	ambient temperature coefficient [10^{-9}/°C]
100 pF AH #1256	50 ± 14	20 ± 10	183 ± 10	-12.3 ± 2.0
10 pF AH #1257	145 ± 14	49 ± 10	294 ± 10	-18.1 ± 2.0
10 pF AH #1258	91 ± 14	18 ± 10	196 ± 10	-11.4 ± 2.0
10 pF AH #1310	-4 ± 14	6 ± 10	134 ± 10	-7.1 ± 2.0

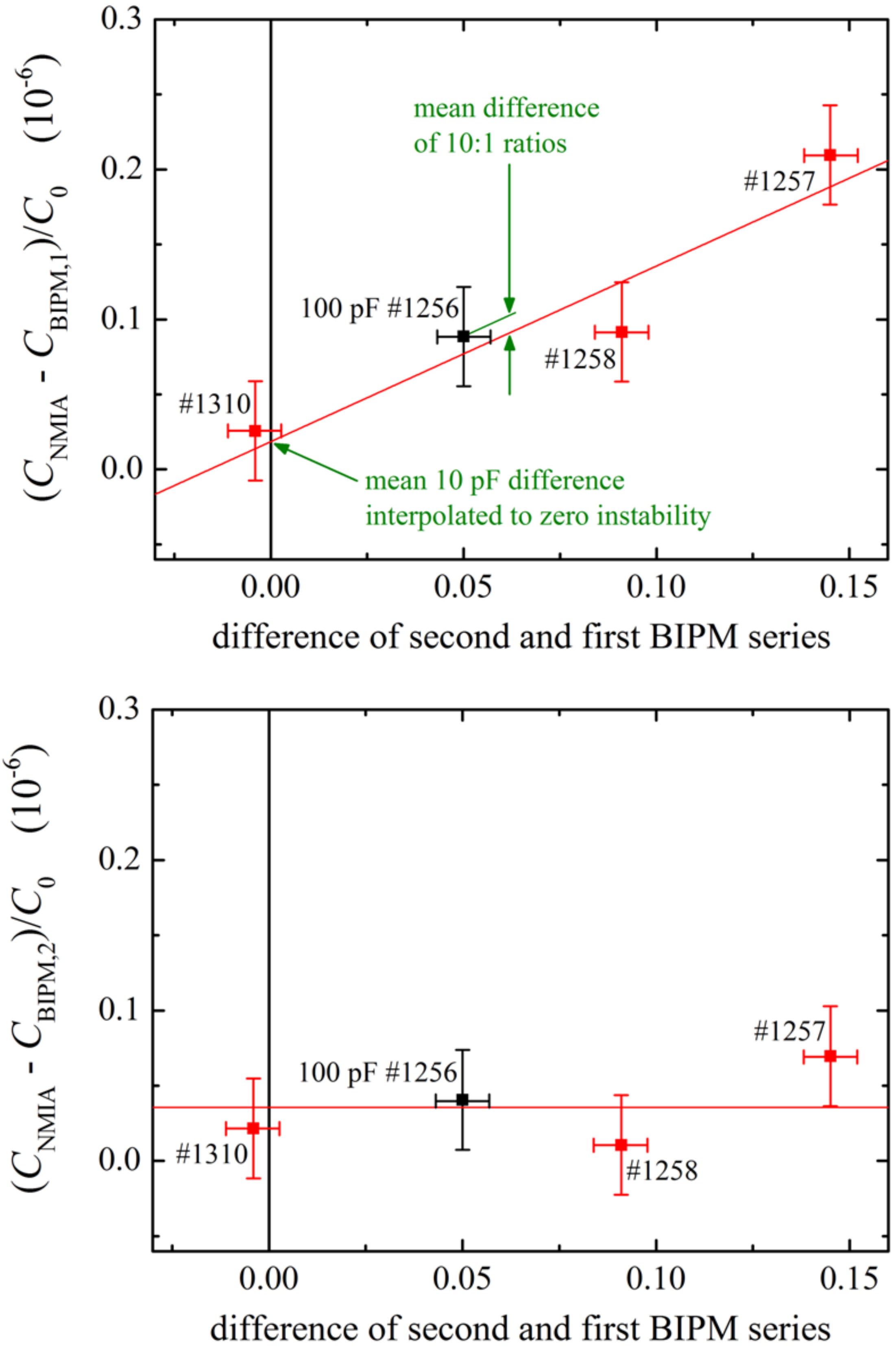

Figure 4.9.1: Top: The difference between the results of NMIA and the first BIPM series, plotted as a function of the difference between the two BIPM series. The uncertainty bars only comprise the statistical uncertainties (k = 1). The solid line is a linear least-squares fit of the 10 pF data. Bottom: The corresponding diagram for the second BIPM series. The solid line indicates the mean value.

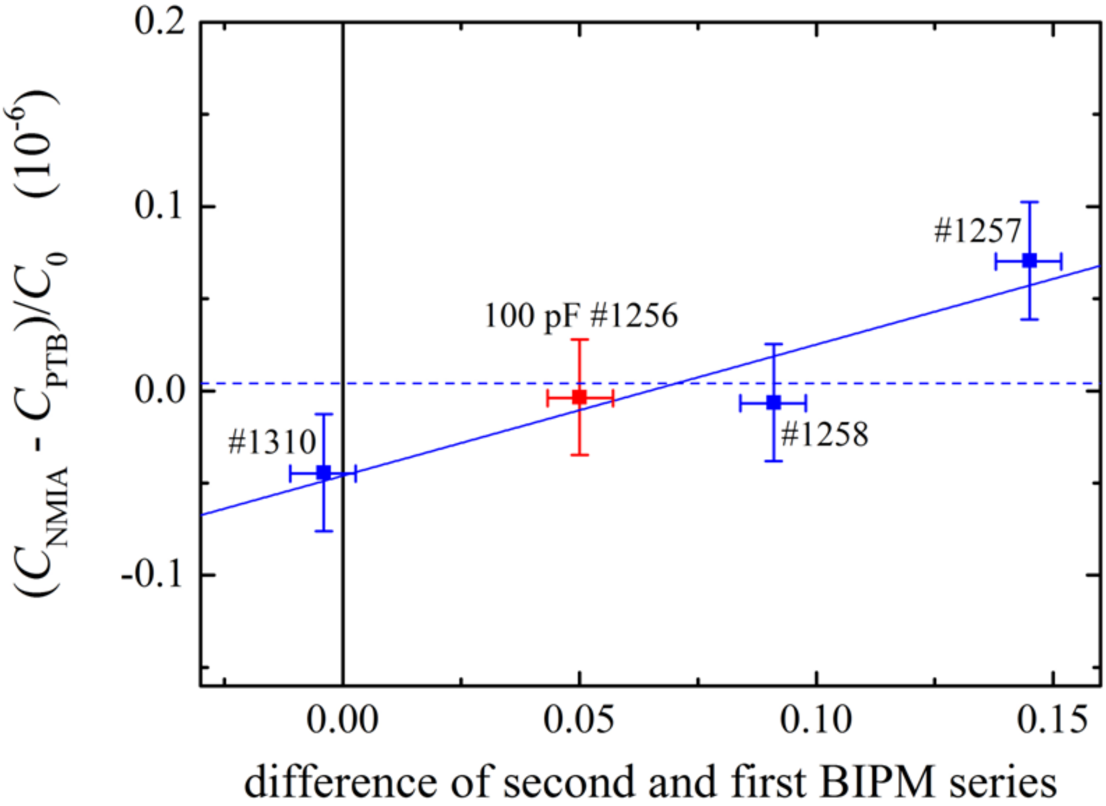

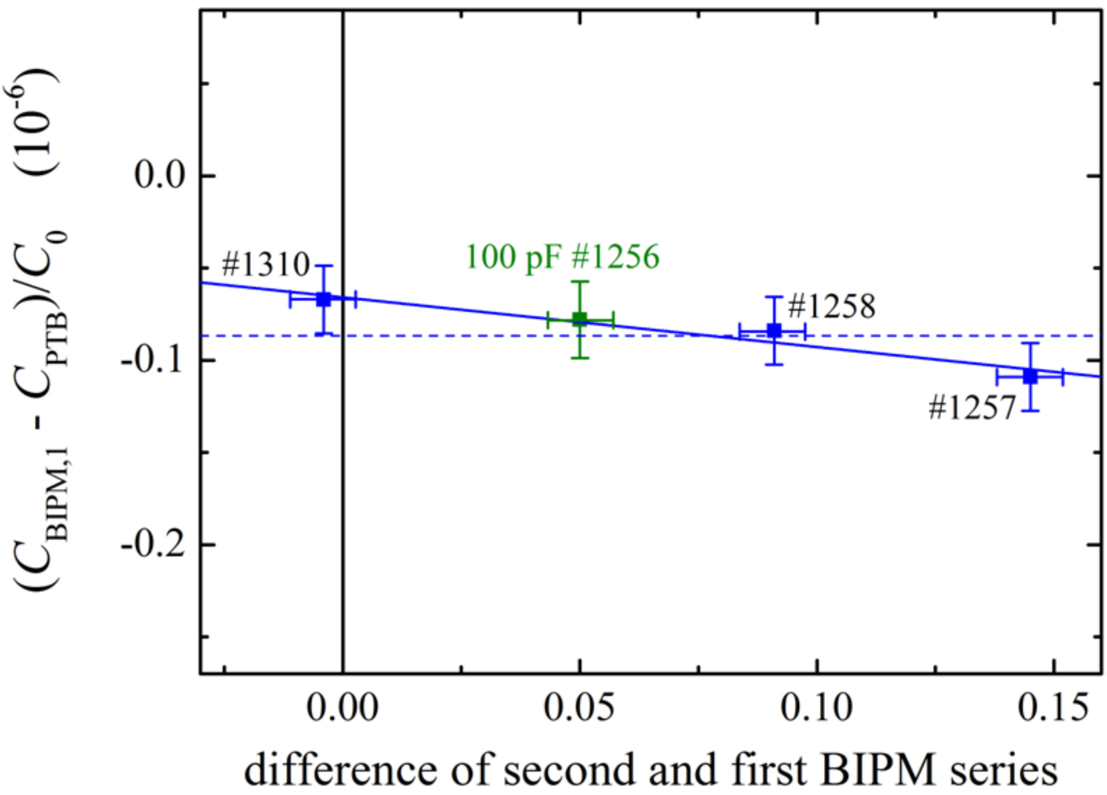

Figure 4.9.2: Top: The difference between the results of NMIA and PTB, plotted as a function of the difference between the two BIPM series. The uncertainty bars only comprise the statistical uncertainties (k = 1). The solid line is a linear least-squares fit of the 10 pF data and the dashed line indicates the mean value (as a guide to the eye). Bottom: The corresponding diagram for the difference between the first BIPM series and the PTB results.

4.9.1.2 Corrected capacitance results at the reference frequency

The final results of the participants either measured at, or interpolated to, the reference frequency of 1233 Hz are shown in Figure 4.9.3 and Figure 4.9.4. They include corrections for the effect of the unthermostated transportations to NMIA (where applicable and as described in Section 4.9.1.1) and they include corrections for deviations from the nominal conditions (in exactly the same manner as for the first capacitance circulation; see Section 4.1.3). The results of the pilot laboratory were already discussed in Section 4.6 (Figure 4.6.1 and Figure 4.6.2); the assigned uncertainty covers not only the calculated measurement uncertainty, but also includes an uncertainty contribution due to the permanent instability of the travelling standards. For the sake of completeness, also the initial LNE results (see Section 4.5) are shown.

Numerical differences of the three 10 pF capacitance values measured by a participant and the pilot laboratory are given in Table 4.9.2. Numerical differences of the results of the BIPM and NMIA are quoted in Table 4.9.3. For all other pairwise differences, the difference in time is too large for a direct comparison, but they can be indirectly calculated from the quoted differences. The numerical values of the correction for the unthermostated transportations are also quoted in these tables. Note that the results without this correction would show a serious scattering and a deviating mean value. With this correction, the standard deviation of the three measurements of each participant is well within the quoted uncertainties. This also shows that the corrections applied as well as the spline approach of the CRV are reasonable within the particular uncertainty.

The 10 pF results of all participants practically agree with each other within the expanded uncertainties. Therefore, the CRV is calculated by a weighted least-squares fit optimisation process (as described in Section 4.7) and includes the results (and uncertainties) of all participants. Numerical differences between the results of the participants and the CRV are given in Table 4.9.4. As follows from this table, all 10 pF results are fully equivalent.

Because the 10 pF results are either traced to the quantum Hall resistance or to the NMIA calculable capacitor, it is also possible to determine a value of the von Klitzing constant. For this purpose, a modified CRV* is calculated which is based only on the results traced to the quantum Hall resistance (Table 4.9.5). Thus the mean difference of this CRV* and the NMIA result (which, as mentioned in Section 4.7, has been converted by the pilot from the SI farad to farad-90) is equal to the relative difference of the von Klitzing constant as determined at this comparison and the conventional value of the von Klitzing constant:

$$(R_{\mathrm{K,comparison}} - R_{\mathrm{K\text{-}90}}) / R_{\mathrm{K\text{-}90}} = (27 \pm 84)\cdot 10^{-9}$$

The quoted uncertainty corresponds to coverage factor $k = 2$. The results can also be expressed in terms of the 2014 CODATA value $R_{\mathrm{K,CODATA}} \equiv h/e^2 = 25812.8074555\ (59)\ \Omega$:

$$(R_{\mathrm{K,comparison}} - R_{\mathrm{K,CODATA}}) / R_{\mathrm{K,CODATA}} = (27 \pm 84 - 18)\cdot 10^{-9} = (9 \pm 84)\cdot 10^{-9}$$

The results of the von Klitzing constant as determined by each participant are given in Table 4.9.6. Within the quoted expanded uncertainties, the agreement is excellent.

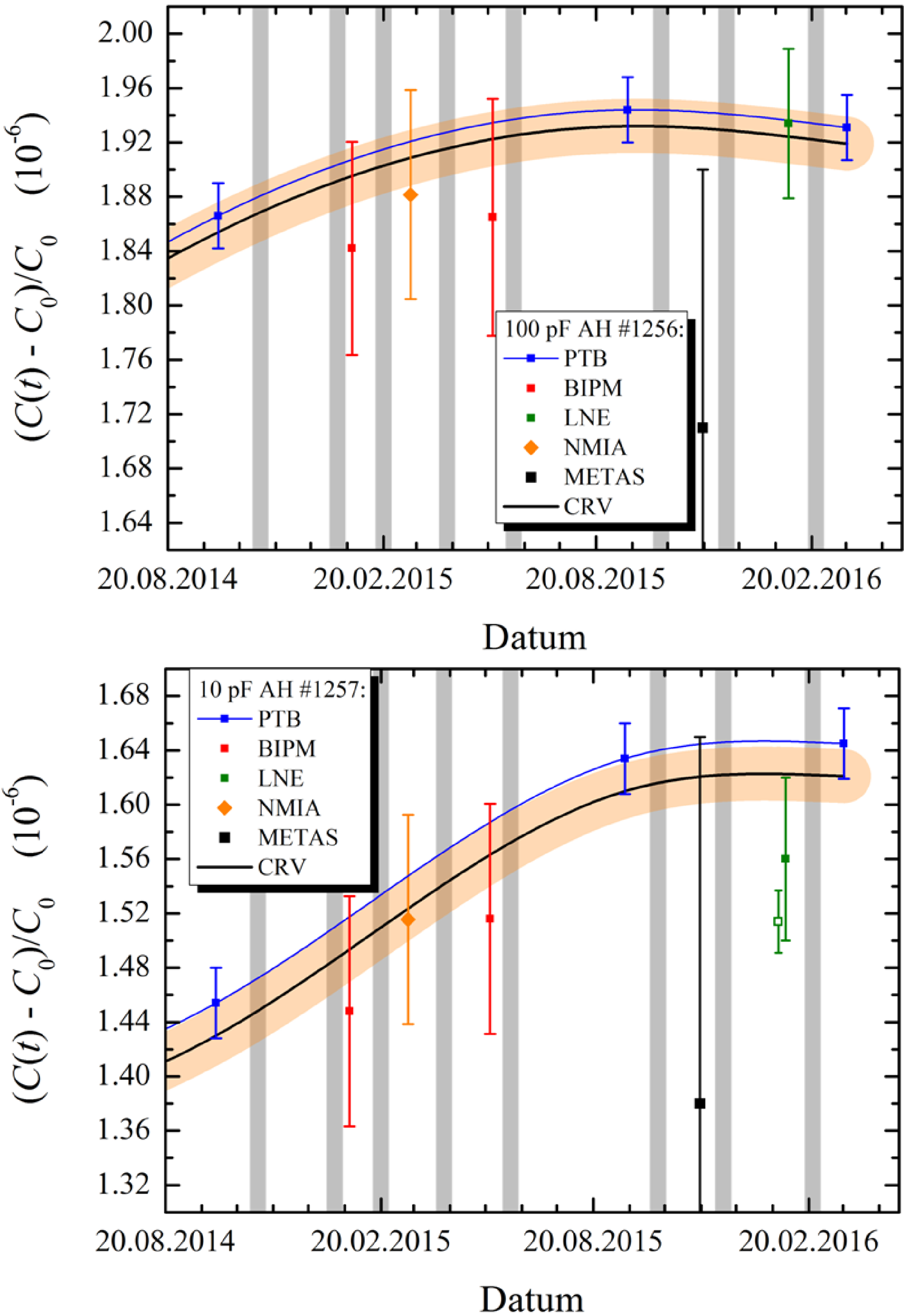

Figure 4.9.3: The capacitance of the travelling standards 100 pF AH #1256 (top) and 10 pF AH #1257 (bottom) as measured by the participants with the corrections discussed in the text. The uncertainty bars correspond to coverage factor $k = 2$. The transportations and the allocated two-week relaxation intervals are indicated in light grey. The solid black line is the CRV with the 95% confidence band in light orange. The open symbol in the bottom diagram indicates the initial 10 pF LNE result and is slightly shifted in time for better visibility.

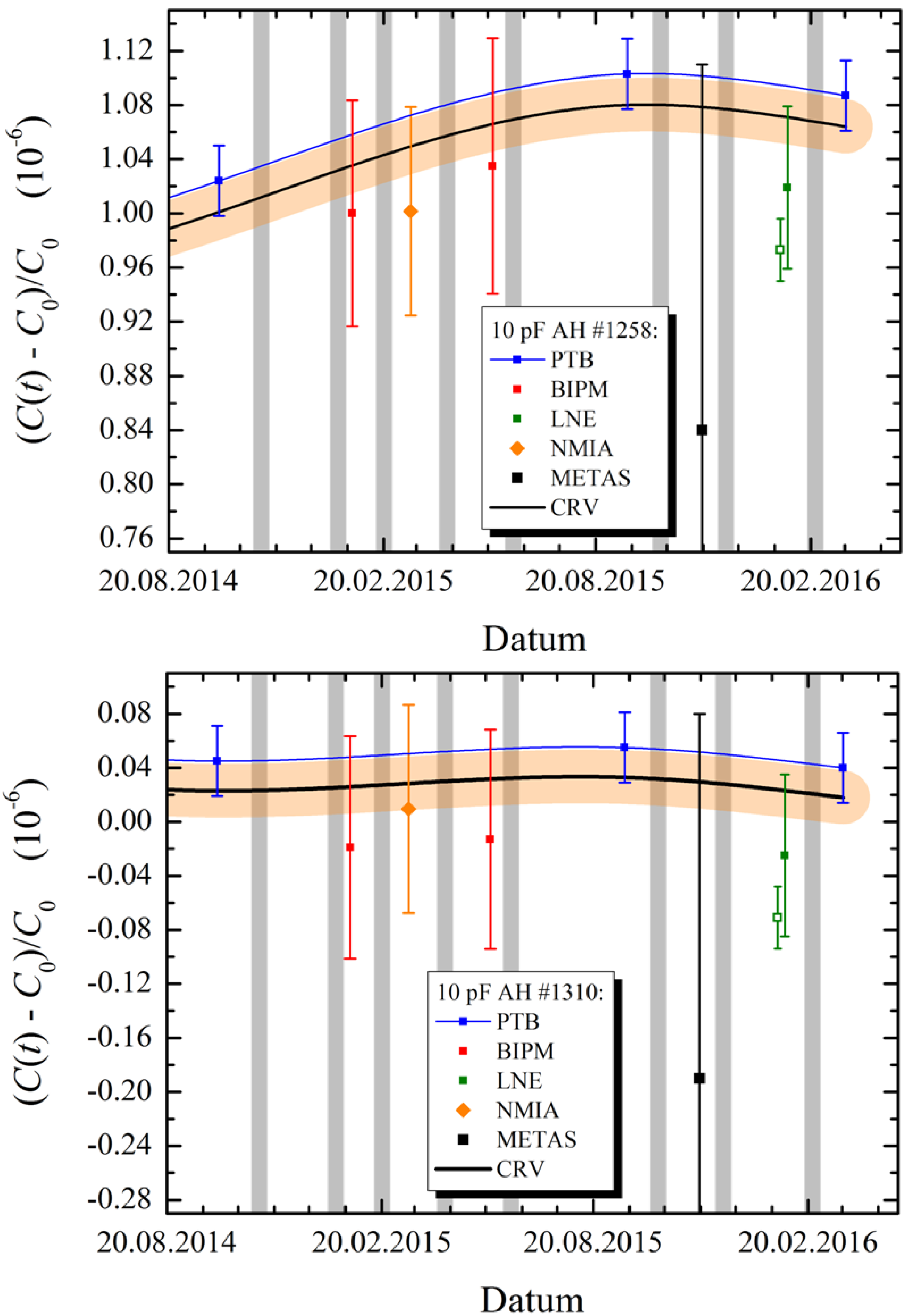

Figure 4.9.4: The capacitance of the travelling standards 10 pF AH #1258 (top) and 10 pF AH #1310 (bottom) as measured by the participants with the corrections discussed in the text. The uncertainty bars correspond to coverage factor $k = 2$. The transportations and the allocated two-week relaxation intervals are indicated in light grey. The solid black line is the CRV with the 95% confidence band in light orange. The open symbols indicate the initial LNE results which are slightly shifted in time for better visibility.

Table 4.9.2: The difference between the results of the 10 pF standards as measured by a participant N and PTB (interpolated to the mean time of the measurement of the particular participant), either measured at, or interpolated to, the reference frequency 1233 Hz. Also the mean 10 pF differences and the standard deviation of the individual differences are quoted. All uncertainties refer to coverage factor *k* = 2. The 100 pF values are also quoted for later calculation of the 10:1 ratios.

Quantity	$dx^{N} - dx^{PTB}$ [10^{-9}]				
	$BIPM_1$ - PTB *)	$BIPM_2$ - PTB *)	LNE - PTB	METAS - PTB	NMIA - PTB *)
100 pF AH #1256	-79 + 14 = -65	-58 - 12 = -70	-2	-232	-3 - 36 = -39
X = AH #1257	-109 + 39 = -70	-38 - 33 = -71	-86	-265	71 -103 = -32
X = AH #1258	-84 + 25 = -59	-33 - 21 = -54	-75	-262	-6 -65 = -71
X = AH #1310	-67 - 1 = -68	-69 + 1 = -68	-70	-242	-44 +3 = -41
mean 10 pF $d^{N} - d^{PTB}$	-66 ± 5	-64 ± 7	-77 ± 7	-256 ± 10	-48 ± 17
uncertainty of d^{N}	84		60	258	80
uncertainty of d^{PTB}	26				
total 10 pF uncertainty	88		65	260	84
final result	-65 ± 88		-77 ± 65	-256 ± 260	-48 ± 84

*) correction for correlation with ($BIPM_2$ - $BIPM_1$)

Table 4.9.3: The differences between the results of the 10 pF standards as measured by the BIPM and NMIA, interpolated to the reference frequency 1233 Hz. Also the mean 10 pF difference and the standard deviation of the individual differences are quoted. All uncertainties refer to coverage factor *k* = 1, apart from the final result with *k* = 2. The 100 pF values are also quoted for later calculation of the 10:1 ratios.

Quantity	$dx^{N1} - dx^{N2}$ [10^{-9}]
	($BIPM_1$ + $BIPM_2$)/2 - NMIA *)
100 pF AH #1256	-65 + 36 = -29
X = AH #1257	-140 +103 = -37
X = AH #1258	-51 +65 = 14
X = AH #1310	-24 -3 = -27
mean 10 pF $d^{N1} - d^{N2}$	-17 ± 22
uncertainty of d^{N1}	84
uncertainty of d^{N2}	80
total 10 pF uncertainty	116
final result	-17 ± 116

*) correction for correlation with ($BIPM_2$ - $BIPM_1$)

Table 4.9.4: Difference between the results of the 10 pF standards of a participant N, either measured at, or interpolated to, the reference frequency 1233 Hz, and the CRV. Also the mean 10 pF differences and the standard deviation of the individual differences are quoted. All uncertainties refer to coverage factor *k* = 2. The 100 pF values are also quoted for later calculation of the 10:1 ratios.

Quantity	$d_X^{N} - d_X^{CRV}$ [10⁻⁹]					
	PTB - CRV	**BIPM1 - CRV**	**BIPM2 - CRV**	**LNE - CRV**	**METAS - CRV**	**NMIA - CRV**
100 pF AH #1256	12	-53	-58	10	-220	-27
X = AH #1257	24	-46	-47	-62	-241	-8
X = AH #1258	23	-36	-31	-52	-239	-48
X = AH #1310	22	-46	-46	-48	-220	-19
mean 10 pF $d^{N} - d^{CRV}$	23 ± 1	-43 ± 5	-41 ± 7	-54 ± 6	-233 ± 10	-25 ± 17
uncertainty of d^{N}	26	84		60	258	80
uncertainty of d^{CRV}	26					
total 10 pF uncertainty	36	88		65	260	84
degree of equivalence	23 ± 36	-42 ± 88		-54 ± 65	-233 ± 260	-25 ± 84

Table 4.9.5: Corresponding to Table 4.9.4, but with a comparison reference value CRV* based only on the 10 pF results traced to the quantum Hall resistance. The difference between CRV* and the NMIA results is thus the difference of von-Klitzing constant determined at this comparison and the conventional value of the von Klitzing constant.

Quantity	$d_X^{N} - d_X^{CRV*}$ [10⁻⁹]					
	PTB - CRV*	**BIPM1 - CRV***	**BIPM2 - CRV***	**LNE - CRV***	**METAS - CRV***	**CRV* - NMIA**
X = AH #1257	23	-47	-48	-63	-209	9
X = AH #1258	20	-39	-34	-55	-242	51
X = AH #1310	21	-47	-47	-49	-221	20
mean 10 pF $d^{N} - d^{CRV*}$	21 ± 1	-44 ± 4	-43 ± 6	-56 ± 6	-224 ± 14	27 ± 18
uncertainty of d^{N}	26	84		60	258	80
uncertainty of d^{CRV*}	26					
total 10 pF uncertainty	36	88		65	260	84
degree of equivalence	21 ± 36	-43 ± 88		-56 ± 65	-224 ± 260	27 ± 84

Table 4.9.6: The von-Klitzing constant as determined from the QHR chain of each participant and the NMIA calculable capacitor, relative to the actual 2014 CODATA value of the von Klitzing constant (*k* = 2).

$(R_K - R_{K,CODATA}) / R_{K,CODATA}$ [10⁻⁹]			
PTB	**BIPM**	**LNE**	**METAS**
-12 ± 88	52 ± 116	65 ± 100	233 ± 270

4.9.2 10:1 capacitance ratio at the reference frequency

The 100 pF:10 pF ratio measured by a participant N is defined here according to

$$\frac{C(100\ \mathrm{pF,N})}{C(10\ \mathrm{pF,X,N})} = 10\left(1 + d^{\mathrm{N}}_{100\ \mathrm{pF}} - d^{\mathrm{N}}_{10\ \mathrm{pF,X}}\right) = 10(1 + d^{\mathrm{N}}_{\mathrm{X}})$$

with $d^{\mathrm{N}}_{100\ \mathrm{pF}}$ the relative deviation of the 100 pF standard #1256 from nominal, $d^{\mathrm{N}}_{10\ \mathrm{pF,X}}$ the relative deviation of the 10 pF standard X from nominal (with X either #1257, #1258, or #1310), and $d^{\mathrm{N}}_{\mathrm{X}}$ the relative deviation from the nominal ratio 10. The results of those participants who did not measure at the reference frequency of 1233 Hz are interpolated to the reference frequency using the frequency dependence measured by the particular participant.

The 100 pF:10 pF ratios are not constant in time, but exhibit a non-linear drift behaviour. The CRV of each 100 pF:10 pF ratio is written as

$$d^{\mathrm{CRV}}_{\mathrm{X}}(t) = d^{\mathrm{PTB}}_{\mathrm{X}}(t) + \Delta_{\mathrm{X}}$$

with Δ_{X} a time-independent parameter determined from a weighted least-squares fit optimisation process including the results (and uncertainties) of all participants.
The results of the 100 pF:10 pF ratios are shown in Figure 4.9.5 and Figure 4.9.6. The agreement of the results of all participants is excellent. For the sake of completeness, also the initial LNE results (see Section 4.5) are shown.

Numerical differences of the three 100 pF:10 pF ratios measured by a participant and the pilot laboratory are given in Table 4.9.7. Numerical differences of the BIPM and NMIA results are given in Table 4.9.8. The standard deviation of the individual results of each participant (shaded in grey and corrected for the change of the standards due to the unthermostated transportations where needed and as indicated) agrees well with the quoted uncertainties. Therefore, the CRV is calculated by a weighted least-squares fit optimisation process (as described in Section 4.7) and includes the results (and uncertainties) of all participants.

Numerical differences between the 100 pF:10 pF ratios of each participant and the CRV are quoted in Table 4.9.9. The results of all participants are fully equivalent with each other and with the CRV; some of the uncertainties even seem to be somewhat overestimated.

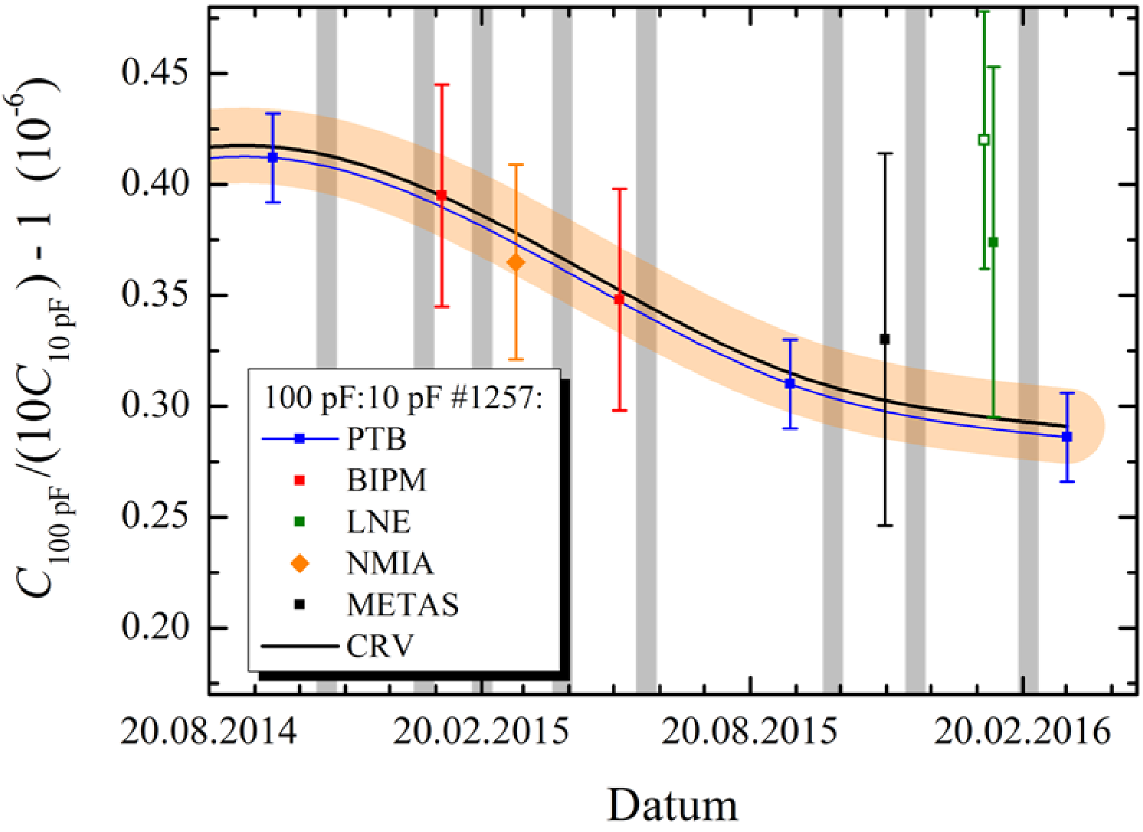

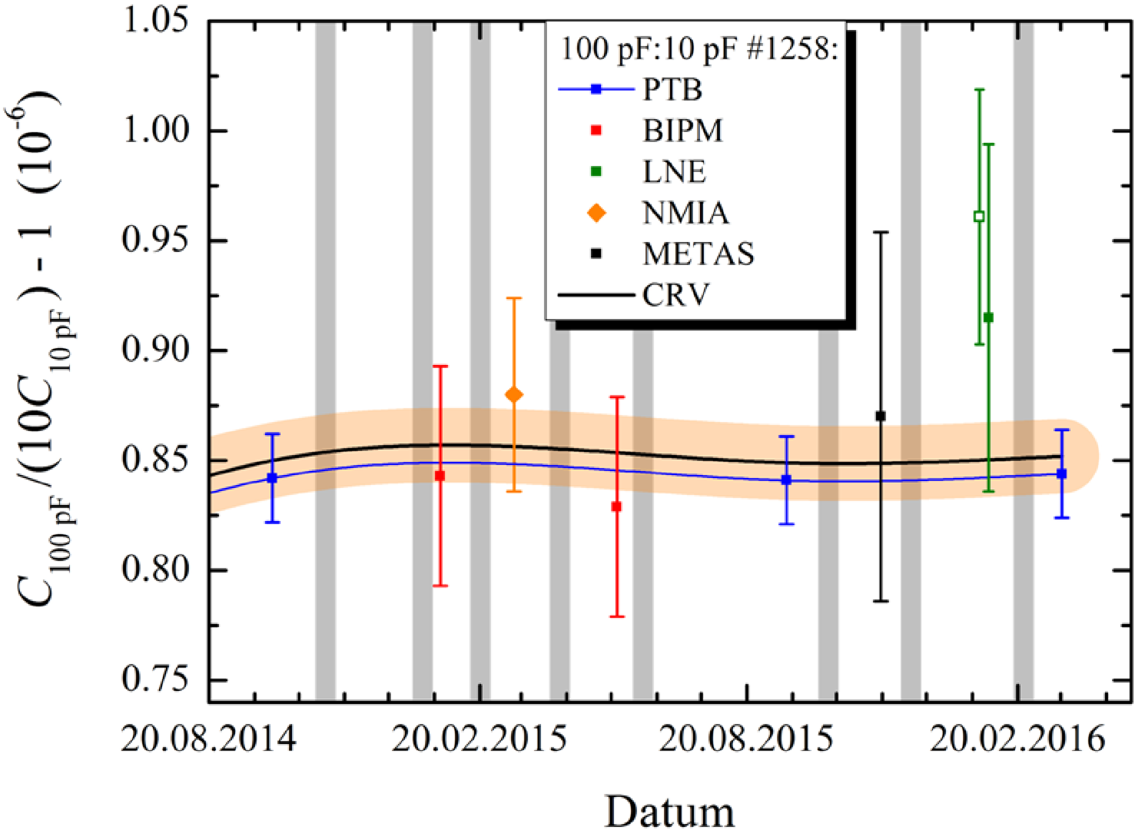

Figure 4.9.5: The ratio of 100 pF AH #1256 to 10 pF AH #1257 (top) and to 10 pF AH #1258 (bottom) at the reference frequency of 1233 Hz (with the corrections as discussed in the text). The uncertainty bars correspond to coverage factor *k* = 2. The transportations and the allocated two-week relaxation intervals are indicated in light grey. The solid black line is the CRV with the 95% confidence band in light orange. The open symbols indicate the initial LNE results which are slightly shifted in time for better visibility.

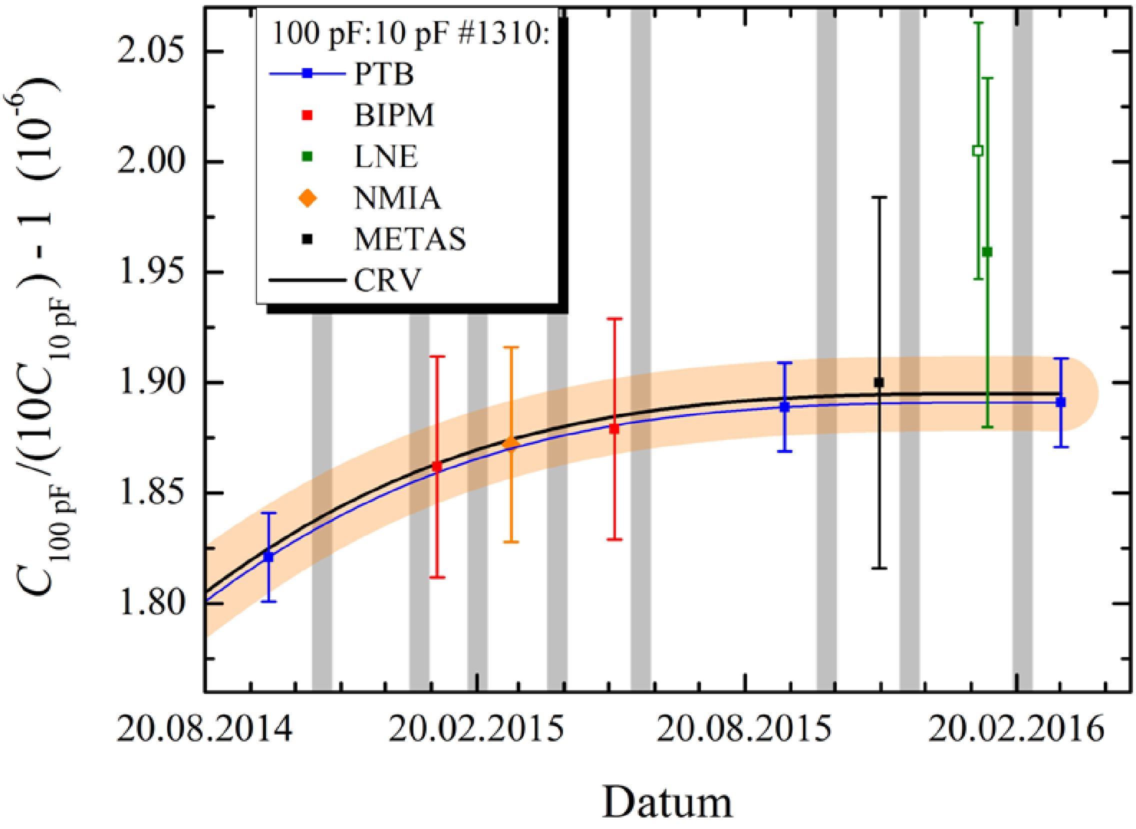

Figure 4.9.6: The ratio of 100 pF AH #1256 to 10 pF AH #1310 at the reference frequency of 1233 Hz (with the corrections as discussed in the text). The uncertainty bars correspond to coverage factor *k* = 2. The transportations and the allocated two-week relaxation intervals are indicated in light grey. The solid black line is the CRV with the 95% confidence band in light orange. The open symbol indicates the initial LNE result which is slightly shifted in time for better visibility.

Table 4.9.7: The differences between the 100 pF:10 pF ratios d_X^N measured by a participant N and PTB (interpolated to the mean time of the measurement of the particular participant), measured at or interpolated to the reference frequency of 1233 Hz. Also the mean differences and the standard deviation of the individual differences are quoted. All uncertainties refer to coverage factor k = 2.

Quantity	$d_X^N - d_X^{PTB}$ [10^{-9}]				
	$BIPM_1$ - PTB *)	**$BIPM_2$ - PTB *)**	**LNE - PTB**	**METAS - PTB**	**NMIA - PTB *)**
X = AH #1257	5	1	84	33	-7
X = AH #1258	-6	-16	73	30	32
X = AH #1310	3	-2	68	10	2
mean value $d^N - d^{PTB}$	1 ± 3	-6 ± 5	75 ± 7	24 ± 7	9 ± 12
uncertainty of d^N	50		79	84	40
uncertainty of d^{PTB}	23				
total uncertainty	55		82	87	46
final result	-3 ± 55		75 ± 82	24 ± 87	9 ± 46

*) includes a correction for correlation with ($BIPM_2$ - $BIPM_1$)

Table 4.9.8: The differences between the 100 pF:10 pF ratios d_X^N measured by the BIPM and NMIA, both interpolated to the reference frequency of 1233 Hz. (The mean BIPM value is used here because a linear drift of the travelling standards cancels from the difference to NMIA.) Also the mean difference and the standard deviation of the individual differences are quoted. The uncertainties refer to coverage factor k = 2.

Quantity	$d_X^{BIPM} - d_X^{NMIA}$ [10^{-9}]
	($BIPM_1$ + $BIPM_2$)/2 - NMIA*)
X = AH #1257	8
X = AH #1258	-43
X = AH #1310	-2
mean $d^{BIPM} - d^{NMIA}$	-12 ± 22
uncertainty of d^{BIPM}	50
uncertainty of d^{NMIA}	40
total uncertainty	64
final result	-12 ± 64

*) includes a correction for correlation with ($BIPM_2$ - $BIPM_1$)

Table 4.9.9: The differences between the 100 pF:10 pF ratios d_X^N measured by a participant N at or interpolated to the reference frequency of 1233 Hz and the CRV. Also the mean differences and the standard deviation of the individual differences are quoted. All uncertainties refer to coverage factor k = 2.

Quantity	$d_X^N - d_X^{CRV}$ [10^{-9}]					
	PTB - CRV	**$BIPM_1$ - CRV**	**$BIPM_2$ - CRV**	**LNE - CRV**	**METAS - CRV**	**NMIA - CRV**
X = AH #1257	-5	0	-4	79	28	-12
X = AH #1258	-8	-14	-24	65	22	24
X = AH #1310	-4	-1	-6	64	6	-2
mean value $d^N - d^{CRV}$	-6 ± 2	-5 ± 6	-11 ± 9	69 ± 7	19 ± 9	11 ± 15
uncertainty of d^N	22	50		79	84	40
uncertainty of d^{CRV}	22					
total uncertainty	31	55		82	87	46
degree of equivalence	-6 ± 31	-8 ± 55		69 ± 82	19 ± 87	11 ± 46

4.9.3 Frequency dependence of the capacitance standards

Measuring the frequency dependence of the travelling standards was an optionally task for those participants which were capable of operating their measuring bridges at multiple frequencies. Results were provided by the BIPM, LNE, NMIA and PTB. The BIPM has measured the frequency dependence at two periods (before and after the NMIA period); because for each travelling standard the difference between the two BIPM frequency dependences is much smaller than the quoted total uncertainty, only the mean BIPM frequency dependence of each standard is presented here. The results of each participant with respect to the reference frequency 1233 Hz are shown in Figure 4.9.7 and Figure 4.9.8 and are found to be in good agreement. For the sake of completeness, also the initial LNE results (without the corrections submitted after the first presentation of Draft A; see Section 4.5) are shown.

The frequency dependence in the kHz range can be approximated either by a linear or a polynomial function or by a power-law (also known as Jonscher law), depending on the number and range of available test frequencies and on the uncertainties. Here the linear approach has been chosen. Even though there is no physical reason to assume a strictly linear frequency dependence, the uncertainty and frequency range of the available data do not allow a significant discrimination of higher order functions. Furthermore, the linear approach characterises the frequency dependence by a *single* parameter, the frequency coefficient (whereas other approaches require a higher number of parameters to be compared). The results are given in Table 4.9.10. For each travelling standard, the results of all contributing participants are found to be in excellent agreement with the particular weighted mean value. The results are also in agreement with those of the first circulation (Section 4.8.3), but at the second circulation, the number of participants and frequencies is larger and the uncertainties are smaller.

The frequency dependence of the travelling standard AH #1310 has also been measured at the BIPM in 2004 [3] and the frequency coefficient around 1233 Hz was (-20 ± 16)·10^{-9}/kHz at $k = 1$ (as can be read from Figure 4 of Ref. 3). The frequency dependence actually measured by the BIPM within the framework of this comparison (marked in Table 4.9.10 with red colour) is in excellent agreement with the former measurement. This shows that the frequency dependence of this standard as well as the measuring bridges of the BIPM have not changed since that time. The frequency coefficients of the other capacitance standards are slightly more negative than for AH #1310.

Because the results of the frequency coefficients are equivalent with each other, the weighted mean values quoted in Table 4.9.10 are taken as the CRV and are used to calculate the degree of equivalence given in Table 4.9.11. In summary, the results of the frequency coefficients are found to be fully equivalent with the CRV and with each other.

Table 4.9.10: Frequency coefficient of the travelling standards around the reference frequency of 1233 Hz and the associated uncertainty (*k* = 2). Also the weighted mean values are given.

Nominal value and SN	Frequency coefficient and the associated $k = 2$ uncertainty (10^{-9}/kHz)				
	PTB	BIPM	NMIA	LNE	weighted mean
100 pF #1256	-105 ± 31	-76 ± 34	-91 ± 78	-111 ± 36	-97 ± 18
10 pF #1257	-118 ± 31	-96 ± 34	-124 ± 77	-86 ± 57	-106 ± 20
10 pF #1258	-131 ± 31	-118 ± 34	-124 ± 78	-111 ± 57	-123 ± 20
10 pF #1310	-74 ± 31	-25 ± 34	-61 ± 72	+10 ± 57	-45 ± 20

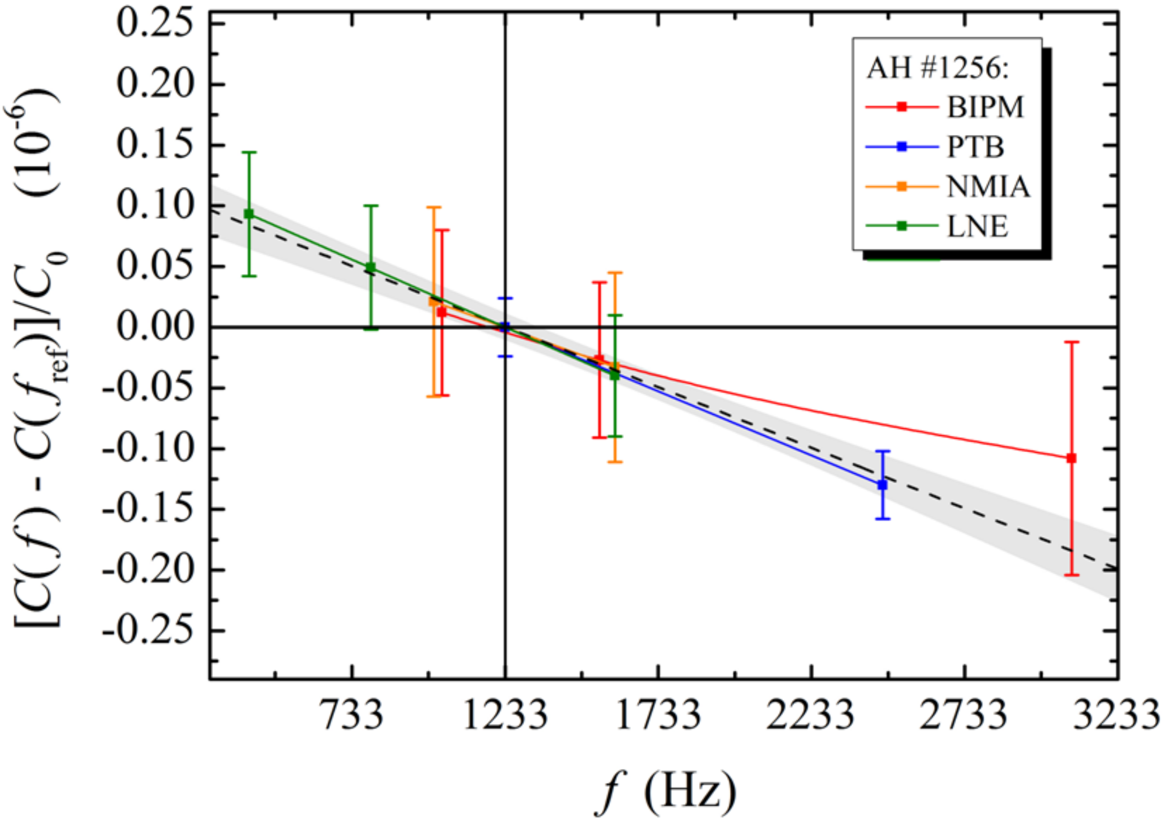

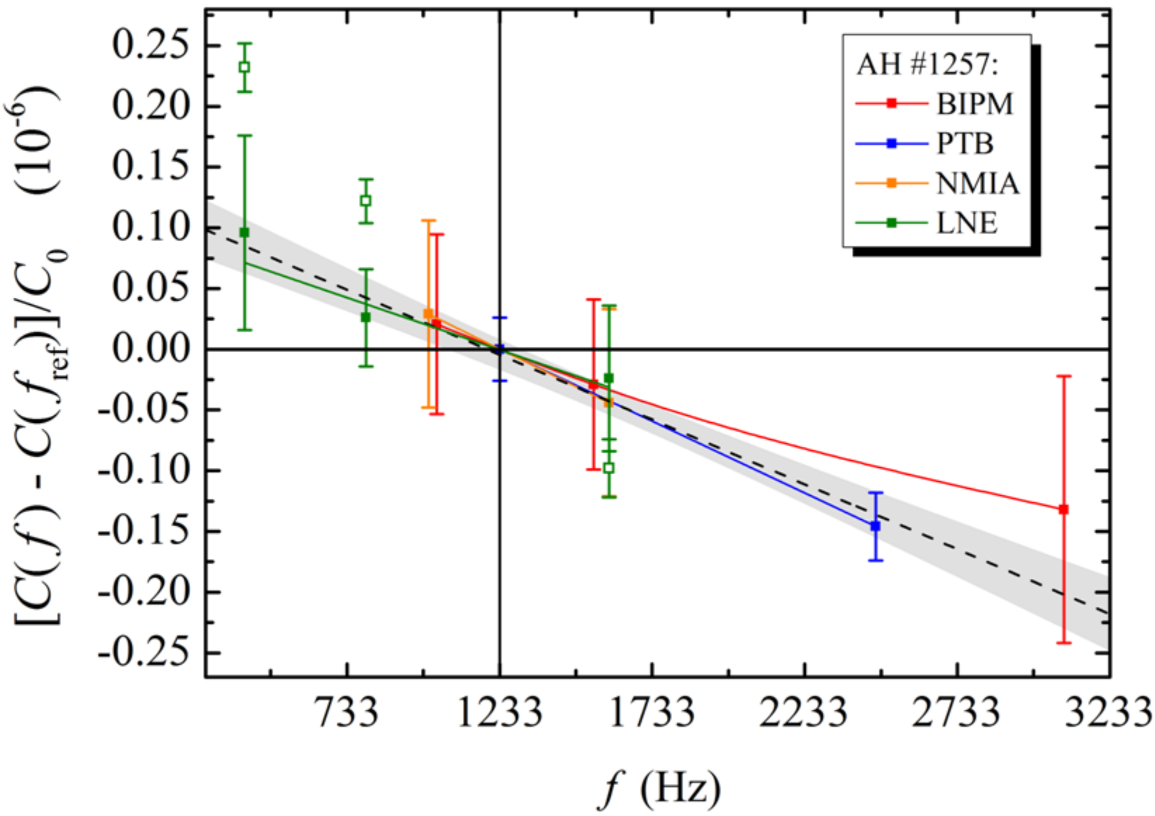

Figure 4.9.7: The frequency dependence of the capacitance standards 100 pF AH #1256 (top) and 10 pF AH #1257 (bottom) with respect to the particular value interpolated to the reference frequency 1233 Hz, as measured by the participants. C_0 is the particular nominal value. All uncertainty bars refer to coverage factor k = 2. The dashed line is a linear least-squares fit of all data with the 95% confidence band in light grey. The coloured solid lines are least-squares fits of the results of each participant and are just a guide to the eye. The open symbols in the bottom diagram are the initial LNE results.

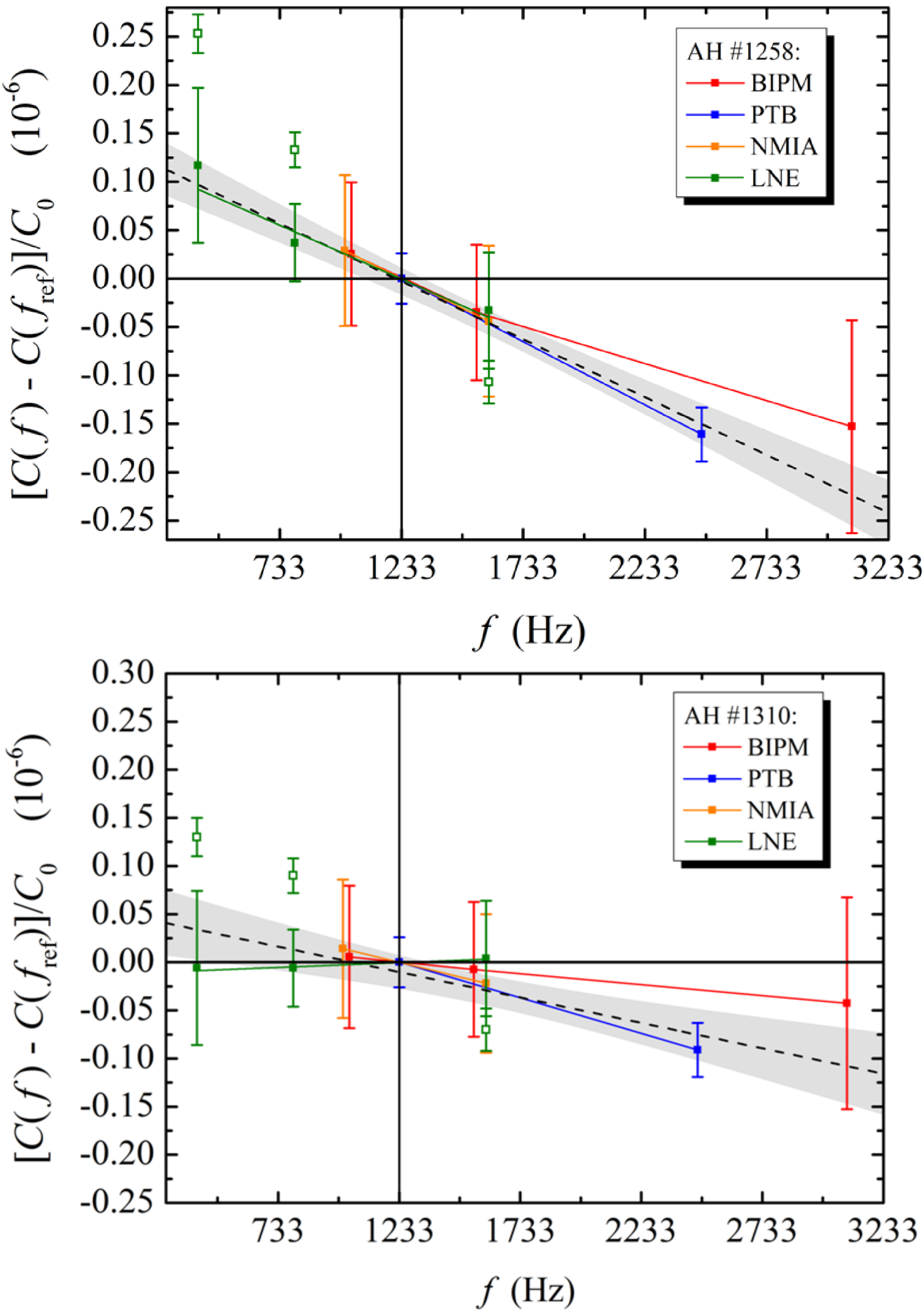

Figure 4.9.8: The frequency dependence of the capacitance standards 10 pF AH #1258 (top) and 10 pF AH #1310 (bottom) with respect to the particular value interpolated to the reference frequency 1233 Hz, as measured by the participants. C_0 is the particular nominal value. All uncertainty bars refer to coverage factor k = 2. The dashed line is a linear least-squares fit of all data with the 95% confidence band in light grey. The coloured solid lines are least-squares fits of the results of each participant and are just a guide to the eye. The open symbols are the initial LNE results.

Table 4.9.11: The differences between the frequency coefficients measured by a participant and the CRV (i.e., the weighted mean value of each particular standard). All quoted uncertainties refer to coverage factor k = 2.

Nominal value and SN	degree of equivalence (10^{-9}/kHz)			
	PTB - CRV	BIPM - CRV	NMIA - CRV	LNE - CRV
100 pF #1256	-8 ± 36	21 ± 39	6 ± 80	-14 ± 41
10 pF #1257	-12 ± 37	10 ± 39	-18 ± 79	20 ± 60
10 pF #1258	-8 ± 37	5 ± 39	-1 ± 80	12 ± 60
10 pF #1310	-29 ± 37	20 ± 39	-16 ± 74	55 ± 60
mean DoE	-14 ± 37	14 ± 39	-7 ± 78	18 ± 44

4.9.4 Summary of the second capacitance circulation

The results of the 10 pF standards at the reference frequency of 1233 Hz, the 100 pF:10 pF ratios at the reference frequency, and also the frequency dependences of the 100 pF and 10 pF travelling standards are found to be in good agreement and fully equivalent (but LNE has submitted corrections after the initial results were distributed). Compared to the first circulation, the expanded relative uncertainty of the 10 pF standards got improved to values as low as $26 \cdot 10^{-9}$, whereas the uncertainties of the 100 pF:10 pF ratios remained practically the same. In addition, the results of those participants who contributed to both capacitance circulations show almost the same pattern relative to each other. (For example, the PTB results are always a bit larger than the BIPM results and the METAS results are always a bit smaller, but in every case covered by the particular uncertainties). This demonstrates that the total uncertainties are dominated by reproducible type B contributions and that the corrections applied as well as the method of analysis are appropriate.

Also the frequency dependence of the capacitance standards was measured again. Compared to the first circulation, the frequency dependence could be determined more reliably and over a much wider frequency range so that the uncertainty of the frequency coefficients got improved.

5. Summary and conclusion

Within the framework of this comparison, three 10 pF and one 100 pF Andeen Hagerling capacitance standards were circulated between the participants and the capacitance values were traced to the quantum Hall resistance, measured either with ac or dc, and expressed in terms of the conventional value of the von Klitzing constant $R_{K\text{-}90}$ = 25812.807 Ω. The comparison comprised one 100 pF capacitance standard to allow testing the 10:1 calibration of the participants because their measuring chains include multiple 10:1 steps. Three 10 pF capacitance standards were circulated for the sake of redundancy.

The first circulation loop of the travelling capacitance standards revealed significant discrepancies. Because the discrepancies were frequency dependent, the ac resistance standards involved in the measuring chain of each participant (i.e., either the ac quantum Hall resistance or calculable ac-dc resistors) were suspected. Therefore, two Vishay resistors with a nominal value of $R_{K\text{-}90}/2$ =12906.4035 Ω were circulated and their frequency dependences were measured traceable to the participant's ac resistance standards. Two resistors (instead of one) were circulated for the sake of redundancy and Vishay resistors were chosen because they are robust and their frequency dependence is not affected by transportation. The results of the linear frequency dependence of the two circulated Vishay resistors were found to be fully equivalent within expanded relative uncertainties of $3.3\cdot10^{-9}$ kHz^{-1} and $4.9\cdot10^{-9}$ kHz^{-1}, respectively, which is excellent. This means that the frequency dependences of the ac-dc resistance standards and the ac quantum Hall resistance used in the measuring chains of the participants conform each other within the particular uncertainties.

While the Vishay resistors were circulated, the participants had a chance to check and, where necessary, to improve their measuring bridges. In fact, some participants discovered systematic bridge errors and submitted corrections. Nevertheless, it was decided to repeat the circulation of the capacitance standards. To yield additional information, it was also decided to transport the travelling capacitance standards to NMIA to get a link to their calculable capacitor. Compared to the first capacitance circulation, the capacitance standards have slightly changed their values by different amount; it thus was ensured that the participants were practically unbiased, which is an important precondition of a comparison.

The comparison also led to new findings regarding the properties of the commercial Andeen Hagerling capacitance standards. The long-term behaviour of these standards is found to exhibit variations on different time scales ranging from a few days up to a few years; the associated relative peak-to-peak amplitudes differ for the individual standards and amount to $(15 - 40)\cdot10^{-9}$ at a time scale of a few days and $(150 - 300)\cdot10^{-9}$ on a time scale of a few years. The magnitude of these variations is found to be correlated with the ambient temperature coefficient of the particular standard. This shows that the instabilities are presumably caused by the imperfection of the internal temperature controllers.

Also the travelling behaviour of the capacitance standards has been investigated. A thermostated transportation by the car of a skilled driver is found to cause no significant jumps and no relaxation effects lasting longer than one week. This also applies to unthermostated transportation by car. Consequently, the results of the first capacitance circulation were not significantly affected, even though the powering of the thermostats has failed during some of the transportations. At the second capacitance circulation, the powering system for the transportations within Europe has been improved and worked successfully. In contrast, the travelling standards were sent unthermostated to, and back from, NMIA by airfreight. Unfortunately, this has caused jumps of the capacitance values, accompanied with long lasting relaxation effects. It turned out that also these effects do not directly originate from the fused-silica elements themselves, but from the internal temperature controllers. Fortunately, these effects could be eliminated by a refined analysis. Most of the imperfections of the four travelling AH capacitance standards are within the specifications of the manufacturer (Annex 13). This demonstrates excellent behaviour of the AH capacitance standards when carefully handled as well as potential for further improvements. So far, the imperfection and the permanent instability of the travelling standards made it necessary to increase the uncertainty of the CRV.

At the end of this comparison, the 10 pF results (either measured at, or interpolated to, the reference frequency of 1233 Hz) obtained by all participants and at both circulations are fully equivalent within expanded relative uncertainties as low as $26\cdot10^{-9}$. Also the 100 pF:10 pF ratios of both circulations are fully equivalent, within expanded relative uncertainties as low as $13\cdot10^{-9}$.

Also the frequency dependence of the travelling capacitance standards has been compared (as far as the participants were capable of measuring it) and is found to be fully equivalent within expanded relative uncertainties as low as $3\cdot10^{-8}$ kHz^{-1}. Measurement of the voltage dependence of the travelling capacitance standards was an optionally task and has been carried out by the BIPM and PTB. The results are found to be equivalent within relative expanded uncertainties of $1.4\cdot10^{-10}$ V^{-1} for the 10 pF standards and $1.4\cdot10^{-9}$ V^{-1} for the 100 pF standard.

Apart from the base uncertainties of the particular measuring chains, the quoted uncertainties include contributions due to the imperfection of the travelling standards, due to corrections for deviations from nominal conditions, and due to corrections of systematic bridge errors (where applicable). In fact, the ac measuring technique is prone to delicate systematic effects at a level of $1\cdot10^{-7}$, whereas the calculated base uncertainty might be much lower (as low as $6\cdot10^{-9}$ at 10 pF and $k = 1$). Thus, a comparison is a proper, and indispensable, instrument to rectify the ac measuring bridges of the participants, indeed at a more moderate level of uncertainty. On the other hand, the uncertainties achieved are excellent and, as far as known to us, a capacitance comparison has never been carried out with a lower uncertainty.

Finally, the capacitance measurements of the participants either traced to the conventional value of the von Klitzing constant or to the NMIA calculable capacitor can be considered as a determination of the von Klitzing constant, with measurements at different countries and across continents. The relative difference of the von Klitzing constant determined at this comparison and the actual 2014 CODATA value R_K = 25812.8074555 (59) Ω is

$$(R_\mathrm{K,comparison} - R_\mathrm{K,CODATA})/\,R_\mathrm{K,CODATA} = (9 \pm 84)\cdot10^{-9}$$

The agreement within the quoted expanded uncertainty is excellent and verifies the reliability of this comparison. (Of course, this value of the von Klitzing constant is not independent of former determinations by NMIA.) The uncertainty is dominated by the NMIA calculable capacitor even though this is a formidable calculable capacitor. Compared to this, the uncertainty of the farad derived from the quantum Hall resistance can be much smaller. This is very promising with respect to the forthcoming revised SI in which the von Klitzing constant $R_\mathrm{K} \equiv h/e^2$ will be an exact quantity because the Planck constant, h, and the elementary charge, e, will be exactly defined.

6. References

[1] D. R. White, „On the analysis of measurement comparisons", *Metrologia* **41/3**, 122-131, 2004.

[2] B. Jeckelmann and M. Zeier, „Analysis of measurement comparison EURO-MET.EM-K2", Conference on precision electromagnetic measurements (CPEM), 8-13 June 2008, Broomfield, CO, USA; conference digest p. 144.

[3] F. Delahaye and R. Goebel, „Evaluation of the frequency dependence of the resistance and capacitance standards in the BIPM quadrature bridge", *IEEE Trans. Instrum. Meas.* **54**, 533-537, 2005.

[4] J. Schurr, V. Bürkel, B. P. Kibble, „Realizing the farad from two ac quantum Hall resistances", *Metrologia* **46**, 619-628, 2009.

[5] D. Cutkosky, „Techniques for comparing Four-Terminal-Pair admittance standards", J*ournal of Research of the NBS*, Vol. 74C, No 3 and 4, p. 63, 1970.

[6] B.P. Kibble, G.H. Rayner, „Coaxial AC Bridges", *Ed. A. E. Bailey*, 1984.

[7] J. Bohácek, „EUROMET project 432: frequency performance of 12906 Ω and 6453 Ω reference resistors for ac quantum Hall effect experiments", *Metrologia* **39**, 231-237, 2002.

[8] F. Overney, „The quantized Hall resistance: towards a primary standard of impedance", *Metrologia* **43**, 409-413, 2006.

[9] A. M. Thompson and D. G. Lampard, „A New Theorem in Electrostatics and its Application to Calculable Standards of Capacitance", Nature, Vol. 177, p. 888, 1956.

[10] A. M. Thompson, „The Cylindrical Cross-capacitor as a Calculable Standard", Proc. IEE, Vol. 106, Part B No. 27, 307-310, 1959.

[11] W. K. Clothier, „A Calculable Standard of Capacitance", Metrologia, Vol. 1, No. 2, 35-56, 1965.

[12] G. W. Small, „Twenty Years of SI Ohm Determinations at NML", IEEE Trans. Instrum. Meas., Vol. IM-36, No. 2, 190-195, 1987.

[13] G. Rietveld, J.M. Williams, E. Houtzager and T.J.B.M. Janssen, "Automated CCC bridge for precision resistance measurements", *CPEM 2006 Conference Digest*, Turino, 496 - 497, 2006.

[14] G. Rietveld and C.J. van Mullem, „Uncertainty analysis of a DVM-based quantum Hall measurement set-up", *CPEM 2000 Conference Digest*, Sydney, 90 - 91, 2000.

[15] B.P. Kibble, A. Hartland and S.W. Chua, „Calculable AC/DC Resistor for AC Quantized Hall Resistance Experiments", *8th Int'l Conf. On Electromagnetic Measurement, BEMC*, November 1997, UK, 34/1-34/4.

[16] J. Boháček, B.M. Wood, „Octofilar resistors with calculable frequency dependence", *Metrologia*, vol. 38, 241-247, 2001.

[17] I. Robinson et al., „Key comparison CCEM-K7: AC voltage ratio", Metrologia, vol. 49, no. 1A, pp. 01007-01007, 2012.

[18] F. Overney, F. Lüönd, and B. Jeanneret, "Broadband fully automated digitally assisted coaxial bridge for high accuracy impedance ratio measurements," *Metrologia*, vol. 53, no. 3, pp. 918–926, 2016.

7. Annex: List of participants

Participant: Physikalisch-Technische Bundesanstalt
Acronym: PTB
Contact person: Jürgen Schurr
Address: Bundesallee 100, D-38116 Braunschweig, Germany
Tel.: +49 531 592 2114
Fax: +49 531 592 2105
E-mail: Juergen.Schurr@ptb.de

Participant: Bureau International de Poids et Mesures
Acronym: BIPM
Contact person: Nick Fletcher
Address: Pavillon de Breteuil, F-92312 Sèvres Cedex, France
Tel.: +33 1 45 07 70 47
E-mail: nick.fletcher@bipm.org

Participant: Laboratoire national de métrologie et d’essais
Acronym: LNE
Contact person: Olivier Thévenot
Address: 1, rue Gaston Boissier, F-75724 Paris Cedex 15, France
Tel.: +33 130 69 2176
E-mail: olivier.thevenot@lne.fr

Participant: Federal Institute of Metrology
Acronym: METAS
Contact person: Frédéric Overney
Address: Lindenweg 50, CH-3003 Bern-Wabern, Switzerland
Tel.: +41 31 32 33 296
Fax: +41 31 32 33 210
E-mail: frederic.overney@metas.ch

Participant: VSL Dutch Metrology Institute
Acronym: VSL
Contact person: Gert Rietfeld
Address: Thijsseweg 11, NL-2629 JA Delft, Netherlands
Tel.: +31 15 269 1500
Fax: +31 15 261 29 71
E-mail: grietfeld@vsl.nl

Participant: National Measurement Institute, Australia
Acronym: NMIA
Contact person: Heather Johnson
Address: Bradfield Road, West Lindfield, NSW 2070, Australia
Tel.: +61 2 8467 3529
Fax: +61 2 8467 3752
E-mail: Leigh.Johnson@measurement.gov.au

8. Annex: Detailed results of travelling AC resistance standards and uncertainty budgets

8.1 Detailed results and uncertainty budget of the BIPM

The following tables give the individual results (for pairs of frequencies), the estimated uncertainties at each frequency, and a summary of the results and total uncertainties (expressed as expanded uncertainties at 95% confidence, using a coverage factor $k = 2$). For all uncertainty components, the effective degree of freedom is estimated to be sufficiently large for this expansion to be valid.

Table 1: individual results for pairs of frequencies on each resistor. The results are expressed as the relative change in the resistance, in parts in 10^6, between the stated frequency, f, and the reference frequency 1610 Hz, such that $\Delta = \frac{R_f - R_{1610}}{R_{1610}} \times 10^6$. The type A standard uncertainty for each measurement is indicated in brackets. Each reported result is the mean difference observed during a series of 11 measurements with interleaved frequencies, taken over a period of around 1 hour.

Date	Resistor	Frequency /Hz	Δ
17/12/2013	BIPM	3210	−0.0716(22)
18/12/2013	BIPM	810	+0.0321(31)
18/12/2013	BIPM	410	+0.0553(33)
21/01/2014	BIPM	410	+0.0619(29)
21/01/2014	BIPM	810	+0.0374(29)
22/01/2014	BIPM	3210	−0.0630(15)
22/01/2014	LNE	3210	−0.0056(15)
23/01/2014	LNE	810	+0.0207(23)
23/01/2014	LNE	410	+0.0430(19)
05/02/2014	LNE	410	+0.0423(31)
05/02/2014	LNE	810	+0.0241(45)
10/02/2014	LNE	3210	+0.0173(27)
05/03/2014	LNE	2	+0.0627(56)
05/03/2014	BIPM	2	+0.0588(27)

Table 2: uncertainty budget for coaxial bridge measurements at each frequency, given as relative standard uncertainties (un-expanded), as parts in 10^9.

Standard uncertainties, relative, parts in 10^9	**410 Hz**	**810 Hz**	**1610 Hz**	**3210 Hz**
Coaxial reference resistor	1	1.5	2.5	14
10:1 divider calibration	10	10	10	20
Realization of 4 term-pair conditions	10	2	2	5
Imperfect cable corrections	1	2	5	15
Imperfect current equalisers	10	10	10	10
Influence of Wagner balance	1	1	1	5
Injector phase	1	1	1	1
RSS	**17**	**14**	**15**	**31**

Table 3: uncertainty for measurements using the room temperature current comparator bridge (at frequency 2 Hz), given as relative standard uncertainties (un-expanded), as parts in 10^9.

Standard uncertainties, relative, parts in 10^9	**2 Hz**
Global uncertainty of RTCC bridge, including 10:1 ratio	10
Uncertainty in correction for 4-term outer resistance	5
Self-heating in coaxial standard	10
RSS	**15**

Table 4: global uncertainties for the results expressed relative to the reference frequency 1610 Hz

Uncertainties, parts in 10^6	**2 Hz**	**410 Hz**	**810 Hz**	**3210 Hz**
Combined standard uncertainty	0.022	0.023	0.021	0.035
Expanded *U*, *k*=2, 95 %	**0.044**	**0.046**	**0.042**	**0.070**

Table 5: Mean results derived from table 1. As in table 1, the results are expressed as the relative change in the resistance, in parts in 10^6, between the stated frequency, *f*, and the reference frequency 1610 Hz, such that $\Delta = \frac{R_f - R_{1610}}{R_{1610}} \times 10^6$. The uncertainties reported in brackets are the overall expanded uncertainties (*k*=2, 95 %) from table 4.

	BIPM Resistor	**LNE Resistor**
2 Hz	+0.063(44)	+0.059(44)
410 Hz	+0.059(46)	+0.043(46)
810 Hz	+0.035(42)	+0.022(42)
1610 Hz	-	-
3210 Hz	−0.067(70)	+0.006(70)

8.2 Detailed results and uncertainty budget of LNE

Ambient conditions

The ambient temperature and the relative humidity of the rooms where the measurements were performed are regulated at (23 ± 0.3) °C and (45 ± 10)% respectively.

Test frequencies

The measurements were made at three frequencies : 397.89 Hz, 795.77 Hz and 1591.55 Hz.

Test voltages

For all three frequencies the applied voltage was equal to 1.3 V on the BIPM resistor (current of 100 µA) and 2 V on the LNE resistor (current of 150 µA).

Period of measurement

The frequency dependence of the resistor RES-ELEC-17 from BIPM was measured from 22 to 29 January 2013.
The frequency dependence of the resistor S/N 1025665 from LNE was measured four times: (1) at the beginning of the circulation from 12 to 24 October 2012, (2) after measurement at PTB from 20 to 22 November 2012, and (3) after measurement at METAS (and stay at BIPM without measurement) from 9 to 14 August 2013 (4) after measurement at BIPM from 05 to 10 june 2014.

Results summary

Resistor BIPM RES-ELEC-17

Nominal value : 12906 Ω Mean resistor temperature: 29.47 kΩ

Test frequency (Hz)	Voltage (V)	Mean date of measurement	Difference from DC ($\times10^{-6}$)	Combined standard uncertainty ($\times10^{-6}$)	Effective degrees of freedom	Expanded uncertainty (95% coverage factor, k=2) ($\times10^{-6}$)
397.89	1.3	25/01/2013	-0.012	0.006	81	0.012
795.77	1.3	25/01/2013	-0.021	0.006	84	0.012
1591.55	1.3	25/01/2013	-0.045	0.008	50	0.016

Resistor LNE S/N 1025665

Nominal value : 12906 Ω Mean resistor temperature: 24.95 °C

Test frequency (Hz)	Voltage (V)	Mean date of measurement	Difference from DC ($\times10^{-6}$)	Combined standard uncertainty ($\times10^{-6}$)	Effective degrees of freedom	Expanded uncertainty (95% coverage factor, k=2) ($\times10^{-6}$)
397.89	2	06/07/2013	-0.008	0.006	81	0.012
795.77	2	06/07/2013	-0.034	0.006	84	0.012
1591.55	2	06/07/2013	-0.049	0.008	50	0.016

The uncertainty budgets for both resistors are presented for each test frequency:

Uncertainty budget : measurements of difference from DC at 397.89 Hz

Quantity X_i	Estimate x_i	Standard uncertainty $u(x_i)$	Probability distribution /method of evaluation (A,B)	Sensitivity coefficient c_i	Uncertainty contribution on difference from DC ($\times 10^{-6}$)	Degree of freedom ν_i
Four terminal-pair resistance bridge						
Frequency	397.89 Hz	1.10^{-2} Hz	rectangular,B	<$0.05.10^{-6}$ /Hz	0.05	infinite
Bridge ratio correction	$0.090.10^{-6}$	3.10^{-9}	gaussian,B	1	0.3	22
Loading					0.2	13
Null current in high potential ports Adjustement of R_H	1293.50 Ω	0.02 Ω	rectangular, B	3.10^{-9}/Ω	0.06	infinite
Adjustement of C_H	7.66 nF	0.006 nF	rectangular, B	2.10^{-6}/nF	0.01	infinite
Null current in low potential ports Adjustement of R_B	1290.99 Ω	0.02 Ω	rectangular, B	4.10^{-9} /Ω	0.08	infinite
Adjustement of C_B	0.79 nF	0.006 nF	rectangular, B	1.10^{-7} /nF	0.06	infinite
Kelvin Arm Adjustement in phase (k_p)	0.0904900	0.00006	rectangular, B	2.10^{-6}	0.01	infinite
Adjustement in quadrature (k_q)	0.0966800	0.00006	rectangular, B	2.10^{-6}	0.01	infinite
Main balance (readings of inductive dividers x100) * Adjustement in phase (kp)	0.0208000	0.00000012	rectangular, B	1	0.12	infinite
Adjustement in quadrature (k_q)	0.0002500	0.00000012	rectangular, B	1.10^{-4}	0	infinite
Frequency effect of the Haddad resistor					0.1	13
Relative uncertainty of the main detector	0 nV	0.1 nV	rectangular, B	5.10^{-9} /nV	0.05	22
Coaxility defect			gaussian,B		0.15	22
Temperature of the Haddad resistor	23°C	0.006 °C	gaussian,B	2.10^{-8} /°C	0.01	22
Temperature of the transfer resistor	25°C	0.006 °C	gaussian,B	2.10^{-8} /°C	0.01	22
Cable correction					0.1	13
Extrapolation of ratio difference from nominal at DC from ratio differences measured at all three frequencies	208.10^{-6}	3.10^{-9}	rectangular, B	1	0.3	13
Variability of repeated measurements			Type A		0.1	17
Combined standard uncertainty on difference from DC at 397.89 Hz					**0.55**	81

(*) Readings of the inductive dividers used to balance the bridge in phase and quadrature; the dividers are followed by an 1:100 injection transformer and the readings must then be divided by 100.

Uncertainty budget : measurements of difference from DC at 795.77 Hz

Quantity X_i	Estimate x_i	Standard uncertainty $u(x_i)$	Probability distribution /method of evaluation (A,B)	Sensitivity coefficient c_i	Uncertainty contribution on difference from DC ($\times 10^{-8}$)	Degree of freedom ν_i
Four terminal-pair resistance bridge						
Frequency	795.77 Hz	1.10^{-2} Hz	rectangular,B	$<0.05.10^{-6}$ /Hz	0.05	infinite
Bridge ratio correction	$0.222.10^{-6}$	3.10^{-9}	gaussian,B	1	0.3	22
Loading					0.2	13
Null current in high potential ports Adjustement of R_H	1293.40 Ω	0.02 Ω	rectangular, B	3.10^{-8}/Ω	0.06	infinite
Adjustement of C_H	7.58 nF	0.006 nF	rectangular, B	2.10^{-6}/nF	0.01	infinite
Null current in low potential ports Adjustement of R_B	1290.96 Ω	0.02 Ω	rectangular, B	4.10^{-8} /Ω	0.08	infinite
Adjustement of C_B	0.75 nF	0.006 nF	rectangular, B	1.10^{-7} /nF	0.06	infinite
Kelvin Arm Adjustement in phase (k_p)	0.0891000	0.00006	rectangular, B	2.10^{-6}	0.01	infinite
Adjustement in quadrature (k_q)	0.0958100	0.00006	rectangular, B	2.10^{-6}	0.01	infinite
Main balance (readings of inductive dividers x100) * Adjustement in phase (kp)	0.0208000	0.00000012	rectangular, B	1	0.12	infinite
Adjustement in quadrature (k_q)	0.0004980	0.00000012	rectangular, B	1.10^{-4}	0	infinite
Frequency effect of the Haddad resistor					0.3	13
Relative uncertainty of the main detector	0 nV	0.1 nV	rectangular, B	5.10^{-9} /nV	0.05	22
Coaxility defect			gaussian,B		0.15	22
Temperature of the Haddad resistor	23°C	0.006 °C	gaussian,B	2.10^{-8} /°C	0.01	22
Temperature of the transfer resistor	25°C	0.006 °C	gaussian,B	2.10^{-8} /°C	0.01	22
Cable correction					0.1	13
Extrapolation of ratio difference from nominal at DC from ratio differences measured at all three frequencies	208.10^{-6}	3.10^{-9}	rectangular, B	1	0.3	13
Variability of repeated measurements			Type A		0.1	17
Combined standard uncertainty on difference from DC at 795.77 Hz					**0.62**	84

(*) Readings of the inductive dividers used to balance the bridge in phase and quadrature; the dividers are followed by an 1:100 injection transformer and the readings must then be divided by 100.

Uncertainty budget : measurements of difference from DC at 1591.55 Hz

Quantity X_i	Estimate x_i	Standard uncertainty $u(x_i)$	Probability distribution /method of evaluation (A,B)	Sensitivity coefficient c_i	Uncertainty contribution on difference from DC ($\times 10^{-8}$)	Degree of freedom v_i
Four terminal-pair resistance bridge						
Frequency	1591.55 Hz	1.10^{-2} Hz	rectangular,B	<$0.05.10^{-6}$ /Hz	0.05	infinite
Bridge ratio correction	$0.762.10^{-6}$	3.10^{-9}	gaussian,B	1	0.3	22
Loading					0.2	13
Null current in high potential ports Adjustement of R_H	1293.40 Ω	0.02 Ω	rectangular, B	3.10^{-8}/Ω	0.06	infinite
Adjustement of C_H	7.57 nF	0.006 nF	rectangular, B	2.10^{-6}/nF	0.01	infinite
Null current in low potential ports Adjustement of R_B	1290.47 Ω	0.02 Ω	rectangular, B	4.10^{-8} /Ω	0.08	infinite
Adjustement of C_B	0.75 nF	0.006 nF	rectangular, B	1.10^{-7} /nF	0.06	infinite
Kelvin Arm Adjustement in phase (k_p)	0.0831000	0.00006	rectangular, B	2.10^{-6}	0.01	infinite
Adjustement in quadrature (k_q)	0.0966800	0.00006	rectangular, B	2.10^{-6}	0.01	infinite
Main balance (readings of inductive dividers x100) * Adjustement in phase (kp)	0.0208000	0.00000012	rectangular, B	1	0.12	infinite
Adjustement in quadrature (k_q)	0.0009990	0.00000012	rectangular, B	1.10^{-4}	0	infinite
Frequency effect of the Haddad resistor					0.5	13
Relative uncertainty of the main detector	0 nV	0.1 nV	rectangular, B	5.10^{-9} /nV	0.05	22
Coaxility defect			gaussian,B		0.15	22
Temperature of the Haddad resistor	23°C	0.006 °C	gaussian,B	2.10^{-8} /°C	0.01	22
Temperature of the transfer resistor	25°C	0.006 °C	gaussian,B	2.10^{-8} /°C	0.01	22
Cable correction					0.1	13
Extrapolation of ratio difference from nominal at DC from ratio differences measured at all three frequencies	208.10^{-6}	3.10^{-9}	rectangular, B	1	0.3	13
Variability of repeated measurements			Type A		0.1	17
Combined standard uncertainty on difference from DC at 1591.55 Hz					**0.74**	50

(*) Readings of the inductive dividers used to balance the bridge in phase and quadrature; the dividers are followed by an 1:100 injection transformer and the readings must then be divided by 100.

8.3 Detailed results and uncertainty budget of METAS

Measurement Conditions

Ambient temperature:	(23.1 ± 0.5) °C
Enclosure temperature:	(24.95 ± 0.01) °C
Relative humidity:	(30 ± 10) %
Voltage:	1.1 Vrms
Frequency:	500 Hz to 10 kHz

Measurement Results

Frequency Hz	Measured Value, δ µΩ/Ω	Relative Uncertainty, U µΩ/Ω
500	-0.020	0.034
1000	-0.036	0.030
2000	-0.052	0.042
3000	-0.068	0.028
4000	-0.075	0.027
5000	-0.095	0.031
6000	-0.108	0.055
7000	-0.140	0.063
8000	-0.170	0.085
9000	-0.205	0.087
10000	-0.251	0.100

Uncertainty of Measurement

The reported uncertainty of measurement is stated as the combined standard uncertainty multiplied by a coverage factor $k = 2$. The measured value (y) and the associated expanded uncertainty (U) represent the interval ($y \pm U$) which contains the value of the measured quantity with a probability of approximately 95 %. The uncertainty was estimated following the guidelines of the ISO (GUM:1995).

The measurement uncertainty contains contributions originating from the measurement standard, from the measurement method, from the environmental conditions and from the object being measured. The long-term characteristic of the object being measured is not included.

8.4 Detailed results and uncertainty budget of PTB

The two travelling Vishay resistors arrived at PTB at 10th December 2012. The temperature control of the LNE resistor was powered during transportation from a battery. The temperature control of the BIPM resistor was set in operation directly after the arrival.

The measurements were carried out in the interval 4th to 8th January 2013, to allow the resistors for relaxation after the transportation. During the measurements, the laboratory temperature was (23.2 ± 0.3) °C, the relative humidity was (35 ± 4) %, and the atmospheric pressure was (1018 ± 3) hPa. The temperature control of the LNE travelling resistors displayed a value of 24.97 °C. The value of the thermistance of the BIPM travelling resistor was 29.5 kΩ (0.8 mK/Ω). Both temperatures were constant during the measurements. The resulting the frequency dependences are given in Table 8.4.1 and Table 8.4.2.

Table 8.4.1: Results for the relative frequency dependence Δ of the travelling LNE resistor, with respect to the value extrapolated to the frequency of 0 Hz. The measuring current was 40 µA (rms).

Frequency (kHz)	Δ (10^{-6})	*k* = 2 uncertainty (10^{-6})
0.507	-0.009	0.016
1.007	-0.019	0.016
1.507	-0.023	0.016
2.007	-0.039	0.016
2.507	-0.053	0.016
3.007	-0.053	0.017
4.007	-0.070	0.018
5.007	-0.094	0.019

Table 8.4.2: Results for the relative frequency dependence Δ of the travelling BIPM resistor, with respect to the value extrapolated to the frequency of 0 Hz. The measuring current was 40 µA (rms).

Frequency (kHz)	Δ (10^{-6})	*k* = 2 uncertainty (10^{-6})
0.507	-0.023	0.016
1.007	-0.038	0.016
1.507	-0.065	0.016
2.007	-0.099	0.016
2.507	-0.120	0.016
3.007	-0.145	0.017
4.007	-0.187	0.018
5.007	-0.222	0.019

Table 8.4.3 specifies the main uncertainty contributions of the coaxial 1:1 resistance ratio bridge. For all uncertainty components, the effective degree of freedom is estimated to be sufficiently large. Because the travelling resistors were measured not directly, but in substitution, against the ac QHR, the final uncertainty of the travelling Vishay resistors as quoted in the tables above is increased by a factor √2.

Table 8.4.3: Uncertainty budget of the coaxial 1:1 ratio bridge for 12.9 kΩ resistances.

Source of uncertainty	***k* = 1 uncertainty contributions (10^{-9})**	
	f = (0.5 - 2.5) kHz	*f* = 5 kHz
detector noise	5	5
cable correction	≤ 0.6	2.3
auxiliary balances	2	2
equalisers	0.6	2.4
main balance injection	0.3	2.2
rms sum	5.5	6.7
***k* = 2 uncertainty**	**11.0**	**13.4**

9. Annex: Diagrams of the bridges for the capacitance realisations

9.1 Bridge diagrams of PTB

The quadrature bridge used at PTB is a four-terminal-pair bridge with two ac quantum resistances R1 and R2, and with two 10 nF capacitances standards C1 and C2 (Figure 9.1.1). The quantum Hall resistances are double-shielded GaAs devices connected according to the triple-series scheme. T2 is a 1:1 ratio transformer; it is built into the same case as the supply transformer, but in such a way that the ratio and supply transformer are not coupled. Its 1:1 deviation is eliminated by reversing the ratio transformer's input leads as well as the output leads at the zero-current detectors T5 and T9.

The main balance is achieved by current injection through two 10 pF capacitance standards C4 and C3, driven by two decade IVDs T4 and T3 for the real and imaginary part of the main balance, respectively. T15 is the Wagner arm. C6 and R6 create the 90° voltage and R12, C12, R14 and C14 constitute a twin-T combining network. The resistor R12 is a fixed value resistor is series with an adjustable low-value resistor (set to typically 6 Ω). R14 and the fixed-value part of R12 are mounted into a liquid-helium dewar because they are the only resistors in the bridge network whose thermal noise fully contributes to the detector signal and otherwise would dominate the detector noise. Because the resistors R1 and R2 are cryogenic quantum Hall resistances, their thermal noise is also very small.

The null detector is a lock-in amplifier provided with an ultra-low-noise preamplifier featuring a noise figure of 0.5 nV/√Hz. At a voltage level of 100 mV_{rms}, an averaging time of 120 s is sufficient to get a relative statistical uncertainty of $2 \cdot 10^{-9}$. The sine generator is a low-distortion precision generator linked to PTB's 10 MHz reference frequency. For more detail see [J. Schurr, V. Bürkel, B. P. Kibble, "Realizing the farad from two ac quantum Hall resistances", *Metrologia* **46**, 619-628, 2009].

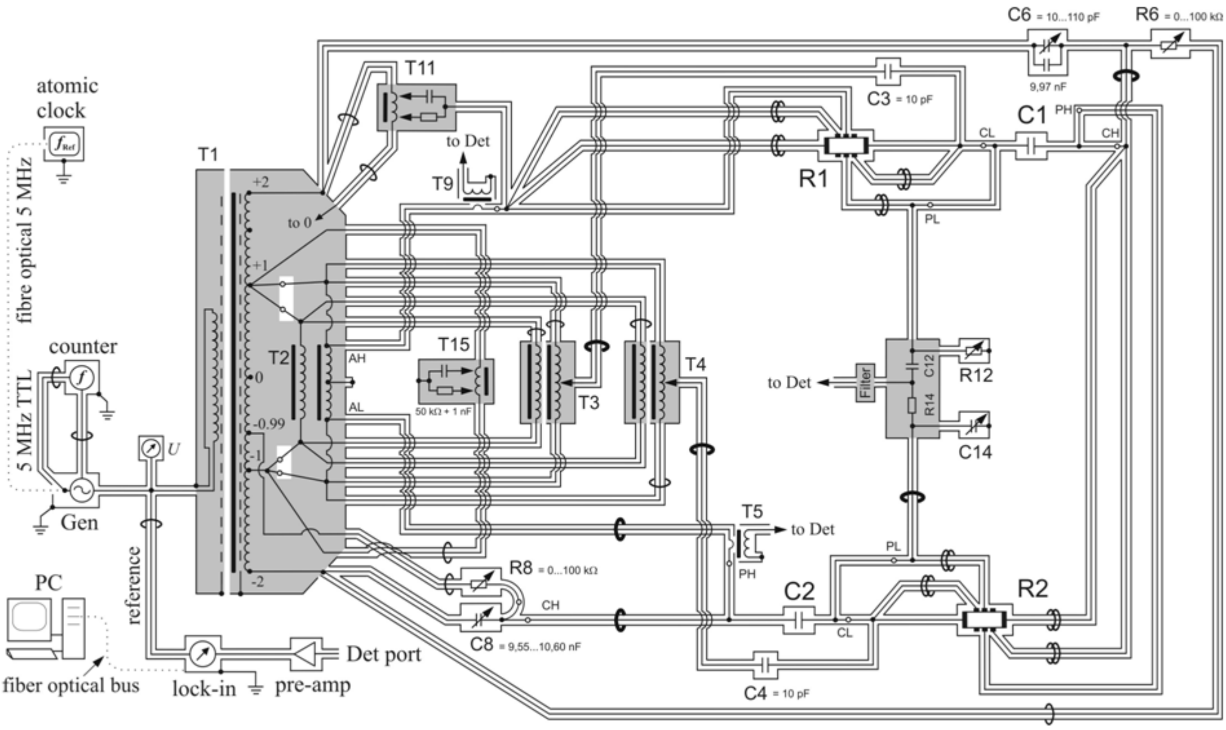

Figure 9.1.1: Four-terminal-pair quadrature bridge with two ac quantum Hall resistances.

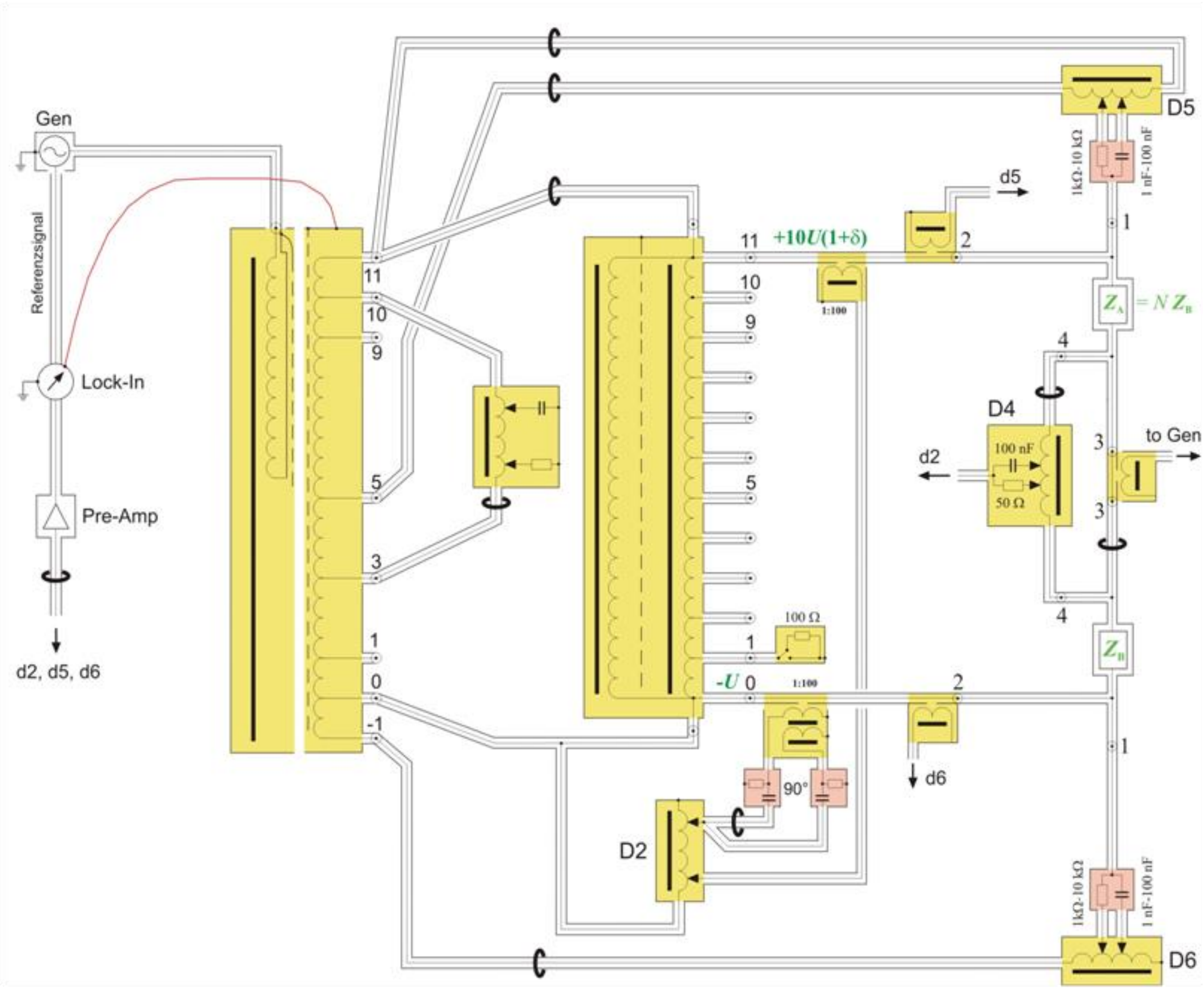

Figure 9.1.2: Four-terminal-pair ratio bridge comparing two impedances Z_A and Z_B.

The four-terminal-pair bridge ratio bridge shown in Figure 9.1.2 is used for the capacitance ratios 10 nF:1 nF, 1 nF:100 pF, and 100 pF:10 pF. In the case of the 100 pF:10 pF ratio, a two-terminal-pair bridge would be sufficient, but to avoid an additional two-terminal-pair bridge or frequent re-configurations of the four-terminal-pair bridge to a two-terminal-pair variant, also this ratio is carried out in the four-terminal-pair configuration.

To meet the four-terminal-pair defining conditions, two current sources, a Kelvin arm and a Wagner arm are used. The main balance is achieved by injecting an in-phase and a 90° phase-shifted voltage. The 90° injection system is realised in a two-staged manner to achieve a better long-term stability of the phase angle and to avoid frequent re-calibrations.

Due to a proper arrangement of the equalisers and because the capacitance bridge does not include high-value resistors whose thermal noise would contribute to the detector noise, the total detector noise is quite small. As a result, a relative statistical uncertainty of $(1\text{ to }2)\cdot10^{-9}$ can be achieved for each capacitance ratio. This requires an averaging time which ranges from 120 s for the 10 nF:1 nF ratio to 20 s for the 100 pF:10 pF ratio.

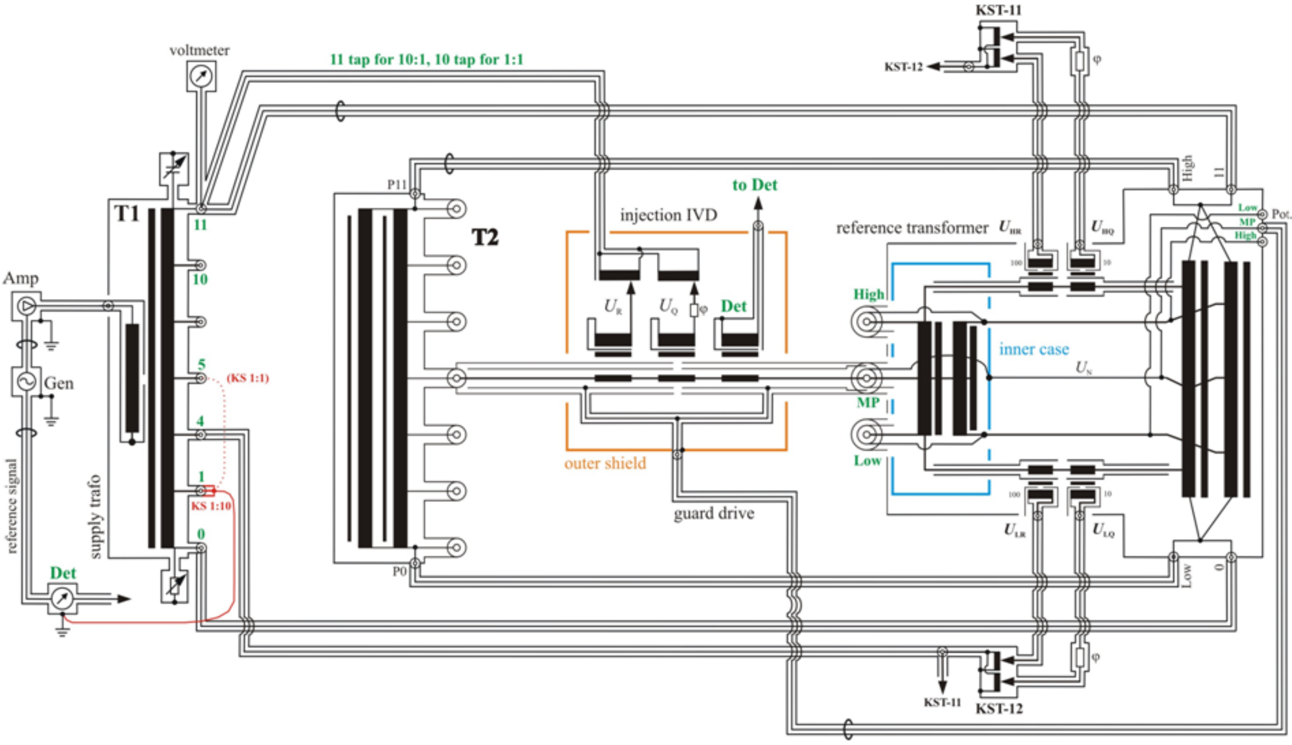

Figure 9.1.3: Straddling bridge for calibration of 10:1 transformer ratio.

The 10:1 deviation of the ratio transformer of the capacitance bridge (Figure 9.1.3) is calibrated by a straddling bridge. The 10:1 ratio of the transformer under calibration T2 can be traced to four 1:1 ratios of a reference transformer whose 1:1 deviation can be eliminated by a reversal measurement. Indeed, the middle tap and the inner case of the 1:1 transformer is not at zero potential, but at an elevated potential. Therefore, the 1:1 transformer requires an inner and an outer shield, and the measuring lead is a triaxial lead whose guard potential depends on the particular configuration. Usually, a straddling bridge uses three triaxial leads simultaneously, but here we use only one triaxial lead sequentially. Because a straddling bridge does not include any large-value resistor creating thermal noise, it has a very low noise level (corresponding to less than $1 \cdot 10^{-9}$ at an averaging time of 10 s and with respect to the output ratio).

9.2 Bridge diagrams of the BIPM

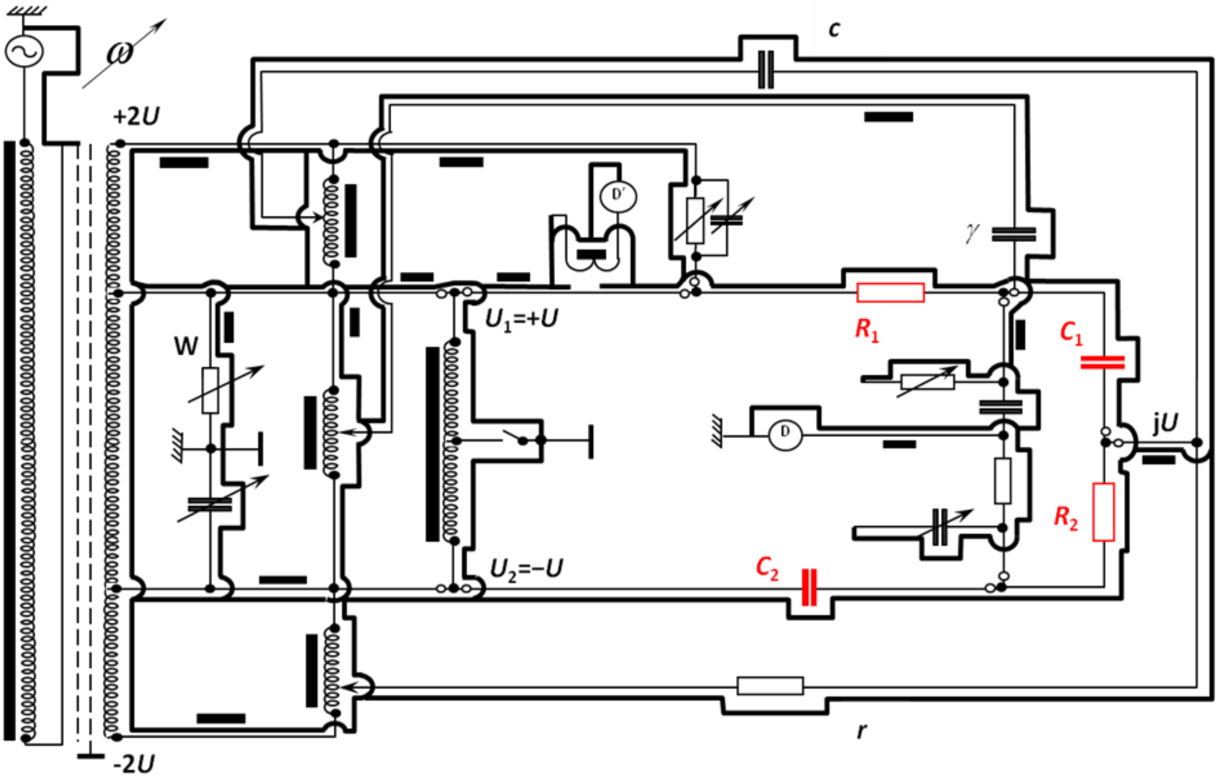

Figure 9.2.1: Scheme of the quadrature bridge.

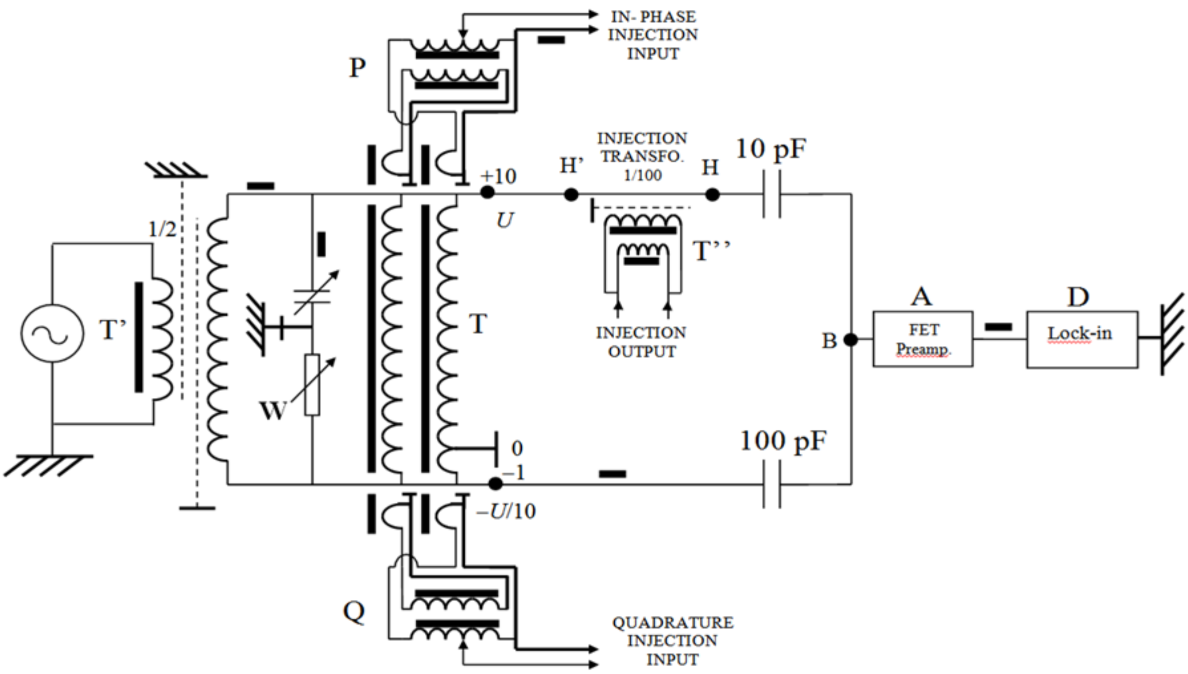

Figure 9.2.2: Scheme of the 10:1 ratio bridge configured for 100 pF:10 pF measurements.

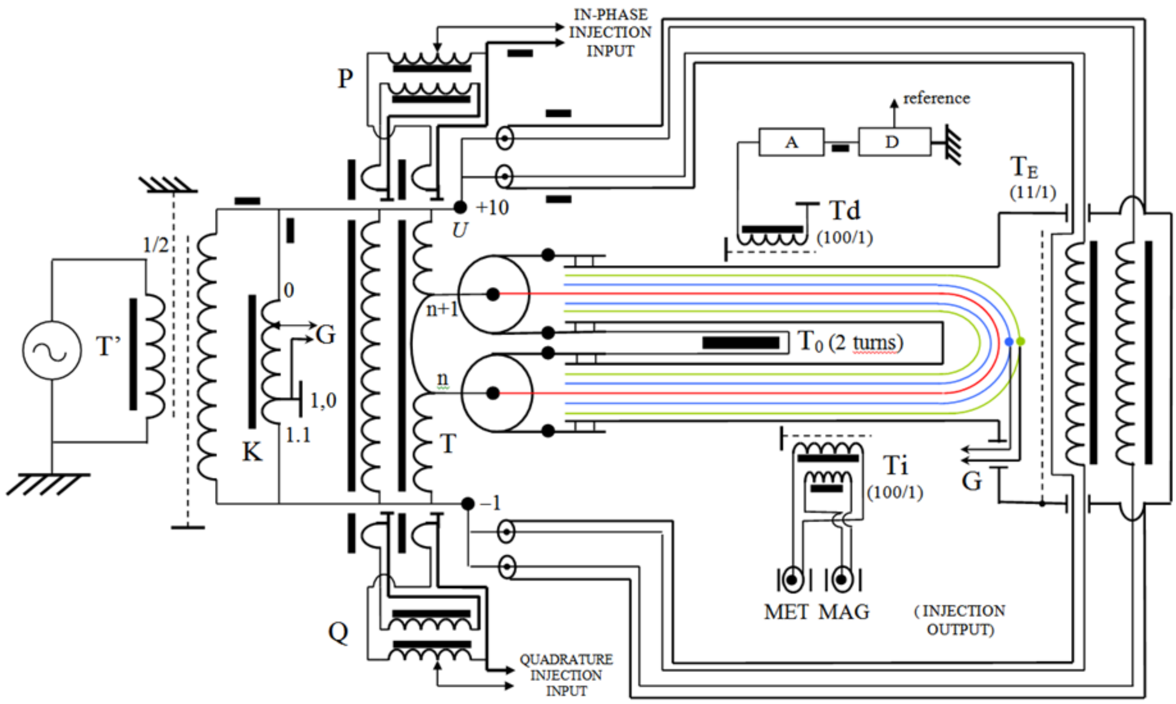

Figure 9.2.3: Divider ratio calibration, performed every 6 month on main 10:1 divider.

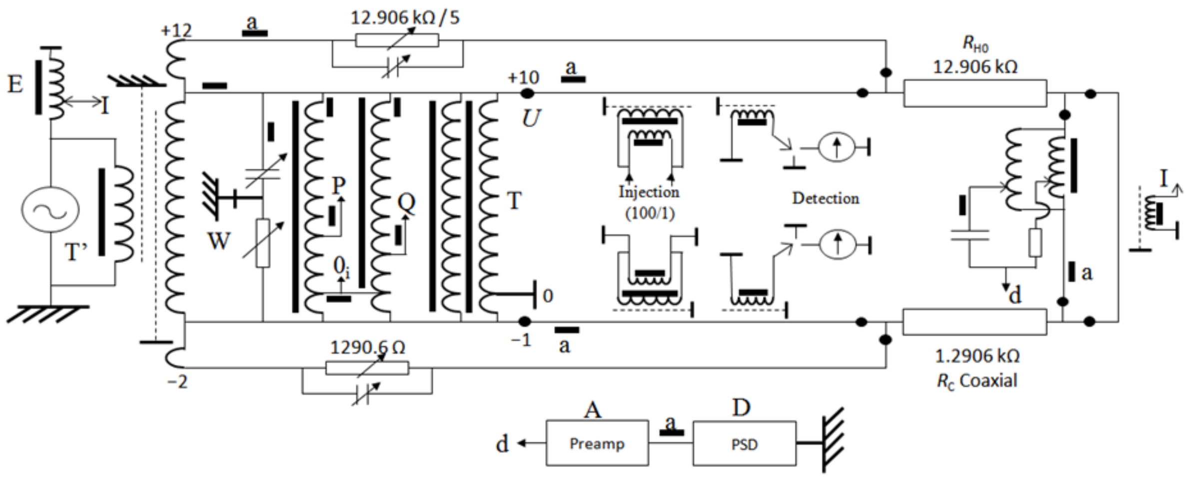

Figure 9.2.4: 4TP bridge for comparison of resistors. Active current equalisers are used for lower frequencies and lower impedances. Injection loads +10:-1 voltages and are compensated by having an unused identical injector and exchange of arms.

9.3 Bridge diagrams of LNE

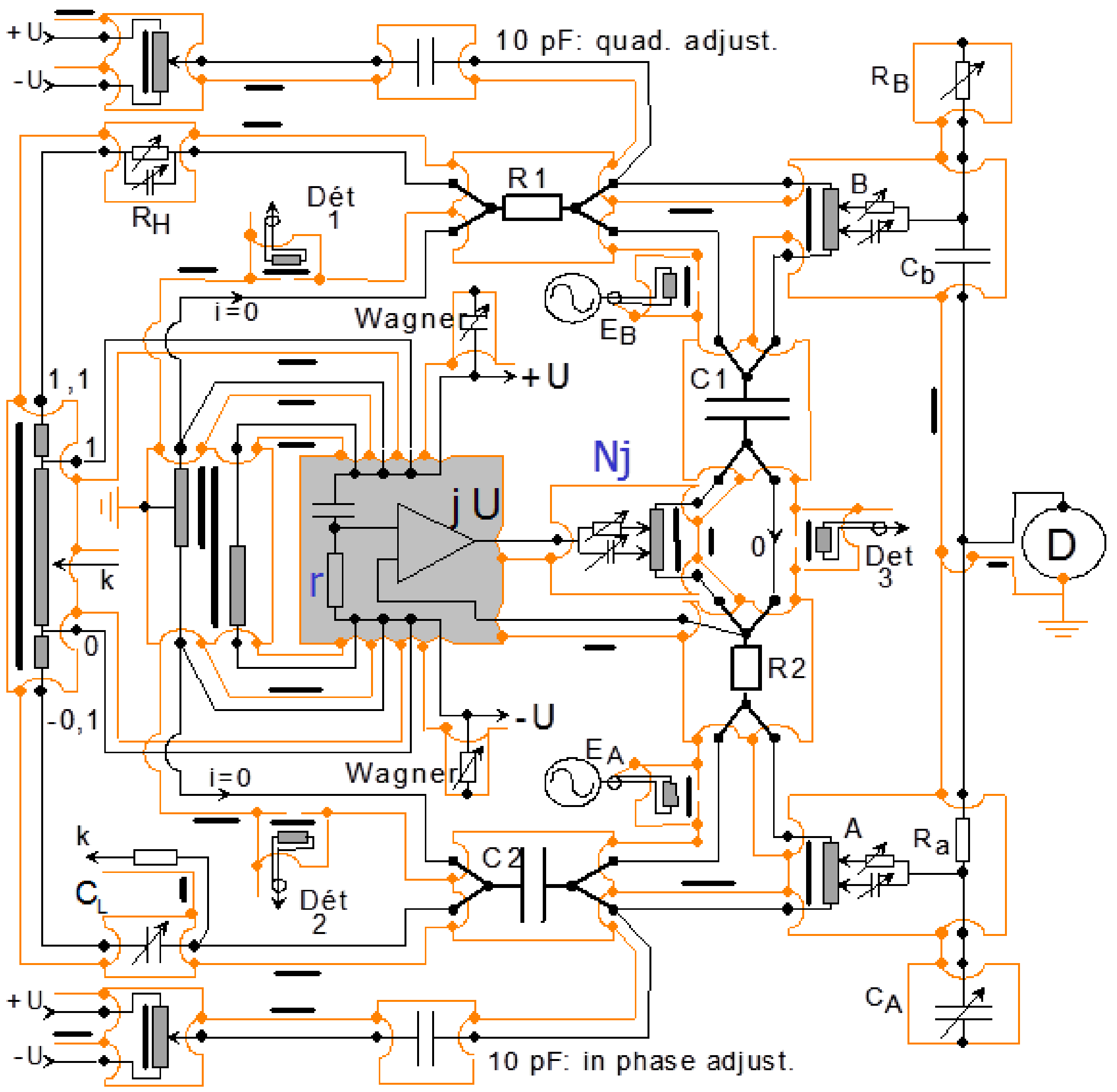

Figure 9.3.1: Four-terminal-pair quadrature bridge.

The quadrature bridge is a four-terminal-pair bridge (Figure 9.3.1) derived from the classical models described by R.D. Cutkosky and B.P. Kibble. Two capacitors, C_1 and C_2, are linked to $R_{K\text{-}90}$ by the relation: $R_1R_2C_1C_2\omega^2 = 1$, where C_1 and C_2 are the values of the two 10 nF capacitors, R_1 and R_2 the couple of resistances and ω is the frequency of the applied voltages.

The three couples of resistors (resistance values are 10 kΩ, 20 kΩ and 40 kΩ respectively at frequencies close to 1600 Hz, 800 Hz and 400 Hz) are of Vishay type resistors. They are thermostated and sealed. The quadrature voltage is provided by means of a RC network and an operational amplifier. An auxiliary RC network drives the reference voltage of the amplifier supply to a value close to the quadrature voltage, providing a high immunity against the amplifier gain instability. The detailed circuit of the quadrature bridge is shown in Figure 9.3.1.

Auxiliary current supplies (R_H and C_L) and compensation Kelvin arms (A, B and Nj) insure the Four-Terminal-Pair definition of the main impedance to be compared (R_1, R_2, C_1 and C_2).
The successive operations leading to the bridge balance are the following:

- The zero current conditions in potential ports are obtained by successive adjustments of R_H, C_L and network Nj in turns, so that the three detectors Det1, Det2, and Det3 (associated with three detection transformers) are respectively nulled.
- Networks B and A are adjusted in turns so that the auxiliary voltage sources E_B and E_A have no effect on the main detector D (thus producing condition equivalent to voltages being zero along the current cables between R_1 and C_1 and between R_2 and C_2, respectively).
- Combining networks (R_B, C_b) and (C_A, R_a) are adjusted to immune the main detector D from the deviation of the quadrature voltage from its nominal value, $-jU$ (for that, the $+U$ and $-U$ sources are disconnected from the main components R_1 and C_2, and the quadrature voltage is applied alone).
- After altering one element of the previous combining network (for example, C_A shorted), the quadrature voltage is adjusted near its nominal value (adjustment of the resistor, r, at the input of the operational amplifier and adjustment of the voltage frequency).
- Finally, the main detector, D, is nulled by means of two adjustable capacitive currents. The first one is injected between R_1 and C_1 for the in quadrature adjustment and the second one is injected between R_2 and C_2 for the in phase adjustment.

The deviation of the 1:1 ratio of the main two-stage transformer is eliminated by the inversion of the impedances to be compared. After the adjustment of all the different combining networks, with the process described above, all parts of errors are compensated, except for the following three parts of uncertainties:

- residual errors due to compensation adjustment detector sensibilities, which are taken into account as type A uncertainties,
- uncertainty of the frequency value of the quadrature bridge supply, which amounts to 2×10^{-10} (1σ),
- reproducibility of the serial inductance of the UHF coaxial tees (estimated to 0.03 μH) used to connect the 10 nF capacitors with a Four-Terminal-Pair definition. The corresponding uncertainty ($LC\omega^2$ form) increases from 0.2×10^{-9} at 400 Hz, to 3×10^{-9} at 1.6 kHz (1σ).

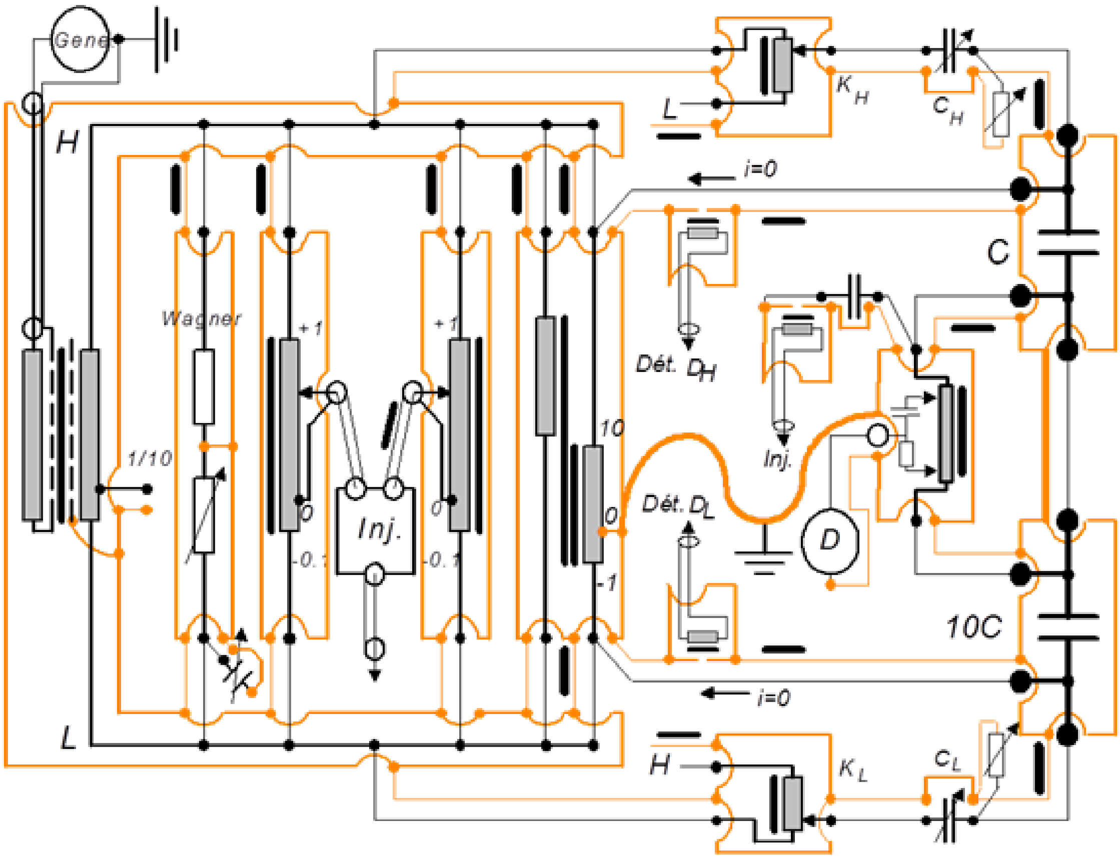

Figure 9.3.2: Four-terminal-pair capacitance bridge.

A four-terminal-pair coaxial capacitance bridge with a 10:1 ratio is used to link the 10 nF capacitors to the 100 pF capacitor (Figure 9.3.2). Two adjustable current sources allow to obtain zero current at the potential ports of the capacitors to be compared and a combining network at the detector node is adjusted so that a small auxiliary voltage injected in the connection cable between “C” and “10C” has no effect on the main detector D, thus producing a condition for which the voltage drop along this cable is zero.

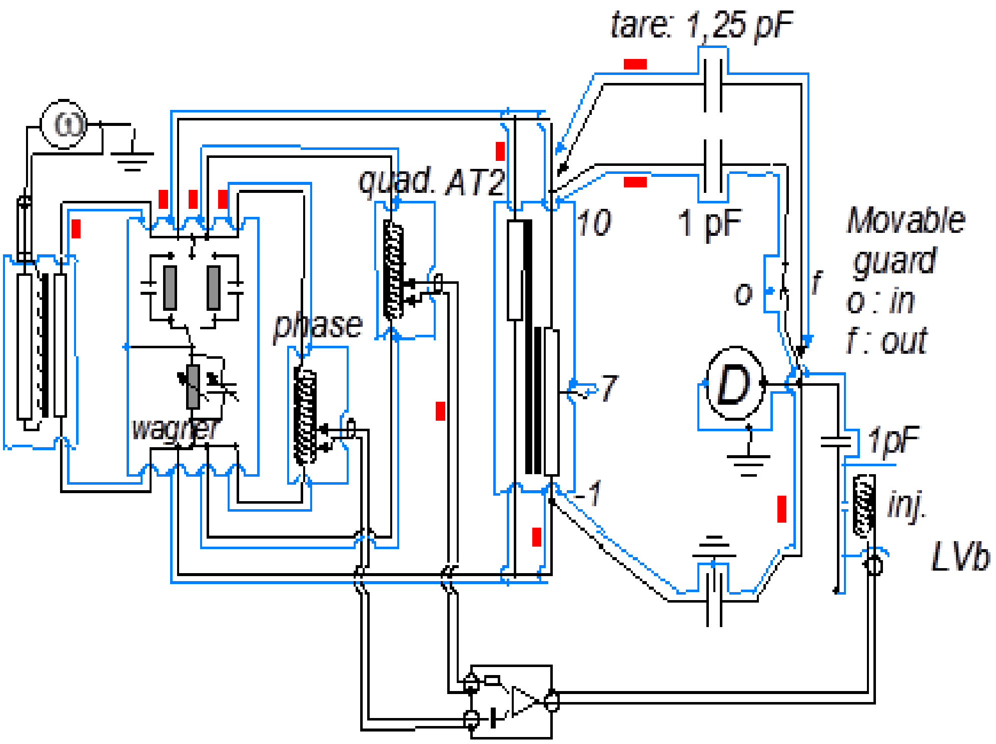

Figure 9.3.3: Two-terminal-pair capacitance bridge (presented here for the comparison of a 1 pF standard capacitor to the calculable capacitor).

The two-terminal-pair coaxial bridge with a 10:1 ratio (Figure 9.3.3) is used to compare a 100 pF capacitor to a 10 pF capacitor. This bridge is also used to compare a 10 pF capacitor to a 1 pF capacitor. The 10:1 ratio can be easily rearranged to obtain an 8:3 ratio. Thus, it is also used to compare a 1 pF capacitor against the capacitance variation generated by the LNE Thompson-Lampard calculable capacitor. The cable corrections have been determined for each capacitance measured.

9.4 Bridge diagrams of METAS

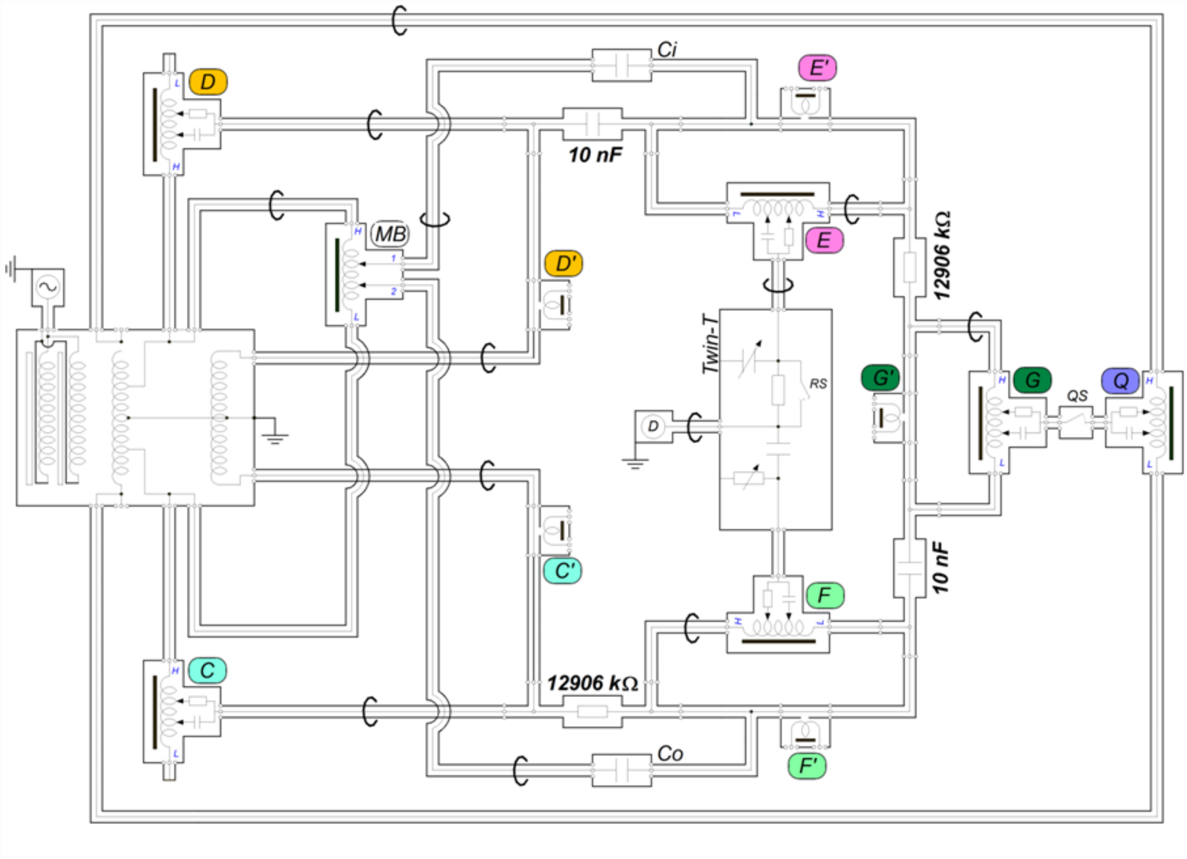

Figure 9.4.1: Four-terminal-pair quadrature bridge used to compare a pair of 10 nF capacitance standards to a pair of 12906.4Ω resistance standards at a frequency of 1233.1471 Hz.

The quadrature bridge compares a pair of 10-nF capacitance standards to a pair of 12.906-kO resistance standards. It is a manual four-terminal-pair bridge. The reference transformer has two secondary windings, the first is supplying the current and the second is making the 1 to -1 voltage ratio. This actual ratio slightly differs from the exact 1 to -1 ratio and therefore the bridge is balanced twice. A first time with the transformer in its forward position and a second time with the transformer in its reverse position. In such a way, the deviation of the 1 to -1 ratio is eliminated and the in-phase balance of the quadrature bridge is
given by:

$$\alpha_{Q} = ½\{\alpha - \alpha'\} C_i / C_{Nom} + 2\Delta v / v$$

where α and α' are the fraction of the reference voltage applied to the injection capacitor C_i in the forward and reverse position respectively. C_{Nom} is the nominal value of the 10-nF capacitance standard. Δv is the deviation of the frequency from its nominal value v.

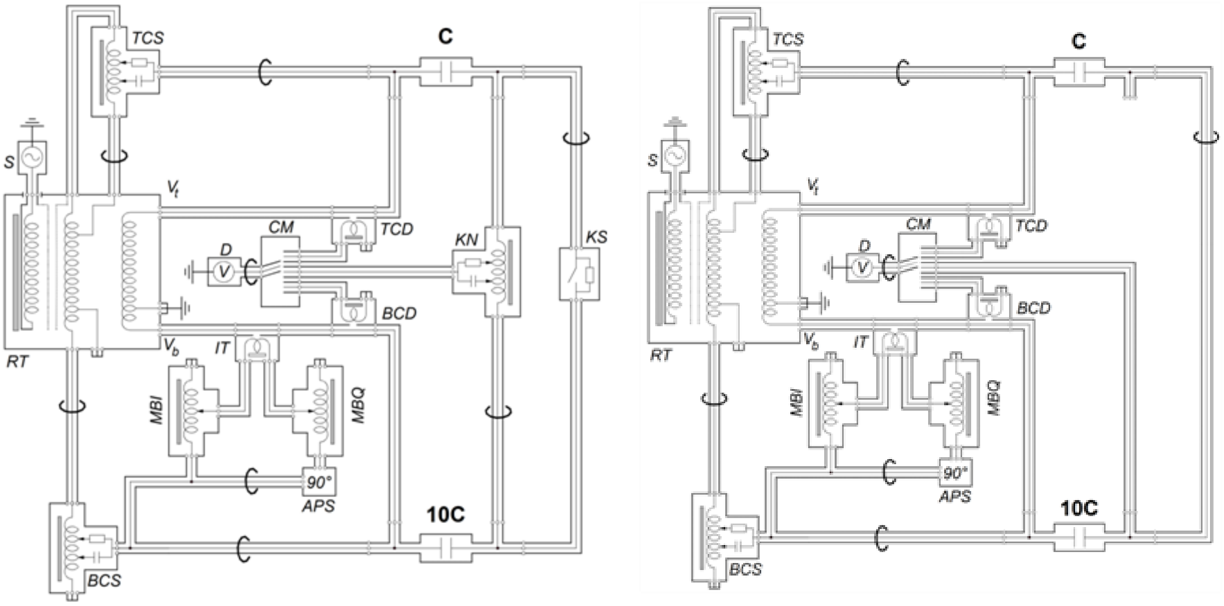

Figure 9.4.2: Schematic of the 10 to -1 bridges used to scale down the capacitance from 10 nF to 10 pF. On the left is the four-terminal-pair version and on the right is the three-terminal-pair version used for the last 100 pF to 10 pF step.

Figure 9.4.2 shows the 10 to -1 ratio bridges used to scale down the capacitance from 10 nF to 10 pF. On the left is the four terminal-pair bridge used for the 10 nF to 1 nF and 1 nF to 100 pF steps and on the right is the three terminal-pair bridge used for the 10 pF to 10 pF step. These two bridges are computer controlled and the balance procedure is automated making the repetition of the comparisons easier.

The realization of the whole measuring chain is a time consuming task requiring a good short term stability of the standards. To be independent of the linear drift of the standards, each step of the chain is repeated in a reversed sequence within one day.

9.5 Bridge diagrams of NMIA

The 10:1 ratio bridge of NMIA is based on a three-winding voltage transformer (Figure 9.5). The main winding of the transformer has taps at n/11, where n = 0, 1,…11 which may be used to supply a precise 10:1 voltage ratio. Additional windings are used as the voltage input to a multi-dial ratio transformer to give an adjustable voltage of (± 500 ± 10j) μV/V relative to one step on the main winding with a resolution of 0.01 μV/V.

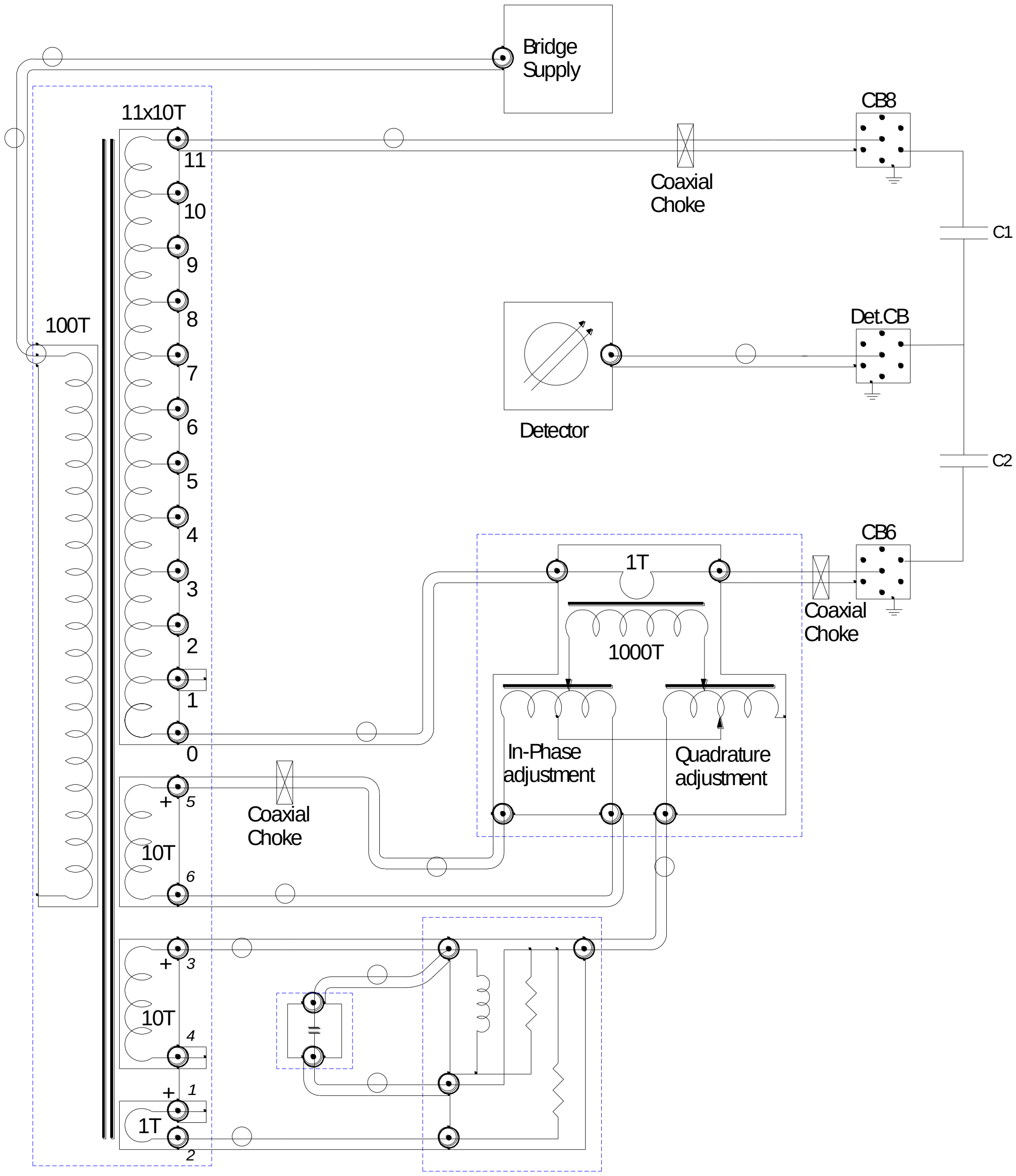

Figure 9.5: The 10:1 ratio bridge.

9.6 Bridge diagrams of VSL

Once the AC-DC resistors are calibrated at DC to the QHRS, they are used to calibrate capacitors via a 4TP quadrature bridge. The capacitors used in this bridge have a nominal value of 10 nF and are thermostated in order the limit the effect of environmental temperature. These are ceramic dielectric capacitors, manufactured by NPL (UK), type C03.

The main components in the bridge are capacitors C_1 and C_3 and resistors R_2 and R_4. The main balance of the bridge is controlled by divider T_2, driving currents through capacitor Δc_1 for in-phase adjustment and through capacitor Δc_4 for quadrature adjustment of the bridge. A quadrature bridge consists of two sections that are to be balanced at the same time.

The quadrature bridge provides the sum of the deviations from nominal of the capacitors C_1 and C_3. With the ratio bridge, the difference between the deviations from nominal can be determined. From the combination of the sum and the difference, the individual values of C_1 and C_3 can be found.

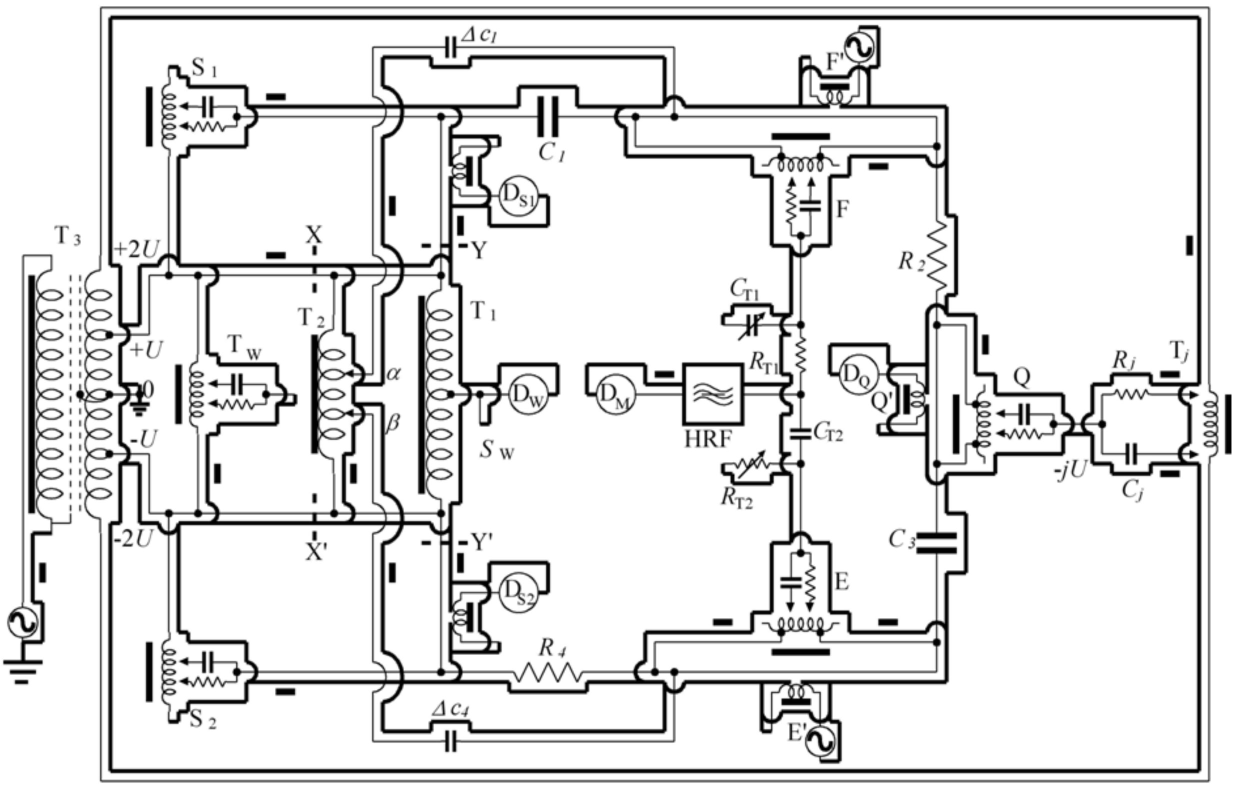

Figure 9.6.1: Four-terminal-pair quadrature bridge.

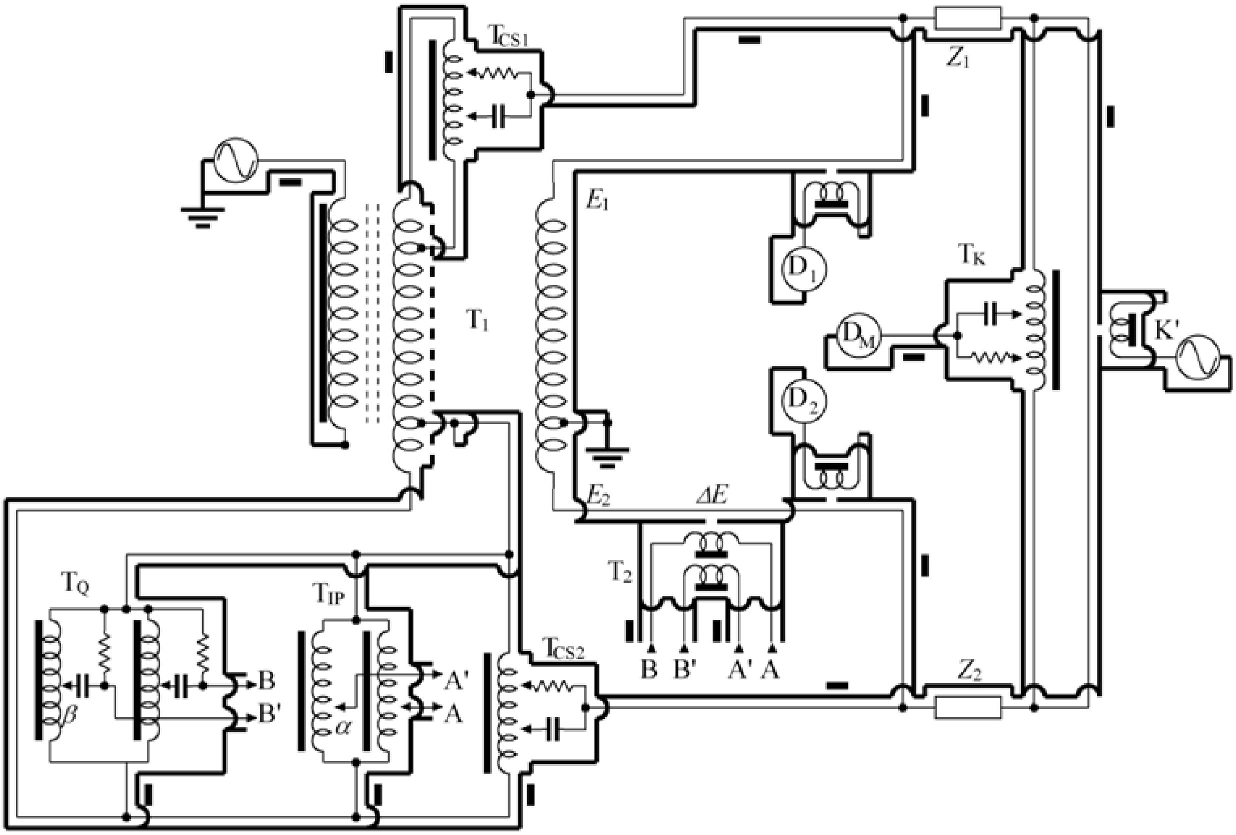

Figure 9.6.2: Four-terminal-pair ratio bridge.

The ratio of the two 10 nF capacitors is determined in a 4TP impedance ratio bridge. The same bridge is also used for scaling to lower values of capacitance with a nominal ratio of 10:1.

The impedances to be compared are Z_1 and Z_2. The heart of the bridge is the main transformer T_1. This transformer has two secondary windings: a current winding (on the left) and a potential winding (on the right). Each winding has 12 output taps, from -1 to 10. The bridge is balanced by injecting a small voltage in the lower potential arm through the 100:1 two-stage injection transformer T_2. This injection voltage is controlled by the networks T_{IP} for the in-phase adjustment and T_Q for the quadrature adjustment.

The injection voltage used to set the main balance of the bridge is derived from the injection networks T_{IP} and T_Q. T_Q is equipped with a network of R_q and C_q to create a phase shift of approximately 90° (R_q = 10 Ω and C_q = 100 nF).

10. Annex: Uncertainty budgets of the capacitance realisations

10.1 PTB uncertainty budgets

Uncertainty contribution of each step of the measuring chain at 1233 Hz (k = 1):

Quantity	distribution	sensitivity coefficient times uncertainty u (10^{-9})		
		for 100 pF	for 10 pF	for 100 pF:10 pF
$\omega^2 R_H^2 C_1 C_2$ with C_1, $C_2 \approx$ 10 nF	normal	0.5 × 6.0	0.5 × 6.0	0
C_1:1 nF bridge	normal	0.5 × 2.4	0.5 × 2.4	0
C_2:1 nF bridge	normal	0.5 × 2.4	0.5 × 2.4	0
1 nF: 100 pF bridge	normal	1 × 2.1	1 × 2.1	0
100 pF: 10 pF bridge	normal	-	1 × 2.6	1 × 2.0
10:1 calibration	normal	2 × 1.4	3 × 1.4	1 × 1.4
total uncertainty (k = 1):		**4.9**	**6.4**	**2.4**
expanded uncertainty		**9.8**	**12.8**	**4.8**

Contributions due to the day-to-day variations of the capacitance standards are not included. The 10 nF and 1 nF standards are just transfer standards and each transfer is accomplished within less than one hour so that day-to-day variation and the long-term drift is not relevant.

The individual results of the travelling standards obtained during a few weeks show a variation with a standard deviation of typically (9-15)·10^{-9} which is clearly larger than the standard deviation of multiple re-measurements within one day. This also applies to a 100 pF:10 pF ratio. Therefore, an additional averaged uncertainty contribution for the instability of the capacitance standards of 11·10^{-9} has been taken into account.

Uncertainty contribution of the quadrature bridge at 1233 Hz:

Source		distribution	uncertainty, sensitivity coefficient	ν	uncertainty (k = 1) (10^{-9})
detector noise and detector offset		normal	2.5 nV at τ = 120 s, 1.21 µV/10^{-6} at U = 100 mV	4	2.1
main in-phase injection		normal		4	0.28
frequency		normal	$\Delta\omega/\omega < 4 \cdot 10^{-11}$, 2	4	0.08
ac QHR		normal		∞	2.4
phase error of quadrature injection		rect.		∞	0.4
residual imbalance of auxiliary balances	Wagner	rect.	4 dials, 13·10^{-8} for imbalance of 2nd dial by 1	∞	0.38
	current source	rect.	2 dials, 1.0·10^{-8} for imbalance of 1st dial by 1	∞	0.3
	twin-T	rect.	5 dials, 1.3·10^{-7} for imbalance of 2nd dial by 1	∞	0.04
harmonic distortion		normal		4	≤ 2.0
lead correction		normal		4	1.4
equaliser evaluation		normal	4.4·10^{-8} x 10%, 1	4	4.4
			effective degree of freedom:	**4.7**	
				total (k = 1):	**6.0**

Uncertainty contribution of the 10:1 ratio bridge at 1233 Hz:

Source		distri-bution	Uncertainty, sensitivity	ν	Uncertainty (k = 1) (10^{-9})
detector noise		normal	U_{Det} = 2.2 nV, τ = 120 s, U = 1.0 V, sens = 3.45 μV / 10^{-6}	4	0.64
			U_{Det} = 2.2 nV, τ = 120 s, U = 10 V, sens = 17.7 μV / 10^{-6}	4	0.12
			U_{Det} = 5 nV, τ = 60 s, U = 100 V, sens = 29.1 μV / 10^{-6}	4	0.17
in-phase injection IVD		normal	$\Delta D_P/D_P = 1.9\cdot10^{-5}$, $D_P = 24\cdot10^{-6}$	∞	0.45
			$D_P \le 10\cdot10^{-6}$	∞	0.19
			$D_P \le 10\cdot10^{-6}$	∞	0.19
phase error of quadrature IVD		rect.	$80\cdot10^{-6} \times 6.2$ μV/V	∞	0.50
cable corrections		rect.		∞	0.17
phase shifter		normal	$\Delta\varphi/\varphi = 4\cdot10^{-5}$, $D_Q = 40\cdot10^{-6}$	4	1.6
			$\Delta\varphi/\varphi = 4\cdot10^{-5}$, $D_Q < 3\cdot10^{-6}$	4	0.12
			$\Delta\varphi/\varphi = 4\cdot10^{-5}$, $D_Q < 3\cdot10^{-6}$	4	0.12
residual imbalance of auxiliary balances	current source 1	rect.	4 dials	∞	0.1
			4 dials	∞	0.1
			4 dials	∞	0.2
	current source 2	rect.	5 dials	∞	0.1
			5 dials	∞	0.1
			5 dials	∞	0.1
	Kelvin	rect.	4 dials	∞	0.3
			3 dials	∞	0.1
			2 dials	∞	0.1
	Wagner	rect.	4 dials	∞	0.05
			4 dials	∞	0.05
			4 dials	∞	0.07
evaluation of equalisers		rect.		∞	1.2 2.0 2.0
detector offset		rect.	≤ 3.0 nV	∞	0.9
			≤ 5.4 nV	∞	0.3
			≤ 45 nV	∞	1.5
			effective degree of freedom:	∞	
			total uncertainty (k = 1):		**2.4** **2.1** **2.6**

The different 10:1 ratios are colour-coded: **10 nF:1 nF**, **1 nF:100 pF** und **100 pF:10 pF**. Uncertainty **c**ontributions quoted in black equally contribute to all 10:1 ratios.

Uncertainty contribution of the 10:1 straddling calibration at 1233 Hz:

Source		distri-bution	uncertainty, sensitivity	ν	uncertainty (k=1) (10^{-9})
detector noise		normal	U_{Det} = 10 nV at τ = 1s, 26 × 900 µV/10^{-6} at U_{Gen} = 37 V	32	0.29
in-phase error of main injection		rect.	in-phase error ≤ $2 \cdot 10^{-5}$ at in-phase component ≤ $1 \cdot 10^{-6}$	∞	≤ 0.02
uncertainty of phase-shifter adjustment		rect.	phase error ≤ $1 \cdot 10^{-4}$ at quadrature component ≤ $1 \cdot 10^{-6}$	∞	≤ 0.1
residual imbalance of auxiliary balances	auxiliary IVD for high adjustment	rect.	in-phase: 8 dials, $5.2 \cdot 10^{-6}$ per imbalance of 4th dial by one	∞	0.15
			In quadrature: 6 dials, $9.0 \cdot 10^{-8}$ per imbalance of 4th dial by one	∞	0.26
	auxiliary IVD for low adjustment	rect.	in-phase: 8 dials, $5.2 \cdot 10^{-6}$ per imbalance of 4th dial by one	∞	0.15
			In quadrature: 6 dials, $9.0 \cdot 10^{-8}$ per imbalance of 4th dial by one	∞	0.26
	cross-capacitance of triaxial lead	rect.	0.25 turns, $1.4 \cdot 10^{-9}$/turn,	∞	0.35
	Wagner arm	rect.	$6 \cdot 10^{-11}$ for C_W, $1 \cdot 10^{-11}$ for R_W	∞	0.06
drift of generator voltage		rect.	$\Delta U_{Gen} / U_{Gen} \leq 1 \cdot 10^{-3}$ over 1 h, $1.2 \cdot 10^{-8}$ per $\Delta U_{Gen} / U_{Gen} = 0.1$	∞	0.07
evaluation of equalisers		normal	$(1.2 \pm 0.7) \cdot 10^{-9}$	4	1.2
uncertainty of guard potential		rect.	$\Delta U_{Guard} / U_{Guard} \leq 1 \cdot 10^{-4}$, $1 \cdot 10^{-8}$ per $\Delta U_{Guard} = 0.1 U_{Guard}$	∞	≤ 0.01
voltage drop at the front panel of the IVD under test		rect.	≤ 0.2 nV	∞	≤ 0.015
cable effects		rect.		∞	0.25
detector offset		rect.	≤ 2 nV	∞	≤ 0.1
voltage dependence of ratio transformer		normal	$(1.2 \pm 0.75) \cdot 10^{-9}$/100 V, calibration at $^{1}/_{3} \cdot$(100 V + 10 V + 1V)	4	≤ 0.3
			total uncertainty, k = 1:		**1.4**
			expanded uncertainty, k = 2:		**2.8**

PTB uncertainty at *f* = 2466 Hz

The whole measuring chain can be carried out at 1233 Hz and 2466 Hz within one day so that the day-to-day fluctuation and the long-term drift of the capacitance standards do not need to be considered in the uncertainty of the frequency coefficient. Some of the uncertainty contributions of the whole measuring chain are proportional to the square of the frequency whereas other contributions are frequency independent. Because PTB measured the frequency coefficient only once, the total uncertainty of a 10 pF or 100 pF value at 2466 Hz is estimated to be $28 \cdot 10^{-9}$ ($k = 1$) and includes a contribution for the variation of the standards during each measuring period of $11 \cdot 10^{-9}$ (as already discussed above).

10.2 BIPM uncertainty budgets

The uncertainty budgets are presented for each operating frequency using several distinct sub-components, each with individual contributions (in some cases the individual contributions could be expanded into separate budgets, but space does not allow such complete detail). All uncertainties are stated as relative standard uncertainties in parts in 10^9. Individual degrees of freedom are not quoted, but in all cases are sufficiently high that the final combined uncertainties can be expanded with a coverage factor k=2 for a confidence level of 95%.

Subcomponent 1: Evaluation of the 1 Hz to operating frequency change of the resistors in the quadrature bridge

		1027 Hz	**1541 Hz**	**3083 Hz**
Contribution	**Comments**	**Value /10^{-9}**	**Value /10^{-9}**	**Value /10^{-9}**
Repeatability	Type A	15	15	15
Frequency dependence of reference 1290.6 Ω coaxial resistor	Type B, from calculation (verified against 645.3 Ω standard)	2	3	6
Transfer to 12.906 kΩ standard on 10:1 ratio bridge	Type B, transformer ratio, equalisers, cable corrections etc	6	5	12
Transfer to 51.624 kΩ standard on 4:1 ratio bridge	Type B, transformer ratio, equalisers, cable corrections etc	5	5	10
Extrapolation to 1 Hz	Type A from fit	8	8	8
Stability of 1 Hz to operating frequency difference	Type B, estimated from experience over several years	10	10	10
Sub total		**21**	**21**	**26**

Subcomponent 2: Measurement at 1 Hz of resistors in quad bridge

Contribution	**Comments**	**Value /10^{-9}**
Repeatability	Type A	10
Link R_{K-90} to 100 Ω	Type B, realisation of R_K, current comparator bridge, etc	7
Link 100 Ω to 51.6 kΩ	Type B, 4:1 Hamon ratio, stability of secondary standards, etc	7
Sub total		**14**

Subcomponent 3: quad bridge, transfer from R to C at the operating frequency

		1027 Hz	1541 Hz	3083 Hz
Contribution	**Comments**	**Value /10^{-9}**	**Value /10^{-9}**	**Value /10^{-9}**
Repeatability	Type A	10	10	15
Residual effects of harmonics	Type B	5	5	5
Imperfect current equalisers	Type B	5	5	5
Two terminal-pair definition of 1000, 2000 or 3000 pF capacitors	Type B	8	5	10
Sub total		**15**	**13**	**19**

Subcomponent 4: scaling from 2000 pF to 10 pF reference capacitor

		1027 Hz	1541 Hz	3083 Hz
Contribution	**Comments**	**Value /10^{-9}**	**Value /10^{-9}**	**Value /10^{-9}**
Repeatability	Type A	10	10	15
Imperfect current equalisers	Type B	5	5	5
Errors in balance injection	Type B	10	5	15
Calibration of 10:1 ratio	Type B	8	8	12
Sub total		**17**	**15**	**25**

Overall budgets

Measurement of 100 pF standard against BIPM 10 pF reference (10 V):

		1027 Hz	1541 Hz	3083 Hz
Contribution	**Comments**	**Value /10^{-9}**	**Value /10^{-9}**	**Value /10^{-9}**
Repeatability	Type A	10	10	10
Drift of mean of reference group	Type B	3	3	3
Imperfect current equalisers	Type B	5	5	5
Errors in balance injection	Type B	8	5	15
Cable corrections	Type B	3	7	18
Calibration of 10:1 ratio	Type B	4	4	4
Sub total		15	15	26
Value of reference group (sub-components 1-4 above)		34	32	43
Total		**37**	**35**	**50**

Measurement of 10 pF standard against BIPM 10 pF reference by substitution (100 V):

		1027 Hz	**1541 Hz**	**3083 Hz**
Contribution	**Comments**	**Value /10^{-9}**	**Value /10^{-9}**	**Value /10^{-9}**
Repeatability	Type A (two 10:1 steps)	14	14	14
Drift of mean of reference group	Type B	3	3	3
Imperfect current equalisers	Type B	7	7	7
Errors in balance injection	Type B	11	7	21
Cable corrections	Type B	4	10	25
Short term stability of 100 pF buffer	Type B	5	5	5
Sub total		20	21	37
Value of reference group (sub-components 1-4 above)		34	32	43
Total		**40**	**38**	**57**

10.3 LNE uncertainty budgets

The uncertainty budget is presented for each test frequency thereafter. The uncertainty of the correction for the deviating ambient temperature and test voltages is not included in the following budget and has been added by the pilot.

Uncertainty budget: measurements performed at 397.88 Hz

Quantity X_i	Estimate x_i	Standard uncertainty $u(x_i)$	Probability distribution /method of evaluation (A,B)	Sensitivity coefficient c_i	Uncertainty contribution $c_i u(x_i)$ (aF)	Degree of freedom ν_i
Quadrature Bridge						
Frequency	397.88 Hz	3.10^{-7} Hz	rectangular, B	$6.7.10^{-12}$ F/Hz	2	50
Resistance (EHQ) (40kΩ//)	20 000 Ω	$8\ 10^{-5}$ Ω	gaussian, B	$5\ 10^{-13}$ F/Ω	40	50
Resistance Frequency effect	$-7.4.10^{-4}$Ω	$9.2.10^{-5}$Ω	gaussian, B	5.10^{-13} F/Ω	46	54
Null current in high potential ports Adjustement of R_H	8000 Ω	0,3 Ω	rectangular, B	1.10^{-17} F/Ω	3	infinite
Adjustement of C_H	3800 pF	12 pF	rectangular, B	$8.33.10^{-8}$	1	infinite
Adjustement of C_B	54500 pF	12 pF	rectangular, B	$8.33.10^{-8}$	1	infinite
Null current in low potential ports Adjustement of kB	-0.0003	0.00006	rectangular, B	1.10^{-15} F	0	infinite
Adjustement of k_p	1.050	0.0006	rectangular, B	1.10^{-16} F	0	infinite
Null voltage condition between R1-C1 Adjustement of kq	0.070	0.0006	rectangular, B	1.10^{-16} F	0	infinite
Adjustement of kp	0.085	0.0006	rectangular, B	1.10^{-16} F	0	infinite
Null voltage condition between R2-C2 Adjustement of kq	1.020	0.0006	rectangular, B	1.10^{-16} F	0	infinite
Main detection arm Adjustement of R_B	495000 Ω	60 Ω	rectangular, B	$1.7.10^{-20}$ F/Ω	1	infinite
Adjustement of C_A	9800 pF	12 pF	rectangular, B	$8.33.10^{-8}$	1	infinite
Main balance Adjustement of kp	0.5000000	0.0000010	rectangular, B	1.10^{-11} F	10	infinite
Adjustement of k_q	0.5000000	0.0000010	rectangular, B	1.10^{-14} F	0	infinite
Relative uncertainty of the main detector	0 nV	50 nV	gaussian, B	1.10^{-10} F/V	5	13
Coaxility defect			gaussian, B		15	13
Reproducibility of the serial inductance of the UHF coaxial tees	0.0 µH	0.03 µH	gaussian, B	$6.7.10^{-11}$ F/H	2	13
Cable correction			gaussian, B		2	8
Temperature of the 10 nF	20°C	0.0006 °C	gaussian, B	$1.7.10^{-15}$ F/°C	1	22
10 nF combined relative standard uncertainty					**$0.6.10^{-8}$**	121
Four terminal pair capacitance bridge						
Frequency	397.88 Hz	1.10^{-2} Hz	rectangular,B	$<1.10^{-19}$ F/Hz	0	infinite
Bridge ratio correction (x2)	$-0,0016.10^{-6}$	$0,3.10^{-8}$	gaussian,B	1.10^{-10} F	0.3	13
loading			gaussian,B		0.2	13
Null current in high potential ports Adjustement of R_H	3340.00 Ω	0,06 Ω	rectangular, B	$1.7.10^{-19}$ F/Ω	0.01	infinite
Adjustement of C_H	999 520 µF	10 µF	rectangular, B	1.10^{-15}	0.01	infinite
Adjustement of k_H	1.0000887	0.00000006	rectangular, B	$1.7.10^{-13}$ F	0.01	infinite
Null current in low potential ports Adjustement of R_B	915.6 Ω	0.06 Ω	rectangular, B	$1.7.10^{-19}$ F/Ω	0.01	infinite
Adjustement of C_B	992.400 µF	10 µF	rectangular, B	1.10^{-15}	0.01	infinite
Adjustement of k_B	-0.0000150	0.00000006	rectangular, B	$1.7.10^{-13}$ F	0.01	infinite
Kelvin Arm Adjustement of k_p	0.55	0.0006	rectangular, B	$1.7.10^{-17}$ F	0.01	infinite
Adjustement of k_q	0.595	0.0006	rectangular, B	$1.7.10^{-17}$ F	0.01	infinite
Main balance Adjustement of kp	0	0.0000001	rectangular, B	1.10^{-12} F	0.1	infinite
Adjustement of k_q	0	0.0000001	rectangular, B	5.10^{-16} F	0	infinite
Relative uncertainty of the main detector	0 nV	50 nV	rectangular, B	1.10^{-12} F/V	0.05	13
Coaxility defect			gaussian,B		0.15	13
Reproducibility of the serial inductance of the UHF coaxial tees	0,0 µH	0.03 µH	gaussian,B	$6.7.10^{-13}$ F/H	0.02	13
Temperature of the 1000 pF	20°C	0.0006 °C	gaussian,B	$1.7.10^{-17}$ F/°C	0.01	22
Température of the 10 nF	20°C	0.0006 °C	gaussian,B	$1.7.10^{-17}$ F/°C	0.01	22
Voltage coefficient (1000 pF)	5.10^{-8} pF/V	1.10^{-8} pF/V	gaussian,B	4.10^{-12} V	0.04	13
Cable correction			gaussian, B		0.2	8
Variability of repeated measurements of the 100 pF			Type A		0.3	15
100 pF combined relative standard uncertainty					**$1.0.10^{-8}$**	172
Two terminal pair capacitance bridge						
Frequency	397.88 Hz	1.10^{-2} Hz	rectangular, B	3.10^{-19} F/Hz	0.003	infinite
Bridge ratio correction	$0.003.10^{-6}$	$0.3.10^{-8}$	gaussian, B	$6.7.10^{-12}$ F	0.02	13
Loading			gaussian, B		0.015	13
Main balance Adjustement of kp	0	0.0000001	rectangular, B	1.10^{-13} F	0.01	infinite
Adjustement of k_q	0	0.0000001	rectangular, B	5.10^{-16} F	0	infinite
Relative uncertainty of the main detector	0 nV	50 nV	gaussian, B	1.10^{-13} F/V	0.005	50
Coaxility defect			gaussian, B		0.015	35
Cable correction	$-0.7.10^{-8}$ pF	1.10^{-8} pF	gaussian, B	1.10^{-12}	0.01	8
Variability of repeated measurements from 10 pF			Type A		0.01	14
10 pF combined relative standard uncertainty					**$1.1.10^{-8}$**	234

Uncertainty budget: measurements performed at 795.77 Hz

Quantity X_i	Estimate x_i	Standard uncertainty $u(x_i)$	Probability distribution /method of evaluation (A,B)	Sensitivity coefficient c_i	Uncertainty contribution $c_i u(x_i)$ (aF)	Degree of freedom ν_i
Quadrature Bridge						
Frequency	795.77 Hz	3.10^{-7} Hz	rectangular, B	$6.7.10^{-12}$ F/Hz	2	50
Resistance (EHQ) (20kΩ//)	10 000 Ω	$6\ 10^{-5}$ Ω	gaussian, B	$5\ 10^{-13}$ F/Ω	30	50
Resistance Frequency effect	$-3.4.10^{-4}$ Ω	$5.3.10^{-5}$Ω	gaussian, B	1.10^{-12} F/Ω	53	42
Null current in high potential ports Adjustement of R_H	8000 Ω	0.3 Ω	rectangular, B	1.10^{-17} F/Ω	3	infinite
Adjustement of C_H	3800 pF	12 pF	rectangular, B	$8.33.10^{-8}$	1	infinite
Adjustement of C_B	54500 pF	12 pF	rectangular, B	$8.33.10^{-8}$	1	infinite
Null current in low potential ports Adjustement of k_B	-0.0003	0.00006	rectangular, B	1.10^{-15} F	0	infinite
Adjustement of k_p	1.050	0.0006	rectangular, B	1.10^{-16} F	0	infinite
Null voltage condition between R1-C1 Adjustement of kq	0.070	0.0006	rectangular, B	1.10^{-16} F	0	infinite
Adjustement of kp	0.085	0.0006	rectangular, B	1.10^{-16} F	0	infinite
Null voltage condition between R2-C2 Adjustement of kq	1.020	0.0006	rectangular, B	1.10^{-16} F	0	infinite
Main detection arm Adjustement of R_B	495000 Ω	60 Ω	rectangular, B	$1.7.10^{-20}$ F/Ω	1	infinite
Adjustement of C_A	9800 pF	12 pF	rectangular, B	$8.33.10^{-8}$	1	infinite
Main balance Adjustement of kp	0.5000000	0.0000010	rectangular, B	1.10^{-11} F	10	infinite
Adjustement of k_q	0.5000000	0.0000010	rectangular, B	1.10^{-14} F	0	infinite
Relative uncertainty of the main detector	0 nV	50 nV	gaussian, B	1.10^{-10} F/V	5	13
Coaxility defect	0		gaussian, B		15	13
Reproducibility of the serial inductance of the UHF coaxial tees	0.0 µH	0.03 µH	gaussian, B	$6.7.10^{-11}$ F/H	2	13
Cable correction			gaussian, B		2	8
Temperature of the 10 nF	20°C	0.0006 °C	gaussian, B	$1.7.10^{-15}$ F/°C	1	22
10 nF combined relative standard uncertainty					$0.6.10^{-8}$	80
Four terminal pair capacitance bridge						
Frequency	795.77 Hz	1.10^{-2} Hz	rectangular, B	$<1.10^{-19}$ F/Hz	0	infinite
Bridge ratio correction (x2)	$0.058.10^{-6}$	$0.3.10^{-8}$	gaussian, B	1.10^{-10} F	0.3	13
Loading			gaussian, B		0.2	13
Null current in high potential ports Adjustement of R_H	3340.00 Ω	0.06 Ω	rectangular,B	$1.7.10^{-19}$ F/Ω	0.01	infinite
Adjustement of C_H	999 520 µF	10 µF	rectangular,B	1.10^{-15}	0.01	infinite
Adjustement of k_H	1.0000887	0.00000006	rectangular,B	$1.7.10^{-13}$ F	0.01	infinite
Null current in low potential ports Adjustement of R_B	915.6 Ω	0.06 Ω	rectangular,B	$1.7.10^{-19}$ F/Ω	0.01	infinite
Adjustement of C_B	992.400 µF	10 µF	rectangular,B	1.10^{-15}	0.01	infinite
Adjustement of k_B	-0.0000150	0.00000006	rectangular,B	$1.7.10^{-13}$ F	0.01	infinite
Kelvin Arm Adjustement of k_p	0.55	0.0006	rectangular,B	$1.7.10^{-17}$ F	0.01	infinite
Adjustement of k_q	0.595	0.0006	rectangular,B	$1.7.10^{-17}$ F	0.01	infinite
Main balance Adjustement of kp	0	0.0000001	rectangular,B	1.10^{-12} F	0.1	infinite
Adjustement of k_q	0	0.0000001	rectangular,B	5.10^{-16} F	0	infinite
relative uncertainty of the main detector main balance	0 nV	50 nV	rectangular,B	1.10^{-12} F/V	0.05	50
Coaxility defect			gaussian, B		0.15	13
Reproducibility of the serial inductance of the UHF coaxial tees	0.0 µH	0.03 µH	gaussian, B	$6.7.10^{-13}$ F/H	0.02	13
Temperature of the 10 nF	20°C	0.0006 °C	gaussian, B	$1.7.10^{-17}$ F/°C	0.01	22
Temperature of the 1000 pF	20°C	0.0006 °C	gaussian, B	$1.7.10^{-17}$ F/°C	0.01	22
Cable correction			gaussian, B		0.2	13
Voltage coefficient (1000 pF)	5.10^{-8} pF/V	1.10^{-8} pF/V	gaussian, B	4.10^{-12} V	0.04	8
Variability of repeated measurements of the 100 pF			Type A		0.4	15
100 pF combined relative standard uncertainty					$0.9.10^{-8}$	128
Two terminal pair capacitance bridge						
Frequency	795.77 Hz	1.10^{-2} Hz	rectangular,B	3.10^{-19} F/Hz	0	infinite
Bridge ratio correction	$0.051.10^{-6}$	$0.3.10^{-8}$	gaussian,B	$6.7.10^{-12}$ F	0.02	13
Loading			gaussian,B		0.015	13
Main balance Adjustement of kp	0	0.0000001	rectangular,B	1.10^{-13} F	0.01	infinite
Adjustement of k_q	0	0.0000001	rectangular,B	5.10^{-16} F	0	infinite
Relative uncertainty of the main detector	0 nV	50 nV	gaussian,B	1.10^{-13} F/V	0.005	50
Coaxility defect	0		gaussian,B		0.015	35
Cable correction	$-2.5.10^{-8}$ pF	1.10^{-8} pF	gaussian,B	1.10^{-12}	0.01	8
Variability of repeated measurements from 10 pF			Type A		0.01	14
10 pF combined relative standard uncertainty					$1.0.10^{-8}$	170

Uncertainty budget: measurements performed at 1591.55 Hz

Quantity X_i	Estimate x_i	Standard uncertainty $u(x_i)$	Probability distribution /method of evaluation (A,B)	Sensitivity coefficient c_i	Uncertainty contribution $c_i u(x_i)$ (aF)	Degree of freedom ν_i
Quadrature Bridge						
Frequency	1591.55 Hz	3.10^{-7} Hz	rectangular, B	$6.7.10^{-12}$ F/Hz	2	50
Resistance (EHQ) (10 kΩ)	10 000 Ω	$4\ 10^{-5}$ Ω	gaussian, B	$5\ 10^{-13}$ F/Ω	20	50
Resistance Frequency effect	0 Ω	$3.5.10^{-5}$ Ω	gaussian, B	2.10^{-12} F/Ω	70	27
Null current in high potential ports Adjustement of R_H	8000 Ω	0.3 Ω	rectangular, B	1.10^{-17} F/Ω	3	infinite
Adjustement of C_H	3800 pF	12 pF	rectangular, B	$8.33.10^{-8}$	1	infinite
Adjustement of C_B	54500 pF	12 pF	rectangular, B	$8.33.10^{-8}$	1	infinite
Null current in low potential ports Adjustement of kB	-0.0003	0.00006	rectangular, B	1.10^{-15} F	0	infinite
Adjustement of k_p	1.050	0.0006	rectangular, B	1.10^{-16} F	0	infinite
Null voltage condition between R1-C1 Adjustement of kq	0.070	0.0006	rectangular, B	1.10^{-16} F	0	infinite
Adjustement of kp	0.085	0.0006	rectangular, B	1.10^{-16} F	0	infinite
Null voltage condition between R2-C2 Adjustement of kq	1.020	0.0006	rectangular, B	1.10^{-16} F	0	infinite
Main detection arm Adjustement of R_B	495000 Ω	60 Ω	rectangular, B	$1.7.10^{-20}$ F/Ω	1	infinite
Adjustement of C_A	9800 pF	12 pF	rectangular, B	$8.33.10^{-8}$	1	infinite
Main balance Adjustement of kp	0.5000000	0.0000010	rectangular, B	1.10^{-11} F	10	infinite
Adjustement of k_q	0.5000000	0.0000010	rectangular, B	1.10^{-14} F	0	infinite
Relative uncertainty of the main detector	0 nV	50 nV	gaussian, B	1.10^{-10} F/V	5	13
Coaxility defect	0		gaussian, B		15	13
Reproducibility of the serial inductance of the UHF coaxial tees	0.0 µH	0.03 µH	gaussian, B	$6.7.10^{-11}$ F/H	2	13
Cable correction			gaussian, B		2	8
Temperature of the 10 nF	20°C	0.0006 °C	gaussian, B	$1.7.10^{-15}$ F/°C	1	22
10 nF combined relative standard uncertainty					$0.8.10^{-8}$	40
Four terminal pair capacitance bridge						
Frequency	1591.55 Hz	1.10^{-2} Hz	rectangular, B	$<1.10^{-19}$ F/Hz	0	infinite
Bridge ratio correction (x2)	$0.275.10^{-6}$	$0.3.10^{-8}$	gaussian, B	1.10^{-10} F	0.3	13
loading			gaussian, B		0.2	13
Null current in high potential ports Adjustement of R_H	3340.00 Ω	0.06 Ω	rectangular, B	$1.7.10^{-19}$ F/Ω	0.01	infinite
Adjustement of C_H	999 520 µF	10 µF	rectangular, B	1.10^{-15}	0.01	infinite
Adjustement of k_H	1.0000887	0.00000006	rectangular, B	$1.7.10^{-13}$ F	0.01	infinite
Null current in low potential ports Adjustement of R_B	915.6 Ω	0.06 Ω	rectangular, B	$1.7.10^{-19}$ F/Ω	0.01	infinite
Adjustement of C_B	992.400 µF	10 µF	rectangular, B	1.10^{-15}	0.01	infinite
Adjustement of k_B	-0.0000150	0.00000006	rectangular, B	$1.7.10^{-13}$ F	0.01	infinite
Kelvin Arm Adjustement of k_p	0.55	0.0006	rectangular, B	$1.7.10^{-17}$ F	0.01	infinite
Adjustement of k_q	0.595	0.0006	rectangular, B	$1.7.10^{-17}$ F	0.01	infinite
Main balance Adjustement of kp	0	0.0000001	rectangular, B	1.10^{-12} F	0.1	infinite
Adjustement of k_q	0	0.0000001	rectangular, B	5.10^{-16} F	0	infinite
Relative uncertainty of the main detector main balance	0 nV	50 nV	gaussian, B	1.10^{-12} F/V	0.05	50
Coaxility defect	0		gaussian, B		0.15	13
Reproducibility of the serial inductance of the UHF coaxial tees	0.0 µH	0.03 µH	gaussian, B	$6.7.10^{-13}$ F/H	0.02	13
Temperature of the 10 nF	20°C	0.0006 °C	gaussian, B	$1.7.10^{-17}$ F/°C	0.01	22
Temperature of the 1000 pF	20°C	0.0006 °C	gaussian, B	$1.7.10^{-17}$ F/°C	0.01	22
Cable correction			gaussian, B		0.20	13
Voltage coefficient (1000 pF)	5.10^{-8} pF/V	1.10^{-8} pF/V	gaussian, B	4.10^{-12} V	0.04	8
Variability of repeated measurements of the 100 pF			Type A		0.5	15
100 pF combined relative standard uncertainty					$1.1.10^{-8}$	74
Two terminal pair capacitance bridge						
Frequency	1591.55 Hz	1.10^{-2} Hz	rectangular, B	3.10^{-19} F/Hz	0.003	infinite
Bridge ratio correction	$0.213.10^{-6}$	$0.3.10^{-8}$	gaussian, B	$6.7.10^{-12}$ F	0.02	13
Loading			gaussian, B		0.015	13
Main balance Adjustement of kp	0	0.0000001	rectangular, B	1.10^{-13} F	0.01	infinite
Adjustement of k_q	0	0.0000001	rectangular, B	5.10^{-16} F	0	infinite
Relative uncertainty of the main detector	0 nV	50 nV	gaussian, B	1.10^{-13} F/V	0.005	50
Coaxility defect	0		gaussian, B		0.015	35
Cable correction	-10.10^{-8} pF	1.10^{-8} pF	gaussian, B	1.10^{-12}	0.01	8
Variability of repeated measurements from 10 pF			Type A		0.02	14
10 pF combined relative standard uncertainty					$1.1.10^{-8}$	98

10.4 METAS uncertainty budgets

Extent of Measurement

Measurement of the capacitance, *C*, of 100 pF and 10 pF capacitance standards at 1233 Hz in agreement with the technical protocol.

Measurement Procedure

The relative deviation of the capacitance from its nominal value can be expressed by

$$\alpha_{100\,\mathrm{pF}} = -\frac{1}{2}\left\{\alpha_{G1} + \alpha_{G2} + \alpha_{Q} + \alpha_{c}\right\} + \frac{\alpha_{S1} + \alpha_{S2}}{2} + \alpha_{S3} - 2\cdot\alpha_{10} + 2\cdot\left(\alpha_c^b - \alpha_c^t\right)$$

for the 100 pF capacitance standard and

$$\alpha_{10\,\mathrm{pF}} = -\frac{1}{2}\left\{\alpha_{G1} + \alpha_{G2} + \alpha_{Q} + \alpha_{c}\right\} + \frac{\alpha_{S1} + \alpha_{S2}}{2} + \alpha_{S3} + \alpha_{S4} - 3\cdot\alpha_{10} + 2\cdot\left(\alpha_c^b - \alpha_c^t\right) + \left(\alpha_c'^b - \alpha_c'^t\right)$$ for

the 10 pF capacitance standards. The different parameters are:

α_{G1}, α_{G2} : are the relative deviation of the calculable resistances (G1 and G2) from the nominal value ($R_{\mathrm{K\text{-}90}}/2$) at the frequency of 1233 Hz.

α_Q : is the in-phase component of the main balance of the quadrature bridge.

α_c : is the cable correction for the quadrature bridge

α_{S1} : is the in-phase balance of the 10 nF(A) -1 nF comparison

α_{S2} : is the in-phase balance of the 10 nF(B) -1 nF comparison

α_{S3} : is the in-phase balance of the 1 nF -100 pF comparison

α_{S4} : is the in-phase balance of the 100 pF -10 pF comparison

α_{10} : is the error of the 10:-1 ratio transformer

α_c^t : is the 4TP cable correction for the top standard of the 10:-1 comparison

α_c^b : is the 4TP cable correction for the bottom standard of the 10:-1 comparison

$\alpha_c'^t$: is the 3TP cable correction for the top standard of the 10:-1 comparison

$\alpha_c'^b$: is the 3TP cable correction for the bottom standard of the 10:-1 comparison

Traceability

The dc value of the resistance is calibrated in terms of $R_{\mathrm{K\text{-}90}}$ and the frequency dependence between dc and 1233 Hz of the calculable resistances as been assessed by an inter-comparison [*Metrologia*, 2002, **39**, 231-237] and by a direct comparison to the ac quantum Hall effect [*Metrologia*, 2006, **43**, 409-413]. The realization of the farad is therefore obtained from the ohm and the second.

U-Budget: Calibration of 100 pF Capacitance Standard

Quantity X_i	Estimate x_i	Standard uncertainty $u(x_i)$	Probability distribution	Method of evaluation (A, B)	Sensitivity coefficient c_i	Relative uncertainty in uF/F c_i*$u(x_i)$	Degrees of freedom ν_i
α_{G1}	33.079	0.021	Normal	A & B	0.5	0.010	12
α_{G2}	44.221	0.021	Normal	A & B	0.5	0.010	12
α_Q	-36.494	0.072	Normal	A & B	0.5	0.036	39
α_c	0.000	0.002	Box	B	0.5	0.001	20
α_{S1}	-8.222	0.018	Normal	A & B	0.5	0.009	23
α_{S2}	-1.164	0.018	Normal	A & B	0.5	0.009	23
α_{S3}	27.628	0.011	Normal	A & B	1.0	0.011	44
α_{10}	0.420	0.070	Box	B	2.0	0.081	20
$\alpha_c{}^b$	-0.002	0.005	Box	B	2.0	0.006	20
$\alpha_c{}^t$	-0.008	0.005	Box	B	2.0	0.006	20
		Combined standard uncertainty			u_c	0.092 ppm	
		Effective degree of freedom			ν_i	32	
		Expanded uncertainty (p=95%)			***U***	**0.187 uF/F**	

U-Budget: Calibration of 10 pF Capacitance Standard

Quantity X_i	Estimate x_i	Standard uncertainty $u(x_i)$	Probability distribution	Method of evaluation (A, B)	Sensitivity coefficient c_i	Relative uncertainty in uF/F c_i*$u(x_i)$	Degrees of freedom ν_i
α_{G1}	33.079	0.021	Normal	A & B	0.5	0.010	12
α_{G2}	44.221	0.021	Normal	A & B	0.5	0.010	12
α_Q	-36.494	0.072	Normal	A & B	0.5	0.036	39
α_c	0.000	0.002	Box	B	0.5	0.001	20
α_{S1}	-8.222	0.018	Normal	A & B	0.5	0.009	23
α_{S2}	-1.164	0.018	Normal	A & B	0.5	0.009	23
α_{S3}	27.628	0.011	Normal	A & B	1.0	0.011	44
α_{S4}	0.100	0.010	Normal	A & B	1.0	0.010	39
α_{10}	0.420	0.070	Box	B	3.0	0.121	20
$\alpha_c{}^b$	-0.002	0.005	Box	B	2.0	0.006	20
$\alpha_c{}^t$	-0.008	0.005	Box	B	2.0	0.006	20
$\alpha'_c{}^b$	-0.001	0.005	Box	B	1.0	0.003	20
$\alpha'_c{}^t$	0.008	0.005	Box	B	1.0	0.003	20
		Combined standard uncertainty			u_c	0.129 ppm	
		Effective degree of freedom			ν_i	26	
		Expanded uncertainty (p=95%)			***U***	**0.266 uF/F**	

U-Budget: α_{G1} and α_{G2} at 1233 Hz

Source of uncertainty	Method of evaluation (A, B)	Relative uncertainty in µΩ/Ω $u(xi)$	Degrees of freedom ν_i
Type A and B uncertainty of the CCC measurement	A & B	0.005	20
Determination of the mean value at mean time	A	0.002	18
Frequency dependence between DC and 1233 Hz	B	0.020	10
Combined standard uncertainty	u_c	0.021 µΩ/Ω	
Effective degree of freedom	ν_i	12	

U-Budget: α_Q

Source of uncertainty	Method of evaluation (A, B)	Relative uncertainty in µΩ/Ω $u(xi)$	Degrees of freedom ν_i
Type A (1 nV after 100 sec)	A	0.042	10
Accuracy on the C_{in}/C_{Nom} ratio	A & B	0.029	18
Frequency accuracy	A	0.016	10
Auxiliary balances	B	0.020	5
Intermodulation distortion	B	0.010	10
Coaxial current inequalities	B	0.010	10
Detector offset	B	0.042	10
Combined standard uncertainty	u_c	0.072 µΩ/Ω	
Effective degree of freedom	ν_i	39	

U-Budget: 10 nF-1 nF, α_{S1} and α_{S2}

Source of uncertainty	Method of evaluation (A, B)	Relative uncertainty in µΩ/Ω $u(xi)$	Degrees of freedom ν_i
noise/sensitivity (1 nV / 70 nV/ppm)	A	0.014	10
in-phase injection	B	0.003	10
phase error of the out of phase injection	B	0.006	10
auxiliary balances	B	0.006	10
coaxial choke effectivness	B	0.002	10
short term stability	B	0.006	10
Combined standard uncertainty	u_c	0.018 µΩ/Ω	
Effective degree of freedom	ν_i	23	

U-Budget: 1 nF-100 pF, α_{S3}

Source of uncertainty	Method of evaluation (A, B)	Relative uncertainty in µΩ/Ω $u(xi)$	Degrees of freedom ν_i
noise/sensitivity (1 nV / 253 nV/ppm)	A	0.004	10
in-phase injection	B	0.003	10
phase error of the out of phase injection	B	0.006	10
auxiliary balances	B	0.006	10
coaxial choke effectivness	B	0.002	10
short term stability	B	0.006	10
Combined standard uncertainty	u_c	0.011 µΩ/Ω	
Effective degree of freedom	ν_i	44	

U-Budget: 100 pF-10 pF, α_{S4}

Source of uncertainty	Method of evaluation (A, B)	Relative uncertainty in µΩ/Ω $u(xi)$	Degrees of freedom ν_i
noise/sensitivity (1 nV / 327 nV/ppm)	A	0.003	10
in-phase injection	B	0.003	10
phase error of the out of phase injection	B	0.006	10
auxiliary balances	B	0.004	10
coaxial choke effectivness	B	0.002	10
short term stability	B	0.006	10
Combined standard uncertainty	u_c	0.010 µΩ/Ω	
Effective degree of freedom	ν_i	39	

10.5 NMIA uncertainty budgets

Uncertainty statement A: 10 pF and 1000 Hz

UNCERTAINTY STATEMENT	Serial No.: 1310				10 pF	1000 Hz
Quantity	**Estimate**	**Standard uncertainty**	**Probability distribution/ method of evaluation (A, B)**	**Sensitivity coefficient**	**Uncertainty contribution**	**Degree of freedom**
X_i	***x_i***	***$u(x_i)$***		***c_i***	***$u(R_i)$***	***v_i***
Calculable capacitor measurements	-	0.002 µF/F	Normal/A	2.65	0.005 µF/F	7
Calculable capacitor	-	0.034 µF/F	Normal/B	1	0.034 µF/F	7.76
Bridge resolution	-	0.003 µF/F	Rectangular/B	2.35	0.007 µF/F	Infinite
Accuracy of two-port definition	-	0.001 µF/F	Normal/B	1	0.001 µF/F	3
Bridge balance injection	-	0.001 µF/F	Normal/B	1	0.001 µF/F	3
Calibration of 10:1 ratio	-	0.002 µF/F	Normal/B	2	0.005 µF/F	102.5
Bridge voltage coefficient: 5I to C½	-	0.001 µF/F	Normal/B	1	0.001 µF/F	5
Voltage coefficient 5I	-	0.008 µF/F	Normal/B	0.99	0.008 µF/F	5
Leads correction	-0.012 µF/F	0.001 µF/F	Rectangular/B	1	0.001 µF/F	infinite
Temperature	-	0.11 °C	Rectangular/B	0.01 µF/F/°C	0.001 µF/F	5
Repeated measurement	0.036 µF/F	0.010 µF/F	Normal/A	1	0.010 µF/F	5
R_x	**10.000 000 24 pF**					
		Combined standard uncertainty			**0.037 µF/F**	
		Effective degrees of freedom			**12**	
		Expanded uncertainty (95% coverage factor)			**0.082 µF/F**	

Uncertainty statement B: 100 pF and 1000 Hz

UNCERTAINTY STATEMENT	Serial No.: 1256				100 pF	1000 Hz
Quantity	**Estimate**	**Standard uncertainty**	**Probability distribution/ method of evaluation (A, B)**	**Sensitivity coefficient**	**Uncertainty contribution**	**Degree of freedom**
X_i	***x_i***	***$u(x_i)$***		***c_i***	***$u(R_i)$***	***v_i***
Calculable capacitor measurements	-	0.002 µF/F	Normal/A	2.65	0.005 µF/F	7
Calculable capacitor	-	0.034 µF/F	Normal/B	1	0.034 µF/F	7.76
Bridge resolution	-	0.003 µF/F	Rectangular/B	2.55	0.007 µF/F	Infinite
Accuracy of two-port definition	-	0.001 µF/F	Normal/B	2	0.002 µF/F	3
Bridge balance injection	-	0.001 µF/F	Normal/B	2	0.002 µF/F	3
Calibration of 10:1 ratio	-	0.002 µF/F	Normal/B	2	0.005 µF/F	102.5
Bridge voltage coefficient: 5I to C½	-	0.001 µF/F	Normal/B	1	0.001 µF/F	5
Voltage coefficient 5I	-	0.008 µF/F	Normal/B	0.99	0.008 µF/F	5
Leads correction	-0.018 µF/F	0.001 µF/F	Rectangular/B	1	0.001 µF/F	infinite
Temperature	-	0.11 °C	Rectangular/B	0.01 µF/F/°C	0.001 µF/F	5
Repeated measurement	1.976 µF/F	0.010 µF/F	Normal/A	1	0.010 µF/F	5
R_x	**10.000 195 8 pF**					
		Combined standard uncertainty			**0.037 µF/F**	
		Effective degrees of freedom			**12**	
		Expanded uncertainty (95% coverage factor)			**0.082 µF/F**	

Uncertainty statement C: 10 pF and 1592 Hz

UNCERTAINTY STATEMENT	Serial No.: 1310				10 pF	1592 Hz
Quantity	**Estimate**	**Standard uncer-tainty**	**Probability distri-bution/ method of evaluation (A, B)**	**Sensitivity coefficient**	**Uncertainty contribution**	**Degree of freedom**
X_i	x_i	$u(x_i)$		c_i	$u(R_i)$	ν_i
Calculable capacitor measurements	-	0.002 µF/F	Normal/A	2.65	0.005 µF/F	7
Calculable capacitor	-	0.034 µF/F	Normal/B	1	0.034 µF/F	7.76
Bridge resolution	-	0.003 µF/F	Rectangular/B	2.35	0.007 µF/F	Infinite
Accuracy of two-port definition	-	0.001 µF/F	Normal/B	1	0.001 µF/F	3
Bridge balance injection	-	0.001 µF/F	Normal/B	1	0.001 µF/F	3
Calibration of 10:1 ratio	-	0.003 µF/F	Normal/B	1	0.003 µF/F	211.5
Bridge voltage coefficient: 5I to C½	-	0.001 µF/F	Normal/B	1	0.001 µF/F	5
Voltage coefficient 5I	-	0.008 µF/F	Normal/B	0.99	0.008 µF/F	5
Leads correction	-0.030 µF/F	0.002 µF/F	Rectangular/B	1	0.002 µF/F	infinite
Temperature	-	0.11 °C	Rectangular/B	0.01 µF/F/°C	0.001 µF/F	5
Repeated measurement	0.019 µF/F	0.011 µF/F	Normal/A	1	0.011 µF/F	5
R_x	**9.999 999 88 pF**					
		Combined standard uncertainty			**0.037 µF/F**	
		Effective degrees of freedom			**12**	
		Expanded uncertainty (95% coverage factor)			**0.081 µF/F**	

Uncertainty statement D: 100 pF and 1592 Hz

UNCERTAINTY STATEMENT	Serial No.: 1256				100 pF	1592 Hz
Quantity	**Estimate**	**Standard uncer-tainty**	**Probability distri-bution/ method of evaluation (A, B)**	**Sensitivity coefficient**	**Uncertainty contribution**	**Degree of freedom**
X_i	x_i	$u(x_i)$		c_i	$u(R_i)$	ν_i
Calculable capacitor measurements	-	0.002 µF/F	Normal/A	2.65	0.005 µF/F	7
Calculable capacitor	-	0.034 µF/F	Normal/B	1	0.034 µF/F	7.76
Bridge resolution	-	0.003 µF/F	Rectangular/B	2.55	0.007 µF/F	Infinite
Accuracy of two-port definition	-	0.001 µF/F	Normal/B	2	0.002 µF/F	3
Bridge balance injection	-	0.001 µF/F	Normal/B	2	0.002 µF/F	3
Calibration of 10:1 ratio	-	0.003 µF/F	Normal/B	2	0.006 µF/F	211.5
Bridge voltage coefficient: 5I to C½	-	0.001 µF/F	Normal/B	1	0.001 µF/F	5
Voltage coefficient 5I	-	0.008 µF/F	Normal/B	0.99	0.008 µF/F	5
Leads correction	-0.046 µF/F	0.002 µF/F	Rectangular/B	1	0.002 µF/F	infinite
Temperature	-	0.11 °C	Rectangular/B	0.01 µF/F/°C	0.001 µF/F	5
Repeated measurement	1.950 µF/F	0.013 µF/F	Normal/A	1	0.013 µF/F	5
R_x	**10.000 190 4 pF**					
		Combined standard uncertainty			**0.039 µF/F**	
		Effective degrees of freedom			**13**	
		Expanded uncertainty (95% coverage factor)			**0.083 µF/F**	

Because the NMIA laboratory runs at a temperature of 20°C which deviates from the nominal 23°C, an uncertainty contribution of 0.006 µF/F (k = 1) for the ambient temperature corrections has to be added.

10.6 VSL uncertainty budgets

Quadrature bridge uncertainty

The main contributions to uncertainty in the quadrature bridge measurement can be seen directly from the balance equation (7) which is repeated here:

$$\frac{dC_1}{C_\mathrm{n}} + \frac{dC_3}{C_\mathrm{n}} \approx \frac{dG_2}{G_\mathrm{n}} + \frac{dG_4}{G_\mathrm{n}} - \frac{(\alpha - \alpha')\Delta c_1}{C_\mathrm{n}} - 2\frac{d\omega}{\omega_\mathrm{n}} \qquad (1)$$

***dG*$_2$*/G*$_\mathrm{n}$ and *dG*$_4$*/G*$_\mathrm{n}$** represent the contributions from resistors R_2 and R_4.
The uncertainty in these resistance values can be separated into 4 different contributions:
- The uncertainty in the DC value of the resistors is subdivided in:

  - Contributions from the DC-QHRS and the potentiometric comparison system: 0.01 µS/S

  - Uncertainty contributions from drift and stability of the AC-DC resistors.
  One of the quadrafilar resistors shows a predictable drift of -0.82 µS/S / year. Its standard uncertainty is 0.014 µS/S for the time period of the comparison.
  The second quadrafilar resistor shows a much stronger drift of -27 µS/S / year. Even more, its behaviour is rather unstable with larger excursions from the nominal drift line. Its standard uncertainty is 0.79 µS/S for the time period of the comparison. Measurements have been performed with this resistor, but these results have not been used for the computations of the values of the 10 nF capacitors due to the large instability. These measurements have only been used to determine the phase-angle of each of the three AC-DC resistors.
  The drift of the octofilar resistor is -3.13 µS/S / year. Every now and then, the value of this resistor shows some small steps up and down with respect to the nominal drift line. Its standard uncertainty is 0.051 µS/S for the time period of the comparison.

- The uncertainty in the determination of the AC-DC difference of the resistance value:
For the quadrafilar resistor, the AC-DC difference at the measurement frequency is estimated to be 0.00 µS/S with an uncertainty of less than 0.02 µS/S [3]. For the octofilar resistor, the AC-DC difference at the measurement frequency is estimated to be 0.00 µS/S with an uncertainty of less than 0.01 µS/S [4].

- The uncertainty of cable corrections:
The four main impedances in the bridge are connected in a 4TP definition of these standards. The cable corrections for these standards are estimated to be 0.00 µS/S with an uncertainty of less than 0.02 µS/S.

- The uncertainty due to imperfect 4TP definition of the standards:
In an ideal 4TP definition, the currents in the high and low potential ports should be zero and the voltage at the low potential port should be zero. In practice, these conditions are met as close as possible with several auxiliary balances in the bridge. Systematic deviations in the impedance values due to their imperfect 4TP definition is estimated to be 0.00 µS/S with an uncertainty of less than 0.01 µS/S.

($\alpha - \alpha'$) is the contribution of the voltage divider T_2 (in Figure 9.6.1) that drives a current through capacitor Δc_1 for adjusting the main balance. The uncertainty in this parameter not only includes the ratio error and high- and low-end errors of divider T_2, but it also includes the effective resolution of the bridge. This divider cannot be adjusted better than 1 part in 10^{-5}, because beyond this point we can no longer discriminate the null-detector reading from its noise.
The standard uncertainty of this parameter is estimated to be 10 µV/V.

Δc_1 is a standard capacitor of 10 pF. Its standard uncertainty is estimated to be 10 µF/F.

$d\omega/\omega_n$ represents the angular measurement frequency.
For the measurements until 25 August, a source was used with a free-running timebase and the frequency was measured with a counter of which the timebase was locked to a 10 MHz reference signal derived from the VSL frequency standard. The reading from the counter was a bit noisy because of the limited stability of the source.
Therefore, from 26 August, another source was used, of which the timebase could also be directly locked to the 10 MHz reference frequency.
The overall frequency uncertainty was less than 0.02 µHz/Hz.

2ω and 3ω harmonics
2nd and 3rd harmonics of the measurement frequency can be introduced by the source or by non-linear behaviour of the bridge components (such as the transformers). These harmonics can result in systematic errors in the null-detector reading and thus affect the bridge balance.
The source used for these measurements was selected for its spectral purity.
Furthermore, a 2nd and 3rd harmonic rejection filter (HRF in Figure 9.6.1) was placed before the null-detector.
Any remaining effects from harmonics are estimated to be less than 0.02 µF/F in the measurement results.

2nd order terms
To simplify the computations, the 2nd order effects have not been included in the balance equation (19). Nevertheless, the magnitude of these effects has been evaluated.
To avoid significant contributions from 2nd order terms, the main impedances should be close to nominal and the frequency should be close to nominal. All impedances used for the computations are within 30 µΩ/Ω from their nominal value.
For the first set of measurements the frequency deviation was about 140 µHz/Hz. Here we have made appropriate corrections for the 2nd order effects. For the next measurements, the frequency was within 25 µHz/Hz from nominal and therefore corrections for 2nd order effects were not needed.
Other important effects arise from the parasitic loss of capacitors C_1 and C_3 and from the phase angles of the resistors R_2 and R_4.
For the capacitors, $G/\omega C$ is about -40 µS/S.
For the quadrifilar resistors, $\omega C/G$ is about -150 µS/S.
For the octofilar resistor, $\omega C/G$ is about -70 µS/S.
The total effect from uncorrected 2nd (and higher) order terms is estimated to be less than 0.01 µF/F.

Chokes
The effectiveness of chokes was tested in three ways.

- Using a magnetic core with a high number of turns of wire, the current unbalance in several cables is measured. The detected signal should be more or less equally small in each of the cables.
- After balancing the bridge, each of the chokes was shorted one after another and the effect of this on the null-detector reading was monitored. In no case a significant effect on the null-detector reading could be observed.

- A sinusoidal current, at the same frequency as the measurement frequency, is passed through several loops of wire to generate and electro-magnetic field. While the bridge is balanced, the loop is moved around the bridge and the effect on the null-detector is monitored.

No significant effects have been seen on the null-detector.

The total uncertainty contribution of imperfect current balances in the cables is estimated to be less than 0.03 µF/F.

Repeatability of the measurements

The standard deviation in the result of $dC_1/C_n + dC_3/C_n$ is 0.02 µF/F.

Correlations

Between the different uncertainty contributions mentioned here, there are no correlations, except for the DC measurements of R_2 and R_4. Even in the DC measurements, the effects of correlation are very small, because the uncertainty from the QHRS and the potentiometric system are smaller than the uncertainty from the stability of the AC-DC resistors. For this reason, neglecting the correlation has no significant effect on the total uncertainty.

Table 10.6.1. Uncertainty budget quadrature bridge

Quantity	Estimate	Standard uncertainty	Probability distribution /method of evaluation (A, B)	Sensitivity coefficient	Uncertainty contribution	Degree of freedom
X_i	x_i	$u(x_i)$		c_i	$u(R_i)$	ν_i
dG_2 value dc	-28.39 µS/S	0.052 µS/S	norm / B	1 (µF/F)/(µS/S)	0.052 µF/F	7
G_2 ac-dc diff	0.00 µS/S	0.006 µS/S	rec / B	1 (µF/F)/(µS/S)	0.006 µF/F	50
G_2 4tp def	0.00 µS/S	0.006 µS/S	rec / B	1 (µF/F)/(µS/S)	0.006 µF/F	50
G_2 cables	0.00 µS/S	0.012 µS/S	rec / B	1 (µF/F)/(µS/S)	0.012 µF/F	50
dG_4 value dc	2.91 µS/S	0.017 µS/S	norm / B	1 (µF/F)/(µS/S)	0.017 µF/F	7
G_4 ac-dc diff	0.00 µS/S	0.012 µS/S	rec / B	1 (µF/F)/(µS/S)	0.012 µF/F	50
G_4 4tp def	0.00 µS/S	0.006 µS/S	rec / B	1 (µF/F)/(µS/S)	0.006 µF/F	50
G_4 cables	0.00 µS/S	0.012 µS/S	rec / B	1 (µF/F)/(µS/S)	0.012 µF/F	50
ω	7748.0919 rad/s	0.012 1.0×10^{-6}	rec / B	-2 µF/F	-0.023 µF/F	100
2ω, 3ω error	0.00 µF/F	0.012 µF/F	rec / B	1 -	0.012 µF/F	50
α−α'	< 0.5 V/V	10 µV/V	norm / B	-0.001 (µF/F)/(µV/V)	-0.010 µF/F	100
Δc_1	10 pF	10 µF/F	norm / B	-0.0005 (µF/F)/(V/V)	-0.005 µF/F	100
2nd order terms	0.00 µF/F	0.006 µF/F	rec / B	1 µF/F	0.006 µF/F	100
chokes	0.00 µF/F	0.017 µF/F	rec / B	1 µF/F	0.017 µF/F	50
stddev	0.00 µF/F	0.020 µF/F	norm / A	1 µF/F	0.020 µF/F	9
$dC_1/C_n + dC_3/C_n$	-38.00 µF/F					
		Combined standard uncertainty:			0.071 µF/F	
		Effective degrees of freedom:		23 k =	2.11	
		Expanded uncertainty (95% coverage factor):			0.150 µF/F	

Ratio bridge uncertainty

The ratio bridge is used in two different configurations:
- in the 1:1 ratio to determine the ratio of the two 10 nF capacitors or
- the 10:1 ratio for scaling from 10 nF to 10 pF.

In both cases, the balance equation can be used as the model equation for the uncertainty analysis. These equations are repeated here:

$$\frac{dC_1}{C_{1\mathrm{n}}} - \frac{dC_2}{C_{2\mathrm{n}}} \approx a - \frac{dE_1}{E_1} \qquad (2)$$

$$a = \frac{\alpha - \beta\left(\omega R_q C_q\right)^2}{100} \qquad (3)$$

In the case of the 1:1 measurement of the two 10 nF capacitors, the quantity to be determined is $dC_1/C_{1\mathrm{n}}$ - $dC_2/C_{2\mathrm{n}}$.

In the case of 10:1 measurements when scaling from 10 nF to 10 pF, capacitor C_2 will be the reference capacitor, and the quantity to be determined is $dC_1/C_{1\mathrm{n}}$.

Transformer ratio error dE_1/E_1

The transformer ratio error dE_1/E_1 in the 1:1 ratio can be eliminated by taking the average of two measurements in which the capacitors are switched from one side of the bridge to the other side. If by this reversed measurement the ratio error is not completely eliminated, the effect will at least be less than 0.01 µV/V

For the 10:1 measurement, the ratio error dE_1/E_1 has been calibrated by the method of permuting 11 capacitors. Ten capacitors of 10 pF were connected in parallel in the C_2 position of the bridge, and the 11th capacitor (also 10 pF) is connected in the C_1 position of the bridge.
Eleven measurements are performed, each time placing another one of the 11 capacitors in the C_1 position. If the values of the capacitors are close to the average of all capacitors, the ratio error of the bridge transformer can be calculated from the 11 measurement results (without the need to know all the individual values of the capacitors precisely). The capacitors should, however, remain stable during the course of the 11 measurements.
This calibration was repeated several times. The error dE_1/E_1 was found to be -0.002 µV/V with an estimated uncertainty of less than 0.03 µV/V.

After the comparison, it was discovered that there were systematic offsets in measured ratios, most probably caused by unproper grounding of the bridge. This grounding problem results in some undefined leakage currents running through the bridge. Effectively, this can be translated into an additional ratio error of the transformer. The corresponding uncertainty contribution is estimated to be:
- less than 0.3 µV/V for 10 nF to 1 nF,
- less than 0.4 µV/V for 1 nF to 100 pF and
- less than 0.5 µV/V for 100 pF to 10 pF.

In-phase injection ratio *a*

The in-phase injection ratio *a* is mainly determined by divider T_{IP} and injection transformer T_2 and, furthermore, a small in-phase contribution from the quadrature injection network T_Q. The in-phase injection ratio is calibrated in a 1:1 ratio measurement of two 10 nF capacitors. First the two capacitors are compared in the normal way, and then a 1 pF capacitor (with known value) is connected in parallel with one of the 10 nF capacitors. The injection ratio error was found to be 0.03 µV/V for an injection of 100 µV/V. In practice during the measurements, all injection voltages were much smaller than 100 µV/V. Therefore, the estimated uncertainty from $\alpha/100$ is less than 0.03 µV/V.

The quadrature injection ratio is calibrated in a similar way. Two resistors of 12.906 kΩ are compared in a 1:1 ratio. Then again a 1 pF capacitor is connected in parallel with one of the resistors. From the difference in the quadrature injection, the error of the T_Q, T_2 network can be found. The estimated uncertainty for $\beta(\omega R_q C_q)^2/100$ is less than 0.02 µV/V.

Standards under test C_1 and C_2

1:1 measurements

- For the 1:1 ratio measurements at 10 nF, we are only interested in the ratio between two capacitors, so there is no "reference" capacitor or capacitor "under test".

- During the period of the comparison, there was no visible drift of the capacitance values, so this effect on the ratio of the two capacitors was neglected.

- Both standards are connected in the bridge with the same type and length of cables. Therefore, any corrections for cables will not lead to significant uncertainty contributions. However, after the comparison, it was discovered that there were some bad connections in feed through connectors between the bridge and the standards under test. This can have affected both the 1:1 measurements of the 10 nF capacitors and the 10:1 measurements from 10 nF down to 10 pF. Therefore, in each of the measurements, additional uncertainties were attributed to the cables. These contributions were estimated to be less than 0.1 µF/F.

- In an ideal 4TP definition, the currents in the high and low potential ports should be zero and the voltage at the low potential port should be zero. In practice, these conditions are met as close as possible with several auxiliary balances in the bridge. Because of the symmetry of the 1:1 bridge and the reversal of the capacitors from one side to the other, it is to be expected that imperfections in the 4TP definition of the capacitors will affect both standards equally, with no significant effect on the ratio.

- The voltage and frequency dependences of the two 10 nF are quite similar for both standards. This is a reasonable assumption, since both standards are of the same type and age. The frequency dependence was also verified by comparing each of the standards against an air-type (dry-nitrogen) capacitor in the frequency range from 1223 Hz to 1243 Hz. Since the capacitors have the same properties, any small variations in voltage or frequency will not affect the measured ratio.

10:1 measurements

- In the 10:1 ratio measurements for scaling from 10 nF down to 1 nF, C_2 is always the reference capacitor and C_1 is the capacitor under test.

The starting point is the 10 nF values determined from the quadrature bridge and the 1:1 measurement of the 10 nF capacitors.
The expanded uncertainty for the 10 nF capacitors is derived from Table 2 and is 0.193 µF/F. The expanded uncertainty for the 1 nF capacitors is derived from Table 3 and is 0.442 µF/F. The expanded uncertainty for the 100 pF capacitors is derived from Table 4 and is 0.670 µF/F.

- The 10 nF, 100 pF, and 10 pF capacitors (either "reference" or "device under test") used in the measurements for this comparison do not show any significant drift during the time period of VSL's measurements for this comparison. The 1 nF capacitors do show a visible drift, however, these are only used as transfer standards.
  To avoid any significant effect from this drift, the transfer from 10 nF to 100 pF was always made within a short period of time: maximum 2 hours. The uncertainty contribution from drift of the reference standards is estimated to be less than 0.005 µF/F.

- The capacitors in the bridge are connected in a 4TP definition. The cable corrections for the standards are estimated to be 0.00 µS/S with an uncertainty of less than 0.02 µS/S.
  After the comparison, it was discovered that there were some bad connections in feed-through connectors between the bridge and the standards under test. This can have affected both the 1:1 measurements of the 10 nF capacitors and the 10:1 measurements from 10 nF down to 10 pF. Therefore, in each of the measurements, additional uncertainties were attributed to the cables. These contributions were estimated to be less than 0.1 µF/F.

- Systematic deviations in the capacitance values due to imperfect 4TP definition is estimated to be 0.00 µS/S with an uncertainty of less than 0.04 µS/S.

- The 10 nF capacitor is calibrated at nominally 1 V and is also used as reference at 1 V for calibrating the 1 nF, at nominally 10 V.
  The 1 nF capacitor is used as a reference at 1 V for calibrating the 100 pF at 10 V. And finally the 100 pF is used as a reference at 10 V for calibrating the 10 pF at 100 V. This shows that any effects of voltage dependence in the 10 nF capacitor and the 100 pF capacitor will not significantly affect the traceability chain, because they are used at the same voltage as the voltage used for their calibration.
  For the 1 nF capacitor this is not the case; it is used at 1 V and calibrated at 10 V. To test the voltage dependence, the 1 nF capacitor was compared with a 100 pF (GR1408 type) capacitor at different voltages from 1 V to 5 V. The differences in the results are within the noise of the bridge.
  We estimate the following contributions for the voltage dependence:
  10 nF: less than 0.01 (µF/F)/V
  1 nF: less than 0.001 (µF/F)/V
  100 pF: less than 0.001 (µF/F)/V

- From the capacitors used in these measurements, only the 10 nF capacitors have a significant frequency dependence. The frequency dependence was verified by comparing the standards against a 1 nF air-type (dry-nitrogen) capacitor in the frequency range from 1223 Hz to 1243 Hz. The frequency dependence was found to be (-0.035 ± 0.003) (µF/F)/Hz.
  For the other standards, the frequency dependence close to 1233 Hz is estimated to be (0.000 ± 0.001) (µF/F)/Hz.

All measurements were performed within 0.2 Hz from the nominal frequency f_n= 1 233.147 12 Hz.

Chokes

The effectiveness of chokes in the ratio bridge has been evaluated in a similar way as in the quadrature bridge. The total uncertainty contribution of imperfect current balances in the cables is estimated to be less than 0.03 µF/F.

2nd order terms

To simply the computations, the 2nd order effects have not been included in the balance equation (20) and equation (21). Nevertheless, the magnitude of these effects has been evaluated. The total effect from uncorrected 2nd (and higher) order terms is estimated to be less than 0.01 µF/F.

Repeatability of the measurements

For the 1:1 ratio measurements at 10 nF, the standard deviation in the result of dC_{1n}/C_n - dC_{2n}/C_n is 0.02 µF/F.
For the 10:1 ratio measurements from 10 nF down to 10 pF, the standard deviation in the results of dC_{1n}/C_n was typically between 0.01 µF/F and 0.02 µF/F.

Correlations

Correlations between uncertainty contributions have not been taken into account in the calculations. Within a single measurement, there are no significant correlations between different uncertainty contributions.
In the different steps of scaling from 10 nF to 10 pF there are correlations between uncertainty contributions in the consecutive steps:

- The error in the 10:1 ratio of the main transformer appears in each of the steps. Not taking into account the correlations between the steps may underestimate the total uncertainty.
- Cable corrections are strongly correlated between consecutive steps. Not taking into account the correlations between the steps may overestimate the total uncertainty.
- Uncertainty contributions from the injection system may be correlated, but the impact of these correlations is expected to be small because the injection ratios differ from one measurement to another.

Uncertainty budget tables for the measurements on the ratio bridge are given on the following pages:
Table 1: Uncertainty budget for 1:1 measurements at 10 nF
Table 3: Uncertainty budget for 10:1 measurements from 10 nF to 1 nF
Table 4: Uncertainty budget for 10:1 measurements from 1 nF to 100 pF
Table 5: Uncertainty budget for 10:1 measurements from 100 pF to 10 pF

Furthermore, Table 2, shows the uncertainty in the 10 nF capacitance values from the combined measurement of the quadrature bridge and the 1:1 ratio bridge.

Table 1. Uncertainty budget ratio bridge 1:1 at 10 nF

Quantity	Estimate	Standard uncertainty	Probability distribution /method of evaluation (A, B)	Sensitivity coefficient	Uncertainty contribution	Degree of freedom
X_i	x_i	$u(x_i)$		c_i	$u(R_i)$	n_i
dC_2/C_n	-16.27 µF/F					
Cables C_2	0.00	0.058		1	0.058	100
dC_1/C_n	-21.73 µF/F					
Cables C_1	0.00	0.058		1	0.058	100
dE_1	0.00 µV/V	0.006 µV/V	rec / B	1 (µF/F)/(µV/V)	0.006 µF/F	100
a_{inj}	-5.38 µV/V	0.017 µV/V	rec / B	1 (µF/F)/(µV/V)	0.017 µF/F	100
$b_{inj\ in\text{-}phase}$	-0.05 µV/V	0.012 µV/V	rec / B	1 (µF/F)/(µV/V)	0.012 µF/F	100
chokes	0 µF/F	0.017 µF/F	rec / B	1	0.017 µF/F	100
2nd order terms	0 µF/F	0.006 µF/F	rec / B	1	0.006 µF/F	100
stddev	0.00 µF/F	0.017 µF/F	norm / A	1	0.017 µF/F	8
dC_1/C_n - dC_2/C_n	-5.46 µF/F					
		Combined standard uncertainty:			0.088 µF/F	
		Effective degrees of freedom:		4943 k =	2.00	
		Expanded uncertainty (95% coverage factor):			0.177 µF/F	

Table 2. Uncertainty budget 10 nF capacitors

Quantity	Estimate	Standard uncertainty	Probability distribution /method of evaluation (A, B)	Sensitivity coefficient	Uncertainty contribution	Degree of freedom
X_i	x_i	$u(x_i)$		c_i	$u(R_i)$	n_i
dC_1/C_n + dC_3/C_n	-38.00 µF/F	0.075 µF/F	norm / B	0.5 -	0.038 µF/F	23
dC_1/C_n - dC_3/C_n	5.46 µF/F	0.177 µF/F	norm / B	0.5 -	0.089 µF/F	4900
dC_1/C_n	-16.27 µF/F					
dC_3/C_n	-21.73 µF/F					
		Combined standard uncertainty:			0.096 µF/F	
		Effective degrees of freedom:		867 k =	2.00	
		Expanded uncertainty (95% coverage factor):			0.193 µF/F	

Table 3. Uncertainty budget ratio bridge 10:1 (10 nF : 1 nF)

Quantity	Estimate	Standard uncer-tainty	Probability distribution /method of evaluation (A, B)	Sensitivity coefficient	Uncertainty contribution	Degree of freedom
X_i	x_i	$u(x_i)$		c_i	$u(R_i)$	ν_i
dC_2/C_n	-16.27 µF/F	0.043 µF/F	norm / B	1	0.043 µF/F	32
C_2 drift	0.00 µF/F	0.003 µF/F	rec / B	1	0.003 µF/F	100
C_2 stability	0.00 µF/F	0.012 µF/F	rec / B	1	0.012 µF/F	100
C_2 Cables	0.00 µF/F	0.058 µF/F	rec / B	1	0.058 µF/F	50
C_2 V dep	0.00 (µF/F)/V	0.006 (µF/F)/V	rec / B	0.1 V	0.001 µF/F	100
C_2 f dep	-0.035 (µF/F)/Hz	0.003 (µF/F)/Hz	rec / B	0.2 Hz	0.001 µF/F	100
C_1 Cables	0.00 µF/F	0.058 µF/F	rec / B	1	0.058 µF/F	50
C_1 C_2 4TP def	0.00 µF/F	0.023 µF/F	rec / B	1	0.023 µF/F	50
dE_1/E_1	0.00 µV/V	0.173 µV/V	rec / B	1 (µF/F)/(µV/V)	0.173 µF/F	50
a_{inj}	-66.52 µV/V	0.017 µV/V	rec / B	1 (µF/F)/(µV/V)	0.017 µF/F	100
$b_{\text{inj in-phase}}$	0.33 µV/V	0.012 µV/V	rec / B	1 (µF/F)/(µV/V)	0.012 µF/F	100
chokes	0.00 µF/F	0.017 µF/F	rec / B	1	0.017 µF/F	50
2nd order terms	0.00 µF/F	0.006 µF/F	rec / B	1	0.006 µF/F	100
stddev	0.00 µF/F	0.020 µF/F	norm / A	1	0.020 µF/F	16
dC_1/C_n	49.92 µF/F					
		Combined standard uncertainty:			0.219 µF/F	
		Effective degrees of freedom:		124 k =	2.02	
		Expanded uncertainty (95% coverage factor):			0.442 µF/F	

Table 4. Uncertainty budget ratio bridge 10:1 (1 nF : 100 pF)

Quantity	Estimate	Standard uncer-tainty	Probability distribution /method of evaluation (A, B)	Sensitivity coefficient	Uncertainty contribution	Degree of freedom
X_i	x_i	$u(x_i)$		c_i	$u(R_i)$	ν_i
dC_2/C_n	49.92 µF/F	0.221 µF/F	norm / B	1	0.221 µF/F	124
C_2 drift	0.00 µF/F	0.003 µF/F	rec / B	1	0.003 µF/F	100
C_2 stability	0.00 µF/F	0.012 µF/F	rec / B	1	0.012 µF/F	100
C_2 Cables	0.00 µF/F	0.058 µF/F	rec / B	1	0.058 µF/F	50
C_2 V dep	0.00 (µF/F)/V	0.001 (µF/F)/V	rec / B	9 V	0.009 µF/F	100
C_2 f dep	0.00 (µF/F)/Hz	0.001 (µF/F)/Hz	rec / B	0.2 Hz	0.000 µF/F	100
C_1 Cables	0.00 µF/F	0.058 µF/F	rec / B	1	0.058 µF/F	50
C_1 C_2 4TP def	0.00 µF/F	0.023 µF/F	rec / B	1	0.023 µF/F	50
dE_1/E_1	0.00 µV/V	0.230 µV/V	rec / B	1 (µF/F)/(µV/V)	0.230 µF/F	50
a_{inj}	48.84 µV/V	0.017 µV/V	rec / B	1 (µF/F)/(µV/V)	0.017 µF/F	100
$b_{\text{inj in-phase}}$	-0.02 µV/V	0.012 µV/V	rec / B	1 (µF/F)/(µV/V)	0.012 µF/F	100
chokes	0.00 µF/F	0.017 µF/F	rec / B	1	0.017 µF/F	50
2nd order terms	0.00 µF/F	0.006 µF/F	rec / B	1	0.006 µF/F	100
stddev	0.00 µF/F	0.02 µF/F	norm / A	1	0.020 µF/F	8
dC_1/C_n	1.10 µF/F					
		Combined standard uncertainty:			0.332 µF/F	
		Effective degrees of freedom:		161 k =	2.01	
		Expanded uncertainty (95% coverage factor):			0.670 µF/F	

Table 5. Uncertainty budget ratio bridge 10:1 (100 pF : 10 pF)

Quantity	Estimate	Standard uncer-tainty	Probability distribution /method of evaluation (A, B)	Sensitivity coefficient	Uncertainty contribution	Degree of freedom
X_i	x_i	$u(x_i)$		c_i	$u(R_i)$	ν_i
dC_2/C_n	1.10 µF/F	0.335 µF/F	norm / B	1	0.335 µF/F	161
C_2 drift	0.00 µF/F	0.003 µF/F	rec / B	1	0.003 µF/F	100
C_2 stability	0.00 µF/F	0.012 µF/F	rec / B	1	0.012 µF/F	100
C_2 Cables	0.00 µF/F	0.058 µF/F	rec / B	1	0.058 µF/F	50
C_2 V dep	0.00 (µF/F)/V	0.001 (µF/F)/V	rec / B	0.1 V	0.000 µF/F	100
C_2 f dep	0.00 (µF/F)/Hz	0.001 (µF/F)/Hz	rec / B	0.2 Hz	0.000 µF/F	100
C_1 Cables	0.00 µF/F	0.058 µF/F	rec / B	1	0.058 µF/F	50
C_1 C_2 4TP def	0.00 µF/F	0.023 µF/F	rec / B	1	0.023 µF/F	50
dE_1/E_1	0.00 µV/V	0.290 µV/V	rec / B	1 (µF/F)/(µV/V)	0.290 µF/F	50
a_{inj}	0.59 µV/V	0.017 µV/V	rec / B	1 (µF/F)/(µV/V)	0.017 µF/F	100
$b_{\text{inj in-phase}}$	0.02 µV/V	0.012 µV/V	rec / B	1 (µF/F)/(µV/V)	0.012 µF/F	100
chokes	0.00 µF/F	0.017 µF/F	rec / B	1	0.017 µF/F	50
2nd order terms	0.00 µF/F	0.006 µF/F	rec / B	1	0.006 µF/F	100
stddev	0.00 µF/F	0.020 µF/F	norm / A	1	0.020 µF/F	11
dC_1/C_n	0.49 µF/F					
		Combined standard uncertainty:			0.453 µF/F	
		Effective degrees of freedom:		191 k =	2.01	
		Expanded uncertainty (95% coverage factor):			0.911 µF/F	

11. Annex: Detailed and summarised results of the capacitance realisations

This section includes the detailed capacitance results of the participants, expressed as the relative deviation from nominal in parts in 10^6. The ambient conditions at the time of the measurements were also monitored and are given here as far as explicitly reported by each participant. The mean values of the individual capacitance measurements and, where needed, the value interpolated to the reference frequency of 1233 Hz are given.

11.1 Detailed and summarised results of PTB

The capacitance of all four AH capacitance standards #1256, #1257, #1258, and #1310 was measured at 1233 Hz at many days distributed over each period. The individual results are quoted in the tables below. At each day, the complete measuring chain from the ac QHR has been carried out. The measuring voltage was 10 V for the 100 pF standard and 100 V for the 10 pF standards. At the end of the last period, all capacitance standards were measured once at 2466 Hz (indicated in red in the table of the fourth PTB period).

The ambient laboratory temperature was monitored during each measurement period and was always in the specified range of (23.0 ± 0.5) °C. Also the barometric pressure and the relative humidity (nominally 50%) were monitored during each measurement period. During period 1-3, the air moistening part of the air condition system did not work reliably so that the humidity was too low.

The chassis temperature as displayed on the front panel of the AH frame was also monitored. All readings are inconspicuous.

Period 1: Results measured at 1233 Hz.

Datum	P [hPa]	rel. H. [%]	AH#1256	AH#1257	AH#1258	AH#1310	$T_{chassis}$ [°C]
08.07.2010	1012	45	1.772	1.319	0.978	0.283	33.9
12.07.2010	1005	53.2	1.800	1.319	0.993	0.292	33.9
14.07.2010	1002	51	1.793	1.319	0.968	0.266	33.8
15.07.2010	1004	48.7	1.812	1.319	0.979	0.282	33.6
22.07.2010	1003	48.2	1.772	1.319	0.935	0.239	33.5
23.07.2010	1007.6	47.3	1.786	1.319	0.948	0.239	33.5
26.07.2010	1002.2	43.5	1.777	1.319	0.936	0.239	33.5
mean date: 17.07.2010, mean capacitance values:			1.787	1.312	0.963	0.263	

Period 2: Results measured at 1233 Hz.

Datum	P [hPa]	rel. H. [%]	AH#1256	AH#1257	AH#1258	AH#1310	$T_{chassis}$ [°C]
24.11.2010	993.9	23	1.832	1.332	0.974	0.214	34
25.11.2010	994.6	22.4	1.786	1.286	0.944	0.177	34
26.11.2010	995.7	20.2	1.791	1.300	0.969	0.208	33.9
02.12.2010	998.9	13.3		1.334	0.987		33.2
03.12.2010	998.9	13.3	1.815	1.279	0.928	0.168	33.1
07.12.2010	997.4	31	1.791	1.281	0.928	0.153	33.1
08.12.2010	997.7	31.8	1.811	1.292	0.934	0.159	33.2
10.12.2010	1016.7	28.7	1.816	1.325	0.971	0.200	33.1
13.12.2010	1013.9	29	1.849	1.341	0.997	0.224	33.1
mean date: 15.12.2010, mean capacitance values:			1.815	1.310	0.960	0.189	

Period 3: Results measured at 1233 Hz.

Datum	P [hPa]	rel. H. [%]	AH#1256	AH#1257	AH#1258	AH#1310	$T_{chassis}$ [°C]
26.05.2011	1003.1	31.5	1.852	1.353	0.977	0.189	33.3
30.05.2011	1007.5	45.2	1.843	1.363	0.996	0.183	33.3
01.06.2011	1010.7	39.2	1.835	1.367		0.184	33.3
06.06.2011	994.9	52	1.820	1.353	0.988	0.176	33.3
08.06.2011	992.7	51.3	1.798	1.352	0.971	0.155	33.2
10.06.2011	1007.7	40.5	1.826	1.339	0.962	0.161	33.3
14.06.2011	1007.6	48.6	1.814	1.342	0.962	0.163	33.3
16.06.2011	1003.9	51	1.810	1.322	0.948	0.124	33.3
17.06.2011	1005.6	40.1	1.791	1.330	0.952	0.117	33.3
20.06.2011	1004.4	43.3	1.787	1.315	0.934	0.119	33.3
23.06.2011	1003	48.5	1.803	1.317	0.938	0.121	33.4
27.06.2011	1004.8	46.3	1.835	1.346	0.979	0.151	33.3
mean date: 12.06.2011, mean capacitance values:			1.817	1.342	0.964	1.534	

Period 4: Results measured at 1233 Hz.

Datum	P [hPa]	rel. H. [%]	AH#1256	AH#1257	AH#1258	AH#1310	$T_{chassis}$ [°C]
22.02.2012	1018.7	-	1.788	1.422	1.059	0.237	33.9
24.02.2012	1009.4	38.2	1.784	1.445	1.065	0.234	34.1
27.02.2012	1016.3	22.5	1.807	1.437	1.074	0.243	33.8
01.03.2012	1014.9	39.7	1.802	1.435	1.062	0.223	33.8
05.03.2012	1007.6	21.0	1.809	1.431	1.065	0.237	33.7
07.03.2012	1015.8	18.5	1.829	1.436	1.070	0.250	33.3
09.03.2012	1026.1	23.1	1.817	1.436	1.068	0.252	33.3
mean date: 28.02.2012, mean capacitance values:			1.805	1.434	1.066	0.239	

Period 5: Results measured at 1233 Hz.

Datum	P [hPa]	rel. H. [%]	AH#1256	AH#1257	AH#1258	AH#1310	$T_{chassis}$ [°C]
23.11.2012	1009.7	25.9	1.795	1.421	1.030	0.151	33.2
26.11.2012	1000.9	28.2	1.794	1.426	1.034	0.152	33.2
27.11.2012	996.0	33.9	1.780	1.409	1.024	0.142	33.2
29.11.2012	991.0	28.3	1.791	1.427	1.032	0.154	33.3
mean date: 26.11.2012, mean capacitance values:			1.790	1.421	1.030	0.150	

Period 6: Results measured at 1233 Hz.

Datum	P [hPa]	rel. H. [%]	AH#1256	AH#1257	AH#1258	AH#1310	$T_{chassis}$ [°C]
05.03.2014	1006.8	28.6	1.772	1.384	0.970	0.047	33.4
07.03.2014	1017.8	24.6	1.776	1.395	0.981	0.061	33.5
10.03.2014	1017.6	25.5	1.780	1.395	0.980	0.058	33.4
12.03.2014	1026.5	23.7	1.791	1.398	0.984	0.061	33.4
14.03.2014	1019.5	22.2	1.778	1.383	0.970	0.054	33.5
mean date: 10.03.2014, mean capacitance values:			1.779	1.391	0.977	0.056	

Period 7: Results measured at 1233 Hz.

Datum	P [hPa]	rel. H. [%]	AH#1256	AH#1257	AH#1258	AH#1310	$T_{chassis}$ [°C]
19.09.2014	1003.6	47.0	1.879	1.473	1.041	0.058	33.0
22.09.2014	1003.6	41.6	1.878	1.467	1.036	0.054	33.0
24.09.2014	1004.8	39.5	1.873	1.450	1.017	0.046	33.0
25.09.2014	1004.2	43.2	1.865	1.447	1.013	0.039	33.1
26.09.2014	1010.6	44.5	1.878	1.462	1.030	0.052	33.1
30.09.2014	1013.9	47.7	1.888	1.472	1.041	0.062	33.7
01.10.2014	1017.7	46.1	1.868	1.434	1.004	0.024	33.8
02.10.2014	1019.9	46.3	1.886	1.469	1.040	0.060	33.8
07.10.2014	996.0	43.3	1.839	1.435	1.001	0.022	33.9
08.10.2014	1001.5	42.8	1.855	1.439	1.012	0.036	33.8
09.10.2014	995.7	46.6	1.849	1.437	1.009	0.030	33.9
13.10.2014	997.9	45.5	1.854	1.444	1.012	0.039	33.9
14.10.2014	999.1	45.8	1.879	1.479	1.050	0.066	33.8
16.10.2014	996.6	43.8	1.855	1.450	1.026	0.047	33.8
17.10.2014	999.7	45.7	1.852	1.452	1.025	0.035	33.9
mean date: 02.10.2014, mean capacitance values:			1.866	1.454	1.024	0.045	

Period 8: Results measured at 1233 Hz.

Datum	P [hPa]	rel. H. [%]	AH#1256	AH#1257	AH#1258	AH#1310	$T_{chassis}$ [°C]
04.09.2015	1004.4	44.3	1.951	1.643	1.111	0.061	33.0
07.09.2015	1010.7	45.0	1.931	1.649	1.119	0.071	33.0
09.09.2015	1015.5	44.1	1.965	1.644	1.114	0.065	32.9
11.09.2015	1012.1	43.8	1.952	1.632	1.103	0.058	33.0
14.09.2015	993.8	46.0	1.928	1.620	1.092	0.041	32.9
16.09.2015	993.5	45.2	1.945	1.638	1.106	0.057	33.1
18.09.2015	1003.9	44.7	1.949	1.635	1.104	0.053	33.1
21.09.2015	1008.3	45.2	1.951	1.632	1.098	0.051	33.1
23.09.2015	995.6	43.7	1.911	1.634	1.103	0.054	33.1
25.09.2015	1011.0	44.8	1.948	1.621	1.092	0.046	33.0
28.09.2015	1027.7	42.4	1.957	1.625	1.097	0.050	33.1
mean date: 16.09.2015, mean capacitance value			1.944	1.634	1.103	0.055	

Period 9: Results measured at 1233 Hz and at 2466 Hz (indicated in red).

Datum	P [hPa]	rel. H. [%]	AH#1256	AH#1257	AH#1258	AH#1310	$T_{chassis}$ [°C]
09.03.2016	1004.3	40.0	1.911	1.641	1.083	0.039	32.6
11.03.2016	1018.9	41.0	1.935	1.653	1.098	0.049	32.6
14.03.2016	1027.7	40.9	1.940	1.654	1.096	0.048	32.6
16.03.2016	1023.8	40.8	1.928	1.646	1.086	0.039	32.5
18.03.2016	1011.1	41.9	1.933	1.637	1.080	0.034	32.7
21.03.2016	1006.0	42.3	1.925	1.642	1.080	0.034	32.6
23.03.2016	999.7	43.3	1.936	1.651	1.091	0.045	32.7
29.03.2016	993.6	41.7	1.936	1.648	1.092	0.041	32.7
31.03.2016	1004.0	43.0	1.936	1.648	1.087	0.039	32.7
06.04.2016	1000.1	43.8	1.930	1.638	1.080	0.028	32.7
	f = 2466 Hz:		1.800	1.492	0.919	-0.063	
08.04.2016	1003.0	41.9	1.933	1.642			32.7
mean date: 21.03.2016, mean capacitance values:			1.931	1.645	1.087	0.040	

Summarised results of PTB at 1233 Hz:

Datum	AH#1256	AH#1257	AH#1258	AH#1310
17.07.2010	1.787	1.312	0.963	0.263
15.12.2010	1.815	1.310	0.960	0.189
12.06.2011	1.817	1.342	0.964	0.154
28.02.2012	1.805	1.434	1.066	0.239
26.11.2012	1.790	1.421	1.030	0.150
10.03.2014	1.779	1.391	0.977	0.056
02.10.2014	1.866	1.454	1.024	0.045
16.09.2015	1.944	1.634	1.103	0.055
21.03.2016	1.931	1.645	1.087	0.040

11.2 Detailed and summarised results of the BIPM

Results of the first capacitance circulation at the principal frequency of 1592 Hz

Date	100 pF 1256	10 pF 1257	10 pF 1258	10 pF 1310
12.04.2011	1.6438	1.178	0.8142	0.0442
14.04.2011	1.643	1.1793	0.8138	0.0499
14.04.2011	-	1.1746	0.8124	0.0476
21.04.2011	1.6192	1.1667	0.8016	0.0315
27.04.2011	1.643	1.1866	0.8196	0.0476
06.05.2011	1.6179	1.1606	0.7947	0.0256
09.05.2011	1.6378	1.1835	0.8156	0.0398
10.05.2011	1.6404	1.1896	0.8201	0.0509
10.05.2011	1.6278	1.1724	0.8042	0.0267
10.05.2011	1.623	1.168	0.8004	0.0245
10.05.2011	1.6239	1.17	0.8026	0.025
11.05.2011	1.6322	1.173	0.8119	0.0421
11.05.2011	1.631	1.17	0.8057	0.0359
11.05.2011	1.6323	1.1751	0.8094	0.0343
12.05.2011	1.644	1.1872	0.8185	0.0411
12.05.2011	1.6275	1.1766	0.8113	0.0323
12.05.2011	1.6277	1.1707	0.8046	0.0274
13.05.2011	1.638	1.1828	0.8149	0.0389
13.05.2011	1.6261	1.1673	0.7997	0.0204

Summarised results of the first capacitance circulation

Frequency (Hz)	Deviation of the mean values from nominal in parts in 10^6			
	100 pF 1256	10 pF 1257	10 pF 1258	10 pF 1310
1000	1.721	1.283	0.922	0.104
1592	1.632	1.175	0.809	0.036

Results of the second capacitance circulation

At the second capacitance circulation, the BIPM carried out two series of measurements, namely before and after the measurements of NMIA. The summarised and detailed results as well as a graphical representation are given in the following.

First series of results of AH#1256, nominal value: 100 pF

Frequency: 1027 Hz   Voltage: 10 V

	Date	Ambient temperature (°C)	Chassis temperature (°C)	Drift	Difference from nominal value (ppm)
	15/01/2015	22.3	33.0	-0.016	1.822
	15/01/2015	22.3	33.0	-0.016	1.820
	16/01/2015	22.6	32.2	-0.013	1.843
	16/01/2015	22.6	32.2	-0.013	1.839
	19/01/2015	22.3	32.9	-0.015	1.842
	19/01/2015	22.3	32.9	-0.015	1.837
	22/01/2015	22.6	33.4	-0.017	1.832
	22/01/2015	22.6	33.4	-0.017	1.831
	27/01/2015	22.4	33.1	-0.015	1.851
	27/01/2015	22.4	33.1	-0.015	1.847
	03/02/2015	22.5	33.9	-0.019	1.816
	03/02/2015	22.5	33.9	-0.019	1.817
	05/02/2015	22.7	34.0	-0.020	1.832
	05/02/2015	22.7	34.0	-0.020	1.830
	09/02/2015	22.7	33.5	-0.016	1.854
	09/02/2015	22.7	35.5	-0.016	1.851
	11/02/2015	22.4	32.7	-0.013	1.855
	11/02/2015	22.4	32.7	-0.013	1.855
	12/02/2015	22.4	33.2	-0.016	1.843
	12/02/2015	22.4	32.2	-0.016	1.842
Mean	**29/01/2015**	**22.5**	**33.2**	**-0.016**	**1.838**
				Std dev:	**0.013**
				Std deviation of the mean:	**0.003**

Frequency: 1541 Hz Voltage: 10 V

	Date	Ambient temperature (°C)	Chassis temperature (°C)	Drift	Difference from nominal value (ppm)
	12/01/2015	22.3	32.8	-0.015	1.800
	12/01/2015	22.3	32.8	-0.015	1.802
	16/01/2015	22.4	32.7	-0.014	1.792
	16/01/2015	22.4	32.7	-0.014	1.792
	19/01/2015	22.4	32.3	-0.013	1.800
	19/01/2015	22.4	32.3	-0.013	1.798
	22/01/2015	22.6	32.9	-0.015	1.792
	22/01/2015	22.6	32.9	-0.015	1.788
	27/01/2015	22.3	32.4	-0.012	1.813
	27/01/2015	22.3	32.4	-0.012	1.806
	03/02/2015	22.4	33.7	-0.018	1.775
	03/02/2015	22.4	33.7	-0.018	1.770
	05/02/2015	22.6	33.7	-0.018	1.792
	05/02/2015	22.6	33.7	-0.018	1.790
	09/02/2015	22.6	33.2	-0.016	1.812
	09/02/2015	22.6	33.2	-0.016	1.808
	11/02/2015	22.4	32.4	-0.013	1.811
	11/02/2015	22.4	32.4	-0.013	1.812
	12/02/2015	22.4	33.3	-0.016	1.794
	12/02/2015	22.4	32.3	-0.016	1.793
Mean	**29/01/2015**	**22.4**	**32.9**	**-0.015**	**1.797**
				Std dev:	**0.012**
				Std deviation of the mean:	**0.003**

Frequency: 3083 Hz Voltage: 10 V

	Date	Ambient temperature (°C)	Chassis temperature (°C)	Drift	Difference from nominal value (ppm)
	03/02/2015	22.5	34.0	-0.020	1.689
	03/02/2015	22.5	34.0	-0.020	1.688
	05/02/2015	22.7	33.9	-0.019	1.716
	05/02/2015	22.7	33.9	-0.019	1.715
	09/02/2015	22.7	33.7	-0.017	1.726
	09/02/2015	22.7	33.7	-0.017	1.726
	11/02/2015	22.3	32.9	-0.014	1.730
	11/02/2015	22.3	32.9	-0.014	1.729
	12/02/2015	22.4	33.2	-0.016	1.720
	12/02/2015	22.4	33.2	-0.016	1.719
Mean	**08/02/2015**	**22.5**	**33.5**	**-0.017**	**1.716**
			Std dev:		**0.015**
			Std deviation of the mean:		**0.003**

First series of results of AH#1257, nominal value: 10 pF

Frequency: 1027 Hz Voltage: 100 V

	Date	Ambient temperature (°C)	Chassis temperature (°C)	Drift	Difference from nominal value (ppm)
	15/01/2015	22.3	33.0	0.008	1.419
	16/01/2015	22.6	32.2	0.011	1.440
	19/01/2015	22.3	32.9	0.009	1.431
	22/01/2015	22.6	33.4	0.008	1.413
	27/01/2015	22.4	33.1	0.010	1.443
	03/02/2015	22.5	33.9	0.007	1.410
	05/02/2015	22.7	34.0	0.007	1.416
	09/02/2015	22.7	33.5	0.008	1.434
	11/02/2015	22.4	32.7	0.009	1.447
Mean	**27/01/2015**	**22.5**	**33.2**	**0.009**	**1.428**
			Std dev:		**0.014**
			Std deviation of the mean:		**0.003**

Frequency: 1541 Hz Voltage: 100 V

	Date	Ambient temperature (°C)	Chassis temperature (°C)	Drift	Difference from nominal value (ppm)
	12/01/2015	22.3	32.8	0.009	1.385
	16/01/2015	22.4	32.7	0.009	1.388
	19/01/2015	22.4	32.3	0.010	1.387
	22/01/2015	22.6	32.9	0.009	1.368
	27/01/2015	22.3	32.4	0.012	1.399
	03/02/2015	22.4	33.7	0.007	1.363
	05/02/2015	22.6	33.7	0.008	1.368
	09/02/2015	22.6	33.2	0.009	1.388
	11/02/2015	22.4	32.4	0.011	1.399
	12/02/2015	22.4	33.3	0.008	1.380
Mean	**29/01/2015**	**22.4**	**32.9**	**0.009**	**1.382**
				Std dev:	**0.013**
				Std deviation of the mean:	**0.003**

Frequency: 3083 Hz Voltage: 100 V

	Date	Ambient temperature (°C)	Chassis temperature (°C)	Drift	Difference from nominal value (ppm)
	03/02/2015	22.5	34.0	0.007	1.263
	05/02/2015	22.7	33.9	0.007	1.274
	09/02/2015	22.7	33.7	0.008	1.287
	11/02/2015	22.3	32.9	0.009	1.298
	12/02/2015	22.4	33.2	0.008	1.290
Mean	**08/02/2015**	**22.5**	**33.5**	**0.008**	**1.282**
				Std dev:	**0.014**
				Std deviation of the mean:	**0.003**

First series of results of AH#1258, nominal value: 10 pF

Frequency: 1027 Hz Voltage: 100 V

	Date	Ambient temperature (°C)	Chassis temperature (°C)	Drift	Difference from nominal value (ppm)
	15/01/2015	22.3	33.0	0.000	0.989
	16/01/2015	22.6	32.2	0.000	1.008
	19/01/2015	22.3	32.9	0.000	1.000
	22/01/2015	22.6	33.4	0.000	0.983
	27/01/2015	22.4	33.1	-0.001	1.011
	03/02/2015	22.5	33.9	-0.001	0.981
	05/02/2015	22.7	34.0	-0.001	0.989
	09/02/2015	22.7	33.5	-0.001	1.006
	11/02/2015	22.4	32.7	0.000	1.012
Mean	**27/01/2015**	**22.5**	**33.2**	**0.000**	**0.998**
				Std dev:	**0.012**
				Std deviation of the mean:	**0.003**

Frequency: 1541 Hz Voltage: 100 V

	Date	Ambient temperature (°C)	Chassis temperature (°C)	Drift	Difference from nominal value (ppm)
	12/01/2015	22.3	32.8	0.000	0.948
	16/01/2015	22.4	32.7	0.000	0.946
	19/01/2015	22.4	32.3	0.000	0.948
	22/01/2015	22.6	32.9	0.000	0.930
	27/01/2015	22.3	32.4	0.000	0.956
	03/02/2015	22.4	33.7	-0.001	0.927
	05/02/2015	22.6	33.7	-0.001	0.935
	09/02/2015	22.6	33.2	-0.001	0.950
	11/02/2015	22.4	32.4	0.000	0.957
	12/02/2015	22.4	33.3	-0.001	0.944
Mean	**29/01/2015**	**22.4**	**32.9**	**0.000**	**0.944**
				Std dev:	**0.010**
				Std deviation of the mean:	**0.002**

Frequency: 3083 Hz Voltage: 100 V

	Date	Ambient temperature (°C)	Chassis temperature (°C)	Drift	Difference from nominal value (ppm)
	03/02/2015	22.5	34.0	-0.001	0.815
	05/02/2015	22.7	33.9	-0.001	0.829
	09/02/2015	22.7	33.7	-0.001	0.839
	11/02/2015	22.3	32.9	0.000	0.845
	12/02/2015	22.4	33.2	-0.001	0.839
Mean	**08/02/2015**	**22.5**	**33.5**	**-0.001**	**0.833**
				Std dev:	**0.012**
				Std deviation of the mean:	**0.003**

First series of results of AH#1310, nominal value: 10 pF

Frequency: 1027 Hz Voltage: 100 V

	Date	Ambient temperature (°C)	Chassis temperature (°C)	Drift	Difference from nominal value (ppm)
	15/01/2015	22.3	33.0	-0.043	-0.023
	16/01/2015	22.6	32.2	-0.037	-0.010
	19/01/2015	22.3	32.9	-0.042	-0.015
	22/01/2015	22.6	33.4	-0.044	-0.016
	27/01/2015	22.4	33.1	-0.047	-0.004
	03/02/2015	22.5	33.9	-0.048	-0.028
	05/02/2015	22.7	34.0	-0.049	-0.020
	09/02/2015	22.7	33.5	-0.046	-0.004
	11/02/2015	22.4	32.7	-0.040	0.001
Mean	**27/01/2015**	**22.5**	**33.2**	**-0.044**	**-0.013**
				Std dev:	**0.010**
				Std deviation of the mean:	**0.002**

Frequency: 1541 Hz Voltage: 100 V

	Date	Ambient temperature (°C)	Chassis temperature (°C)	Drift	Difference from nominal value (ppm)
	12/01/2015	22.3	32.8	-0.040	-0.022
	16/01/2015	22.4	32.7	-0.040	-0.031
	19/01/2015	22.4	32.3	-0.040	-0.027
	22/01/2015	22.6	32.9	-0.042	-0.030
	27/01/2015	22.3	32.4	-0.043	-0.018
	03/02/2015	22.4	33.7	-0.047	-0.045
	05/02/2015	22.6	33.7	-0.047	-0.035
	09/02/2015	22.6	33.2	-0.044	-0.018
	11/02/2015	22.4	32.4	-0.038	-0.016
Mean	**27/01/2015**	**22.4**	**32.9**	**-0.042**	**-0.027**
				Std dev:	**0.009**
				Std deviation of the mean:	**0.002**

Frequency: 3083 Hz Voltage: 100 V

	Date	Ambient temperature (°C)	Chassis temperature (°C)	Drift	Difference from nominal value (ppm)
	03/02/2015	22.5	34.0	-0.049	-0.081
	05/02/2015	22.7	33.9	-0.048	-0.067
	09/02/2015	22.7	33.7	-0.048	-0.055
	11/02/2015	22.3	32.9	-0.042	-0.052
	12/02/2015	22.4	33.2	-0.044	-0.061
Mean	**08/02/2015**	**22.5**	**33.5**	**-0.046**	**-0.063**
				Std dev:	**0.011**
				Std deviation of the mean:	**0.003**

Second series of results of AH#1256, nominal value: 100 pF

Frequency: 1027 Hz   Voltage: 10 V

	Date	Ambient temperature (°C)	Chassis temperature (°C)	Drift	Difference from nominal value (ppm)
	27/04/2015	22.1	35.3	-0.007	1.948
	27/04/2015	22.1	35.3	-0.007	1.944
	30/04/2015	22.1	34.9	-0.004	1.934
	30/04/2015	22.1	34.9	-0.004	1.933
	05/05/2015	22.0	35.1	-0.006	1.891
	05/05/2015	22.0	35.1	-0.006	1.892
	12/05/2015	22.1	35.5	-0.007	1.900
	12/05/2015	22.1	35.5	-0.007	1.900
	18/05/2015	21.9	34.4	-0.001	1.892
	18/05/2015	21.9	34.4	-0.001	1.885
	26/05/2015	22.0	34.9	-0.003	1.894
	26/05/2015	22.0	34.9	-0.003	1.888
	01/06/2015	22.0	34.5	-0.002	1.891
	01/06/2015	22.0	34.5	-0.002	1.890
Mean	**12/05/2015**	**22.0**	**34.9**	**-0.004**	**1.906**
				Std dev:	**0.023**
				Std deviation of the mean:	**0.005**

Frequency: 1541 Hz Voltage: 10 V

	Date	Ambient temperature (°C)	Chassis temperature (°C)	Drift	Difference from nominal value (ppm)
	27/04/2015	22.2	35.1	-0.005	1.904
	27/04/2015	22.2	35.1	-0.005	1.902
	30/04/2015	22.1	35.1	-0.005	1.889
	30/04/2015	22.1	35.1	-0.005	1.886
	04/05/2015	22.0	34.6	-0.003	1.866
	04/05/2015	22.0	34.6	-0.003	1.861
	07/05/2015	22.0	34.7	-0.004	1.867
	07/05/2015	22.0	34.7	-0.004	1.865
	12/05/2015	22.1	35.4	-0.008	1.859
	12/05/2015	22.1	35.4	-0.008	1.857
	15/05/2015	22.0	34.4	-0.002	1.863
	15/05/2015	22.0	34.4	-0.002	1.861
	18/05/2015	21.9	34.1	-0.001	1.850
	18/05/2015	21.9	34.1	-0.001	1.850
	22/05/2015	22.0	35.3	-0.006	1.848
	22/05/2015	22.0	35.3	-0.006	1.848
	26/05/2015	22.0	34.5	-0.002	1.855
	26/05/2015	22.0	34.5	-0.002	1.851
	29/05/2015	22.1	34.4	-0.001	1.846
	29/05/2015	22.1	34.4	-0.001	1.840
	01/06/2015	22.0	34.3	-0.002	1.848
	01/06/2015	22.0	34.3	-0.002	1.845
Mean	**14/05/2015**	**22.0**	**34.7**	**-0.004**	**1.862**
				Std dev:	**0.018**
				Std deviation of the mean:	**0.004**

Frequency: 3083 Hz Voltage: 10 V

	Date	Ambient temperature (°C)	Chassis temperature (°C)	Drift	Difference from nominal value (ppm)
	27/04/2015	22.1	35.4	-0.007	1.824
	27/04/2015	22.1	35.4	-0.007	1.820
	30/04/2015	22.0	34.2	-0.001	1.829
	30/04/2015	22.0	34.2	-0.001	1.826
	05/05/2015	22.0	35.2	-0.006	1.781
	05/05/2015	22.0	35.2	-0.006	1.778
	12/05/2015	22.1	35.5	-0.008	1.779
	12/05/2015	22.1	35.5	-0.004	1.780
	18/05/2015	21.9	34.8	-0.004	1.768
	18/05/2015	21.9	34.8	-0.005	1.765
	26/05/2015	22.0	35.1	-0.005	1.771
	26/05/2015	22.0	35.1	-0.005	1.774
	01/06/2015	22.0	34.7	-0.003	1.772
	01/06/2015	22.0	34.7	-0.003	1.769
Mean	**12/05/2015**	**22.0**	**35.0**	**-0.005**	**1.788**
				Std dev:	**0.025**
				Std deviation of the mean:	**0.005**

Second series of results of AH#1257, nominal value: 10 pF

Frequency: 1027 Hz Voltage: 100 V

	Date	Ambient temperature (°C)	Chassis temperature (°C)	Drift	Difference from nominal value (ppm)
	27/04/2015	22.1	35.3	0.016	1.604
	30/04/2015	22.1	34.9	0.018	1.590
	05/05/2015	22.0	35.1	0.016	1.577
	12/05/2015	22.1	35.5	0.015	1.578
	18/05/2015	21.9	34.4	0.017	1.564
	26/05/2015	22.0	34.9	0.016	1.565
	01/06/2015	22.0	34.5	0.016	1.571
Mean	**12/05/2015**	**22.0**	**34.9**	**0.016**	**1.578**
				Std dev:	**0.014**
				Std deviation of the mean:	**0.003**

Frequency: 1541 Hz Voltage: 100 V

	Date	Ambient temperature (°C)	Chassis temperature (°C)	Drift	Difference from nominal value (ppm)
	27/04/2015	22.2	35.1	0.017	1.546
	30/04/2015	22.1	35.1	0.016	1.531
	04/05/2015	22.0	34.6	0.018	1.528
	07/05/2015	22.0	34.7	0.018	1.520
	12/05/2015	22.1	35.4	0.015	1.524
	15/05/2015	22.0	34.4	0.018	1.520
	18/05/2015	21.9	34.1	0.019	1.516
	22/05/2015	22.0	35.3	0.014	1.506
	26/05/2015	22.0	34.5	0.018	1.516
	29/05/2015	22.1	34.4	0.018	1.512
	01/06/2015	22.0	34.3	0.017	1.515
Mean	**14/05/2015**	**22.0**	**34.7**	**0.017**	**1.521**
				Std dev:	**0.011**
				Std deviation of the mean:	**0.002**

Frequency: 3083 Hz Voltage: 100 V

	Date	Ambient temperature (°C)	Chassis temperature (°C)	Drift	Difference from nominal value (ppm)
	27/04/2015	22.1	35.4	0.016	1.434
	30/04/2015	22.0	34.2	0.019	1.441
	05/05/2015	22.0	35.2	0.016	1.420
	12/05/2015	22.1	35.5	0.015	1.419
	18/05/2015	21.9	34.8	0.016	1.399
	26/05/2015	22.0	35.1	0.015	1.408
	01/06/2015	22.0	34.7	0.015	1.412
Mean	**12/05/2015**	**22.0**	**35.0**	**0.016**	**1.419**
				Std dev:	**0.015**
				Std deviation of the mean:	**0.003**

Second series of results of AH#1258, nominal value: 10 pF

Frequency: 1027 Hz Voltage: 100 V

	Date	Ambient temperature (°C)	Chassis temperature (°C)	Drift	Difference from nominal value (ppm)
	27/04/2015	22.1	35.3	0.004	1.138
	30/04/2015	22.1	34.9	0.004	1.115
	05/05/2015	22.0	35.1	0.004	1.098
	12/05/2015	22.1	35.5	0.003	1.099
	18/05/2015	21.9	34.4	0.004	1.074
	26/05/2015	22.0	34.9	0.003	1.075
	01/06/2015	22.0	34.5	0.003	1.072
Mean	**12/05/2015**	**22.0**	**34.9**	**0.004**	**1.096**
				Std dev:	**0.025**
				Std deviation of the mean:	**0.005**

Frequency: 1541 Hz Voltage: 100 V

	Date	Ambient temperature (°C)	Chassis temperature (°C)	Drift	Difference from nominal value (ppm)
	27/04/2015	22.2	35.1	0.004	1.065
	30/04/2015	22.1	35.1	0.004	1.044
	04/05/2015	22.0	34.6	0.004	1.034
	07/05/2015	22.0	34.7	0.004	1.027
	12/05/2015	22.1	35.4	0.004	1.031
	15/05/2015	22.0	34.4	0.004	1.022
	18/05/2015	21.9	34.1	0.004	1.013
	22/05/2015	22.0	35.3	0.003	1.006
	26/05/2015	22.0	34.5	0.004	1.011
	29/05/2015	22.1	34.4	0.004	1.003
	01/06/2015	22.0	34.3	0.004	1.006
Mean	**14/05/2015**	**22.0**	**34.7**	**0.004**	**1.024**
				Std dev:	**0.019**
				Std deviation of the mean:	**0.004**

Frequency: 3083 Hz   Voltage: 100 V

	Date	Ambient temperature (°C)	Chassis temperature (°C)	Drift	Difference from nominal value (ppm)
	27/04/2015	22.1	35.4	0.004	0.930
	30/04/2015	22.0	34.2	0.005	0.929
	05/05/2015	22.0	35.2	0.004	0.907
	12/05/2015	22.1	35.5	0.003	0.905
	18/05/2015	21.9	34.8	0.004	0.884
	26/05/2015	22.0	35.1	0.003	0.886
	26/05/2015	22.0	34.7	0.003	0.886
	01/06/2015	22.0	34.4	0.004	0.886
Mean	**14/05/2015**	**22.0**	**34.9**	**0.004**	**0.902**
				Std dev:	**0.019**
				Std deviation of the mean:	**0.004**

Second series of results of AH#1310, nominal value: 10 pF

Frequency: 1027 Hz Voltage: 100 V

	Date	Ambient temperature (°C)	Chassis temperature (°C)	Drift	Difference from nominal value (ppm)
	27/04/2015	22.1	35.3	-0.069	-0.0062
	30/04/2015	22.1	34.9	-0.066	-0.0049
	05/05/2015	22.0	35.1	-0.067	-0.0238
	12/05/2015	22.1	35.5	-0.070	-0.0089
	18/05/2015	21.9	34.4	-0.063	-0.0117
	26/05/2015	22.0	34.9	-0.066	-0.0070
	01/06/2015	22.0	34.5	-0.063	-0.0066
Mean	**12/05/2015**	**22.0**	**34.9**	**-0.066**	**-0.010**
				Std dev:	**0.007**
				Std deviation of the mean:	**0.001**

Frequency: 1541 Hz Voltage: 100 V

	Date	Ambient temperature (°C)	Chassis temperature (°C)	Drift	Difference from nominal value (ppm)
	27/04/2015	22.2	35.1	-0.067	-0.0205
	30/04/2015	22.1	35.1	-0.068	-0.0174
	04/05/2015	22.0	34.6	-0.065	-0.0285
	07/05/2015	22.0	34.7	-0.065	-0.0224
	12/05/2015	22.1	35.4	-0.069	-0.0230
	15/05/2015	22.0	34.4	-0.064	-0.0150
	18/05/2015	21.9	34.1	-0.061	-0.0234
	22/05/2015	22.0	35.3	-0.068	-0.0234
	26/05/2015	22.0	34.5	-0.063	-0.0210
	29/05/2015	22.1	34.4	-0.062	-0.0256
	01/06/2015	22.0	34.3	-0.062	-0.0243
Mean	**14/05/2015**	**22.0**	**34.7**	**-0.065**	**-0.022**
				Std dev:	**0.004**
				Std deviation of the mean:	**0.001**

Frequency: 3083 Hz Voltage: 100 V

	Date	Ambient temperature (°C)	Chassis temperature (°C)	Drift	Difference from nominal value (ppm)
	27/04/2015	22.1	35.4	-0.070	-0.0529
	30/04/2015	22.0	34.2	-0.062	-0.0428
	05/05/2015	22.0	35.2	-0.067	-0.0670
	12/05/2015	22.1	35.5	-0.070	-0.0575
	18/05/2015	21.9	34.8	-0.065	-0.0598
	26/05/2015	22.0	35.1	-0.067	-0.0540
	01/06/2015	22.0	34.7	-0.064	-0.0558
Mean	**12/05/2015**	**22.0**	**35.0**	**-0.066**	**-0.056**
				Std dev:	**0.007**
				Std deviation of the mean:	**0.002**

During the first series of measurements, the observed stability of the travelling standards over the measurement period at the BIPM was good. There was no evidence of systematic drift or of adverse effects of transport for any of the standards. In all cases there was a random scatter of two or three parts in 10^8 (peak-peak) over the measurement period of several weeks, which is consistent with the normal behaviour of good quality fused silica standards of this type on the BIPM measurement system.

During the second series of measurements a clear drift, most probably a consequence of the transportation from NMIA to BIPM, is observable on three of the standards (AH #1256, AH #1257 and AH #1258, see plots 1 to 3 below). This drift, more pronounced at the beginning of the measurement period, seems to attenuate with time. It is difficult to say if the standards are continuing to drift at the end of the measuring period but, it may be noticed that non-negligible differences remain between the mean capacitance value of the two series of measurements at least for capacitors #1256 ($\approx 5.10^{-8}$), #1257 ($\approx 1.10^{-7}$) and #1258 ($\approx 5.10^{-8}$), whatever the operating frequency. The capacitor #1310 has not significantly changed over the same time period although it has been submitted to similar treatment (transportation and measurement conditions).

Plots 1-4 show the individual data points for each standard for the three frequencies considered and for the two periods of measurements.

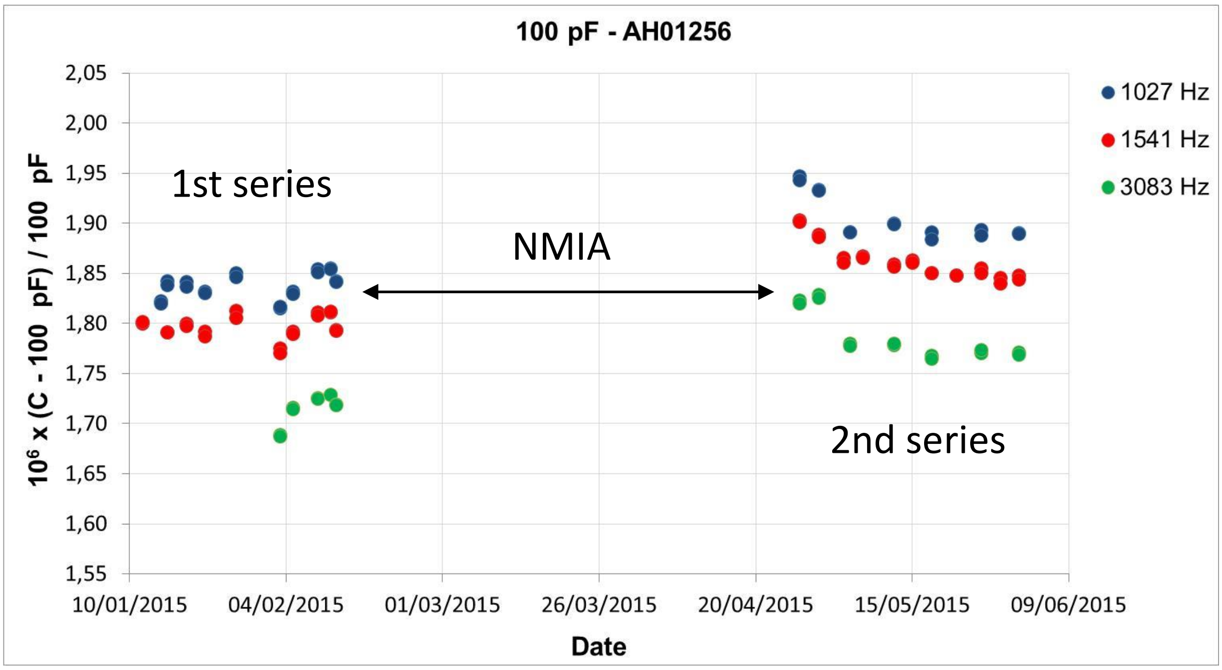

Plot 1: Individual measurements on 100 pF standard serial number 1256

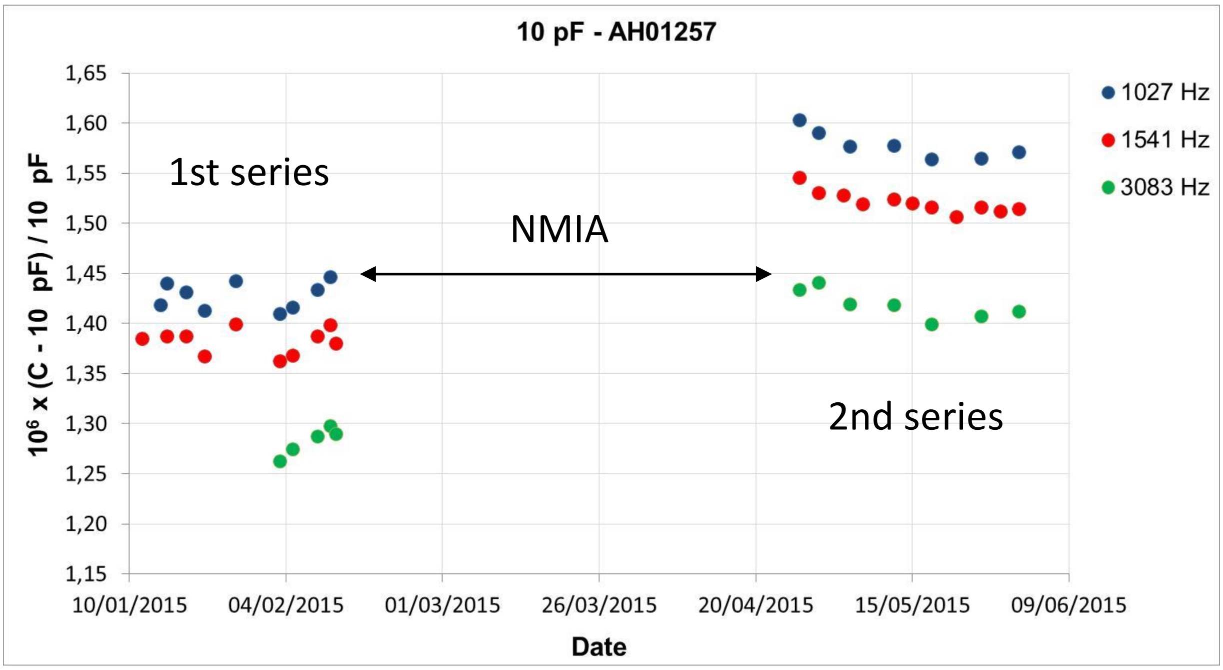

Plot 2: Individual measurements on 10 pF standard serial number 1257

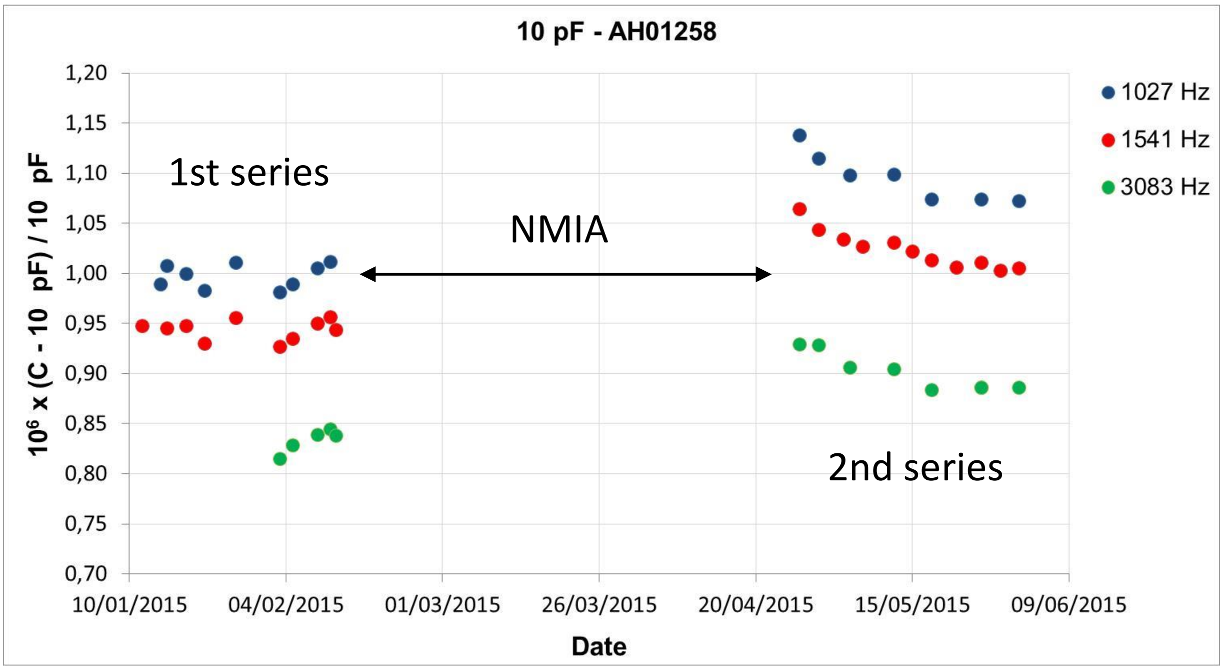

Plot 3: Individual measurements on 10 pF standard serial number 1258

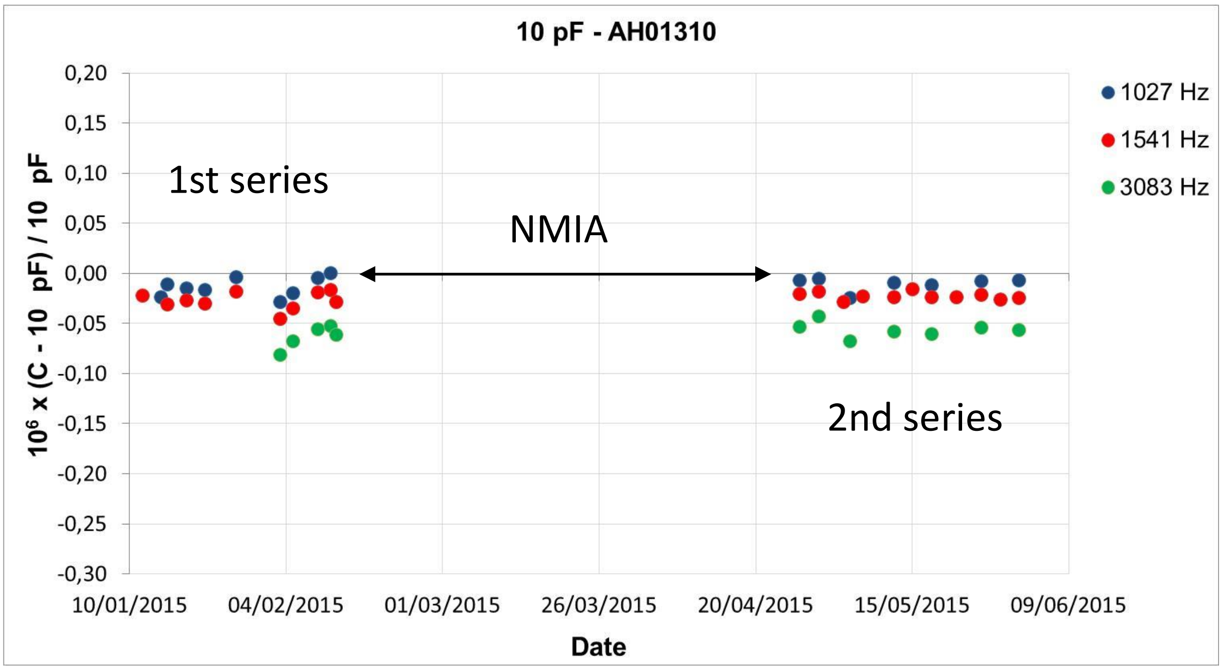

Plot 4: Individual measurements on 10 pF standard serial number 1310

Summarised BIPM results of the second capacitance circulation

The standard deviation quoted in the tables below is just an indication of the stability of the standards over the two measurement periods. These tables include, for each operating frequency, the mean values (deviation from nominal) of each standard over the given measurement period plus standard deviation of all measurements (expressed in parts in 10^6).

First series of measurements (5 January to 13 February 2015)

1027 Hz	**100 pF - SN 1256**	**10 pF - SN 1257**	**10 pF - SN 1258**	**10 pF – SN 1310**
Mean value $/10^{-6}$	+1.838	+1.428	+0.998	−0.013
sd $/10^{-6}$	0.013	0.014	0.012	0.010

1541 Hz	**100 pF - SN 1256**	**10 pF - SN 1257**	**10 pF - SN 1258**	**10 pF – SN 1310**
Mean value $/10^{-6}$	+1.797	+1.382	+0.944	−0.027
sd $/10^{-6}$	0.012	0.013	0.010	0.009

3083 Hz	**100 pF - SN 1256**	**10 pF - SN 1257**	**10 pF - SN 1258**	**10 pF – SN 1310**
Mean value $/10^{-6}$	+1.716	+1.282	+0.833	−0.063
sd $/10^{-6}$	0.015	0.014	0.012	0.011

Second series of measurements (17 April to 3 June 2015)

i) Means and standard deviations including initial drift

1027 Hz	**100 pF - SN 1256**	**10 pF - SN 1257**	**10 pF - SN 1258**	**10 pF – SN 1310**
Mean value $/10^{-6}$	+1.906	+1.578	+1.096	−0.010
sd $/10^{-6}$	0.023	0.014	0.025	0.007

1541 Hz	**100 pF - SN 1256**	**10 pF - SN 1257**	**10 pF - SN 1258**	**10 pF – SN 1310**
Mean value $/10^{-6}$	+1.862	+1.521	+1.024	−0.022
sd $/10^{-6}$	0.018	0.011	0.019	0.004

3083 Hz	**100 pF - SN 1256**	**10 pF - SN 1257**	**10 pF - SN 1258**	**10 pF – SN 1310**
Mean value $/10^{-6}$	+1.788	+1.419	+0.902	−0.056
sd $/10^{-6}$	0.025	0.015	0.019	0.007

ii) Means and standard deviations eliminating the few first measurement values (for which the drift is the most pronounced) for the three standards 1256, 1257 and 1258 (starting on 5 May 2015)

1027 Hz	**100 pF - SN 1256**	**10 pF - SN 1257**	**10 pF - SN 1258**
Mean value $/10^{-6}$	+1.892	+1.571	+1.084
sd $/10^{-6}$	0.005	0.006	0.014

1541 Hz	**100 pF - SN 1256**	**10 pF - SN 1257**	**10 pF - SN 1258**
Mean value $/10^{-6}$	+1.855	+1.518	+1.017
sd $/10^{-6}$	0.008	0.007	0.012

3083 Hz	**100 pF - SN 1256**	**10 pF - SN 1257**	**10 pF - SN 1258**
Mean value $/10^{-6}$	+1.774	+1.412	+0.892
sd $/10^{-6}$	0.006	0.008	0.010

11.3 Detailed and summarised results of LNE

Because LNE carried out the 100 pF measurements at a voltage level of 45 V_{rms} (instead of 10 V_{rms}) and the 10 pF measurements at 398 Hz at a voltage level of 63 V_{rms} (instead of 100 V_{rms}), a correction with the corresponding uncertainty has been added by the pilot, as explained in Section 4.7.

Further, because the LNE laboratory runs at a deviating temperature of 20°C, the pilot applied a correction with an associated uncertainty of $6 \cdot 10^{-9}$, as described in Section 12.1. In the following, the uncorrected LNE results are given.

Summarised LNE results of the first capacitance circulation

Capacitor AH 1256
Nominal value : 100 pF

Test frequency (Hz)	Voltage (V)	Mean date of measurement	Measurement result : Deviation from nominal value (µF/F)	Combined standard uncertainty (µF/F)	Effective degrees of freedom	Expanded uncertainty (95% coverage factor, k=2)
397.89	5	18/03/2011	1.899	0.010	57	0.020
795.77	10	11/03/2011	1.820	0.009	103	0.018
1591.55	10	14/03/2011	1.767	0.011	62	0.022

AH 1100 Frame informations : Drift : -0.36 / Chassis Temp. °C : 32.9

Capacitor AH 1257
Nominal value : 10 pF

Test frequency (Hz)	Voltage (V)	Mean date of measurement	Measurement result : Deviation from nominal value (µF/F)	Combined standard uncertainty (µF/F)	Effective degrees of freedom	Expanded uncertainty (95% coverage factor, k=2)
397.89	50	28/03/2011	1.482	0.011	76	0.022
795.77	100	27/03/2011	1.394	0.010	146	0.020
1591.55	100	27/03/2011	1.339	0.012	80	0.024

AH 1100 Frame informations : Drift : 0.017 / Chassis Temp. °C : 32.9

Capacitor AH 1258
Nominal value : 10 pF

Test frequency (Hz)	Voltage (V)	Mean date of measurement	Measurement result : Deviation from nominal value (µF/F)	Combined standard uncertainty (µF/F)	Effective degrees of freedom	Expanded uncertainty (95% coverage factor, k=2)
397.89	50	28/03/2011	1.118	0.011	76	0.022
795.77	100	27/03/2011	1.033	0.010	146	0.020
1591.55	100	27/03/2011	0.957	0.011	80	0.022

AH 1100 Frame informations : Drift : -0.002 / Chassis Temp. °C : 32.9

Capacitor AH 1310
Nominal value : 10 pF

Test frequency (Hz)	Voltage (V)	Mean date of measurement	Measurement result : Deviation from nominal value (µF/F)	Combined standard uncertainty (µF/F)	Effective degrees of freedom	Expanded uncertainty (95% coverage factor, k=2)
397.89	50	28/03/2011	0.218	0.010	76	0.020
795.77	100	27/03/2011	0.181	0.010	146	0.020
1591.55	100	27/03/2011	0.176	0.011	80	0.022

AH 1100 Frame informations : Drift : -0.051 / Chassis Temp. °C : 32.9

Detailed LNE results of the first capacitance circulation

AH1256

Serial N°. Of the standard : **AH1256 (PTB)** Nominal value : **100 pF** Voltage : **45 V** Test frequency : **397,89 Hz**

	Date	Test frequency (Hz)	Ambient temperature and uncertainty T_{amb} (°C)	Humidity (%)	Barometric pressure (Pa)	Drift	Chassis temperature (°C)	Measurement result: deviation from nominal value (µF/F)	Type A uncertainty (µF/F)	Type B uncertainty (µF/F)	Combined uncertainty (µF/F)
	14/03/2011	397.89	(20,7+/- 0,3)°C	50+/-10	992	-0.036	33.1	1.866	0.020	0.008	0.022
	15/03/2011	397.89	(20,7+/- 0,3)°C	50+/-10	991	-0.036	33.2	1.897	0.020	0.008	0.022
	15/03/2011	397.89	(20,7+/- 0,3)°C	50+/-10	990	-0.036	33.1	1.866	0.020	0.008	0.022
	15/03/2011	397.89	(20,7+/- 0,3)°C	50+/-10	988	-0.036	33.3	1.911	0.020	0.008	0.022
	18/03/2011	397.89	(20,7+/- 0,3)°C	50+/-10	1003	-0.036	32.2	1.894	0.020	0.008	0.022
	18/03/2011	397.89	(20,7+/- 0,3)°C	50+/-10	1002	-0.033	32.2	1.897	0.020	0.008	0.022
	18/03/2011	397.89	(20,7+/- 0,3)°C	50+/-10	1002	-0.036	33.3	1.909	0.020	0.008	0.022
	18/03/2011	397.89	(20,7+/- 0,3)°C	50+/-10	1002	-0.036	33.0	1.921	0.020	0.008	0.022
	23/03/2011	397.89	(20,7+/- 0,3)°C	50+/-10	1015	-0.035	33.0	1.910	0.020	0.008	0.022
	23/03/2011	397.89	(20,7+/- 0,3)°C	50+/-10	1014	-0.036	33.1	1.923	0.020	0.008	0.022
Mean	**17/03/11**	**397.89**	**(20,7+/-0,3)°C**	**50+/-10**	**1000**	**-0.036**	**33.0**	**1.899**	**0.006**	**0.008**	**0.010**

Serial N°. Of the standard : **AH1256 (PTB)** Nominal value : **100 pF** Voltage : **45 V** Test frequency : **795,77 Hz**

	Date	Test frequency (Hz)	Ambient temperature and uncertainty T_{amb} (°C)	Humidity (%)	Barometric pressure (Pa)	Drift	Chassis temperature (°C)	Measurement result: deviation from nominal value (µF/F)	Type A uncertainty (µF/F)	Type B uncertainty (µF/F)	Combined uncertainty (µF/F)
	08/03/2011	795,77	(20,7+/- 0,3)°C	50+/-10	1001	-0.036	33.1	1.835	0.013	0.008	0.016
	09/03/2011	795,77	(20,7+/- 0,3)°C	50+/-10	1001	-0.036	33.1	1.811	0.013	0.008	0.016
	09/03/2011	795,77	(20,7+/- 0,3)°C	50+/-10	1000	-0.036	33.1	1.809	0.013	0.008	0.016
	09/03/2011	795,77	(20,7+/- 0,3)°C	50+/-10	999	-0.036	33.0	1.808	0.013	0.008	0.016
	10/03/2011	795,77	(20,7+/- 0,3)°C	50+/-10	1001	-0.036	33.2	1.830	0.013	0.008	0.016
	10/03/2011	795,77	(20,7+/- 0,3)°C	50+/-10	1000	-0.036	33.1	1.834	0.013	0.008	0.016
	11/03/2011	795,77	(20,7+/- 0,3)°C	50+/-10	998	-0.036	33.2	1.834	0.013	0.008	0.016
	11/03/2011	795,77	(20,7+/- 0,3)°C	50+/-10	997	-0.036	31.9	1.797	0.013	0.008	0.016
	14/03/2011	795,77	(20,7+/- 0,3)°C	50+/-10	993	-0.036	33.3	1.817	0.013	0.008	0.016
	14/03/2011	795,77	(20,7+/- 0,3)°C	50+/-10	993	-0.033	32.2	1.813	0.013	0.008	0.016
	21/03/2011	795,77	(20,7+/- 0,3)°C	50+/-10	1012	-0.036	33.1	1.833	0.013	0.008	0.016
Mean	**11/03/11**	**795.77**	**(20,7+/-0,3)°C**	**50+/-10**	**1000**	**-0.036**	**32.9**	**1.820**	**0.004**	**0.008**	**0.009**

Serial N°. Of the standard : **AH1256 (PTB)** Nominal value : **100 pF** Voltage : **45 V** Test frequency : **1591,55 Hz**

	Date	Test frequency (Hz)	Ambient temperature and uncertainty T_{amb} (°C)	Humidity (%)	Barometric pressure (Pa)	Drift	Chassis temperature (°C)	Measurement result: deviation from nominal value (µF/F)	Type A uncertainty (µF/F)	Type B uncertainty (µF/F)	Combined uncertainty (µF/F)
	03/03/11	1591.55	(20,7+/- 0,3)°C	50+/-10	1008	-0.035	32.9	1.767	0.022	0.009	0.023
	07/03/11	1591.55	(20,7+/- 0,3)°C	50+/-10	1006	-0.036	33.1	1.807	0.022	0.009	0.023
	08/03/11	1591.55	(20,7+/- 0,3)°C	50+/-10	1004	-0.036	33.2	1.765	0.022	0.009	0.023
	08/03/11	1591.55	(20,7+/- 0,3)°C	50+/-10	1002	-0.036	33.1	1.742	0.022	0.009	0.023
	10/03/11	1591.55	(20,7+/- 0,3)°C	50+/-10	999	-0.036	33.2	1.791	0.022	0.009	0.023
	11/03/11	1591.55	(20,7+/- 0,3)°C	50+/-10	1000	-0.036	33.0	1.753	0.022	0.009	0.023
	11/03/11	1591.55	(20,7+/- 0,3)°C	50+/-10	999	-0.036	33.2	1.764	0.022	0.009	0.023
	21/03/11	1591.55	(20,7+/- 0,3)°C	50+/-10	1013	-0.036	33.0	1.788	0.022	0.009	0.023
	21/03/11	1591.55	(20,7+/- 0,3)°C	50+/-10	1013	-0.033	32.3	1.747	0.022	0.009	0.023
	21/03/11	1591.55	(20,7+/- 0,3)°C	50+/-10	1013	-0.036	33.2	1.731	0.022	0.009	0.023
	24/03/11	1591.55	(20,7+/- 0,3)°C	50+/-10	1013	-0.035	33.0	1.761	0.022	0.009	0.023
	24/03/11	1591.55	(20,7+/- 0,3)°C	50+/-10	1011	-0.036	33.1	1.770	0.022	0.009	0.023
	24/03/11	1591.55	(20,7+/- 0,3)°C	50+/-10	1008	-0.036	33.0	1.786	0.022	0.009	0.023
Mean	**14/03/11**	**1591.55**	**(20,7+/-0,3)°C**	**50+/-10**	**1007**	**-0.036**	**33.0**	**1.767**	**0.006**	**0.009**	**0.011**

AH1257

Serial N°. Of the standard : **AH1257 (PTB)** Nominal value : **10 pF** Voltage : **63 V** Test frequency : **397,89 Hz**

	Date	Test frequency (Hz)	Ambient temperature and uncertainty T_{amb} (°C)	Humidity (%)	Barometric pressure (Pa)	Drift	Chassis temperature (°C)	Measurement result: deviation from nominal value (µF/F)	Type A uncertainty (µF/F)	Type B uncertainty (µF/F)	Combined uncertainty (µF/F)
	25/03/11	397.89	(20,7+/- 0,3)°C	50+/-10	1017	0.014	33.1	1.473	0.006	0.010	0.012
	25/03/11	397.89	(20,7+/- 0,3)°C	50+/-10	1017	0.016	32.5	1.468	0.006	0.010	0.012
	28/03/11	397.89	(20,7+/- 0,3)°C	50+/-10	1002	0.018	31.7	1.482	0.006	0.010	0.012
	28/03/11	397.89	(20,7+/- 0,3)°C	50+/-10	1002	0.017	31.9	1.486	0.006	0.010	0.012
	28/03/11	397.89	(20,7+/- 0,3)°C	50+/-10	1003	0.016	32.1	1.482	0.006	0.010	0.012
	28/03/11	397.89	(20,7+/- 0,3)°C	50+/-10	1003	0.018	31.9	1.484	0.006	0.010	0.012
	28/03/11	397.89	(20,7+/- 0,3)°C	50+/-10	1003	0.018	31.6	1.482	0.006	0.010	0.012
	29/03/11	397.89	(20,7+/- 0,3)°C	50+/-10	1000	0.018	31.6	1.488	0.006	0.010	0.012
	29/03/11	397.89	(20,7+/- 0,3)°C	50+/-10	1000	0.018	31.7	1.487	0.006	0.010	0.012
	30/03/11	397.89	(20,7+/- 0,3)°C	50+/-10	990	0.019	31.4	1.486	0.006	0.010	0.012
	30/03/11	397.89	(20,7+/- 0,3)°C	50+/-10	991	0.018	31.5	1.484	0.006	0.010	0.012
	31/03/11	397.89	(20,7+/- 0,3)°C	50+/-10	989	0.018	31.5	1.484	0.006	0.010	0.012
Mean	**28/03/11**	**397.89**	**(20,7+/-0,3)°C**	**50+/-10**	**1001**	**0.017**	**31.9**	**1.482**	**0.002**	**0.010**	**0.011**

Serial N°. Of the standard : **AH1257 (PTB)** Nominal value : **10 pF** Voltage : **100 V** Test frequency : **795,77 Hz**

	Date	Test frequency (Hz)	Ambient temperature and uncertainty T_{amb} (°C)	Humidity (%)	Barometric pressure (Pa)	Drift	Chassis temperature (°C)	Measurement result: deviation from nominal value (µF/F)	Type A uncertainty (µF/F)	Type B uncertainty (µF/F)	Combined uncertainty (µF/F)
	25/03/11	795,77	(20,7+/- 0,3)°C	50+/-10	1017	0.016	32.6	1.389	0.008	0.009	0.013
	25/03/11	795,77	(20,7+/- 0,3)°C	50+/-10	1017	0.016	32.4	1.382	0.008	0.009	0.013
	25/03/11	795,77	(20,7+/- 0,3)°C	50+/-10	1017	0.016	32.3	1.392	0.008	0.009	0.013
	25/03/11	795,77	(20,7+/- 0,3)°C	50+/-10	1017	0.016	32.6	1.379	0.008	0.009	0.013
	28/03/11	795,77	(20,7+/- 0,3)°C	50+/-10	1003	0.018	31.8	1.397	0.008	0.009	0.013
	28/03/11	795,77	(20,7+/- 0,3)°C	50+/-10	1003	0.018	31.6	1.401	0.008	0.009	0.013
	28/03/11	795,77	(20,7+/- 0,3)°C	50+/-10	1003	0.018	31.9	1.409	0.008	0.009	0.013
	28/03/11	795,77	(20,7+/- 0,3)°C	50+/-10	1003	0.018	31.9	1.397	0.008	0.009	0.013
	29/03/11	795,77	(20,7+/- 0,3)°C	50+/-10	1000	0.018	31.6	1.398	0.008	0.009	0.013
	29/03/11	795,77	(20,7+/- 0,3)°C	50+/-10	1000	0.018	31.6	1.398	0.008	0.009	0.013
	30/03/11	795,77	(20,7+/- 0,3)°C	50+/-10	991	0.018	31.5	1.402	0.008	0.009	0.013
	31/03/11	795,77	(20,7+/- 0,3)°C	50+/-10	989	0.018	31.5	1.395	0.008	0.009	0.013
Mean	**27/03/11**	**795.77**	**(20,7+/-0,3)°C**	**50+/-10**	**1005**	**0.017**	**31.9**	**1.394**	**0.002**	**0.009**	**0.010**

Serial N°. Of the standard : **AH1257 (PTB)** Nominal value : **10 pF** Voltage : **100 V** Test frequency : **1591,55 Hz**

	Date	Test frequency (Hz)	Ambient temperature and uncertainty T_{amb} (°C)	Humidity (%)	Barometric pressure (Pa)	Drift	Chassis temperature (°C)	Measurement result: deviation from nominal value (µF/F)	Type A uncertainty (µF/F)	Type B uncertainty (µF/F)	Combined uncertainty (µF/F)
	25/03/11	1591.55	(20,7+/- 0,3)°C	50+/-10	1017	0.015	32.6	1.332	0.012	0.011	0.016
	25/03/11	1591.55	(20,7+/- 0,3)°C	50+/-10	1017	0.016	32.4	1.322	0.012	0.011	0.016
	25/03/11	1591.55	(20,7+/- 0,3)°C	50+/-10	1017	0.014	33.1	1.317	0.012	0.011	0.016
	28/03/11	1591.55	(20,7+/- 0,3)°C	50+/-10	1003	0.017	32.1	1.335	0.012	0.011	0.016
	28/03/11	1591.55	(20,7+/- 0,3)°C	50+/-10	1003	0.018	31.6	1.348	0.012	0.011	0.016
	28/03/11	1591.55	(20,7+/- 0,3)°C	50+/-10	1003	0.016	32.3	1.328	0.012	0.011	0.016
	28/03/11	1591.55	(20,7+/- 0,3)°C	50+/-10	1003	0.017	32.0	1.342	0.012	0.011	0.016
	28/03/11	1591.55	(20,7+/- 0,3)°C	50+/-10	1003	0.018	31.6	1.343	0.012	0.011	0.016
	29/03/11	1591.55	(20,7+/- 0,3)°C	50+/-10	1000	0.018	31.6	1.349	0.012	0.011	0.016
	29/03/11	1591.55	(20,7+/- 0,3)°C	50+/-10	1000	0.018	31.6	1.349	0.012	0.011	0.016
	30/03/11	1591.55	(20,7+/- 0,3)°C	50+/-10	991	0.019	31.4	1.348	0.012	0.011	0.016
	31/03/11	1591.55	(20,7+/- 0,3)°C	50+/-10	989	0.018	31.5	1.351	0.012	0.011	0.016
Mean	**27/03/11**	**795.77**	**(20,7+/-0,3)°C**	**50+/-10**	**1004**	**0.017**	**32.0**	**1.339**	**0.003**	**0.011**	**0.012**

AH1258

Serial N°. Of the standard : **AH1258 (PTB)** Nominal value : **10 pF** Voltage : **63 V** Test frequency : **397,89 Hz**

	Date	Test frequency (Hz)	Ambient temperature and uncertainty T_{amb} (°C)	Humidity (%)	Barometric pressure (Pa)	Drift	Chassis temperature (°C)	Measurement result: deviation from nominal value (µF/F)	Type A uncertainty (µF/F)	Type B uncertainty (µF/F)	Combined uncertainty (µF/F)
	25/03/2011	397.89	(20,7+/- 0,3)°C	50+/-10	1017	-0.002	33.1	1.106	0.006	0.010	0.012
	25/03/2011	397.89	(20,7+/- 0,3)°C	50+/-10	1017	-0.002	32.5	1.102	0.006	0.010	0.012
	28/03/2011	397.89	(20,7+/- 0,3)°C	50+/-10	1002	-0.001	31.7	1.117	0.006	0.010	0.012
	28/03/2011	397.89	(20,7+/- 0,3)°C	50+/-10	1002	-0.002	31.8	1.123	0.006	0.010	0.012
	28/03/2011	397.89	(20,7+/- 0,3)°C	50+/-10	1003	-0.002	32.0	1.118	0.006	0.010	0.012
	28/03/2011	397.89	(20,7+/- 0,3)°C	50+/-10	1003	-0.002	31.9	1.118	0.006	0.010	0.012
	28/03/2011	397.89	(20,7+/- 0,3)°C	50+/-10	1003	-0.002	31.6	1.123	0.006	0.010	0.012
	29/03/2011	397.89	(20,7+/- 0,3)°C	50+/-10	1000	-0.002	31.7	1.123	0.006	0.010	0.012
	29/03/2011	397.89	(20,7+/- 0,3)°C	50+/-10	1000	-0.002	31.7	1.122	0.006	0.010	0.012
	30/03/2011	397.89	(20,7+/- 0,3)°C	50+/-10	990	-0.002	31.4	1.116	0.006	0.010	0.012
	30/03/2011	397.89	(20,7+/- 0,3)°C	50+/-10	991	-0.002	31.5	1.122	0.006	0.010	0.012
	31/03/2011	397.89	(20,7+/- 0,3)°C	50+/-10	989	-0.002	31.5	1.119	0.006	0.010	0.012
Mean	**28/03/11**	**397.89**	**(20,7+/-0,3)°C**	**50+/-10**	**1001**	**-0.002**	**31.9**	**1.118**	**0.002**	**0.010**	**0.011**

Serial N°. Of the standard : **AH1258 (PTB)** Nominal value : **10 pF** Voltage : **100 V** Test frequency : **795,77 Hz**

	Date	Test frequency (Hz)	Ambient temperature and uncertainty T_{amb} (°C)	Humidity (%)	Barometric pressure (Pa)	Drift	Chassis temperature (°C)	Measurement result: deviation from nominal value (µF/F)	Type A uncertainty (µF/F)	Type B uncertainty (µF/F)	Combined uncertainty (µF/F)
	25/03/2011	795,77	(20,7+/- 0,3)°C	50+/-10	1017	-0.002	32.6	1.033	0.006	0.009	0.011
	25/03/2011	795,77	(20,7+/- 0,3)°C	50+/-10	1017	-0.002	32.4	1.029	0.006	0.009	0.011
	25/03/2011	795,77	(20,7+/- 0,3)°C	50+/-10	1017	-0.002	32.3	1.027	0.006	0.009	0.011
	28/03/2011	795,77	(20,7+/- 0,3)°C	50+/-10	1017	-0.002	32.6	1.021	0.006	0.009	0.011
	28/03/2011	795,77	(20,7+/- 0,3)°C	50+/-10	1003	-0.002	31.8	1.031	0.006	0.009	0.011
	28/03/2011	795,77	(20,7+/- 0,3)°C	50+/-10	1003	-0.002	31.6	1.034	0.006	0.009	0.011
	28/03/2011	795,77	(20,7+/- 0,3)°C	50+/-10	1003	-0.002	31.9	1.033	0.006	0.009	0.011
	29/03/2011	795,77	(20,7+/- 0,3)°C	50+/-10	1003	-0.002	31.9	1.037	0.006	0.009	0.011
	29/03/2011	795,77	(20,7+/- 0,3)°C	50+/-10	1000	-0.002	31.6	1.035	0.006	0.009	0.011
	30/03/2011	795,77	(20,7+/- 0,3)°C	50+/-10	1000	-0.002	31.6	1.038	0.006	0.009	0.011
	31/03/2011	795,77	(20,7+/- 0,3)°C	50+/-10	991	-0.002	31.5	1.043	0.006	0.009	0.011
	31/03/2011	795,77	(20,7+/- 0,3)°C	50+/-10	989	-0.002	31.5	1.0351	0.006	0.009	0.011
Mean	**28/03/11**	**795.77**	**(20,7+/-0,3)°C**	**50+/-10**	**1005**	**-0.002**	**31.9**	**1.033**	**0.002**	**0.009**	**0.010**

Serial N°. Of the standard : **AH1258 (PTB)** Nominal value : **10 pF** Voltage : **100 V** Test frequency : **1591,55 Hz**

	Date	Test frequency (Hz)	Ambient temperature and uncertainty T_{amb} (°C)	Humidity (%)	Barometric pressure (Pa)	Drift	Chassis temperature (°C)	Measurement result: deviation from nominal value (µF/F)	Type A uncertainty (µF/F)	Type B uncertainty (µF/F)	Combined uncertainty (µF/F)
	25/03/11	1591.55	(20,7+/- 0,3)°C	50+/-10	1017	-0.002	32.6	0.952	0.008	0.011	0.014
	25/03/11	1591.55	(20,7+/- 0,3)°C	50+/-10	1017	-0.002	32.5	0.944	0.008	0.011	0.014
	25/03/11	1591.55	(20,7+/- 0,3)°C	50+/-10	1017	-0.002	33.1	0.944	0.008	0.011	0.014
	28/03/11	1591.55	(20,7+/- 0,3)°C	50+/-10	1003	-0.002	32.0	0.957	0.008	0.011	0.014
	28/03/11	1591.55	(20,7+/- 0,3)°C	50+/-10	1003	-0.002	31.6	0.968	0.008	0.011	0.014
	28/03/11	1591.55	(20,7+/- 0,3)°C	50+/-10	1003	-0.002	32.2	0.951	0.008	0.011	0.014
	28/03/11	1591.55	(20,7+/- 0,3)°C	50+/-10	1003	-0.002	32.0	0.957	0.008	0.011	0.014
	28/03/11	1591.55	(20,7+/- 0,3)°C	50+/-10	1003	-0.002	31.7	0.961	0.008	0.011	0.014
	29/03/11	1591.55	(20,7+/- 0,3)°C	50+/-10	1000	-0.001	31.6	0.961	0.008	0.011	0.014
	29/03/11	1591.55	(20,7+/- 0,3)°C	50+/-10	1000	-0.001	31.6	0.964	0.008	0.011	0.014
	30/03/11	1591.55	(20,7+/- 0,3)°C	50+/-10	991	-0.001	31.4	0.964	0.008	0.011	0.014
	31/03/11	1591.55	(20,7+/- 0,3)°C	50+/-10	989	-0.002	31.7	0.966	0.008	0.011	0.014
Mean	**27/03/11**	**1591.55**	**(20,7+/-0,3)°C**	**50+/-10**	**1004**	**-0.002**	**32.0**	**0.957**	**0.002**	**0.011**	**0.011**

AH1310

Serial N°. Of the standard : **AH1310 (BIPM)** Nominal value : **10 pF** Voltage : **63 V** Test frequency : **397,89 Hz**

	Date	Test frequency (Hz)	Ambient temperature and uncertainty T_{amb} (°C)	Humidity (%)	Barometric pressure (Pa)	Drift	Chassis temperature (°C)	Measurement result: deviation from nominal value (µF/F)	Type A uncertainty (µF/F)	Type B uncertainty (µF/F)	Combined uncertainty (µF/F)
	25/03/2011	397.89	(20,7+/- 0,3)°C	50+/-10	1017	-0.058	33.1	0.218	0.004	0.010	0.011
	25/03/2011	397.89	(20,7+/- 0,3)°C	50+/-10	1017	-0.055	32.5	0.205	0.004	0.010	0.011
	28/03/2011	397.89	(20,7+/- 0,3)°C	50+/-10	1002	-0.050	31.7	0.218	0.004	0.010	0.011
	28/03/2001	397.89	(20,7+/- 0,3)°C	50+/-10	1002	-0.050	31.8	0.221	0.004	0.010	0.011
	28/03/2011	397.89	(20,7+/- 0,3)°C	50+/-10	1003	-0.052	32.0	0.217	0.004	0.010	0.011
	28/03/2011	397.89	(20,7+/- 0,3)°C	50+/-10	1003	-0.051	32.0	0.221	0.004	0.010	0.011
	28/03/2011	397.89	(20,7+/- 0,3)°C	50+/-10	1003	-0.049	31.6	0.220	0.004	0.010	0.011
	29/03/2011	397.89	(20,7+/- 0,3)°C	50+/-10	1000	-0.050	31.7	0.218	0.004	0.010	0.011
	29/03/2011	397.89	(20,7+/- 0,3)°C	50+/-10	1000	-0.049	31.6	0.219	0.004	0.010	0.011
	30/03/2011	397.89	(20,7+/- 0,3)°C	50+/-10	990	-0.048	31.4	0.220	0.004	0.010	0.011
	30/03/2011	397.89	(20,7+/- 0,3)°C	50+/-10	991	-0.049	31.5	0.221	0.004	0.010	0.011
	31/03/2011	397.89	(20,7+/- 0,3)°C	50+/-10	989	-0.048	31.5	0.221	0.004	0.010	0.011
Mean	**27/05/10**	**397.89**	**(20,7+/-0,3)°C**	**50+/-10**	**1001**	**-0.051**	**31.9**	**0.218**	**0.001**	**0.010**	**0.010**

Serial N°. Of the standard : **AH1310 (BIPM)** Nominal value : **10 pF** Voltage : **100 V** Test frequency : **795,77 Hz**

	Date	Test frequency (Hz)	Ambient temperature and uncertainty T_{amb} (°C)	Humidity (%)	Barometric pressure (Pa)	Drift	Chassis temperature (°C)	Measurement result: deviation from nominal value (µF/F)	Type A uncertainty (µF/F)	Type B uncertainty (µF/F)	Combined uncertainty (µF/F)
	25/03/2011	795,77	(20,7+/- 0,3)°C	50+/-10	1017	-0.056	32.6	0.182	0.009	0.009	0.013
	25/03/2011	795,77	(20,7+/- 0,3)°C	50+/-10	1017	-0.054	32.4	0.159	0.009	0.009	0.013
	25/03/2011	795,77	(20,7+/- 0,3)°C	50+/-10	1017	-0.054	32.3	0.169	0.009	0.009	0.013
	28/03/2011	795,77	(20,7+/- 0,3)°C	50+/-10	1017	-0.055	32.5	0.177	0.009	0.009	0.013
	28/03/2011	795,77	(20,7+/- 0,3)°C	50+/-10	1003	-0.050	31.9	0.183	0.009	0.009	0.013
	28/03/2011	795,77	(20,7+/- 0,3)°C	50+/-10	1003	-0.049	31.7	0.184	0.009	0.009	0.013
	28/03/2011	795,77	(20,7+/- 0,3)°C	50+/-10	1003	-0.051	31.9	0.182	0.009	0.009	0.013
	29/03/2011	795,77	(20,7+/- 0,3)°C	50+/-10	1003	-0.050	31.9	0.186	0.009	0.009	0.013
	29/03/2011	795,77	(20,7+/- 0,3)°C	50+/-10	1000	-0.055	31.6	0.184	0.009	0.009	0.013
	30/03/2011	795,77	(20,7+/- 0,3)°C	50+/-10	1000	-0.049	31.7	0.187	0.009	0.009	0.013
	31/03/2011	795,77	(20,7+/- 0,3)°C	50+/-10	991	-0.049	31.5	0.189	0.009	0.009	0.013
	31/03/2011	795,77	(20,7+/- 0,3)°C	50+/-10	989	-0.048	31.5	0.186	0.009	0.009	0.013
Mean	**28/03/11**	**795.77**	**(20,7+/-0,3)°C**	**50+/-10**	**1005**	**-0.052**	**32.0**	**0.181**	**0.002**	**0.009**	**0.010**

Serial N°. Of the standard : **AH1310 (BIPM)** Nominal value : **10 pF** Voltage : **100 V** Test frequency : **1591,55 Hz**

	Date	Test frequency (Hz)	Ambient temperature and uncertainty T_{amb} (°C)	Humidity (%)	Barometric pressure (Pa)	Drift	Chassis temperature (°C)	Measurement result: deviation from nominal value (µF/F)	Type A uncertainty (µF/F)	Type B uncertainty (µF/F)	Combined uncertainty (µF/F)
	25/03/11	1591.55	(20,7+/- 0,3)°C	50+/-10	1017	-0.055	32.6	0.172	0.006	0.011	0.012
	25/03/11	1591.55	(20,7+/- 0,3)°C	50+/-10	1017	-0.055	32.6	0.168	0.006	0.011	0.012
	25/03/11	1591.55	(20,7+/- 0,3)°C	50+/-10	1017	-0.059	33.1	0.169	0.006	0.011	0.012
	28/03/11	1591.55	(20,7+/- 0,3)°C	50+/-10	1003	-0.051	31.9	0.176	0.006	0.011	0.012
	28/03/11	1591.55	(20,7+/- 0,3)°C	50+/-10	1003	-0.050	31.7	0.186	0.006	0.011	0.012
	28/03/11	1591.55	(20,7+/- 0,3)°C	50+/-10	1003	-0.053	32.2	0.172	0.006	0.011	0.012
	28/03/11	1591.55	(20,7+/- 0,3)°C	50+/-10	1003	-0.051	32.0	0.173	0.006	0.011	0.012
	28/03/11	1591.55	(20,7+/- 0,3)°C	50+/-10	1003	-0.049	31.7	0.185	0.006	0.011	0.012
	29/03/11	1591.55	(20,7+/- 0,3)°C	50+/-10	1000	-0.049	31.6	0.176	0.006	0.011	0.012
	29/03/11	1591.55	(20,7+/- 0,3)°C	50+/-10	1000	-0.050	31.6	0.178	0.006	0.011	0.012
	30/03/11	1591.55	(20,7+/- 0,3)°C	50+/-10	991	-0.048	31.4	0.178	0.006	0.011	0.012
	31/03/11	1591.55	(20,7+/- 0,3)°C	50+/-10	989	-0.049	31.7	0.177	0.006	0.011	0.012
Mean	**27/03/11**	**1591.55**	**(20,7+/-0,3)°C**	**50+/-10**	**1004**	**-0.052**	**32.0**	**0.176**	**0.002**	**0.011**	**0.011**

Summarised LNE results of the second capacitance circulation

The following detailed results do neither include the correction of
(-0.09 ± 0.04)·10^{-6} at 397.88 Hz
(-0.05 ± 0.02)·10^{-6} at 795.77 Hz
(0.12 ± 0.02)·10^{-6} at 1591.5 Hz
for the magnetisation of the injection system nor the correction for the deviating ambient temperature and test voltages.

Capacitor AH 1256, Nominal value: 100 pF

Test frequency (Hz)	Voltage (V)	Mean date of measurement	Deviation from nominal (µF/F)	Combined uncertainty (µF/F)	Effective degrees of freedom	Expanded uncertainty (95%, k=2)
397.89	45	26/01/2016	2.085	0.009	172	0.020
795.77	45	25/01/2016	2.041	0.009	128	0.018
1591.55	45	27/01/2016	1.952	0.010	74	0.020

AH 1100 Frame information: Drift: 0.015 / Chassis Temp. °C: 31.4

Capacitor AH 1257: Nominal value: 10 pF

Test frequency (Hz)	Voltage (V)	Mean date of measurement	Deviation from nominal (µF/F)	Combined uncertainty (µF/F)	Effective degrees of freedom	Expanded uncertainty (95%, k=2)
397.89	100	11/02/2016	1.71	0.04	234	0.08
795.77	100	11/02/2016	1.64	0.02	170	0.04
1591.55	100	11/02/2016	1.59	0.03	98	0.06

AH 1100 Frame information: Drift: 0.014 / Chassis Temp. °C: 31.8

Capacitor AH 1258: Nominal value: 10 pF

Test frequency (Hz)	Voltage (V)	Mean date of measurement	Deviation from nominal (µF/F)	Combined uncertainty (µF/F)	Effective degrees of freedom	Expanded uncertainty (95%, k=2)
397.89	100	11/02/2016	1.17	0.04	234	0.08
795.77	100	11/02/2016	1.09	0.02	170	0.04
1591.55	100	11/02/2016	0.02	0.03	98	0.06

AH 1100 Frame information: Drift: 0.000 / Chassis Temp. °C: 31.8

Capacitor AH 1310: Nominal value: 10 pF

Test frequency (Hz)	Voltage (V)	Mean date of measurement	Deviation from nominal (µF/F)	Combined uncertainty (µF/F)	Effective degrees of freedom	Expanded uncertainty (95%, k=2)
397.89	100	11/02/2016	-0.01	0.04	234	0.08
795.77	100	11/02/2016	-0.01	0.02	170	0.04
1591.55	100	11/02/2016	0.00	0.03	98	0.06

AH 1100 Frame information: Drift: -0.051 / Chassis Temp. °C: 31.8

Detailed LNE results of the second capacitance circulation

The following detailed results do neither include the correction of the magnetisation of the injection system nor for the deviating ambient temperature and test voltage.

AH1256

Serial N°. Of the standard : **AH1256 (PTB)** Nominal value : **100 pF** Voltage : **45 V** Test frequency **397,89 Hz**

	Date	Test frequency (Hz)	Ambient temperature and uncertainty T_{amb} (°C)	Humidity (%)	Barometric pressure (Pa)	Drift	Chassis temperature (°C)	Measurement result: deviation from nominal value (µF/F)	Type A uncertainty (µF/F)	Type B uncertainty (µF/F)	Combined uncertainty (µF/F)
	20/01/2016	397.89	20,1+/- 0,3	50+/-10	1000	0.014	31.3	2.098	0.013	0.010	0.016
	21/01/2016	397.89	20,1+/- 0,3	50+/-10	1004	0.015	31.4	2.100	0.013	0.010	0.016
	21/01/2016	397.89	20,1+/- 0,3	50+/-10	1005	0.014	31.5	2.102	0.013	0.010	0.016
	21/01/2016	397.89	20,1+/- 0,3	50+/-10	1004	0.016	31.3	2.071	0.013	0.010	0.016
	25/01/2016	397.89	20,1+/- 0,3	50+/-10	1005	0.015	31.5	2.092	0.013	0.010	0.016
	25/01/2016	397.89	20,1+/- 0,3	50+/-10	1005	0.014	31.4	2.072	0.013	0.010	0.016
	25/01/2016	397.89	20,1+/- 0,3	50+/-10	1005	0.014	31.6	2.068	0.013	0.010	0.016
	25/01/2016	397.89	20,1+/- 0,3	50+/-10	1005	0.014	31.4	2.070	0.013	0.010	0.016
	25/01/2016	397.89	20,1+/- 0,3	50+/-10	1005	0.015	31.4	2.093	0.013	0.010	0.016
	27/01/2016	397.89	20,1+/- 0,3	50+/-10	998	0.015	31.6	2.072	0.013	0.010	0.016
	27/01/2016	397.89	20,1+/- 0,3	50+/-10	998	0.015	31.2	2.080	0.013	0.010	0.016
	27/01/2016	397.89	20,1+/- 0,3	50+/-10	997	0.015	31.4	2.072	0.013	0.010	0.016
	27/01/2016	397.89	20,1+/- 0,3	50+/-10	997	0.014	31.6	2.080	0.013	0.010	0.016
	01/02/2016	397.89	20,1+/- 0,3	50+/-10	1006	0.016	31.5	2.099	0.013	0.010	0.016
	01/02/2016	397.89	20,1+/- 0,3	50+/-10	1005	0.014	31.3	2.085	0.013	0.010	0.016
	01/02/2016	397.89	20,1+/- 0,3	50+/-10	1005	0.015	31.4	2.092	0.013	0.010	0.016
	01/02/2016	397.89	20,1+/- 0,3	50+/-10	1005	0.015	31.2	2.103	0.013	0.010	0.016
Mean	**26/01/16**	**397.89**	**20,1+/-0,3**	**50+/-10**	**1003**	**0.015**	**31.4**	**2.085**	**0.003**	**0.008**	**0.009**

Serial N°. Of the standard : **AH1256 (PTB)** Nominal value : **100 pF** Voltage : **45 V** Test frequency **795,77 Hz**

	Date	Test frequency (Hz)	Ambient temperature and uncertainty T_{amb} (°C)	Humidity (%)	Barometric pressure (Pa)	Drift	Chassis temperature (°C)	Measurement result: deviation from nominal value (µF/F)	Type A uncertainty (µF/F)	Type B uncertainty (µF/F)	Combined uncertainty (µF/F)
	20/01/2016	795,77	20,1+/- 0,3	50+/-10	999	0.015	31.4	2.013	0.019	0.009	0.021
	20/01/2016	795,77	20,1+/- 0,3	50+/-10	1000	0.015	31.3	2.034	0.019	0.009	0.021
	20/01/2016	795,77	20,1+/- 0,3	50+/-10	1000	0.014	31.5	2.026	0.019	0.009	0.021
	20/01/2016	795,77	20,1+/- 0,3	50+/-10	1000	0.015	31.3	2.049	0.019	0.009	0.021
	21/01/2016	795,77	20,1+/- 0,3	50+/-10	1004	0.016	31.4	2.044	0.019	0.009	0.021
	21/01/2016	795,77	20,1+/- 0,3	50+/-10	1004	0.015	31.3	2.055	0.019	0.009	0.021
	26/01/2016	795,77	20,1+/- 0,3	50+/-10	1006	0.015	31.5	2.059	0.019	0.009	0.021
	26/01/2016	795,77	20,1+/- 0,3	50+/-10	1006	0.015	31.7	2.068	0.019	0.009	0.021
	26/01/2016	795,77	20,1+/- 0,3	50+/-10	1005	0.015	31.4	2.083	0.019	0.009	0.021
	26/01/2016	795,77	20,1+/- 0,3	50+/-10	1004	0.015	31.7	2.034	0.019	0.009	0.021
	26/01/2016	795,77	20,1+/- 0,3	50+/-10	1003	0.015	31.5	2.045	0.019	0.009	0.021
	26/01/2016	795,77	20,1+/- 0,3	50+/-10	1001	0.015	31.6	2.036	0.019	0.009	0.021
	26/01/2016	795,77	20,1+/- 0,3	50+/-10	1001	0.015	31.4	2.039	0.019	0.009	0.021
	26/01/2016	795,77	20,1+/- 0,3	50+/-10	1000	0.015	31.6	2.045	0.019	0.009	0.021
	02/02/2016	795,77	20,1+/- 0,3	50+/-10	999	0.012	31.4	2.011	0.019	0.009	0.021
	02/02/2016	795,77	20,1+/- 0,3	50+/-10	1001	0.015	31.4	2.026	0.019	0.009	0.021
	02/02/2016	795,77	20,1+/- 0,3	50+/-10	1000	0.014	31.5	2.023	0.019	0.009	0.021
Mean	**25/01/16**	**795.77**	**20,1+/-0,3**	**50+/-10**	**1000**	**0.014**	**31.5**	**2.041**	**0.005**	**0.008**	**0.009**

	Serial N°. Of the standard :	AH1256 (PTB)		Nominal value :	100 pF	Voltage :	45 V	Test frequency	1591,55 Hz	
	Date	Test frequency (Hz)	Ambient temperature and uncertainty T_{amb} (°C)	Humidity (%)	Barometric pressure (Pa)	Drift	Chassis temperature (°C)	Measurement result: deviation from nominal value (µF/F)	Type A uncertainty (µF/F)	Type B uncertainty (µF/F)	Combined uncertainty (µF/F)
	18/01/2016	1591.55	20,1+/- 0,3	50+/-10	994	0.015	31.7	1.961	0.015	0.011	0.018
	18/01/2016	1591.55	20,1+/- 0,3	50+/-10	992	0.015	31.5	1.928	0.015	0.011	0.018
	18/01/2016	1591.55	20,1+/- 0,3	50+/-10	992	0.015	31.1	1.927	0.015	0.011	0.018
	18/01/2016	1591.55	20,1+/- 0,3	50+/-10	992	0.016	31.4	1.939	0.015	0.011	0.018
	19/01/2016	1591.55	20,1+/- 0,3	50+/-10	994	0.015	31.8	1.956	0.015	0.011	0.018
	19/01/2016	1591.55	20,1+/- 0,3	50+/-10	994	0.015	31.7	1.923	0.015	0.011	0.018
	19/01/2016	1591.55	20,1+/- 0,3	50+/-10	995	0.015	31.5	1.957	0.015	0.011	0.018
	29/01/2016	1591.55	20,1+/- 0,3	50+/-10	1010	0.015	31.6	1.964	0.015	0.011	0.018
	29/01/2016	1591.55	20,1+/- 0,3	50+/-10	1001	0.017	31.4	1.963	0.015	0.011	0.018
	03/02/2016	1591.55	20,1+/- 0,3	50+/-10	1005	0.015	31.5	1.969	0.015	0.011	0.018
	04/02/2016	1591.55	20,1+/- 0,3	50+/-10	1009	0.015	31.3	1.947	0.015	0.011	0.018
	04/02/2016	1591.55	20,1+/- 0,3	50+/-10	1009	0.013	31.5	1.965	0.015	0.011	0.018
	04/02/2016	1591.55	20,1+/- 0,3	50+/-10	1007	0.013	31.4	1.958	0.015	0.011	0.018
	04/02/2016	1591.55	20,1+/- 0,3	50+/-10	1008	0.015	31.6	1.953	0.015	0.011	0.018
	05/02/2016	1591.55	20,1+/- 0,3	50+/-10	1006	0.015	31.1	1.952	0.015	0.011	0.018
	05/02/2016	1591.55	20,1+/- 0,3	50+/-10	1006	0.016	31.5	1.972	0.015	0.011	0.018
	05/02/2016	1591.55	20,1+/- 0,3	50+/-10	1003	0.015	31.5	1.956	0.015	0.011	0.018
Mean	**27/01/16**	**1591.55**	**20,1+/-0,3**	**50+/-10**	**1006**	**0.015**	**31.4**	**1.952**	**0.004**	**0.009**	**0.010**

AH 1257

	Serial N°. Of the standard :	AH1257 (PTB)		Nominal value :	10 pF	Voltage :	100 V	Test frequency	397,89 Hz	
	Date	Test frequency (Hz)	Ambient temperature and uncertainty T_{amb} (°C)	Humidity (%)	Barometric pressure (Pa)	Drift	Chassis temperature (°C)	Measurement result: deviation from nominal value (µF/F)	Type A uncertainty (µF/F)	Type B uncertainty (µF/F)	Combined uncertainty (µF/F)
	10/02/16	397.89	20,2+/- 0,3	50+/-10	1001	0.015	32.7	1.797	0.004	0.011	0.012
	11/02/16	397.89	20,2+/- 0,3	50+/-10	1006	0.013	33.0	1.800	0.004	0.011	0.012
	11/02/16	397.89	20,2+/- 0,3	50+/-10	1007	0.013	31.8	1.797	0.004	0.011	0.012
	11/02/16	397.89	20,2+/- 0,3	50+/-10	1007	0.015	31.5	1.798	0.004	0.011	0.012
	11/02/16	397.89	20,2+/- 0,3	50+/-10	1007	0.015	31.6	1.794	0.004	0.011	0.012
	11/02/16	397.89	20,2+/- 0,3	50+/-10	1006	0.014	31.5	1.795	0.004	0.011	0.012
	11/02/16	397.89	20,2+/- 0,3	50+/-10	1006	0.014	31.5	1.797	0.004	0.011	0.012
	11/02/16	397.89	20,2+/- 0,3	50+/-10	1007	0.014	31.5	1.796	0.004	0.011	0.012
	11/02/16	397.89	20,2+/- 0,3	50+/-10	1007	0.015	31.5	1.795	0.004	0.011	0.012
	12/02/16	397.89	20,2+/- 0,3	50+/-10	991	0.014	31.5	1.797	0.004	0.011	0.012
	12/02/16	397.89	20,2+/- 0,3	50+/-10	992	0.014	31.8	1.802	0.004	0.011	0.012
	12/02/16	397.89	20,2+/- 0,3	50+/-10	992	0.014	31.8	1.803	0.004	0.011	0.012
	12/02/16	397.89	20,2+/- 0,3	50+/-10	992	0.014	31.8	1.798	0.004	0.011	0.012
	12/02/16	397.89	20,2+/- 0,3	50+/-10	992	0.014	31.8	1.804	0.004	0.011	0.012
	12/02/16	397.89	20,2+/- 0,3	50+/-10	992	0.014	31.8	1.803	0.004	0.011	0.012
	12/02/16	397.89	20,2+/- 0,3	50+/-10	992	0.014	31.8	1.805	0.004	0.011	0.012
Mean	**11/02/16**	**397.89**	**20,2+/-0,3**	**50+/-10**	**995**	**0.014**	**31.7**	**1.800**	**0.001**	**0.010**	**0.010**

	Serial N°. Of the standard :		**AH1257 (PTB)**		Nominal value : **10 pF**		Voltage : **100 V**		Test frequency	**795,77 Hz**	
	Date	Test frequency (Hz)	Ambient temperature and uncertainty T_{amb} (°C)	Humidity (%)	Barometric pressure (Pa)	Drift	Chassis temperature (°C)	Measurement result: deviation from nominal value (µF/F)	Type A uncertainty (µF/F)	Type B uncertainty (µF/F)	Combined uncertainty (µF/F)
	10/02/16	795.77	20,2+/- 0,3	50+/-10	1001	0.015	32.7	1.688	0.003	0.011	0.011
	11/02/16	795.77	20,2+/- 0,3	50+/-10	1006	0.013	33	1.687	0.003	0.011	0.011
	11/02/16	795.77	20,2+/- 0,3	50+/-10	1007	0.013	31.8	1.687	0.003	0.011	0.011
	11/02/16	795.77	20,2+/- 0,3	50+/-10	1007	0.015	31.5	1.686	0.003	0.011	0.011
	11/02/16	795.77	20,2+/- 0,3	50+/-10	1007	0.015	31.6	1.685	0.003	0.011	0.011
	11/02/16	795.77	20,2+/- 0,3	50+/-10	1006	0.014	31.5	1.686	0.003	0.011	0.011
	11/02/16	795.77	20,2+/- 0,3	50+/-10	1006	0.014	31.5	1.686	0.003	0.011	0.011
	11/02/16	795.77	20,2+/- 0,3	50+/-10	1007	0.014	31.5	1.686	0.003	0.011	0.011
	11/02/16	795.77	20,2+/- 0,3	50+/-10	1007	0.015	31.5	1.683	0.003	0.011	0.011
	12/02/16	795.77	20,2+/- 0,3	50+/-10	991	0.014	31.5	1.688	0.003	0.011	0.011
	12/02/16	795.77	20,2+/- 0,3	50+/-10	992	0.014	31.8	1.688	0.003	0.011	0.011
	12/02/16	795.77	20,2+/- 0,3	50+/-10	992	0.014	31.8	1.691	0.003	0.011	0.011
	12/02/16	795.77	20,2+/- 0,3	50+/-10	992	0.014	31.8	1.690	0.003	0.011	0.011
	12/02/16	795.77	20,2+/- 0,3	50+/-10	992	0.014	31.8	1.690	0.003	0.011	0.011
	12/02/16	795.77	20,2+/- 0,3	50+/-10	992	0.014	31.8	1.692	0.003	0.011	0.011
	12/02/16	795.77	20,2+/- 0,3	50+/-10	992	0.014	31.8	1.693	0.003	0.011	0.011
Mean	**11/02/16**	**795.77**	**20,2+/-0,3**	**50+/-10**	**1000**	**0.014**	**31.8**	**1.688**	**0.001**	**0.009**	**0.009**

	Serial N°. Of the standard :		**AH1257 (PTB)**		Nominal value : **10 pF**		Voltage : **100 V**		Test frequency	**1591,55 Hz**	
	Date	Test frequency (Hz)	Ambient temperature and uncertainty T_{amb} (°C)	Humidity (%)	Barometric pressure (Pa)	Drift	Chassis temperature (°C)	Measurement result: deviation from nominal value (µF/F)	Type A uncertainty (µF/F)	Type B uncertainty (µF/F)	Combined uncertainty (µF/F)
	10/02/16	1591.55	20,2+/- 0,3	50+/-10	1001	0.015	32.7	1.520	0.013	0.011	0.017
	11/02/16	1591.55	20,2+/- 0,3	50+/-10	1006	0.013	33.0	1.469	0.013	0.011	0.017
	11/02/16	1591.55	20,2+/- 0,3	50+/-10	1007	0.013	31.8	1.468	0.013	0.011	0.017
	11/02/16	1591.55	20,2+/- 0,3	50+/-10	1007	0.015	31.5	1.463	0.013	0.011	0.017
	11/02/16	1591.55	20,2+/- 0,3	50+/-10	1007	0.015	31.6	1.467	0.013	0.011	0.017
	11/02/16	1591.55	20,2+/- 0,3	50+/-10	1006	0.014	31.5	1.465	0.013	0.011	0.017
	11/02/16	1591.55	20,2+/- 0,3	50+/-10	1006	0.014	31.5	1.465	0.013	0.011	0.017
	11/02/16	1591.55	20,2+/- 0,3	50+/-10	1007	0.014	31.5	1.463	0.013	0.011	0.017
	11/02/16	1591.55	20,2+/- 0,3	50+/-10	1007	0.015	31.5	1.464	0.013	0.011	0.017
	12/02/16	1591.55	20,2+/- 0,3	50+/-10	991	0.014	31.5	1.468	0.013	0.011	0.017
	12/02/16	1591.55	20,2+/- 0,3	50+/-10	992	0.014	31.8	1.468	0.013	0.011	0.017
	12/02/16	1591.55	20,2+/- 0,3	50+/-10	992	0.014	31.8	1.470	0.013	0.011	0.017
	12/02/16	1591.55	20,2+/- 0,3	50+/-10	992	0.014	31.8	1.471	0.013	0.011	0.017
	12/02/16	1591.55	20,2+/- 0,3	50+/-10	992	0.014	31.8	1.471	0.013	0.011	0.017
	12/02/16	1591.55	20,2+/- 0,3	50+/-10	992	0.014	31.8	1.472	0.013	0.011	0.017
	12/02/16	1591.55	20,2+/- 0,3	50+/-10	992	0.014	31.8	1.473	0.013	0.011	0.017
Mean	**11/02/16**	**1591.55**	**20,2+/-0,3**	**50+/-10**	**1000**	**0.014**	**31.8**	**1.471**	**0.003**	**0.011**	**0.012**

AH 1258

	Serial N°. Of the standard :	AH1258 (PTB)			Nominal value :	10 pF		Voltage : 100 V	Test frequency	397,89 Hz	
	Date	Test frequency (Hz)	Ambient temperature and uncertainty T_{amb} (°C)	Humidity (%)	Barometric pressure (Pa)	Drift	Chassis temperature (°C)	Measurement result: deviation from nominal value (µF/F)	Type A uncertainty (µF/F)	Type B uncertainty (µF/F)	Combined uncertainty (µF/F)
	10/02/2016	397.89	20,2+/- 0,3	50+/-10	1001	0.000	32.7	1.261	0.004	0.011	0.012
	11/02/2016	397.89	20,2+/- 0,3	50+/-10	1006	0.000	33.0	1.263	0.004	0.011	0.012
	11/02/2016	397.89	20,2+/- 0,3	50+/-10	1007	0.000	31.8	1.261	0.004	0.011	0.012
	11/02/2016	397.89	20,2+/- 0,3	50+/-10	1007	0.001	31.5	1.264	0.004	0.011	0.012
	11/02/2016	397.89	20,2+/- 0,3	50+/-10	1007	0.000	31.6	1.262	0.004	0.011	0.012
	11/02/2016	397.89	20,2+/- 0,3	50+/-10	1006	0.000	31.5	1.262	0.004	0.011	0.012
	11/02/2016	397.89	20,2+/- 0,3	50+/-10	1006	0.000	31.5	1.269	0.004	0.011	0.012
	11/02/2016	397.89	20,2+/- 0,3	50+/-10	1007	0.000	31.5	1.262	0.004	0.011	0.012
	11/02/2016	397.89	20,2+/- 0,3	50+/-10	1007	0.000	31.5	1.269	0.004	0.011	0.012
	12/02/2016	397.89	20,2+/- 0,3	50+/-10	991	0.000	31.5	1.264	0.004	0.011	0.012
	12/02/2016	397.89	20,2+/- 0,3	50+/-10	992	0.000	31.8	1.268	0.004	0.011	0.012
	12/02/2016	397.89	20,2+/- 0,3	50+/-10	992	0.000	31.8	1.271	0.004	0.011	0.012
	12/02/2016	397.89	20,2+/- 0,3	50+/-10	992	0.000	31.8	1.260	0.004	0.011	0.012
	12/02/2016	397.89	20,2+/- 0,3	50+/-10	992	0.000	31.8	1.269	0.004	0.011	0.012
	12/02/2016	397.89	20,2+/- 0,3	50+/-10	992	0.000	31.8	1.271	0.004	0.011	0.012
	12/02/2016	397.89	20,2+/- 0,3	50+/-10	992	0.000	31.8	1.268	0.004	0.011	0.012
Mean	**11/02/16**	**397.89**	**20,2+/-0,3**	**50+/-10**	**1000**	**0.000**	**31.8**	**1.265**	**0.001**	**0.010**	**0.010**

	Serial N°. Of the standard :	AH1258 (PTB)			Nominal value :	10 pF		Voltage : 100 V	Test frequency	795,77 Hz	
	Date	Test frequency (Hz)	Ambient temperature and uncertainty T_{amb} (°C)	Humidity (%)	Barometric pressure (Pa)	Drift	Chassis temperature (°C)	Measurement result: deviation from nominal value (µF/F)	Type A uncertainty (µF/F)	Type B uncertainty (µF/F)	Combined uncertainty (µF/F)
	10/02/2016	795,77	20,2+/- 0,3	50+/-10	1001	0.000	32.7	1.137	0.004	0.010	0.011
	11/02/2016	795,77	20,2+/- 0,3	50+/-10	1006	0.000	33	1.137	0.004	0.010	0.011
	11/02/2016	795,77	20,2+/- 0,3	50+/-10	1007	0.000	31.8	1.139	0.004	0.010	0.011
	11/02/2016	795,77	20,2+/- 0,3	50+/-10	1007	0.001	31.5	1.136	0.004	0.010	0.011
	11/02/2016	795,77	20,2+/- 0,3	50+/-10	1007	0.000	31.6	1.136	0.004	0.010	0.011
	11/02/2016	795,77	20,2+/- 0,3	50+/-10	1006	0.000	31.5	1.141	0.004	0.010	0.011
	11/02/2016	795,77	20,2+/- 0,3	50+/-10	1006	0.000	31.5	1.140	0.004	0.010	0.011
	11/02/2016	795,77	20,2+/- 0,3	50+/-10	1007	0.000	31.5	1.150	0.004	0.010	0.011
	11/02/2016	795,77	20,2+/- 0,3	50+/-10	1007	0.000	31.5	1.143	0.004	0.010	0.011
	12/02/2016	795,77	20,2+/- 0,3	50+/-10	991	0.000	31.5	1.146	0.004	0.010	0.011
	12/02/2016	795,77	20,2+/- 0,3	50+/-10	992	0.000	31.8	1.150	0.004	0.010	0.011
	12/02/2016	795,77	20,2+/- 0,3	50+/-10	992	0.000	31.8	1.149	0.004	0.010	0.011
	12/02/2016	795,77	20,2+/- 0,3	50+/-10	992	0.000	31.8	1.138	0.004	0.010	0.011
	12/02/2016	795,77	20,2+/- 0,3	50+/-10	992	0.000	31.8	1.142	0.004	0.010	0.011
	12/02/2016	795,77	20,2+/- 0,3	50+/-10	992	0.000	31.8	1.145	0.004	0.010	0.011
	12/02/2016	795,77	20,2+/- 0,3	50+/-10	992	0.000	31.8	1.144	0.004	0.010	0.011
Mean	**11/02/16**	**795.77**	**20,2+/-0,3**	**50+/-10**	**995**	**0.000**	**31.7**	**1.145**	**0.001**	**0.009**	**0.009**

	Serial N°. Of the standard :	AH1258 (PTB)			Nominal value :	10 pF		Voltage : 100 V	Test frequency	1591,55 Hz	
	Date	Test frequency (Hz)	Ambient temperature and uncertainty T_{amb} (°C)	Humidity (%)	Barometric pressure (Pa)	Drift	Chassis temperature (°C)	Measurement result: deviation from nominal value (µF/F)	Type A uncertainty (µF/F)	Type B uncertainty (µF/F)	Combined uncertainty (µF/F)
	10/02/16	1591.55	20,2+/- 0,3	50+/-10	1001	0.000	32.7	0.900	0.004	0.011	0.012
	11/02/16	1591.55	20,2+/- 0,3	50+/-10	1006	0.000	33.0	0.902	0.004	0.011	0.012
	11/02/16	1591.55	20,2+/- 0,3	50+/-10	1007	0.000	31.8	0.902	0.004	0.011	0.012
	11/02/16	1591.55	20,2+/- 0,3	50+/-10	1007	0.001	31.5	0.898	0.004	0.011	0.012
	11/02/16	1591.55	20,2+/- 0,3	50+/-10	1007	0.000	31.6	0.902	0.004	0.011	0.012
	11/02/16	1591.55	20,2+/- 0,3	50+/-10	1006	0.000	31.5	0.904	0.004	0.011	0.012
	11/02/16	1591.55	20,2+/- 0,3	50+/-10	1006	0.000	31.5	0.904	0.004	0.011	0.012
	11/02/16	1591.55	20,2+/- 0,3	50+/-10	1007	0.000	31.5	0.909	0.004	0.011	0.012
	11/02/16	1591.55	20,2+/- 0,3	50+/-10	1007	0.000	31.5	0.907	0.004	0.011	0.012
	12/02/16	1591.55	20,2+/- 0,3	50+/-10	991	0.000	31.5	0.908	0.004	0.011	0.012
	12/02/16	1591.55	20,2+/- 0,3	50+/-10	992	0.000	31.8	0.908	0.004	0.011	0.012
	12/02/16	1591.55	20,2+/- 0,3	50+/-10	992	0.000	31.8	0.910	0.004	0.011	0.012
	12/02/16	1591.55	20,2+/- 0,3	50+/-10	992	0.000	31.8	0.900	0.004	0.011	0.012
	12/02/16	1591.55	20,2+/- 0,3	50+/-10	992	0.000	31.8	0.906	0.004	0.011	0.012
	12/02/16	1591.55	20,2+/- 0,3	50+/-10	992	0.000	31.8	0.908	0.004	0.011	0.012
	12/02/16	1591.55	20,2+/- 0,3	50+/-10	992	0.000	31.8	0.911	0.004	0.011	0.012
Mean	**11/02/16**	**1591.55**	**20,2+/-0,3**	**50+/-10**	**1000**	**0.000**	**31.8**	**0.905**	**0.001**	**0.011**	**0.011**

AH1310

	Serial N°. Of the standard :	AH1310 (BIPM)		Nominal value :	10 pF		Voltage :	100 V	Test frequency	397,89 Hz	
	Date	Test frequency (Hz)	Ambient temperature and uncertainty T_{amb} (°C)	Humidity (%)	Barometric pressure (Pa)	Drift	Chassis temperature (°C)	Measurement result: deviation from nominal value (µF/F)	Type A uncertainty (µF/F)	Type B uncertainty (µF/F)	Combined uncertainty (µF/F)
	10/02/2016	397.89	20,2+/- 0,3	50+/-10	1001	-0.049	32.7	0.076	0.004	0.011	0.012
	11/02/2016	397.89	20,2+/- 0,3	50+/-10	1006	-0.051	33.0	0.076	0.004	0.011	0.012
	11/02/2016	397.89	20,2+/- 0,3	50+/-10	1007	-0.051	31.8	0.077	0.004	0.011	0.012
	11/02/2016	397.89	20,2+/- 0,3	50+/-10	1007	-0.053	31.5	0.083	0.004	0.011	0.012
	11/02/2016	397.89	20,2+/- 0,3	50+/-10	1007	-0.053	31.6	0.081	0.004	0.011	0.012
	11/02/2016	397.89	20,2+/- 0,3	50+/-10	1006	-0.053	31.5	0.085	0.004	0.011	0.012
	11/02/2016	397.89	20,2+/- 0,3	50+/-10	1006	-0.053	31.5	0.082	0.004	0.011	0.012
	11/02/2016	397.89	20,2+/- 0,3	50+/-10	1007	-0.053	31.5	0.083	0.004	0.011	0.012
	11/02/2016	397.89	20,2+/- 0,3	50+/-10	1007	-0.053	31.5	0.083	0.004	0.011	0.012
	12/02/2016	397.89	20,2+/- 0,3	50+/-10	991	-0.053	31.5	0.087	0.004	0.011	0.012
	12/02/2016	397.89	20,2+/- 0,3	50+/-10	992	-0.050	31.8	0.085	0.004	0.011	0.012
	12/02/2016	397.89	20,2+/- 0,3	50+/-10	992	-0.050	31.8	0.085	0.004	0.011	0.012
	12/02/2016	397.89	20,2+/- 0,3	50+/-10	992	-0.052	31.8	0.086	0.004	0.011	0.012
	12/02/2016	397.89	20,2+/- 0,3	50+/-10	992	-0.049	31.8	0.085	0.004	0.011	0.012
	12/02/2016	397.89	20,2+/- 0,3	50+/-10	992	-0.049	31.8	0.085	0.004	0.011	0.012
Mean	**11/02/16**	**397.89**	**20,2+/-0,3**	**50+/-10**	**1000**	**-0.051**	**31.8**	**0.082**	**0.001**	**0.010**	**0.010**

	Serial N°. Of the standard :	AH1310 (BIPM)		Nominal value :	10 pF		Voltage :	100 V	Test frequency	795,77 Hz	
	Date	Test frequency (Hz)	Ambient temperature and uncertainty T_{amb} (°C)	Humidity (%)	Barometric pressure (Pa)	Drift	Chassis temperature (°C)	Measurement result: deviation from nominal value (µF/F)	Type A uncertainty (µF/F)	Type B uncertainty (µF/F)	Combined uncertainty (µF/F)
	10/02/2016	795,77	20,2+/- 0,3	50+/-10	1001	-0.049	32.7	0.034	0.006	0.011	0.012
	11/02/2016	795,77	20,2+/- 0,3	50+/-10	1006	-0.051	33.0	0.031	0.006	0.010	0.012
	11/02/2016	795,77	20,2+/- 0,3	50+/-10	1007	-0.051	31.8	0.030	0.006	0.010	0.012
	11/02/2016	795,77	20,2+/- 0,3	50+/-10	1007	-0.053	31.5	0.035	0.006	0.010	0.012
	11/02/2016	795,77	20,2+/- 0,3	50+/-10	1007	-0.053	31.6	0.039	0.006	0.010	0.012
	11/02/2016	795,77	20,2+/- 0,3	50+/-10	1006	-0.053	31.5	0.038	0.006	0.010	0.012
	11/02/2016	795,77	20,2+/- 0,3	50+/-10	1006	-0.053	31.5	0.033	0.006	0.010	0.012
	11/02/2016	795,77	20,2+/- 0,3	50+/-10	1007	-0.053	31.5	0.041	0.006	0.010	0.012
	11/02/2016	795,77	20,2+/- 0,3	50+/-10	1007	-0.053	31.5	0.039	0.006	0.010	0.012
	12/02/2016	795,77	20,2+/- 0,3	50+/-10	991	-0.053	31.5	0.045	0.006	0.010	0.012
	12/02/2016	795,77	20,2+/- 0,3	50+/-10	992	-0.050	31.8	0.053	0.006	0.010	0.012
	12/02/2016	795,77	20,2+/- 0,3	50+/-10	992	-0.050	31.8	0.042	0.006	0.010	0.012
	12/02/2016	795,77	20,2+/- 0,3	50+/-10	992	-0.052	31.8	0.043	0.006	0.010	0.012
	12/02/2016	795,77	20,2+/- 0,3	50+/-10	992	-0.051	31.8	0.042	0.006	0.010	0.012
	12/02/2016	795,77	20,2+/- 0,3	50+/-10	992	-0.049	31.8	0.041	0.006	0.010	0.012
	12/02/2016	795,77	20,2+/- 0,3	50+/-10	992	-0.049	31.8	0.041	0.006	0.010	0.012
Mean	**11/02/16**	**795.77**	**(20,7+/-0,3)°C**	**50+/-10**	**1000**	**-0.051**	**31.8**	**0.039**	**0.001**	**0.009**	**0.010**

	Serial N°. Of the standard :	AH1310 (BIPM)	Nominal value :	10 pF		Voltage :	100 V	Test frequency	1591,55 Hz	
	Date	Test frequency (Hz)	Ambient temperature and uncertainty T_{amb} (°C)	Humidity (%)	Barometric pressure (Pa)	Drift	Chassis temperature (°C)	Measurement result: deviation from nominal value (µF/F)	Type A uncertainty (µF/F)	Type B uncertainty (µF/F)	Combined uncertainty (µF/F)
	10/02/16	1591.55	(20,7+/- 0,3)°C	50+/-10	1001	-0.049	32.7	-0.125	0.005	0.011	0.012
	11/02/16	1591.55	(20,7+/- 0,3)°C	50+/-10	1006	-0.051	33.0	-0.133	0.005	0.011	0.012
	11/02/16	1591.55	(20,7+/- 0,3)°C	50+/-10	1007	-0.051	31.8	-0.132	0.005	0.011	0.012
	11/02/16	1591.55	20,2+/- 0,3	50+/-10	1007	-0.053	31.5	-0.127	0.005	0.011	0.012
	11/02/16	1591.55	20,2+/- 0,3	50+/-10	1007	-0.053	31.6	-0.121	0.005	0.011	0.012
	11/02/16	1591.55	20,2+/- 0,3	50+/-10	1006	-0.053	31.5	-0.123	0.005	0.011	0.012
	11/02/16	1591.55	20,2+/- 0,3	50+/-10	1006	-0.053	31.5	-0.120	0.005	0.011	0.012
	11/02/16	1591.55	20,2+/- 0,3	50+/-10	1007	-0.053	31.5	-0.122	0.005	0.011	0.012
	11/02/16	1591.55	20,2+/- 0,3	50+/-10	1007	-0.053	31.5	-0.122	0.005	0.011	0.012
	12/02/16	1591.55	20,2+/- 0,3	50+/-10	991	-0.053	31.5	-0.119	0.005	0.011	0.012
	12/02/16	1591.55	20,2+/- 0,3	50+/-10	992	-0.050	31.8	-0.117	0.005	0.011	0.012
	12/02/16	1591.55	20,2+/- 0,3	50+/-10	992	-0.050	31.8	-0.120	0.005	0.011	0.012
	12/02/16	1591.55	20,2+/- 0,3	50+/-10	992	-0.052	31.8	-0.119	0.005	0.011	0.012
	12/02/16	1591.55	20,2+/- 0,3	50+/-10	992	-0.051	31.8	-0.120	0.005	0.011	0.012
	12/02/16	1591.55	20,2+/- 0,3	50+/-10	992	-0.049	31.8	-0.118	0.022	0.011	0.025
	12/02/16	1591.55	20,2+/- 0,3	50+/-10	992	-0.049	31.8	-0.122	0.005	0.011	0.012
Mean	**11/02/16**	**1591.55**	**(20,7+/-0,3)°C**	**50+/-10**	**1000**	**-0.051**	**31.8**	**-0.123**	**0.001**	**0.011**	**0.011**

11.4 Detailed and summarised results of METAS

Measurement Conditions at the first measurement period

Ambient temperature:	(23.1 ± 0.5) °C
Relative humidity:	(26 ± 10) %
Voltage:	10 V at 100 pF
	100 V at 10 pF
Frequency:	1233.1 Hz

Measurement Conditions at the second measurement period

Ambient temperature:	(23.9 ± 0.5) °C
Relative humidity:	(35 ± 10) %
Voltage:	10 V at 100 pF
	100 V at 10 pF
Frequency:	1233.1 Hz

Summarised results of the first measurement period

Nominal value pF	S/N	Measured value, *y*		Relative uncertainty, *U* µF/F
		C pF	Δ*C*/*C* µF/F	
100	1256	100.000146	1.46	0.15
10	1257	10.0000098	0.98	0.20
10	1258	10.0000063	0.63	0.20
10	1310	9.9999989	-0.11	0.20

Summarised results of the second measurement period

Nominal value pF	S/N	Measured value, *y*		Relative uncertainty, *U* µF/F
		C pF	Δ*C*/*C* µF/F	
100	1256	100.000171	1.71	0.19
10	1257	10.0000138	1.38	0.27
10	1258	10.0000084	0.84	0.27
10	1310	9.9999981	-0.19	0.27

Detailed results

Datum	*P* [hPa]	rel. H. [%]	AH#1256	AH#1257	AH#1258	AH#1310	$T_{ambient}$ [°C]
12.11.2010	945	26	1.500	1.013	0.661	-0.079	23.2 ± 0.5
10.11.2010	930	25	1.412	0.933	0.578	-0.161	23.1 ± 0.5
08.11.2010	924	26	1.377	0.897	0.551	-0.188	23.1 ± 0.5
03.11.2010	958	26	1.449	0.963	0.615	-0.130	23.1 ± 0.5
29.10.2010	951	26	1.434	0.945	0.597	-0.142	23.0 ± 0.5
26.10.2010	960	26	1.464	0.977	0.625	-0.113	23.1 ± 0.5
15.10.2010	949	25	1.446	0.956	0.607	-0.125	23.1 ± 0.5
13.10.2010	947	26	1.458	0.971	0.619	-0.116	23.1 ± 0.5
11.10.2010	944	26	1.474	0.988	0.641	-0.095	23.1 ± 0.5
08.10.2010	955	27	1.499	1.004	0.659	-0.077	23.1 ± 0.5
06.10.2010	950	27	1.502	1.032	0.685	-0.053	23.1 ± 0.5
05.10.2010	946	28	1.493	1.011	0.665	-0.078	23.1 ± 0.5
01.10.2010	952	27	1.489	0.998	0.660	-0.082	23.1 ± 0.5
mean date: 21.10.2010, mean capacitance values:			1.461	0.976	0.628	-0.111	
26.11.2015	949.7	34.7	1.671	1.342	0.797	-0.237	24.0 ± 0.5
20.11.2015	948.5	35.8	1.717	1.376	0.841	-0.187	24.0 ± 0.5
18.11.2015	959.5	35.6	1.733	1.427	0.888	-0.149	24.0 ± 0.5
16.11.2015	957.0	34.7	1.722	1.375	0.843	-0.180	23.8 ± 0.5
13.11.2015	964.1	34.3	1.694	1.359	0.835	-0.207	23.9 ± 0.5
12.11.2015	963.2	34.6	1.693	1.373	0.829	-0.204	23.9 ± 0.5
mean date: 17.11.2015, mean capacitance values:			1.705	1.375	0.839	-0.194	

11.5 Detailed and summarised results of NMIA

The capacitance of all four AH11A capacitance standards #1257, #1258, #1310 and #1256, was measured at 1000 Hz and 1592 Hz. A measurement voltage of 100 V was used for each of the 10 pF standards, and 10 V for the 100 pF standard.

The ambient laboratory temperature was nominally 20 °C and the ambient relative humidity was nominally 50%. The ambient laboratory temperature, humidity and barometric pressure were monitored during the measurement period.

The "Chassis Temperature" and "Drift" as displayed on the front panel of the AH1100 Capacitance Standard Frame were also monitored. All readings were within expected limits.

Measurements at 1592 Hz				
Date	**SN1256**	**SN1257**	**SN1258**	**SN1310**
03.03.2015	1.941	1.643	1.074	0.013
04.03.2015	1.916	1.617	1.039	-0.003
05.03.2015	1.916	1.627	1.059	-0.003
06.03.2015	1.924	1.635	1.072	0.010
09.03.2015	1.861	1.572	0.989	-0.048
11.03.2015	1.868	1.570	1.001	-0.040
mean date: 06.03.2015, mean values:	1.904	1.611	1.039	-0.012

Measurements at 1000 Hz				
Date	**SN1256**	**SN1257**	**SN1258**	**SN1310**
16.03.2015	1.935	1.655	1.101	-0.005
17.03.2015	1.966	1.686	1.122	0.032
18.03.2015	1.930	1.660	1.083	0.000
19.03.2015	1.948	1.673	1.099	0.013
20.03.2015	1.982	1.712	1.138	0.052
24.03.2015	1.987	1.717	1.133	0.052
mean date: 19.03.2015, mean values:	1.958	1.684	1.112	0.024

Summary of results: 1000 Hz

Capacitor	Serial No. Nominal value	1257 10 pF	1258 10 pF	1310 10 pF	1256 100 pF
Test parameters	Mean date	19 March 2015			
	Test voltage (V)	100	100	100	10
Measurement result (μF/F)	Deviation from nominal value	**1.684**	**1.112**	**0.024**	**1.958**
	Type A uncertainty	0.012	0.010	0.012	0.011
	Type B uncertainty	0.035	0.035	0.035	0.036
	Combined uncertainty	0.037	0.037	0.037	0.037
	Degrees of freedom	12	11	12	12
	Expanded uncertainty†	0.082	0.081	0.082	0.082
Ambient temperature (°C)	Mean value	19.90	19.90	19.90	19.90
	Combined uncertainty	0.11	0.11	0.11	0.11
	Degrees of freedom	74	74	74	74
	Minimum value	19.44	19.44	19.44	19.44
	Maximum value	20.53	20.53	20.53	20.53
Relative ambient humidity (%)	Mean value	54	54	54	54
	Combined uncertainty	2	2	2	2
	Degrees of freedom	33340	33340	33340	33340
	Minimum value	51	51	51	51
	Maximum value	59	59	59	59
P (Pa)	Barometric Pressure	100 740	100 740	100 740	100 740
AH11A chassis temperature (°C)	Mean value	29.0			
	Minimum value	28.8			
	Maximum value	29.2			
AH11A drift (ppm)	Mean value	0.030	0.011	-0.016	0.018
	Minimum value	0.030	0.010	-0.017	0.018
	Maximum value	0.031	0.011	-0.014	0.019

† 95% factor

Summary of results: 1592 Hz

Capacitor	Serial No. Nominal value	1257 10 pF	1258 10 pF	1310 10 pF	1256 100 pF
Test param-eters	Mean date	6 March 2015			
	Test voltage (V)	100	100	100	10
Measure-ment result (µF/F)	Deviation from nominal value	**1.611**	**1.039**	**-0.012**	**1.904**
	Type A uncertainty	0.014	0.016	0.012	0.014
	Type B uncertainty	0.035	0.035	0.035	0.036
	Combined uncertainty	0.038	0.039	0.037	0.039
	Degrees of freedom	12	13	12	13
	Expanded uncertainty†	0.083	0.084	0.081	0.083
Ambient temperature (°C)	Mean value	19.91	19.91	19.91	19.91
	Combined uncertainty	0.11	0.11	0.11	0.11
	Degrees of freedom	74	74	74	74
	Minimum value	19.45	19.45	19.45	19.45
	Maximum value	20.45	20.45	20.45	20.45
Relative ambient humidity (%)	Mean value	53	53	53	53
	Combined uncertainty	2	2	2	2
	Degrees of freedom	34266	34266	34266	34266
	Minimum value	50	50	50	50
	Maximum value	59	59	59	59
P (Pa)	Barometric Pressure	100 390	100 390	100 390	100 390
AH11A chassis temperature (°C)	Mean value	29.0			
	Minimum value	28.9			
	Maximum value	29.6			
AH11A drift (ppm)	Mean value	0.031	0.011	-0.016	0.015
	Minimum value	0.028	0.010	-0.020	0.012
	Maximum value	0.031	0.011	-0.015	0.017

† 95% coverage factor

<u>Summarised results and associated uncertainties (*k* = 1):</u>

Datum	*f* [Hz]	AH#1256	AH#1257	AH#1258	AH#1310
19.03.2015	1000	1.958 ± 0.037 -0.037 ± 0.006 +0.0176	1.684 ± 0.037 -0.054 ± 0.006 +0.0176	1.112 ± 0.037 -0.034 ± 0.006 +0.0176	0.024 ± 0.037 -0.021 ± 0.006 +0.0176
06.03.2015	1592	1.904 ± 0.039 -0.037 ± 0.006 +0.0176	1.611 ± 0.038 -0.054 ± 0.006 +0.0176	1.039 ± 0.039 -0.034 ± 0.006 +0.0176	-0.012 ± 0.039 -0.021 ± 0.006 +0.0176
Interpol.	1233	1.937 ± 0.038 -0.037 ± 0.006 +0.0176	1.655 ± 0.038 -0.054 ± 0.006 +0.0176	1.083 ± 0.038 -0.034 ± 0.006 +0.0176	0.010 ± 0.038 -0.021 ± 0.006 +0.0176

<u>Comments:</u>

- The effect of the deviating ambient temperature (20°C instead of 23°C) has been taken into account as described in Section 4.7.
- To convert the SI capacitance values obtained by NMIA to farad-90, the pilot has added a relative correction of (+17.6 ± 0.2)·10^{-9}, as explained in Section 4.7.

11.6 Detailed and summarised results of VSL

A summary of the ambient temperature, relative humidity and barometric pressure during the measurement of the travelling standards of this comparison is given in Table 11.6.1. A summary of the capacitance measurement results is given in Table 11.6.2.

Table 11.6.1: Summary of ambient conditions

		Average	Unc.	Minimum	Maximum
Temperature	°C	22.9	0.5	22.6	23.8
Humidity	%	44	5	40	48
Pressure	Pa	101439	10	99632	102551

Table 11.6.2: Summary of capacitance measurement results

SN	Date	Test frequency (Hz)	Test voltage (V)	Nominal value (pF)	Deviation from nominal (µF/F)	Type A uncertainty (µF/F)	Type B uncertainty (µF/F)	Comb. uncertainty (µF/F)	*k*	Expanded uncertainty (µF/F)
01256	23-08-2010	1233.09472	10.0	100	1.10	0.020	0.332	0.332	2.02	0.670
01257	21-08-2010	1233.07474	100	10	0.49	0.020	0.452	0.453	2.01	0.911
01258	21-08-2010	1233.07474	100	10	0.14	0.020	0.452	0.453	2.01	0.911
01310	21-08-2010	1233.07474	100	10	-0.61	0.020	0.452	0.453	2.01	0.911

100 pF Capacitor

Serial No. of the standard: 01256 Nominal value: 100 pF

Date	Test frequency (Hz)	Test voltage (V)	Ambient temp. T_{amb} (°C)	Humidity (%)	Pressure (Pa)	Result (µF/F)	Type A unc. (µF/F)	Type B unc. (µF/F)	Comb. unc. (µF/F)	Drift	Chassis Temp (°C)
06-08-2010	1232.97480	10.0	23.0	43	101700	1.11	0.015	0.332	0.332	-0.021	32.7
06-08-2010	1232.97480	10.0	23.0	43	101700	1.06	0.015	0.332	0.332	-0.021	32.7
16-08-2010	1232.97480	10.0	23.0	43	100700	1.05	0.015	0.332	0.332	-0.022	32.8
16-08-2010	1232.97480	10.0	23.0	43	100700	1.03	0.015	0.332	0.332	-0.022	32.8
30-08-2010	1233.17466	10.0	23.0	43	101700	1.11	0.015	0.332	0.332	-0.023	32.9
30-08-2010	1233.17466	10.0	23.0	43	101700	1.11	0.015	0.332	0.332	-0.023	32.9
31-08-2010	1233.17468	10.0	23.0	43	102500	1.17	0.015	0.332	0.332	-0.023	32.8
01-09-2010	1233.17468	10.0	23.0	43	102200	1.15	0.015	0.332	0.332	-0.023	32.8
01-09-2010	1233.17468	10.0	23.0	43	102200	1.15	0.015	0.332	0.332	-0.023	32.8
06-09-2010	1233.17468	10.0	23.0	43	102000	1.09	0.015	0.332	0.332	-0.024	32.9

10 pF Capacitors

Serial No. of the standard: 01257 Nominal value: 10 pF

Date	Test frequency (Hz)	Test voltage (V)	Ambient temp. T_{amb} (°C)	Humidity (%)	Pressure (Pa)	Result (µF/F)	Type A unc. (µF/F)	Type B unc. (µF/F)	Comb. unc. (µF/F)	Drift	Chassis Temp (°C)
05-08-2010	1232.97480	100	23.0	43	101000	0.48	0.014	0.452	0.452	0.019	32.9
06-08-2010	1232.97480	100	23.0	43	101700	0.46	0.014	0.452	0.452	0.018	32.8
06-08-2010	1232.97480	100	23.0	43	101700	0.46	0.014	0.452	0.452	0.018	32.8
17-08-2010	1232.97480	100	23.0	44	100900	0.41	0.014	0.452	0.452	0.019	32.6
17-08-2010	1232.97480	100	23.0	44	100900	0.43	0.014	0.452	0.452	0.019	32.6
17-08-2010	1232.97480	100	23.0	44	100900	0.46	0.014	0.452	0.452	0.019	32.6
30-08-2010	1233.17466	100	23.0	43	101700	0.51	0.014	0.452	0.452	0.018	32.8
30-08-2010	1233.17466	100	23.0	43	101700	0.47	0.014	0.452	0.452	0.018	32.8
31-08-2010	1233.17468	100	23.0	43	102500	0.55	0.014	0.452	0.452	0.018	32.7
31-08-2010	1233.17468	100	23.0	43	102500	0.54	0.014	0.452	0.452	0.018	32.7
01-09-2010	1233.17468	100	23.0	43	102200	0.55	0.014	0.452	0.452	0.018	32.8
01-09-2010	1233.17468	100	23.0	43	102200	0.53	0.014	0.452	0.452	0.018	32.8

Serial No. of the standard: 01258 Nominal value: 10 pF

Date	Test frequency (Hz)	Test voltage (V)	Ambient temp. T_{amb} (°C)	Humidity (%)	Pressure (Pa)	Result (μF/F)	Type A unc. (μF/F)	Type B unc. (μF/F)	Comb. unc. (μF/F)	Drift	Chassis Temp (°C)
05-08-2010	1232.97480	100	23.0	43	101000	0.13	0.013	0.452	0.452	-0.002	32.9
06-08-2010	1232.97480	100	23.0	43	101700	0.12	0.013	0.452	0.452	-0.002	32.8
06-08-2010	1232.97480	100	23.0	43	101700	0.12	0.013	0.452	0.452	-0.002	32.8
17-08-2010	1232.97480	100	23.0	44	100900	0.07	0.013	0.452	0.452	-0.002	32.6
17-08-2010	1232.97480	100	23.0	44	100900	0.08	0.013	0.452	0.452	-0.002	32.6
17-08-2010	1232.97480	100	23.0	44	100900	0.11	0.013	0.452	0.452	-0.002	32.6
30-08-2010	1233.17466	100	23.0	43	101700	0.17	0.013	0.452	0.452	-0.002	32.8
30-08-2010	1233.17466	100	23.0	43	101700	0.14	0.013	0.452	0.452	-0.002	32.9
31-08-2010	1233.17468	100	23.0	43	102500	0.20	0.013	0.452	0.452	-0.002	32.7
31-08-2010	1233.17468	100	23.0	43	102500	0.19	0.013	0.452	0.452	-0.002	32.7
01-09-2010	1233.17468	100	23.0	43	102200	0.19	0.013	0.452	0.452	-0.002	32.8
01-09-2010	1233.17468	100	23.0	43	102200	0.19	0.013	0.452	0.452	-0.002	32.8

Serial No. of the standard: 01310 Nominal value: 10 pF

Date	Test frequency (Hz)	Test voltage (V)	Ambient temp. T_{amb} (°C)	Humidity (%)	Pressure (Pa)	Result (μF/F)	Type A unc. (μF/F)	Type B unc. (μF/F)	Comb. unc. (μF/F)	Drift	Chassis Temp (°C)
05-08-2010	1232.97480	100	23.0	43	101000	-0.63	0.014	0.452	0.452	-0.087	32.8
06-08-2010	1232.97480	100	23.0	43	101700	-0.62	0.014	0.452	0.452	-0.087	32.8
06-08-2010	1232.97480	100	23.0	43	101700	-0.63	0.014	0.452	0.452	-0.087	32.8
17-08-2010	1232.97480	100	23.0	44	100900	-0.69	0.014	0.452	0.452	-0.086	32.6
17-08-2010	1232.97480	100	23.0	44	100900	-0.67	0.014	0.452	0.452	-0.086	32.6
17-08-2010	1232.97480	100	23.0	44	100900	-0.63	0.014	0.452	0.452	-0.086	32.6
30-08-2010	1233.17466	100	23.0	43	101700	-0.57	0.014	0.452	0.452	-0.087	32.8
30-08-2010	1233.17466	100	23.0	43	101700	-0.62	0.014	0.452	0.452	-0.087	32.9
31-08-2010	1233.17468	100	23.0	43	102500	-0.56	0.014	0.452	0.452	-0.086	32.7
31-08-2010	1233.17468	100	23.0	43	102500	-0.56	0.014	0.452	0.452	-0.086	32.7
01-09-2010	1233.17468	100	23.0	43	102200	-0.54	0.014	0.452	0.452	-0.086	32.8
01-09-2010	1233.17468	100	23.0	43	102200	-0.56	0.014	0.452	0.452	-0.086	32.8

12. Annex: Supplementary measurements

12.1 Influence of the ambient temperature

To determine the effect of the ambient temperature on the capacitance values, the pilot laboratory performed test measurements with the capacitance standards placed in a temperature cabinet with an adjustable temperature while the capacitance of the AH standards has been monitored by an AH capacitance bridge. (The essential property of the AH capacitance bridge is the resolution of $1 \cdot 10^{-8}$, or even $1 \cdot 10^{-9}$, and not the absolute precision.) To get reliable and reproducible results, it is important to avoid that the air circulation is too strong and air is blown too strongly onto the AH frame, because this may lead to an unrealistic heat removal from the AH frame. A measurement for the 100 pF standard AH#1256 is shown in Figure 12.1. All four travelling standards have repeatedly been measured. The resulting ambient temperature coefficients are listed in Table 12.1. Because LNE and NMIA run their laboratory at a temperature of 20°C, their results have been corrected for the deviating ambient temperature.

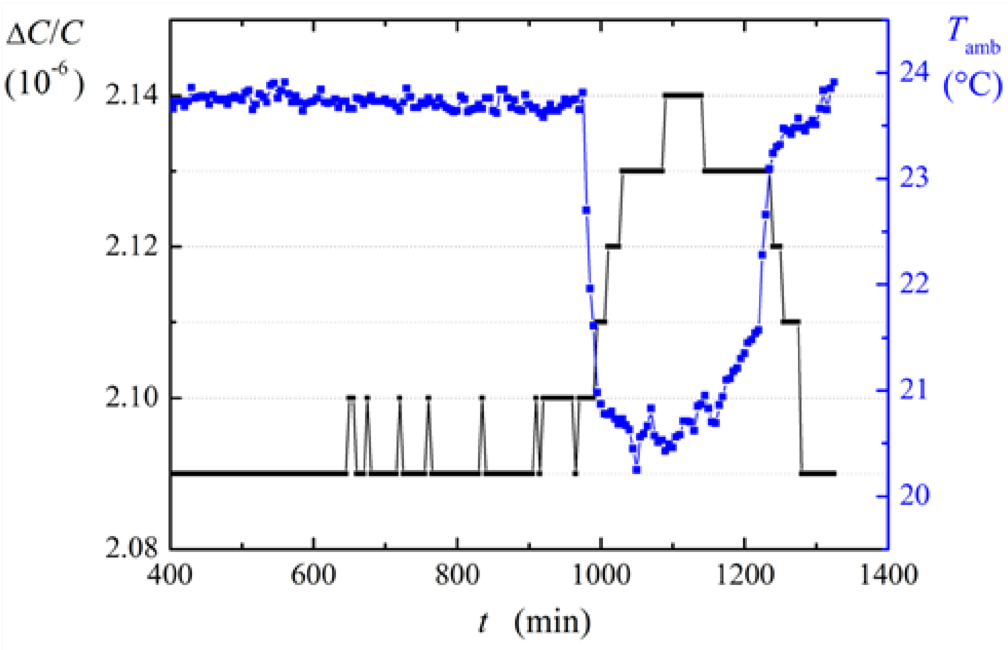

Figure 12.1: Changes of the 100 pF capacitance standard AH#1256 with the ambient temperature, measured with an AH capacitance bridge.

Table 12.1: Ambient temperature coefficient of the travelling capacitance standards and the estimated uncertainty (k = 1).

Standard	Ambient temperature coefficient	
	[10^{-9}/°C]	[10^{-9}/3°C]
100 pF #1256	-12.3 ± 2.0	-37 ± 6
10 pF #1257	-18.1 ± 2.0	-54 ± 6
10 pF #1258	-11.4 ± 2.0	-34 ± 6
10 pF #1310	-7.1 ± 2.0	-21 ± 6

12.2 Influence of mains voltage

The AH frame is powered by mains voltage. The nominal mains voltage within Europe is 230 V, but 240 V has been used at NMIA. Furthermore, during the measurements the mains voltage was not monitored by each participant and may have deviated from nominal by a few volts. A change of the mains voltage may affect the capacitance standards, for example, because a change of the heat dissipated in the internal AH mains transformer may affect the temperature of the capacitance standards. Therefore, the pilot laboratory investigated by means of an adjustable mains transformer to which extent the capacitance of the standard located closest to the internal AH mains transformer depends on the mains voltage level. The mains voltage was changed a few times between 225 V and 240 V, but the capacitance did not show a significant change within a relative uncertainty of $5 \cdot 10^{-9}$ per 15 V. This corresponds to an upper limit of $3 \cdot 10^{-9}$ per 10 V difference of the mains voltage and is negligible.

12.3 Data logger

Before the first circulation, a data logger model MSR 145 was mounted into the AH frame to automatically record accelerations in three axes above a certain threshold and to record the temperature at fixed intervals of 10 minutes. The battery of the data logger needs recharging every 8 weeks, as tested at the pilot laboratory. Therefore, the participants were asked to recharge the battery.

During the first capacitance circulation, the recharging of the data-logger battery failed a few times so that only incomplete data are available. Because the data logger was built into the chassis of the AH frame, the failure was not visible from outside. The available data of the first capacitance circulation are shown in Figure 12.3. During the transportations, the acceleration did not exceed ±1.5g in horizontal direction and 2.8g in vertical direction. To value these accelerations, one should have in mind that horizontal accelerations in normal traffic, for example when starting or stopping at a traffic light, are typically in the range of (0.5 to 1)g. Road irregularities typically cause vertical accelerations of 2g. Shock events during standard freight can be in the range of (50 to 100) g or even higher (for objects of similar mass and volume) and this is the limit where solid transport packages become damaged. Such events were not recorded here. During the stays at the laboratories, no shock events were detected at all, as it should be.

At the second capacitance circulation and the first return to PTB, the software of the data logger was found to be completely corrupted and data were not recorded or lost. Because the data logger was not satisfying at the first capacitance circulation and a quick replacement was not possible, the pilot decided to proceed without shock and temperature monitoring.

However, at the end of the circulation the packaging did not show any visible damage. This demonstrates that the transportations were really careful. In addition, the travelling standards were packed into shock-absorbing foam plastic.

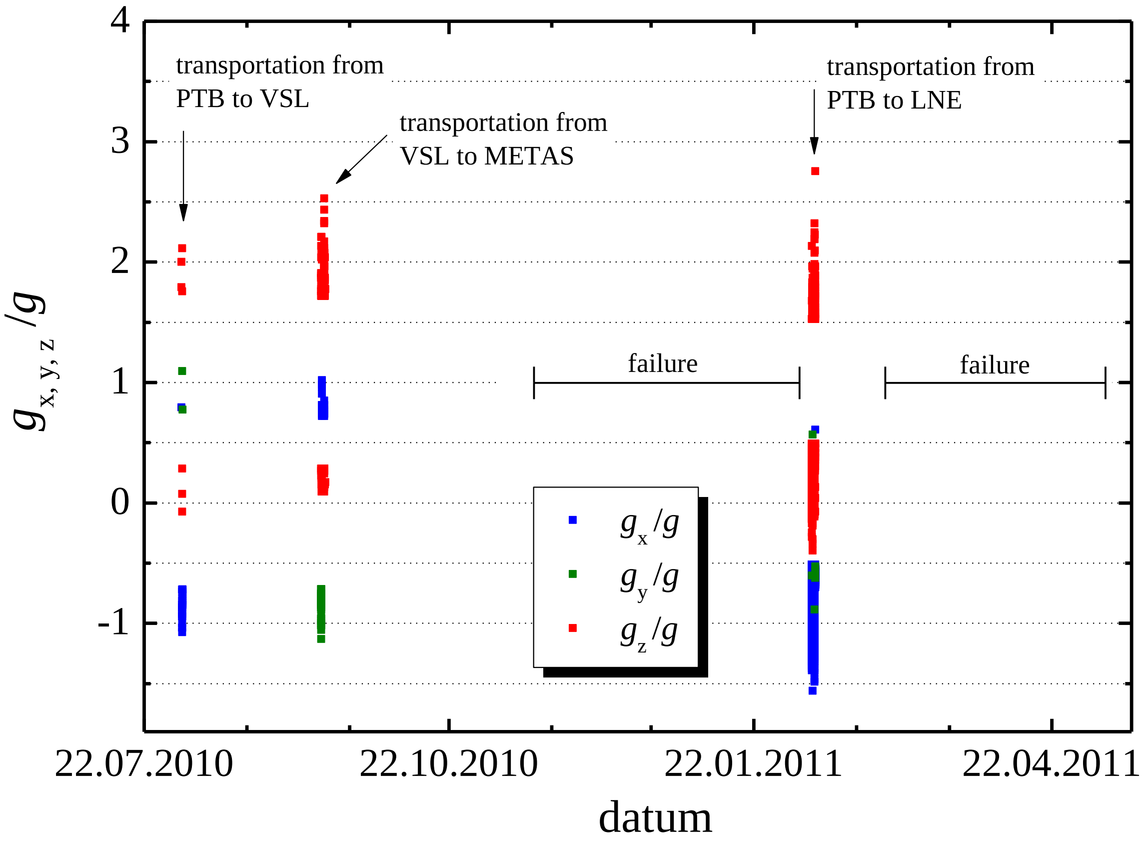

Figure 12.3: Accelerations in three axes, in terms of the gravitational acceleration *g*, recorded by the data logger during the first capacitance circulation.

13. Annex: Comparison with AH specifications

Table 13 compares the AH 11A specifications which are relevant in the context of this report with the results obtained during this comparison. Most results meet or beat the specifications, but two quantities exceed the specifications (marked in red).

Table 13: Comparison of AH 11A specifications and results obtained at this comparison. Results which do not comply with the AH specifications are marked in red.

Quantity	AH specifications	Results obtained at this comparison
Accuracy	initial setting: 2 ppm	after more than 15 years: ≤ 2 ppm (at other standards: 2.5 ppm to maximal 5 ppm after more than 15 years)
Stability	0.3 ppm/year	(0.1 to 0.3) ppm/year
Ambient temperature coefficient	0.01 ppm/°C	(-7 to **-18) ppb/°C**
Hysteresis from temperature cycling	0.05 ppm	maximal 0.05 ppm
Hysteresis from mechanical shock	0.05 ppm	(0.0 to **0.15) ppm**
AC voltage coefficient	3 ppb/volt rms	maximal 0.4 ppb/volt rms
Sensitivity to power line voltage	0.3 ppb per 1% change in power line voltage	smaller than measurement uncertainty of 0.8 ppb per 1% change in power line voltage